

Brackish Groundwater in Aquifers of the Upper Coastal Plains, Central Texas

John E. Meyer, P.G., Andrea D. Croskrey, P.G., Alysa K. Suydam, P.G.,
and Nathaniel van Oort

Report 385
December 2020

Texas Water Development Board
www.twdb.texas.gov



Texas Water Development Board

Report 385

Brackish Groundwater in Aquifers of the Upper Coastal Plains, Central Texas

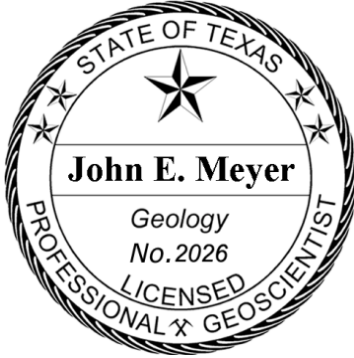
by
John E. Meyer, P.G.
Andrea D. Croskrey, P.G.
Alysa K. Suydam, P.G.
Nathaniel van Oort

December 2020



Geoscientist Seal

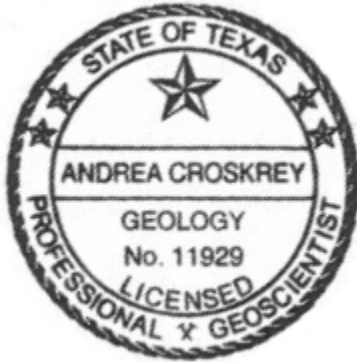
The contents of this report (including figures, tables, and plates) document the work of the following licensed Texas geoscientists:



John E. Meyer, P.G., No. 2026


Mr. Meyer was responsible for working on all aspects of the study and preparing the report. The seal appearing on this document was authorized on December 24, 2020.

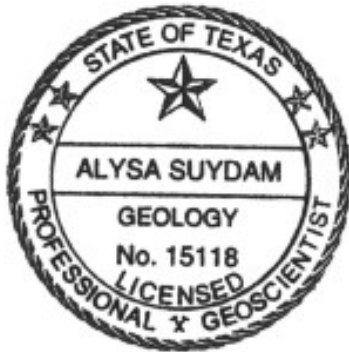

John E. Meyer



Andrea Croskrey, P.G., No. 11929


Ms. Croskrey was responsible for working on all aspects of the study and preparing the report. The seal appearing on this document was authorized on December 28, 2020.


Andrea Croskrey



Alysa Suydam, P.G., No. 15118

Ms. Suydam interpreted stratigraphy, lithology, and total dissolved solids from geophysical well logs, interpolated net sand GIS rasters, delineated salinity classes, calculated groundwater volumes, created report figures, and prepared cross-sections. Ms. Suydam completed this work as a G.I.T. under the direct supervision of Mr. Meyer and Ms. Croskrey. The seal appearing on this document was authorized on December 28, 2020.


Alysa Suydam

Nathaniel van Oort under the direct supervision of Mr. Meyer and Ms. Croskrey, collected well information, interpreted stratigraphy and lithology from geophysical well logs, prepared stratigraphic surface GIS rasters, and prepared report figures.

Cover photo courtesy of John Meyer

“Lower Carrizo Formation (above) truncating upper Calvert Bluff Formation channel, Bastrop County, Texas”

Texas Water Development Board

Peter Lake
Chairman

Kathleen Jackson
Member

Brooke Paup
Member

Leading the state's efforts in ensuring a secure water future for Texas and its citizens.

*The Texas Water Development Board freely grants permission to copy and distribute its materials.
The agency would appreciate acknowledgment.*

Published and distributed by the
Texas Water Development Board
P.O. Box 13231, Capitol Station
Austin, Texas 78711-3231

(Printed on recycled paper)

This page is intentionally blank.

Table of Contents

1.	Executive summary.....	1
2.	Introduction.....	3
3.	Project deliverables.....	6
4.	Study area.....	7
5.	Geologic setting.....	18
5.1	Stratigraphy, lithology, and depositional environments.....	18
5.1.1	Wilcox Group.....	21
5.1.2	Carrizo Formation.....	23
5.1.3	Reklaw Formation.....	23
5.1.4	Queen City Formation.....	24
5.1.5	Weches Formation.....	24
5.1.6	Sparta Formation.....	24
5.1.7	Cook Mountain Formation.....	24
5.1.8	Yegua Formation.....	25
5.2	Structural geology.....	25
6.	Methodology.....	34
6.1	Previous investigations.....	34
6.2	Data collection and analysis.....	39
6.3	Stratigraphic interpretation.....	43
6.4	Net sand analysis.....	44
6.5	Aquifer determination.....	47
6.6	Water Quality.....	50
6.6.1	Sources of dissolved minerals.....	51
6.6.2	Parameters of concern for desalination.....	52
6.7	Aquifer hydraulic properties.....	52
6.8	Formation porosity.....	54
6.9	Geophysical well log analysis for interpreted total dissolved solids concentration.....	61
6.9.1	R _{WA} Minimum Method input parameters.....	63
6.9.2	R _{WA} Minimum Method formulas.....	73
6.9.3	Geophysical well log tools.....	75
6.10	Salinity class delineation.....	77
6.11	Groundwater volumes.....	78
7.	Results.....	81
7.1	Wilcox Group.....	86
7.1.1	Well control.....	86
7.1.2	Stratigraphic analysis.....	87
7.1.3	Formation top, bottom, and thickness.....	91
7.1.4	Net sand.....	96
7.1.5	Salinity classes.....	98
7.1.6	Volume of brackish groundwater.....	101
7.1.7	Aquifer hydraulic properties.....	103
7.2	Carrizo Formation.....	105
7.2.1	Well control.....	105
7.2.2	Stratigraphic analysis.....	105
7.2.3	Formation top, bottom, thickness.....	110

7.2.4	Net sand	115
7.2.5	Salinity classes	117
7.2.6	Volume of brackish groundwater.....	120
7.2.7	Aquifer hydraulic properties	121
7.3	Reklaw Formation.....	123
7.3.1	Well control	123
7.3.2	Stratigraphic analysis.....	123
7.3.3	Formation top, bottom, thickness.....	125
7.3.4	Net sand	132
7.3.5	Salinity classes	132
7.3.6	Volume of brackish groundwater.....	132
7.4	Queen City Formation.....	132
7.4.1	Well control	132
7.4.2	Stratigraphic analysis.....	132
7.4.3	Formation top, bottom, thickness.....	136
7.4.4	Net sand	141
7.4.5	Salinity classes	143
7.4.6	Volume of brackish groundwater.....	146
7.4.7	Aquifer hydraulic properties	147
7.5	Weches Formation	150
7.5.1	Well control	150
7.5.2	Stratigraphic analysis.....	150
7.5.3	Formation top, bottom, thickness.....	152
7.5.4	Net sand	158
7.5.5	Salinity classes.....	158
7.5.6	Volume of brackish groundwater.....	158
7.6	Sparta Formation.....	158
7.6.1	Well control	158
7.6.2	Stratigraphic analysis.....	158
7.6.3	Formation top, bottom, thickness.....	160
7.6.4	Net sand	167
7.6.5	Salinity classes	168
7.6.6	Volume of brackish groundwater.....	172
7.6.7	Aquifer hydraulic properties	172
7.7	Cook Mountain Formation.....	175
7.7.1	Well control	175
7.7.2	Stratigraphic analysis.....	175
7.7.3	Formation top, bottom, thickness.....	179
7.7.4	Net sand	185
7.7.5	Salinity classes	185
7.7.6	Volume of brackish groundwater.....	185
7.8	Yegua Formation	185
7.8.1	Well control	185
7.8.2	Stratigraphic analysis.....	186
7.8.3	Formation top, bottom, thickness.....	190
7.8.4	Net sand	195

7.8.5	Salinity classes	197
7.8.6	Volume of brackish groundwater.....	200
7.8.7	Aquifer hydraulic properties	200
8.	Desalination concentrate disposal.....	203
9.	Future improvements	205
10.	Conclusions.....	206
11.	Acknowledgments.....	207
12.	References.....	208
13.	Appendices.....	218
13.1	Geological formation brackish groundwater volumes per administrative boundary..	218
13.1.1	Wilcox Group.....	218
13.1.2	Carrizo Formation.....	221
13.1.3	Queen City Formation.....	223
13.1.4	Sparta Formation.....	225
13.1.5	Yegua Formation	227
13.2	Calculation of groundwater volumes in GIS	229
13.2.1	Area.....	230
13.2.2	Saturated thickness.....	231
13.2.3	Specific yield	233
13.3	List of reports performed in the study area.....	235
13.4	BRACS Database.....	239
13.4.1	Table relationships	239
13.5	Geographic Information System analysis and datasets.....	244
13.5.1	GIS filename codes	245
13.5.2	Study GIS files organized by folder structure.....	247
13.6	Raster interpolation documentation	258
13.6.1	Stratigraphic surface interpolation.....	258
13.6.2	Net sand thickness raster interpolation	268
13.6.3	Static water level raster interpolation	276

List of Figures

Figure 4-1.	Study area location map	7
Figure 4-2.	Map legend for Figures 4-3 through 4-5	8
Figure 4-3.	City and public water supply system limits: western study area.....	11
Figure 4-4.	City and public water supply system limits: central study area	12
Figure 4-5.	City and public water supply system limits: eastern study area.....	13
Figure 4-6.	Administrative districts within the study area.....	15
Figure 4-7.	Existing and recommended brackish groundwater desalination plants	17
Figure 5.2-1.	Regional geologic structure map.....	26
Figure 5.2-2.	Fault zones within the Milano Fault Zone	28
Figure 5.2-3.	Diagrammatic cross-section across an unnamed fault zone.....	30
Figure 5.2-4.	Diagrammatic cross-section across the Karnes Trough	31
Figure 5.2-5.	Diagrammatic cross-section across the Luling Fault Zone	32
Figure 6.1-1.	Cross-section lines and points reviewed for the study	35
Figure 6.1-2.	Estimated cross-section lines and points reviewed for the study	36

Figure 6.1-3.	Geological formations outcropping within the study area	38
Figure 6.2-1.	Study well control	40
Figure 6.2-2.	Symbolic Venn diagram of geologic evaluation well control.....	43
Figure 6.5-1.	Modified geological formation outcrops with region codes	49
Figure 6.7-1.	Study area wells with aquifer hydraulic data	54
Figure 6.8-1.	Wilcox Group estimated total porosity versus depth plot.....	59
Figure 6.8-2.	Carrizo Sand estimated total porosity versus depth plot.....	59
Figure 6.8-3.	Queen City Sand estimated total porosity versus depth plot.....	60
Figure 6.8-4.	Wilcox Group estimated total porosity versus temperature plot.....	61
Figure 7-1.	Structural strike and dip cross-section name and location	82
Figure 7-2.	Aquifer salinity classes along structural dip cross-section X-X', Plate 7	83
Figure 7-3.	Aquifer salinity classes along structural dip cross-section Y-Y', Plate 8	84
Figure 7-4.	Aquifer salinity classes along structural dip cross-section Z-Z', Plate 9	85
Figure 7.1.2-1.	Wilcox Group top depth interpreted on a geophysical well log	88
Figure 7.1.2-2.	Wilcox Group bottom depth interpreted on a geophysical well log.....	89
Figure 7.1.2-3.	Wilcox Group top depth interpreted on a geophysical well log	90
Figure 7.1.2-4.	Wilcox Group bottom depth interpreted on a geophysical well log	91
Figure 7.1.3-1.	Wilcox Group top elevation surface	92
Figure 7.1.3-2.	Wilcox Group bottom elevation surface	93
Figure 7.1.3-3.	Wilcox Group top depth surface	94
Figure 7.1.3-4.	Wilcox Group bottom depth surface.....	95
Figure 7.1.3-5.	Wilcox Group thickness.....	96
Figure 7.1.4-1.	Wilcox Group net sand thickness	97
Figure 7.1.5-1.	Wilcox Group salinity classes.....	99
Figure 7.1.5-2.	Wilcox Group salinity classes and well control.....	100
Figure 7.1.5-3.	Wells with water quality data from the Simsboro Formation.....	101
Figure 7.1.7-1.	Wilcox Group hydraulic properties	104
Figure 7.2.2-1.	Carrizo Sand top depth interpreted on a geophysical well log	107
Figure 7.2.2-2.	Carrizo Sand bottom depth interpreted on a geophysical well log	108
Figure 7.2.2-3.	Carrizo Sand top depth interpreted on a geophysical well log	109
Figure 7.2.2-4.	Carrizo Sand bottom depth interpreted on a geophysical well log	110
Figure 7.2.3-1.	Carrizo Sand top elevation surface	111
Figure 7.2.3-2.	Carrizo Sand bottom elevation surface	112
Figure 7.2.3-3.	Carrizo Sand top depth surface	113
Figure 7.2.3-4.	Carrizo Sand bottom depth surface.....	114
Figure 7.2.3-5.	Carrizo Sand thickness.....	115
Figure 7.2.4-1.	Carrizo Sand net sand thickness	116
Figure 7.2.5-1.	Carrizo Sand salinity classes.....	118
Figure 7.2.5-2.	Carrizo Sand salinity classes and well control.....	119
Figure 7.2.7-1.	Hydraulic properties of the Carrizo Sand	122
Figure 7.3.2-1.	Reklaw Formation top and bottom depths interpreted on a log.....	124
Figure 7.3.2-2.	Reklaw Formation top and bottom depths interpreted on a log.....	125
Figure 7.3.3-1.	Reklaw Formation top elevation surface	127
Figure 7.3.3-2.	Reklaw Formation bottom elevation surface	128
Figure 7.3.3-3.	Reklaw Formation top depth surface	129
Figure 7.3.3-4.	Reklaw Formation bottom depth surface.....	130

Figure 7.3.3-5.	Reklaw Formation thickness.....	131
Figure 7.4.2-1.	Queen City Sand top depth interpreted on a well log.....	133
Figure 7.4.2-2.	Queen City Sand bottom depth interpreted on a well log.....	134
Figure 7.4.2-3.	Queen City Sand top depth interpreted on a well log.....	135
Figure 7.4.2-4.	Queen City Sand bottom depth interpreted on a well log.....	135
Figure 7.4.3-1.	Queen City Sand top elevation surface.....	137
Figure 7.4.3-2.	Queen City Sand bottom elevation surface.....	138
Figure 7.4.3-3.	Queen City Sand top depth surface.....	139
Figure 7.4.3-4.	Queen City Sand bottom depth surface.....	140
Figure 7.4.3-5.	Queen City Sand thickness.....	141
Figure 7.4.4-1.	Queen City Sand net sand thickness.....	142
Figure 7.4.5-1.	Queen City Sand salinity classes.....	144
Figure 7.4.5-2.	Queen City Sand salinity classes and well control.....	145
Figure 7.4.7-1.	Queen City Sand hydraulic properties.....	149
Figure 7.5.2-1.	Weches Formation top and bottom depths interpreted on a well log.....	151
Figure 7.5.2-2.	Weches Formation top and bottom depths interpreted on a well log.....	151
Figure 7.5.3-1.	Weches Formation top elevation surface.....	153
Figure 7.5.3-2.	Weches Formation bottom elevation surface.....	154
Figure 7.5.3-3.	Weches Formation top depth surface.....	155
Figure 7.5.3-4.	Weches Formation bottom depth surface.....	156
Figure 7.5.3-5.	Weches Formation thickness.....	157
Figure 7.6.2-1.	Sparta Sand top and bottom depths interpreted on a well log.....	159
Figure 7.6.2-2.	Sparta Sand top and bottom depths interpreted on a well log.....	160
Figure 7.6.3-1.	Sparta Sand top elevation surface.....	162
Figure 7.6.3-2.	Sparta Sand bottom elevation surface.....	163
Figure 7.6.3-3.	Sparta Sand top depth surface.....	164
Figure 7.6.3-4.	Sparta Sand bottom depth surface.....	165
Figure 7.6.3-5.	Sparta Sand thickness.....	166
Figure 7.6.4-1.	Sparta Sand net sand thickness.....	168
Figure 7.6.5-1.	Sparta Sand salinity classes.....	170
Figure 7.6.5-2.	Sparta Sand salinity classes and well control.....	171
Figure 7.6.7-1.	Sparta Sand hydraulic properties.....	174
Figure 7.7.2-1.	Cook Mountain Formation top depth interpreted on a well log.....	176
Figure 7.7.2-2.	Cook Mountain Formation bottom depth interpreted on a well log.....	177
Figure 7.7.2-3.	Cook Mountain Formation top depth interpreted on a well log.....	178
Figure 7.7.2-4.	Cook Mountain Formation bottom depth interpreted on a well log.....	179
Figure 7.7.3-1.	Cook Mountain Formation top elevation surface.....	180
Figure 7.7.3-2.	Cook Mountain Formation bottom elevation surface.....	181
Figure 7.7.3-3.	Cook Mountain Formation top depth surface.....	182
Figure 7.7.3-4.	Cook Mountain Formation bottom depth surface.....	183
Figure 7.7.3-5.	Cook Mountain Formation thickness.....	184
Figure 7.8.2-1.	Yegua Formation top depth interpreted on a geophysical well log.....	187
Figure 7.8.2-2.	Yegua Formation bottom depth interpreted on a geophysical well log.....	188
Figure 7.8.2-3.	Yegua Formation top depth interpreted on a geophysical well log.....	189
Figure 7.8.2-4.	Yegua Formation bottom depth interpreted on a geophysical well log.....	190
Figure 7.8.3-1.	Yegua Formation top elevation surface.....	191

Figure 7.8.3-2.	Yegua Formation bottom elevation surface.....	192
Figure 7.8.3-3.	Yegua Formation top depth surface.....	193
Figure 7.8.3-4.	Yegua Formation bottom depth surface.....	194
Figure 7.8.3-5.	Yegua Formation thickness.....	195
Figure 7.8.4-1.	Yegua Formation net sand thickness	196
Figure 7.8.5-1.	Yegua Formation salinity classes.....	198
Figure 7.8.5-2.	Yegua Formation salinity classes and well control.....	199
Figure 7.8.7-1.	Yegua Formation hydraulic properties	202
Figure 13.2-1.	Model Builder diagram of inputs for the Fishnet tool	229
Figure 13.2-2.	Grid cells assignment.....	230
Figure 13.2.2-1.	Model builder steps.....	232
Figure 13.2.3-1.	Sparta Aquifer GRID_ID cells 1254692 and 1256087.....	234
Figure 13.4.1-1.	BRACS Database table relationships.....	240
Figure 13.6.1-1.	Sample of point inputs to interpolate Sparta bottom elevation.....	260
Figure 13.6.1-2.	Iterative formation raster work flow	265
Figure 13.6.2-1.	Wilcox net sand rasters in the Yoakum Canyon area	270
Figure 13.6.2-2.	Iterative net sand raster work flow.....	275

List of Tables

Table 2-1.	Groundwater salinity classification.....	4
Table 4-1.	Cross-reference table for map identification number and city name.....	8
Table 4-2.	Cross-reference table for map identification number and public water supply	9
Table 4-3.	Cross-reference table for existing and recommended new desalination plants	16
Table 5-1.	Stratigraphic column showing sequence stratigraphy.....	19
Table 5-2.	Stratigraphic column showing aquifer nomenclature	20
Table 6.1-1.	Geological formation map-unit symbol labels for Figure 6.1-3.....	37
Table 6.2-1.	Study area well control and use.....	42
Table 6.4-1.	Summary of study area well control for geological formation net sand maps....	47
Table 6.5-1.	Regions 1 through 11 of the study area.....	48
Table 6.6.2-1.	Parameters of concern for desalination.....	52
Table 6.7-1.	Study area aquifer hydraulic property records	53
Table 6.8-1.	Summary of well control used for porosity versus depth correlations.....	55
Table 6.9.1-1.	Input parameters for the R _{WA} Minimum Method	63
Table 6.9.1-2.	Estimated total porosity for each study area geological formation.....	66
Table 6.9.1-4.	Wilcox Group groundwater quality data.....	69
Table 6.9.1-5.	Carrizo Sand groundwater quality data.....	70
Table 6.9.1-6.	Queen City Sand groundwater quality data	71
Table 6.9.1-7.	Sparta Sand groundwater quality data	72
Table 6.9.1-8.	Yegua Formation groundwater quality data	73
Table 7-1.	Structural cross-section plate number, name, and type.....	81
Table 7.1.1-1.	Wilcox Group well control data points.....	87
Table 7.1.6-1.	Total volume of in-place groundwater in the Wilcox Group.....	102
Table 7.1.7-1.	Hydraulic properties of the Wilcox Group	103
Table 7.2.1-1.	Carrizo Sand well control data points.....	105
Table 7.2.6-1.	Total volume of in-place groundwater in the Carrizo Sand.....	120

Table 7.2.7-1.	Hydraulic properties of the Carrizo Sand	121
Table 7.3.1-1.	Reklaw Formation well control data points	123
Table 7.4.1-1.	Queen City Sand well control data points.....	132
Table 7.4.6-1.	Total volume of in-place groundwater in the Queen City Sand	147
Table 7.4.7-1.	Hydraulic properties of the Queen City Sand	148
Table 7.5.1-1.	Weches Formation well control data points.....	150
Table 7.6.1-1.	Sparta Sand well control data points.....	158
Table 7.6.6-1.	Total volume of in-place groundwater in the Sparta Sand	172
Table 7.6.7-1.	Hydraulic properties of the Sparta Sand	173
Table 7.7.1-1.	Cook Mountain Formation well control data points	175
Table 7.8.1-1.	Yegua Formation well control data points.....	186
Table 7.8.6-1.	Total volume of in-place groundwater in the Yegua Formation.....	200
Table 7.8.7-1.	Hydraulic properties of the Yegua Formation	201
Table 13.1.1-1.	Groundwater volume of the Wilcox Group per county	218
Table 13.1.1-2.	Groundwater volume of the Wilcox Group per RWPA.....	219
Table 13.1.1-3.	Groundwater volume of the Wilcox Group per GMA.....	219
Table 13.1.1-4.	Groundwater volume of the Wilcox Group per GCD.....	220
Table 13.1.2-1.	Groundwater volume of the Carrizo Sand per county	221
Table 13.1.2-2.	Groundwater volume of the Carrizo Sand per RWPA.....	222
Table 13.1.2-3.	Groundwater volume of the Carrizo Sand per GMA.....	222
Table 13.1.2-4.	Groundwater volume of the Carrizo Sand per GCD.....	223
Table 13.1.3-1.	Groundwater volume of the Queen City Sand per county	223
Table 13.1.3-2.	Groundwater volume of the Queen City Sand per RWPA	224
Table 13.1.3-3.	Groundwater volume of the Queen City Sand per GMA	224
Table 13.1.3-4.	Groundwater volume of the Queen City Sand per GCD	225
Table 13.1.4-1.	Groundwater volume of the Sparta Sand per county	225
Table 13.1.4-2.	Groundwater volume of the Sparta Sand per RWPA	226
Table 13.1.4-3.	Groundwater volume of the Sparta Sand per GMA.....	226
Table 13.1.4-4.	Groundwater volume of the Sparta Sand per GCD	226
Table 13.1.5-1.	Groundwater volume of the Yegua Formation per county	227
Table 13.1.5-2.	Groundwater volume of the Yegua Formation per RWPA	227
Table 13.1.5-3.	Groundwater volume of the Yegua Formation per GMA.....	227
Table 13.1.5-4.	Groundwater volume of the Yegua Formation per GCD.....	228
Table 13.2.3-1.	Aquifer specific yield values	233
Table 13.5.1-1.	GIS filename codes applied to the study.....	245
Table 13.5.2-1.	GIS files for regional geology.....	247
Table 13.5.2-2.	GIS files for the lithologic analysis	249
Table 13.5.2-3.	GIS files for geological formation salinity class.....	250
Table 13.5.2-4.	GIS files for geologic formation surfaces.....	251
Table 13.5.2-5.	Study support GIS files.....	254
Table 13.5.2-6.	Geological formation groundwater volume files	256
Table 13.6.1-1.	Minimum, maximum, and mean offsets: raster and stratigraphic pick.....	266
Table 13.6.2-1.	Minimum, maximum, and mean differences: raster and net sand pick	273

1. Executive summary

Estimated at more than 2.7 billion acre-feet, brackish groundwater (water with total dissolved solids concentrations of 1,000 to 10,000 milligrams per liter) with the appropriate treatment (desalination) constitutes an important water supply option in Texas. However, one of the more challenging issues that may limit the potential for future development is the scarcity of detailed geological characterization for the brackish sections of Texas Water Development Board (TWDB) designated major and minor aquifers.

We selected the aquifers of the Upper Coastal Plains in the Central Texas region as a study area because of the anticipated need for additional brackish groundwater in the region. These aquifers include, from oldest to youngest, the Wilcox, Carrizo, Queen City, Sparta, and Yegua. We evaluated each of these stacked aquifers in one study due to the economy of scale when collecting and interpreting data and conducting Geographic Information System (GIS) analysis.

The study area encompasses parts of Atascosa, Bastrop, Bexar, Caldwell, Dewitt, Fayette, Gonzales, Guadalupe, Karnes, Lavaca, Lee, Live Oak, Williamson, and Wilson counties. It includes parts of regional water planning areas G, K, L, N, and P. Parts of the study area lie within nine groundwater conservation districts. The aquifers in the study area underlie an area of about 5,900 square miles.

For the project, we collected, analyzed, and interpreted thousands of water well logs and geophysical well logs to map the geologic units and establish stratigraphic relationships. We also gathered water chemistry, water level, and aquifer test data from a wide variety of sources to characterize groundwater in the five aquifers. From this information, we mapped salinity classes that are three-dimensional regions within the aquifers containing groundwater of a similar salinity range: fresh groundwater (0 to 999 milligrams per liter total dissolved solids), slightly saline groundwater (1,000 to 2,999 milligrams per liter total dissolved solids), moderately saline groundwater (3,000 to 9,999 milligrams per liter total dissolved solids), very saline groundwater (10,000 to 34,999 milligrams per liter total dissolved solids), brine (greater than 35,000 milligrams per liter total dissolved solids), or some mixture of two or more salinity classes.

We calculated the volume of brackish groundwater in the study area. Even with a perfectly designed well field, not all of the brackish groundwater can be produced or be economically developed, but the estimates provide an indication of the potential availability of this important resource. Within the study area, the Wilcox Group contains 112 million acre-feet of in-place brackish groundwater with additional significant brackish water in mixed classes (classes containing a mixture of two or more salinities in areas that cannot be easily subdivided horizontally and/or vertically). The Carrizo Sand contains more than 57 million acre-feet of in-place brackish groundwater with additional significant brackish water in mixed classes. The Queen City Sand contains more than 20 million acre-feet of in-place brackish groundwater with additional significant brackish water in mixed classes. The Sparta Sand contains more than 6 million acre-feet of in-place brackish groundwater. The Yegua Formation contains more than 42 million acre-feet of in-place brackish groundwater with additional significant brackish water in mixed classes.

The Carrizo-Wilcox Aquifer, one of the state's major aquifers, is the principal source of groundwater in the region. Six entities in the 2012 State Water Plan and five entities in the 2017 State Water Plan recommended brackish groundwater desalination using the Carrizo-Wilcox

Aquifer as a water management strategy. There is also interest from other public water suppliers in the region. There is one operating desalination plant in the study area located at the San Antonio Water System's H₂Oaks Center in southern Bexar County. The desalination plant produces lower Wilcox Group brackish groundwater from 12 production wells and uses two Class I injection wells for concentrate disposal into the saline Edwards Formation. Phase 1 of this plant became operational in 2017 and provides 12 million gallons per day of desalinated groundwater. Phase 2 will produce an additional 12 million gallons per day by 2021, and Phase 3 will add another 6 million gallons per day by 2026 for a total production goal of 30 million gallons per day.

Two out of the five regional water planning areas within the study area (regions L and N) included groundwater desalination as a recommended water management strategy in the 2017 State Water Plan. If water user groups implemented these 10 recommended water strategies and the four associated projects, desalination would produce about 8,400 acre-feet per year of new water supplies by 2070. A water management strategy is a plan to meet a water need, whereas a project is the infrastructure required to implement the strategy. Additionally, there are two recommended water management strategies in region L not currently assigned to serve a specific water user group.

This aquifer study generated new interpretation techniques, data, and maps for detailed regional stratigraphy, new or reaffirmed aquifer assignments for existing wells, four-tier lithology intervals and net sands, and groundwater salinity calculations and classes. All the results of this analysis are contained in the database, GIS datasets, and raw well records assembled for this study. These records and files contain a wealth of groundwater data useful to water planners for site selection and evaluation. The report can be used to evaluate potential sites for brackish groundwater production well fields. However, information produced from the study is not intended to serve as a substitute for desalination plant well field characterization using test well drilling and groundwater modeling of aquifer conditions.

2. Introduction

A 2003 TWDB-funded study (LBG-Guyton Associates, 2003) provided an estimate of the total volume of brackish groundwater in the state. However, the study was by design regional in scope, limited in areal extent, and narrow in its assessment of groundwater quality. To improve on the 2003 study, the TWDB requested and received funding from the 81st Texas Legislature (2009) to implement the Brackish Resources Aquifer Characterization System (BRACS) program to more thoroughly characterize the brackish aquifers for the purpose of aiding in the exploration and development of brackish groundwater resources and providing a basis for site-specific studies. The 83rd, 84th, and 86th Texas Legislatures (2013, 2015, and 2019) provided additional funding to increase the number of TWDB staff assigned to this program. The 84th Texas Legislature approved House Bill 30 that instructed the TWDB to map brackish groundwater production zones in Texas aquifers by December 1, 2022. The 86th Texas Legislature extended this deadline to December 1, 2032, and passed House Bill 722 creating a framework for permitting brackish groundwater production within designated brackish groundwater production zones located in groundwater conservation districts.

The goals of the BRACS program are to (1) map and characterize the brackish parts of the major and minor aquifers of the state in greater detail using existing water well reports, geophysical well logs, and available aquifer data; (2) build datasets that can be used for groundwater exploration; and (3) provide data for replicable numerical groundwater flow models. The objective of this study is to map the brackish groundwater resources of the Wilcox, Carrizo, Queen City, Sparta, and Yegua aquifers in Central Texas. Volumes of brackish water resources were calculated to aid in the identification of potential brackish groundwater production zones and should not be used for regional planning of desired future conditions, which instead relies on volumes of total estimated recoverable storage (TERS) as determined by the TWDB Groundwater Availability Modeling program (Wade and Bradley, 2013; Wade and Shi, 2014).

Groundwater contains dissolved minerals, is measured in units of milligrams per liter total dissolved solids, and is classified in five categories by Winslow and Kister (1956). The same groundwater salinity classification was used in the LBG-Guyton (2003) study and in previous studies completed in the TWDB's BRACS program (Meyer and others, 2014). We modified the Winslow and Kister classification by adding mixed salinity classes where salinity variability precluded mapping a single class (Table 2-1).

Table 2-1. Groundwater salinity classification used in the study. This table was modified from Winslow and Kister (1956) with the addition of mixed salinity classes. Salinity class codes are used in report tables, the BRACS Database, and the GIS file-naming scheme (Section 13.5.1). Colors used in this table for each salinity classification are consistent throughout the report and GIS datasets.

Groundwater salinity classification	Salinity class code	Total dissolved solids concentration (milligrams per liter)
Fresh	Fr	0 to 999
Fresh and slightly saline	Fr-Ss	0 to 999 and 1,000 to 2,999
Fresh, slightly, and moderately Saline	Fr-Ss-Ms	0 to 999; 1,000 to 2,999; and 3,000 to 9,999
Slightly saline	Ss	1,000 to 2,999
Slightly and moderately saline	Ss-Ms	1,000 to 2,999 and 3,000 to 9,999
Slightly, moderately, and very saline	Ss-Ms-Vs	1,000 to 2,999; 3,000 to 9,999; and 10,000 to 34,999
Moderately saline	Ms	3,000 to 9,999
Moderately and very saline	Ms-Vs	3,000 to 9,999 and 10,000 to 34,999
Moderately, very saline, and brine	Ms-Vs-Br	3,000 to 9,999; 10,000 to 34,999; and greater than 35,000
Very saline	Vs	10,000 to 34,999
Very saline and brine	Vs-Br	10,000 to 34,999 and greater than 35,000
Brine	Br	Greater than 35,000

To place the salinity classification into context, 1,000 milligrams per liter of total dissolved solids is a secondary water quality limit set by the Texas Commission on Environmental Quality for public water systems (TCEQ, 2015). The Underground Source of Drinking Water is defined as an aquifer with less than 10,000 milligrams per liter total dissolved solids and is therefore ineligible for disposal of wastewater by injection without an aquifer exemption from the U.S. Environmental Protection Agency. The Railroad Commission of Texas defines Base of Useable Quality (BUQ) water generally at 3,000 milligrams per liter total dissolved solids for protection of aquifers with oil and gas well cemented surface casing. Brackish groundwater in Texas is not defined by statute but is considered 1,000 to 10,000 milligrams per liter total dissolved solids. Finally, for additional context, seawater has approximately 35,000 milligrams per liter of total dissolved solids (Hem, 1985).

For the study, we collected more than 8,100 well records for geologic, water chemistry, water level, and aquifer test data from a wide variety of sources to characterize groundwater in the study area aquifers. From this information, we interpreted and mapped geological formation stratigraphy, lithology, and salinity classes. Salinity classes are three-dimensional regions within the aquifer containing groundwater of a similar salinity. Areas with variable salinity within an aquifer were mapped as mixed salinity classes. Examples include well clusters where individual wells exhibit more than one salinity class within a geological formation or closely spaced wells exhibit different salinity classes.

We calculated the volume of in-place groundwater in the Wilcox, Carrizo, Queen City, Sparta, and Yegua aquifers based on salinity classes, percent sand, and specific yield. We did not attempt to determine the volume of confined storage; the amount of water derived from confined storage would represent less than 1 percent of the total volume. These values are based on total groundwater in place, however not all this brackish groundwater can be produced or is economic to develop. All the aquifers except the Sparta contain areas of mixed salinity classes. There are significant brackish groundwater resources in these mixed classes.

Information contained in the report is not intended to serve as a substitute for more localized well field characterization of aquifer conditions. The next logical step will be to study potential well field sites in greater detail, targeting individual sands or zones, identifying lateral and vertical distribution and connectivity, identifying facies and structural faulting, and assessing source water. If an initial site assessment indicates feasibility, test well drilling and logging, aquifer analysis, and aquifer modeling should be conducted to prove water quality and quantity. Capacity and availability of the brackish groundwater resources in the study area will need to be determined during well field design and development using test, monitor, and production wells and groundwater modeling. Existing TWDB regional groundwater models are designed for regional assessment and are not suitable for localized well field analysis. Regional models were not constructed to analyze the effect of salinity on groundwater flow and in general should not be used for estimating withdrawal of brackish groundwater. Groundwater quantity and quality changes, potential subsidence, and sustainability are significant factors that must be evaluated before developing brackish groundwater.

3. Project deliverables

This report contains a discussion of methodology and conclusions and is available for download from the TWDB website (www.twdb.texas.gov/). In addition, this report contains sections describing data collection, previous investigations, hydrogeologic setting, aquifer determination, aquifer hydraulic properties, groundwater chemistry, net sand analysis, geophysical well log interpretation, groundwater salinity classes, groundwater volume methodology, desalination concentrate disposal, and study deliverables.

An equally important objective is to make the information and datasets gathered for the study readily available to the public. Thus, all information collected is non-confidential. The information includes raw data such as water well reports and digital geophysical well logs, processed data such as lithology, simplified lithologic descriptions, stratigraphic picks, aquifer water chemistry and salinity analysis, and interpreted results in the form of GIS datasets. The BRACS Database and BRACS Database Data Dictionary (Meyer, 2020) and all GIS datasets are available for download from the TWDB BRACS website (www.twdb.texas.gov/innovativewater/bracs/). Geophysical well logs are available upon request or can be downloaded from the TWDB Water Data Interactive web viewer (www3.twdb.texas.gov/apps/waterdatainteractive/).

4. Study area

The study area encompasses parts of 14 counties (Atascosa, Bastrop, Bexar, Caldwell, Dewitt, Fayette, Gonzales, Guadalupe, Karnes, Lavaca, Lee, Live Oak, Williamson, and Wilson) that are underlain by the study aquifers (Figure 4-1).

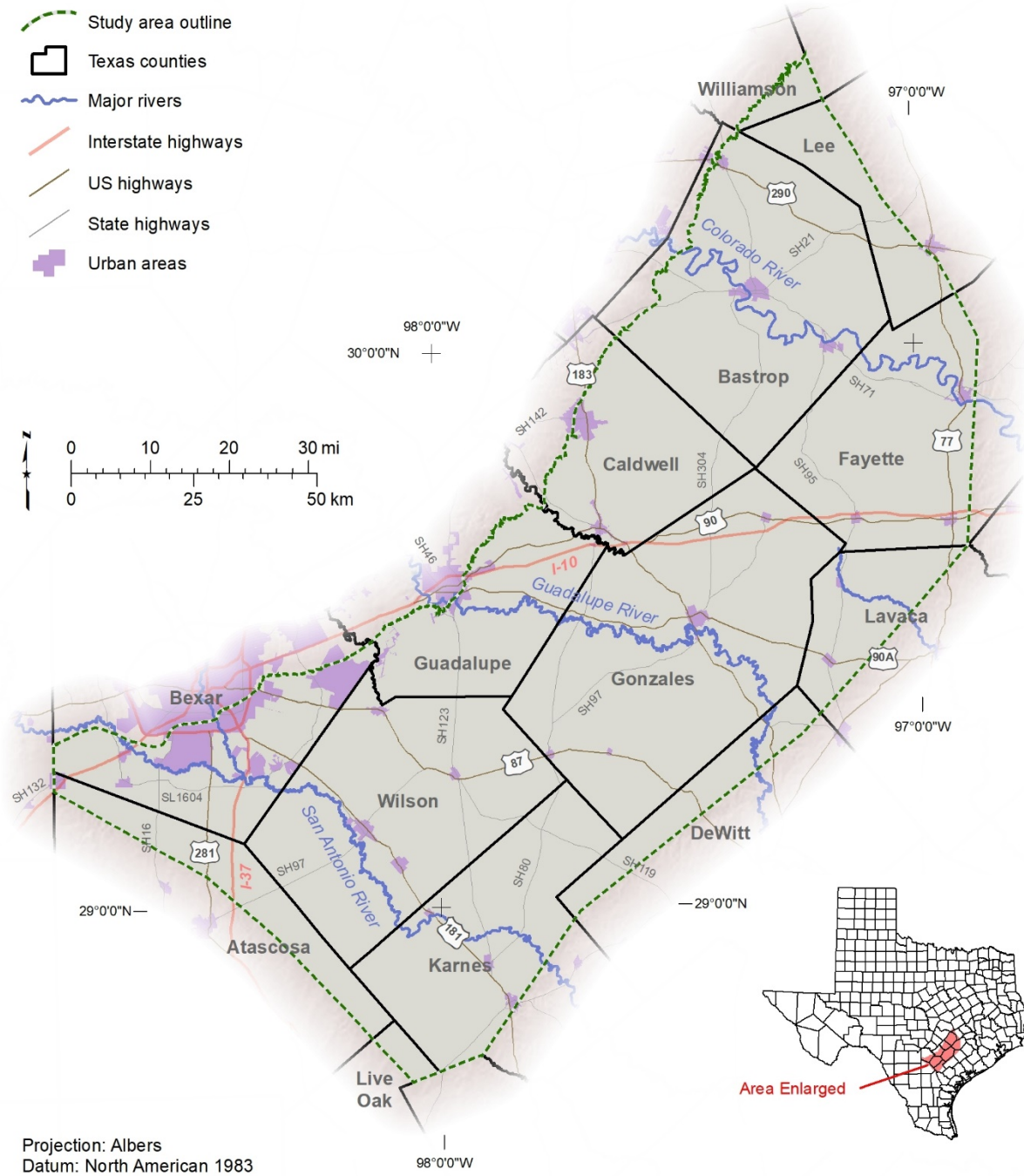


Figure 4-1. Study area location map.

Cities and the boundaries of the larger public water supply systems in the study area are presented in Figures 4-2 through 4-5. A cross-reference between the city name and map identification number used on the figures is provided in Table 4-1. A cross-reference between the public water supply system name, map identification number, and public water supply identification number assigned by the Texas Commission on Environmental Quality is provided in Table 4-2. The public water supply name or identification number can be used to query public water system information from the Texas Commission Environmental Quality website using the Drinking Water Watch (dww2.tceq.texas.gov/DWW/).

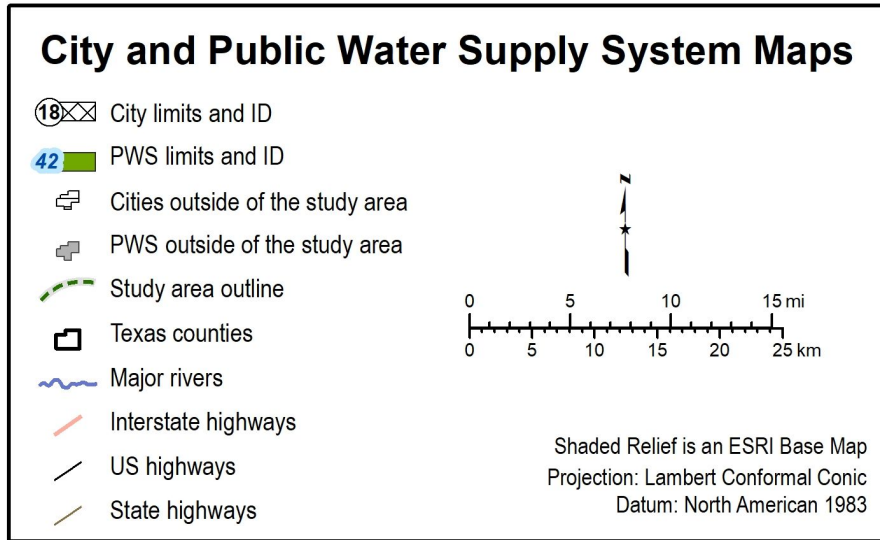








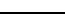
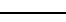



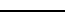
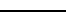







































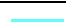

























Figure 4-2. Map legend for Figures 4-3 through 4-5. ID = identification number, PWS = public water supply system. Source of the water system boundaries is a 2011 study contracted by the TWDB (HDR Engineering, 2011) using 2010 data. Not all public water supply systems are present in this dataset, and water system boundaries may have changed since this project was completed. The location and name of cities are from a dataset provided by Texas Department of Transportation in 2014.

Table 4-1. Cross-reference table between the map identification (ID) number and the city name used in Figures 4-3 through 4-5.

Map ID	City name	Map ID	City name	Map ID	City name
1	Bastrop	12	La Grange	23	Schulenburg
2	China Grove	13	La Vernia	24	Seguin
3	Elgin	14	Lockhart	25	Shiner
4	Elmendorf	15	Luling	26	Smiley
5	Falls City	16	Lytle	27	Smithville
6	Flatonia	17	Moulton	28	Somerset
7	Floresville	18	New Berlin	29	Stockdale
8	Giddings	19	Nixon	30	Von Ormy
9	Gonzales	20	Poth	31	Waelder
10	Karnes City	21	Saint Hedwig		
11	Kenedy	22	San Antonio		

Table 4-2. Cross-reference table relating the map identification number (ID) and public water supply system (PWS) name, and PWS identification number (PWD ID) used in Figures 4-3 through 4-5. The Texas Commission on Environmental Quality official PWS name and PWS ID are used in this table.

Symbol	Map ID	PWS ID	PWS name	Symbol	Map ID	PWS ID	PWS name
	1	0110013	Aqua WSC		41	0150082	East Central SUD Palm Park Water
	2	2470025	Arrowhead WS		42	1630010	East Medina County SUD unit 1
	3	0150040	Atascosa Rural WSC		43	1280007	El Oso WSC
	4	0110049	Bastrop County MUD 1		44	0070018	Fashing Peggy WSC
	5	0110014	Bastrop County WCID 1		45	0750009	Fayette County WCID Monument Hill
	6	0110020	Bastrop County WCID 2		46	0750034	Fayette WSC East
	7	0110047	Bastrop West Water Supply		47	0750022	Fayette WSC West
	8	1630034	Benton City WSC		48	0890006	Gonzales County WSC
	9	2470019	C Willow Water Co		49	0940020	Green Valley SUD
	10	0750008	Cistern Water Well Company		50	0110045	K & K Water Company
	11	0110001	City of Bastrop		51	0940029	Lago Vista WS
	12	0110002	City of Elgin		52	2470020	Lake Valley Water Company
	13	0150048	City of Elmendorf		53	1440005	Lee County WSC
	14	1280004	City of Falls City		54	1440006	Lincoln WSC
	15	0750002	City of Flatonia		55	2270033	Manville WSC
	16	2470001	City of Floresville		56	0280003	Maxwell WSC
	17	1440001	City of Giddings		57	0070023	McCoy WSC
	18	0890001	City of Gonzales		58	2470023	Moss Woods Subdivision WS
	19	1280001	City of Karnes City		59	0150486	Nico Tyme Water Co-Op
	20	1280002	City of Kenedy		60	0940085	Oak Hills Ranch Water
	21	0750003	City of La Grange		61	2470009	Oak Hills WSC
	22	2470004	City of La Vernia		62	0890024	Ottine WSC
	23	0280001	City of Lockhart		63	2470026	Picosa WSC
	24	0280002	City of Luling		64	0280007	Polonia WSC North
	25	0070004	City of Lytle		65	0280020	Polonia WSC South
	26	1430002	City of Moulton		66	2470015	S S WSC
	27	0890002	City of Nixon		67	0150018	San Antonio WS
	28	2470002	City of Poth		68	0150171	San Antonio WS North West
	29	0750004	City of Schulenburg		69	0150249	San Antonio WS Southside
	30	0940002	City of Seguin		70	2470016	Seven Oaks Water Supply
	31	1430003	City of Shiner		71	2470017	Shady Oaks Water Company
	32	0890004	City of Smiley		72	1660015	Southwest Milam WSC
	33	0110003	City of Smithville		73	0940022	Springs Hill WSC
	34	2470003	City of Stockdale		74	0940017	Staples Farmers Corp

Symbol	Map ID	PWS ID	PWS name	Symbol	Map ID	PWS ID	PWS name
	35	0890003	City of Waelder		75	2470005	Sunko WSC
	36	2470021	Creekwood Estates		76	2470007	Three Oaks WSC
	37	0940015	Crystal Clear WSC		77	0280012	Tri Community WSC
	38	0280005	Dale WSC		78	0750039	Vista Ranch WS
	39	2470022	Eagle Creek Ranch		79	1440014	Westwood Villa Apartments
	40	0150138	East Central SUD				

Notes:

Co = Company

Co-Op = Cooperative

Corp = Corporation

SUD = Special Utility District

WCID = Water Control and Improvement District

WS = Water Supply

WSC = Water Supply Corporation

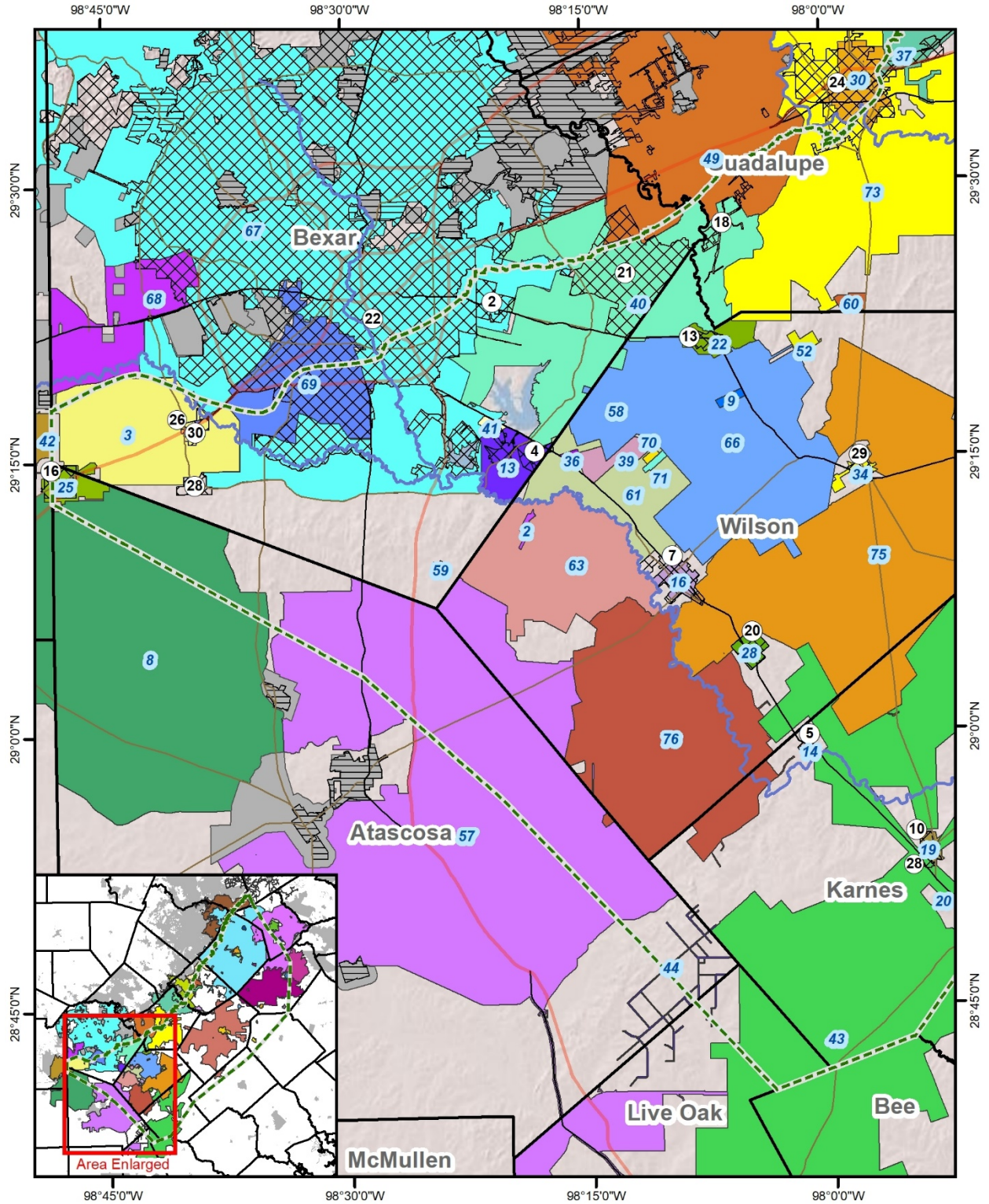


Figure 4-3. City and public water supply system limits in the western part of the study area. Figure 4-2 is the legend for this map. Table 4-1 is a cross-reference of city map numbers and names. Table 4-2 is a cross-reference of public water system map numbers and names.

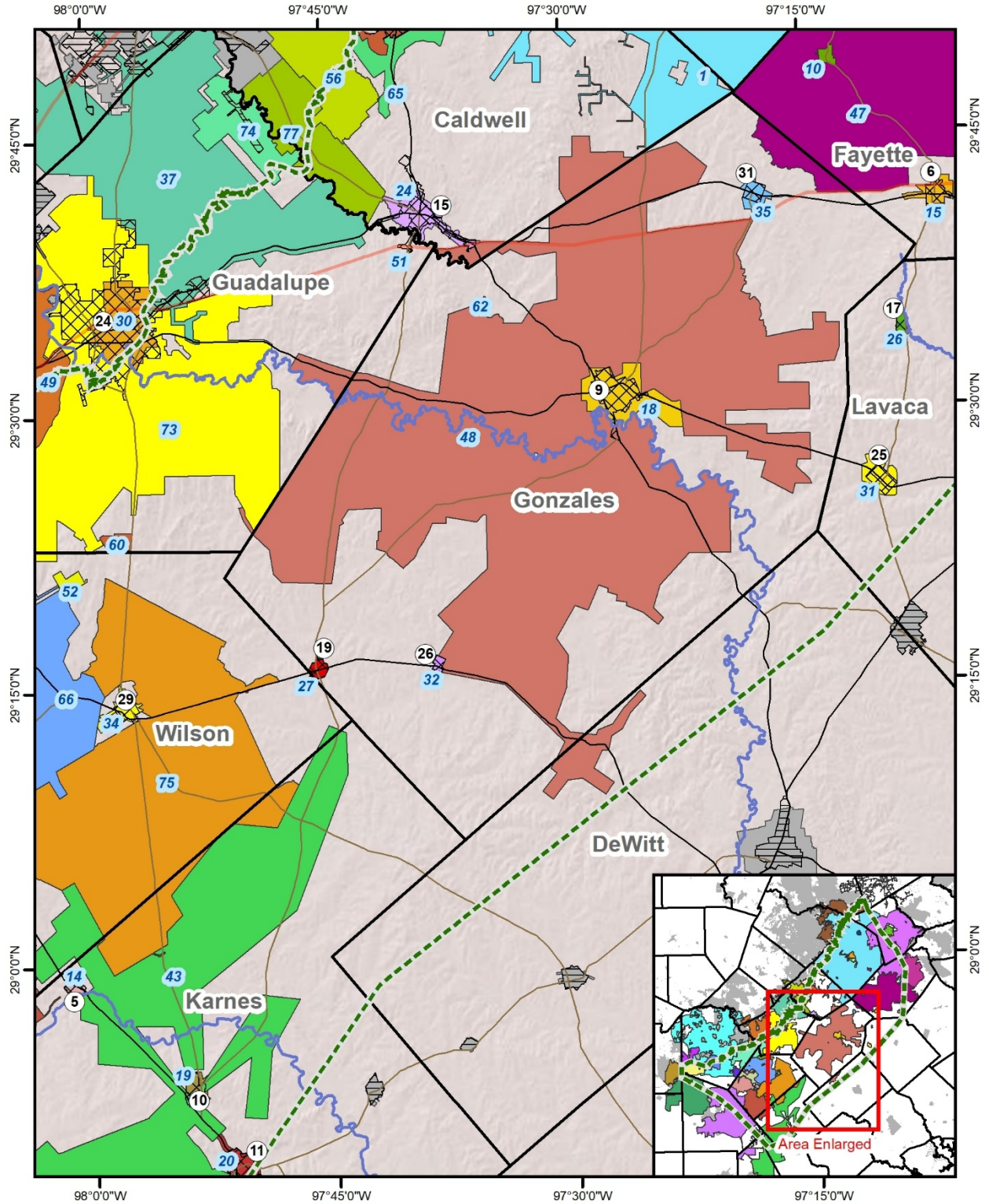


Figure 4-4. City and public water supply system limits in the central part of the study area. Figure 4-2 is the legend for this map. Table 4-1 is a cross-reference of city map numbers and names. Table 4-2 is a cross-reference of public water system map numbers and names.

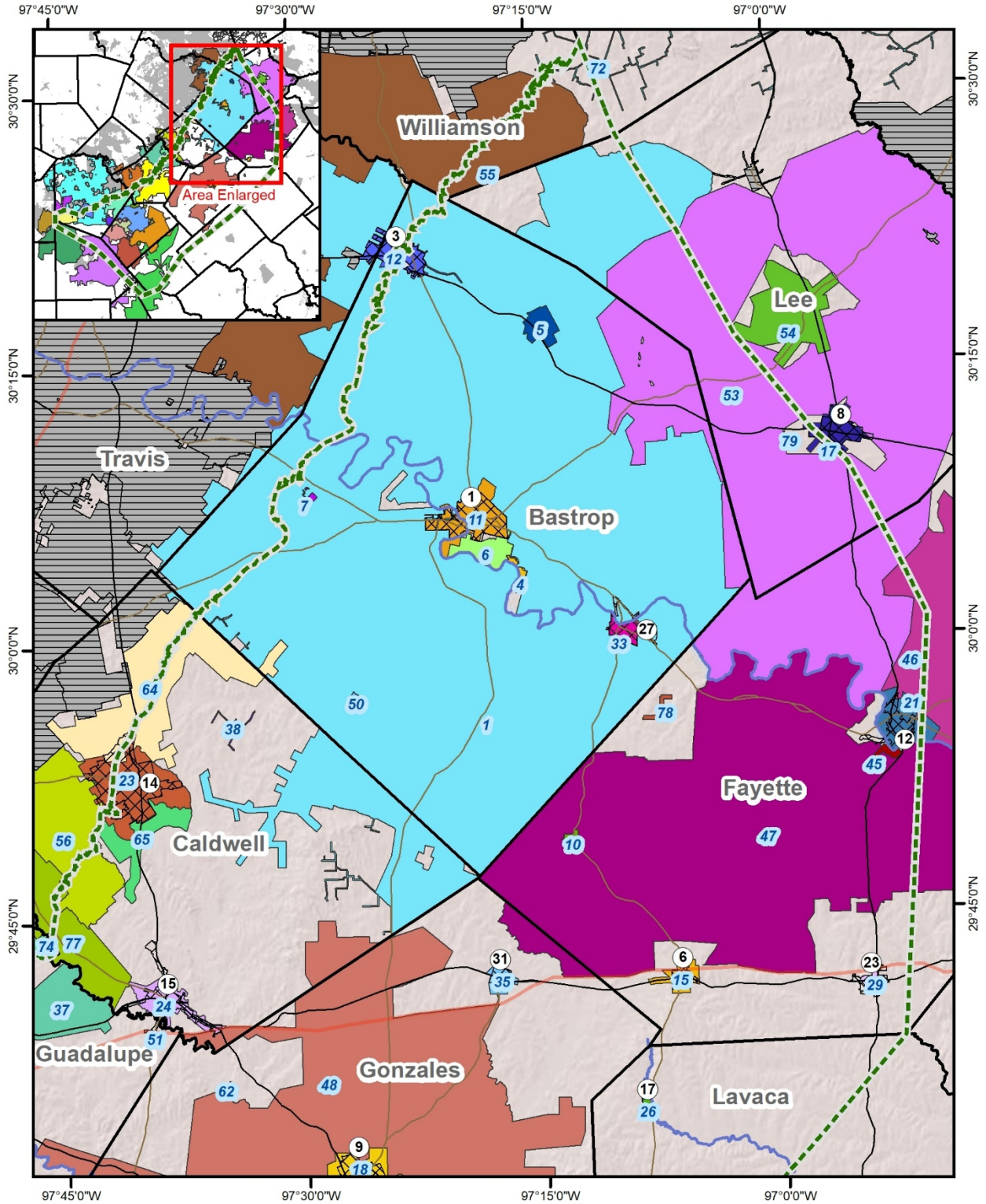


Figure 4-5. City and public water supply system limits in the eastern part of the study area. Figure 4-2 is the legend for this map. Table 4-1 is a cross-reference of city map numbers and names. Table 4-2 is a cross-reference of public water system map numbers and names.

The study area lies within parts of five Regional Water Planning Areas (G, K, L, N, and P) and six Groundwater Management Areas (8, 10, 12, 13, 15, and 16) (Figure 4-6). The southeastern boundaries of Groundwater Management Areas 8 and 10 are based on the official TWDB aquifer boundary shapefiles whereas the northwestern boundary of our study area is based on the digitized version of the updip extent of the Wilcox Group from the Geologic Atlas of Texas (TWDB, 2007b). Volumes were not estimated for Groundwater Management Areas 8 and 10 since only small tracts overlap with the study area, due to discrepancies in the extent of the Wilcox Group outcrop. The study area contains parts of nine groundwater conservation districts: Edwards Aquifer Authority, Evergreen Underground Water Conservation District, Fayette County Groundwater Conservation District, Gonzales County Underground Water Conservation District, Guadalupe County Groundwater Conservation District, Live Oak Underground Water Conservation District, Lost Pines Groundwater Conservation District, Pecan Valley Groundwater Conservation District, and Plum Creek Conservation District (Figure 4-6).

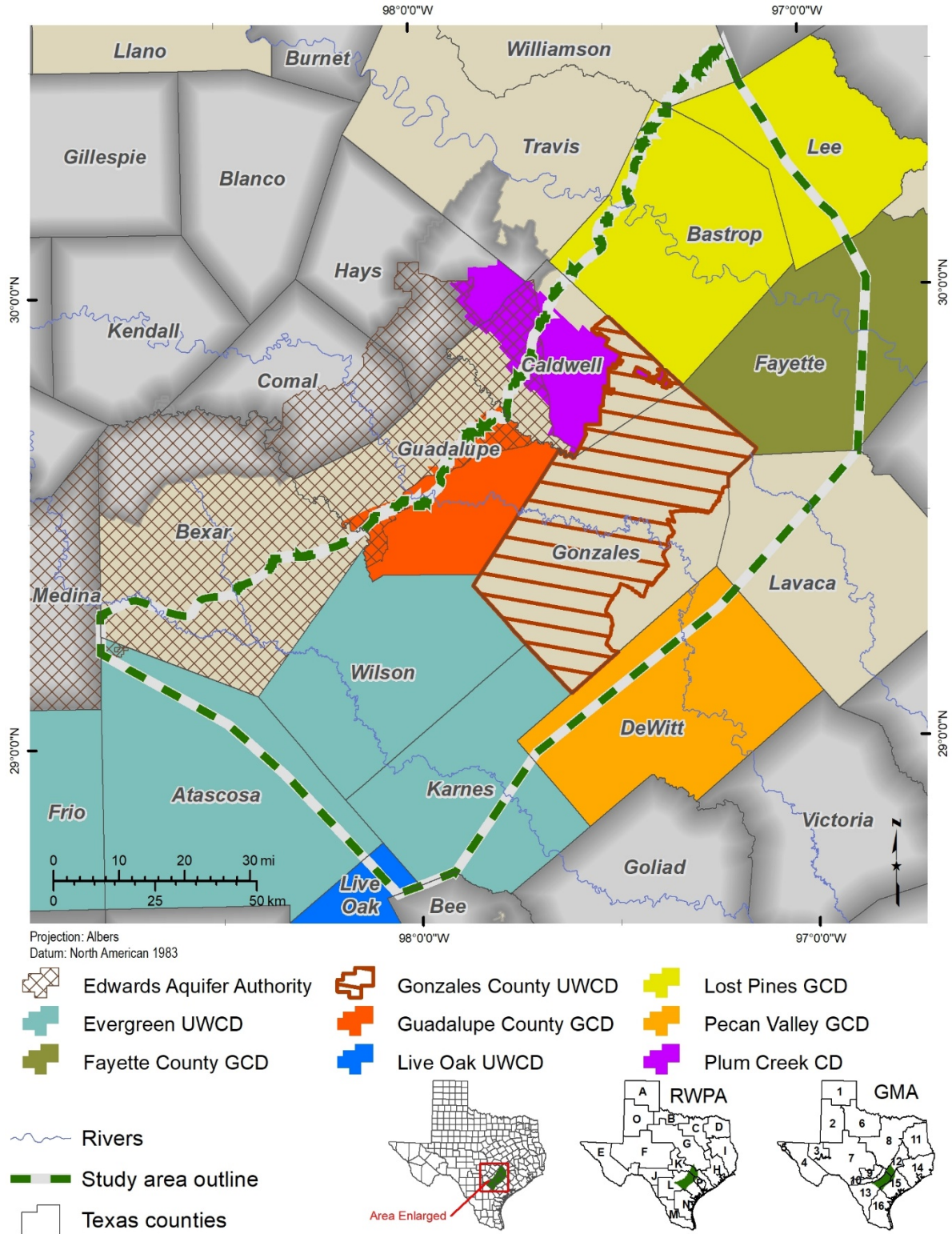


Figure 4-6. Administrative boundaries within the study area encompass groundwater conservation districts (GCDs), Groundwater Management Areas (GMAs), and Regional Water Planning Areas (RWPAs). CD = conservation district, UWCD = underground water conservation district.

The study area presently contains one municipal brackish groundwater desalination plant (Figure 4-7; Table 4-3) and four desalination projects in the 2017 State Water Plan (TWDB, 2017). The municipal desalination plant is owned by the San Antonio Water System. It treats brackish groundwater from the lower Wilcox Aquifer. The San Antonio Water System plant is being constructed in three phases with estimated production capacity and completion dates of: Phase 1, 12 million gallons per day, October 2016; Phase 2, 12 million gallons per day, 2021; and Phase 3, 6 million gallons per day, 2026 for a total production of 30 million gallons per day (Shirazi, 2015, personal communication).

The four desalination projects from the 2017 State Water Plan are Canyon Regional Water Authority, San Antonio Water System (an expanded brackish project in Wilson County), Schertz-Seguin Local Government Corporation, and SS Water Supply Corporation. In 2070, brackish groundwater desalination is expected to provide 111,000 acre-feet per year (1.3 percent of the recommended water management strategies) of new water to the region.

Additionally, the City of Kenedy municipal desalination plant is just outside of the study area and treats brackish groundwater from the Gulf Coast Aquifer.

Table 4-3. Cross-reference table relating the map identification number (ID) and existing and recommended new desalination plants from the 2017 State Water Plan mapped in Figure 4-7. The City of Kenedy plant is adjacent to the study area and produces from the Gulf Coast Aquifer.

Map ID	Name	Source
A	City of Kenedy	brackish Gulf Coast Aquifer
B	San Antonio Water System, H2Oaks Center	brackish Wilcox Aquifer
1	Canyon Regional Water Authority	brackish Wilcox Aquifer
2	SS Water Supply Corporation	brackish Wilcox Aquifer
3	Schertz-Seguin Local Government Corporation	brackish Wilcox Aquifer
4	San Antonio Water System, expanded	brackish Wilcox Aquifer

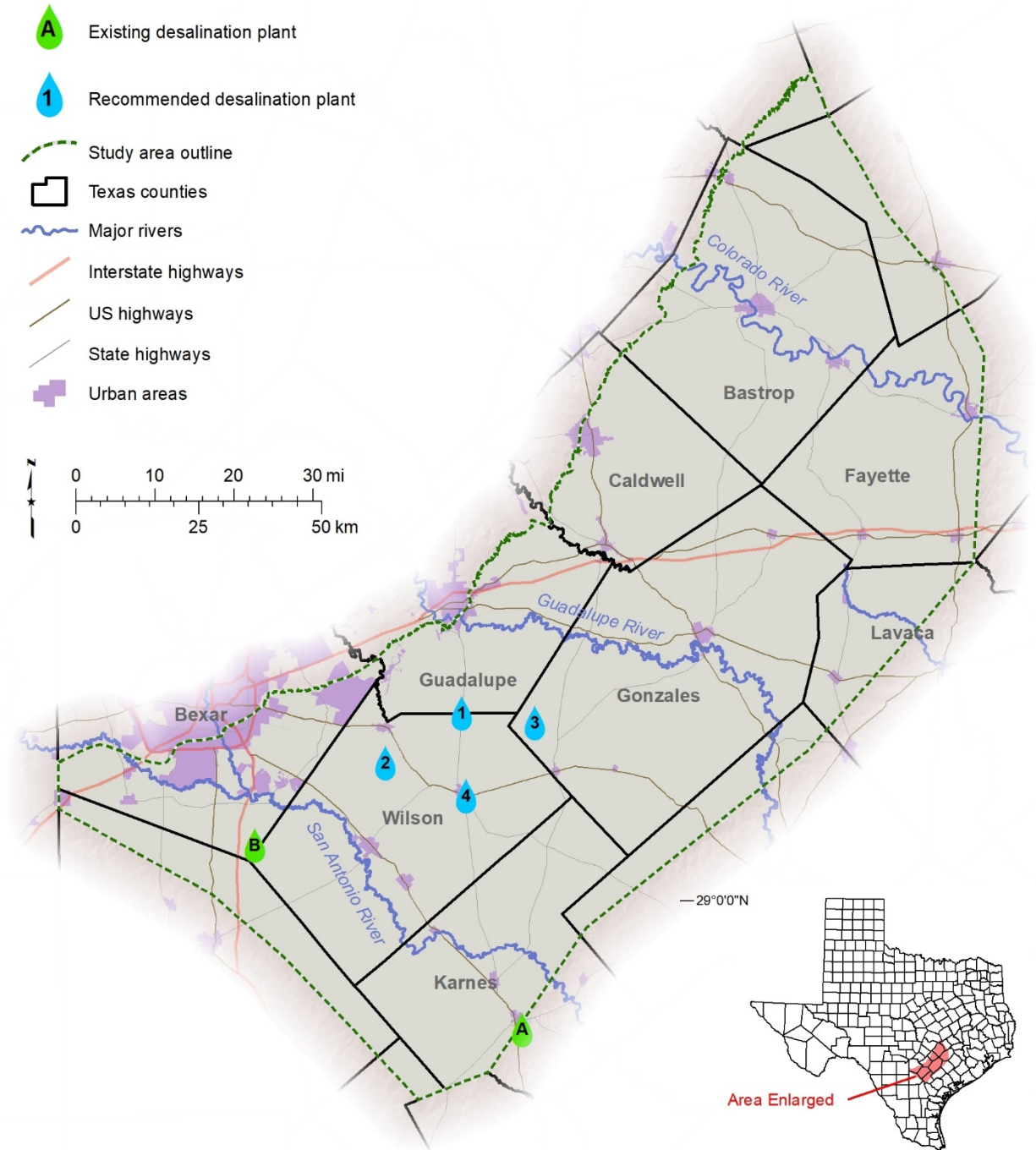


Figure 4-7. Existing and recommended brackish groundwater desalination plants used for public water supply in and near the study area. Table 4-3 is a cross-reference of plant map identification label, name, and source.

5. Geologic setting

Aquifers within the Upper Coastal Plains consist of a large swath of sedimentary rocks that span Texas, from the southwest border with the Republic of Mexico to the northeast border with the states of Arkansas and Louisiana. The TWDB designated aquifers within the study area include the Carrizo-Wilcox, Queen City, Sparta, Yegua-Jackson, and Brazos River Alluvium (Davidson and others, 2009; George and others, 2011). These aquifers underlie approximately 5,900 square miles in the study area. The U.S. Geological Survey publications refer to these aquifers as the Texas coastal uplands aquifer system (Ryder, 1996). Geological formations within the study area generally strike sub-parallel to the current coast and dip in wedges that thicken toward the Gulf of Mexico (Galloway and other, 2000).

The primary focus of this study was the Carrizo-Wilcox Aquifer, the source of brackish groundwater for the current desalination plant (San Antonio Water System, H₂Oaks Center) and several future desalination projects in Central Texas. We also included the overlying Queen City, Sparta, and Yegua aquifers and the Reklaw, Weches, and Cook Mountain aquitards because there is an economy of scale when evaluating several stacked aquifers in a study area.

5.1 Stratigraphy, lithology, and depositional environments

We prepared Table 5-1 showing the stratigraphic relationship between the geologic units, their age, systems tracts, and unconformities from the Wheeler Chart prepared by Brown and Loucks (2009). The Wheeler Chart scratches the surface of incredible complexity reflected in the Paleocene and Eocene geologic record in the Gulf of Mexico Basin. The objective of this study is the characterization of brackish groundwater in these aquifers, not systematic stratigraphic mapping. However, linking the study area aquifers into the sequence stratigraphic construct explains some of the interesting relationships between these geologic units and offers insight into the problems associated with lithostratigraphic mapping of geologic units using geophysical well logs (Table 5-2).

Table 5-1. Stratigraphic column with systems tracts, age, and unconformities (modified from Brown and Loucks, 2009). Age of surface is in millions of years before present (MA) and applies to the line below the number. Note the decision to limit age assignments based on Lawless and others (1997). Maximum flooding surface (MFS) and unconformity (T1, T2, TS) labels apply to the line below the label. This table does not reflect the entire Jackson or Midway group stratigraphy. This table is not scaled vertically in uniform units of time.

Epoch	Group	Formation	Member	Systems tracts	Age (MA)	MFS	Unconformity	
Eocene	Jackson	Caddell		HST	38.7	MFS		
		Moodys Branch		TST	39.0		TS	
	Claiborne	Hiatus		LST	40.0		T1	
		Yegua		HST	41.3	MFS		
		Cook Mountain		TST	42.3		TS	
		Hiatus		LST	43.6		T1	
		Sparta		HST	44.5	MFS		
		Weches		TST	45.0		TS	
		Hiatus		LST	46.5		T1	
		Queen City		HST	47.6	MFS		
		Reklaw		TST				
		Hiatus			48.5		T1	
				HST	48.8	MFS		
				TST	49.1		TS	
				LST	49.5		T1	
	Wilcox	Carrizo		HST				
			Hiatus			52.5	MFS	
		Sabinetown		TST				
		Rockdale	Calvert Bluff			54.1		TS
			Hiatus		LST	54.9		T1
Simsboro				HST				
Butler				HST				
Seguin				TST	56.55	MFS		
		Caldwell Knob		TST				
		Solomon Creek			57.7		TS	
			LST	58.5		T1		
	Hooper		HST	59.2	MFS			
Paleocene	Midway	Wills Point		TST	59.99		TS	
				SMST	60.9		T2	
				HST	61.5	MFS		
				TST				
			Wortham			62.88		TS
			Mexia		SMST	64.05		T2

Notes:

HST: highstand systems tract

LST: lowstand systems tract

TST: transgressive systems tract

MFS: maximum flooding surface

SMST: shelf-margin systems tract

T1: type 1 unconformity, a subaerial and submarine unconformity, occurs at base of LST

T2: type 2 unconformity, occurs at base of shelf-margin systems tract

TS: transgressive surface, occurs at base of TST

Table 5-2. Stratigraphic column showing the epochs, formations, and hydrogeologic units. The epoch, group, and formation organization is consistent with the design of Table 5-1 to facilitate comparison. The United States Geological Survey (USGS) nomenclature is based on Ryder (1996). Texas hydrogeologic units are based on TWDB (2007a) and George and others (2011). This table does not reflect the entire Jackson or Midway group stratigraphy. This table is not scaled vertically in uniform units of time.

Epoch	Group	Formation	USGS aquifer name	Texas aquifer name	Aquifer system	
Eocene	Jackson	Caddell	Vicksburg-Jackson confining unit	Yegua-Jackson Aquifer	Upper Coastal Plains	
		Moodys Branch				
		Hiatus				
	Claiborne	Yegua	Upper Claiborne Aquifer	Confining unit		
		Cook Mountain	Middle Claiborne confining unit			
		Hiatus	Middle Claiborne Aquifer	Sparta Aquifer		
		Sparta Sand		Confining unit		
		Weches		Queen City Aquifer		
		Hiatus	Lower Claiborne confining unit	Confining unit		
		Queen City Sand				
		Reklaw	Lower Claiborne – upper Wilcox Aquifer	Carrizo-Wilcox Aquifer		
		Hiatus				
		Carrizo Sand				
		Wilcox	Hiatus	Middle Wilcox Aquifer		
			Sabinetown			
Rockdale						
Seguin						
Paleocene	Midway	Wills Point	Midway confining unit	Confining unit		

These geological formations were deposited during the upper Paleocene and Eocene epochs of the Tertiary (Paleogene) Period, approximately 59.2 to 40 million years ago, along the ancient coast of the Gulf of Mexico (Brown and Loucks, 2009). Formation lithology is predominantly gravel, sand, silt, clay, and occasionally lignite. Depositional environments responsible for the sediment packages include fluvial, strandplain, marsh and swamp, delta, prodelta, barrier island, lagoon, and open marine. The depositional systems were fed by erosion of landscape uplifted during the Laramide Orogeny, which built the modern-day Rocky Mountains (Galloway and others, 2011). A brief description of the depositional setting using sequence stratigraphic terminology will provide context of how these aquifers and aquitards were formed.

Deposition during and following maximum sea level is termed a highstand systems tract (HST) and includes on-shelf basinward progradation (also termed regression) where the coastline shifts toward the Gulf of Mexico basin. It consists of fluvial, deltaic, strandplain, barrier bar, and shelf environments with moderate to very high rates of sediment accumulation (Galloway and others, 1994). The upper surface of the systems tract consists of a subaerial or submarine regional unconformity (Brown and Loucks, 2009) representing a depositional hiatus of 0.5 to 3 million years duration. Highstand systems tract examples include the Hooper and Simsboro formations of the Wilcox Group, initial Carrizo Sand deposition, Queen City, Sparta, and Yegua formations. These formations are regional aquifers.

Deposition during sea level fall is termed a lowstand systems tract (LST) and includes on-shelf basinward progradation (also termed forced regression) where the coastline shifts toward the Gulf of Mexico basin, often to the shelf edge. Shelf erosion may create incised valleys into subjacent sediment with sediment accumulation during subsequent sea level rise (Brown and Loucks, 2009). Sediment consists of coarse-grained sand and gravel deposited in fluvial deltaic environments. Upper Carrizo Sand strata are an excellent example. The Carrizo is a unique, regional aquifer with fresh water extending tens of miles downdip from the outcrop in the region south of the San Marcos Arch (Plate 8).

Deposition during sea level rise is termed a transgressive systems tract (TST) and includes wave-dominated strandplain, barrier bar, and shelf depositional systems where the coastline shifts landward (Brown and Loucks, 2009). The lower strata may include reworking of the subjacent sediment and the upper surface consists of a marine condensed section (glauconite, organic shale, and highly fossiliferous) representing the maximum flooding surface of the transgression reflecting low to very low rates of sediment accumulation (Galloway and others, 1994). Examples include the Calvert Bluff Formation of the Wilcox Group, Reklaw, Weches, and Cook Mountain formations. These formations form regional aquitards, although sands in the Calvert Bluff Formation can form local aquifers.

Sediment accumulation was affected by rate, volume, and location of primary axes of sediment input, sediment reworking, sea-level fluctuations, basin subsidence, sediment compaction, growth faults, and normal faults formed from syndepositional movement of underlying Jurassic Louann Salt deposits. Each of the geological formations evaluated in this study is unique, based on the previously mentioned variables, and is discussed in the following sections.

5.1.1 Wilcox Group

In terms of sequence stratigraphic nomenclature, the Wilcox Group represents highstand systems tract (Hooper and Simsboro formations; Lower Wilcox) and transgressive systems tract (Calvert

Bluff Formation; Middle Wilcox). Wilcox deposition was interrupted by two significant hiatuses, the first after deposition of the Hooper Formation and the second after deposition of the Simsboro Formation (each less than 1 million years in duration). The Calvert Bluff Formation (top of the Wilcox Group) post-deposition hiatus was approximately 2.5 million years in duration (Brown and Loucks, 2009).

The Wilcox Group lithology contains a heterogeneous mixture of sediment resulting from deposition by (1) the Mount Pleasant Fluvial System within the Wilcox Group outcrop chiefly north of the Colorado River and the northern part of the Sabine Uplift, (2) multiple mostly river-dominated deltaic systems within the Rockdale Delta System north of the San Marcos Arch, and (3) the San Marcos strandplain bay system transitioning to the Cotulla barrier bar system within the Rio Grande Embayment south of the San Marcos Arch (Fisher and McGowan, 1967). Clay, silt, sand, gravel, and lignite deposited in fluvial, deltaic, and marine depositional environments are characteristic of the group. Wilcox Group deposition represents the first major progradational expansion of the northwestern margin of the Gulf of Mexico up to 40 miles gulfward from the Cretaceous position during the Paleocene (Ewing, 2016; Galloway and others, 2011).

The Hooper Formation provides a limited amount of groundwater primarily near the outcrop where the sands of the Simsboro Formation are absent. The Simsboro Formation is a prolific aquifer within the region between the Colorado and Trinity rivers. The Calvert Bluff Formation provides limited amounts of water for shallow wells in the region. This formation hosts several economic lignite deposits used for thermoelectric power generation in Texas ranging from Bastrop County northeast to Titus County.

The Yoakum Canyon (also known as the Yoakum channel, Hoyt, 1959) is a significant geologic feature in the Middle Wilcox that extends from outcrop in southwestern Bastrop County downdip through Gonzales, DeWitt, and Lavaca counties to the Wilcox Growth Fault zone downdip of the shelf edge, nearly 67 miles in length. Canyon width ranges from 4 miles in the updip to 12 miles in the downdip section near the shelf edge (Plate 6). The canyon is filled primarily with shale, although sand beds occur in the upper and mid-range sections. Canyon-fill thickness is zero at outcrop to over 2,500 feet in western Lavaca County (Hoyt, 1959). Dingus and Galloway (1990) postulate that decompaction of the shale indicates the original canyon could have been approximately 3,500 feet deep. The upper shale within the Middle Wilcox is referred to as the Yoakum shale by Hargis (2010). The Carrizo Sand thickens along the Yoakum Canyon axis and is reflected on the net sand map and those of Hoyt (1959). Origin of the Yoakum Canyon is still debated in literature, although Brown and Loucks (2009) report that the top of the submarine canyon system terminates at a regional marine condensed shale representing the maximum extent of marine transgression in the Middle Wilcox. They postulate that the Yoakum Canyon and similar structures elsewhere along the Gulf of Mexico margin (Hardin Channel) were formed by cannibalization of sediment and gravity-induced slumping.

Wilcox sandstones are very fine to fine-grained and poorly to moderately sorted in south central Texas (Fisher, 1982). Quartz is the most abundant mineral (averaging 64 percent framework grains), with plagioclase and potassium feldspars (7 percent and 3 percent framework grains, respectively). Silicified volcanic rock fragments (6 percent framework grains) and shale fragments and clay clasts are the most abundant rock fragments (8 percent framework grains) (Fisher, 1982). Diagenetic mineralogy has affected the primary and secondary porosity of Wilcox sandstones. In order of formation, quartz overgrowths, precipitation of kaolinite and

chlorite (clay minerals) in pore spaces and minor grain-replacement mineral, calcite as pore-fill and grain replacement, leaching of calcite, and precipitation of minor amounts of ferroan calcite and dolomite (Fisher, 1982). Fisher (1982) determined that this diagenetic sequence was initiated and completed at shallow depths in south central Texas. Kaolinite is more abundant in the shallow sandstones, possibly developed from leached plagioclase feldspar (Fisher, 1982). Chlorite is found at greater depths with higher temperatures (Dutton and Loucks, 2014). Calcite and ankerite are the most abundant cement (as much as 38 percent of the whole rock), but calcite is not found in samples deeper than 10,800 feet below ground surface (Fisher, 1982). Aquifer transmissivity and porosity will decrease with depth due to compaction and diagenesis. An increase in kaolinite in the primary and secondary porosity with depth in conjunction with primary dispersed and layered clay minerals will probably decrease the formation resistivity as measured by geophysical well logs, increase the formation clay content as measured with gamma ray logs, and decrease the amount of deflection on the spontaneous potential tool (Estepp, 1998; Schlumberger, 1987).

5.1.2 Carrizo Sand

In terms of sequence stratigraphic nomenclature, the Carrizo Sand represents an initial highstand systems tract that prograded across the Wilcox Group that was preceded by a depositional hiatus of approximately 3 million years. Younger Carrizo Sand deposition was in a lowstand systems tract with erosion into underlying older Carrizo Sand sediments, termed incised valley fill (Brown and Loucks, 2009). An unnamed transgression, highstand systems tract, and depositional hiatus (Brown and Loucks, 2009) followed Carrizo Sand deposition prior to Reklaw Formation deposition.

The Carrizo Sand lithology is mostly composed of medium-grained sands with a minor amount of sandy clays. There are localized areas of high iron content (Sellards and others, 1932). Major sediment input of Carrizo Sand fluvial-deltaic sands was south of the San Marcos Arch, the hypothesis being the Wilcox Group depositional axis shifted from the Rockdale Deltaic system in the Houston Embayment to the Rosita Deltaic System in the Rio Grande Embayment (Ayers and Lewis, 1985; Ewing, 2016; Galloway and others, 2011).

Hamlin (1988) characterized the Carrizo Sand in south Texas as two sand-rich fluvial depositional systems that provided sediment to deltaic deposits downdip. One of these fluvial axes is located in northern Wilson County, within the study area. The fluvial axes contain bedload channel systems containing primarily sand with discontinuous clay lenses.

5.1.3 Reklaw Formation

In terms of sequence stratigraphic nomenclature, the Reklaw Formation represents a transgressive systems tract preceded by a depositional hiatus of approximately 1 million years (Brown and Loucks, 2009).

The Reklaw Formation lithology is made up of clay and sandstone (Sellards and others, 1932). As with other aquitards in the study area, the sediment deposited in the Reklaw Formation was the product of marine transgression, possibly in several pulses (Hargis, 2009b), with the coastline moving inland. Reklaw Formation sands may represent re-working and cannibalization of underlying Carrizo Sand sediments during the transgression (Sams, 1990). Bulling and Breyer

(1989) describe depositional environments (for example, barrier bar and associated crevasse splay deposits) and exploration potential of these sands.

5.1.4 Queen City Sand

In terms of sequence stratigraphic nomenclature, the Queen City Sand represents a highstand systems tract overlain by an unconformity (Brown and Loucks, 2009).

The Queen City Sand lithology is made up of sand, sandy silty clay, lignite, and bentonite. The Queen City Sand was deposited in a strike-oriented, strandplain (shore-zone) environment that received sediment via longshore currents from the northeast (Guevara and Garcia, 1972). The strandplain environment was located between Wilson and Fayette counties. The Queen City Sand was deposited in a high-constructive lobate delta system eastward from Fayette County. In South Texas (Wilson County and to the southwest) the Queen City was deposited in a high-destructive, wave-dominated delta system consisting of meanderbelt sand, lagoonal mud, stacked coastal barriers, and prodelta facies (Guevara and Garcia, 1972). Eargle (1968) reported radioactive anomalies in the middle Queen City Sand in south-central Texas that may represent placer concentrations of heavy mineral sands.

5.1.5 Weches Formation

In terms of sequence stratigraphic nomenclature, the Weches Formation represents a transgressive systems tract preceded by a depositional hiatus of approximately 1.5 million years (Brown and Loucks, 2009).

The Weches Formation lithology consists of widespread deposition of clay, glauconitic sand, clay and limonite representing a marine transgression and contains a marine condensed section.

5.1.6 Sparta Sand

In terms of sequence stratigraphic nomenclature, the Sparta Sand represents a highstand systems tract overlain by an unconformity (Brown and Loucks, 2009).

The Sparta Sand lithology is sand, sandy clay, glauconitic sand, and limonite (Sellards and others, 1932) deposited during a progradational period. In East Texas, the Sparta Sand was deposited in high-constructive delta facies consisting of five major delta lobes oriented generally perpendicular to regional strike (Ricoy and Brown, 1977). The high-constructive delta, located from Fayette County northeast to Louisiana, consists of upper delta plain in outcrop and lower delta plain, delta front, and prodelta fine-grained sediment in the subsurface (Ricoy and Brown, 1977). In Central Texas, the Sparta Sand was deposited in a strike-oriented strandplain (shore-zone)/barrier bar system fed by longshore currents from reworked high-constructive delta facies (Ricoy and Brown, 1977). The strandplain/barrier bar system occurs approximately between Fayette and Atascosa counties. Southwest of the study area, Ricoy and Brown (1977) document a high-destructive, wave-dominated delta system in South Texas.

5.1.7 Cook Mountain Formation

In terms of sequence stratigraphic nomenclature, the Cook Mountain Formation represents a transgressive systems tract preceded by a depositional hiatus of approximately 1 million years (Brown and Loucks, 2009).

The Cook Mountain Formation lithology consists of clay, shale, sandy shale, sand, glauconite, and limestone (Sellards and others, 1932) representing a marine transgression. It was mostly deposited in shallow and deep marine environments with some littoral and continental deposits.

5.1.8 Yegua Formation

In terms of sequence stratigraphic nomenclature, the Yegua Formation represents a highstand systems tract overlain by an unconformity representing a hiatus of deposition lasting approximately 1 million years (Brown and Loucks, 2009). The Yegua Formation records five to eight low-stand events that reflect eustatic sea level fluctuations (Ewing, 2016). Incised valleys present on the shelf fed sediment to shelf-edge deltas and slope-fans downdip from the Liberty Delta in East Texas (Ewing, 2016).

The Yegua Formation lithology is made up of sand, sandy clay, and clay deposited during a progradational period of deposition. Multiple regionally extensive marine shales can be used for correlation of units that were deposited during episodic sea-level fluctuations across the near-shore deltaic and off-shore marine depositional environments. Depositional environments include fluvial systems (primarily within the outcrop) feeding deltas and strandplain facies (primarily downdip of the outcrop), and shelf facies (primarily downdip from the study area).

5.2 Structural geology

There are several regional geologic structures that have modified syn- and post-deposition geological formations within the study area (Figure 5.2-1). Regional strike of study area geological formations is southwest – northeast with dip generally to the southeast. The San Marcos Arch, a positive structural feature, bisects the study area separating the Houston Embayment to the northeast from the Rio Grande Embayment to the southwest. Each embayment is characterized by subsidence and sediment loading and contains a salt diapir province. Salt diapirs have not been mapped in the study area, although salt movement is responsible for normal faulting in the Milano Fault Zone and Karnes Trough. The updip limit of Jurassic Louann salt deposition is plotted on the eastern side of the San Marcos Arch. Normal faults of the Luling Fault Zone are updip of the Milano Fault Zone and their development may be unrelated to salt movement.

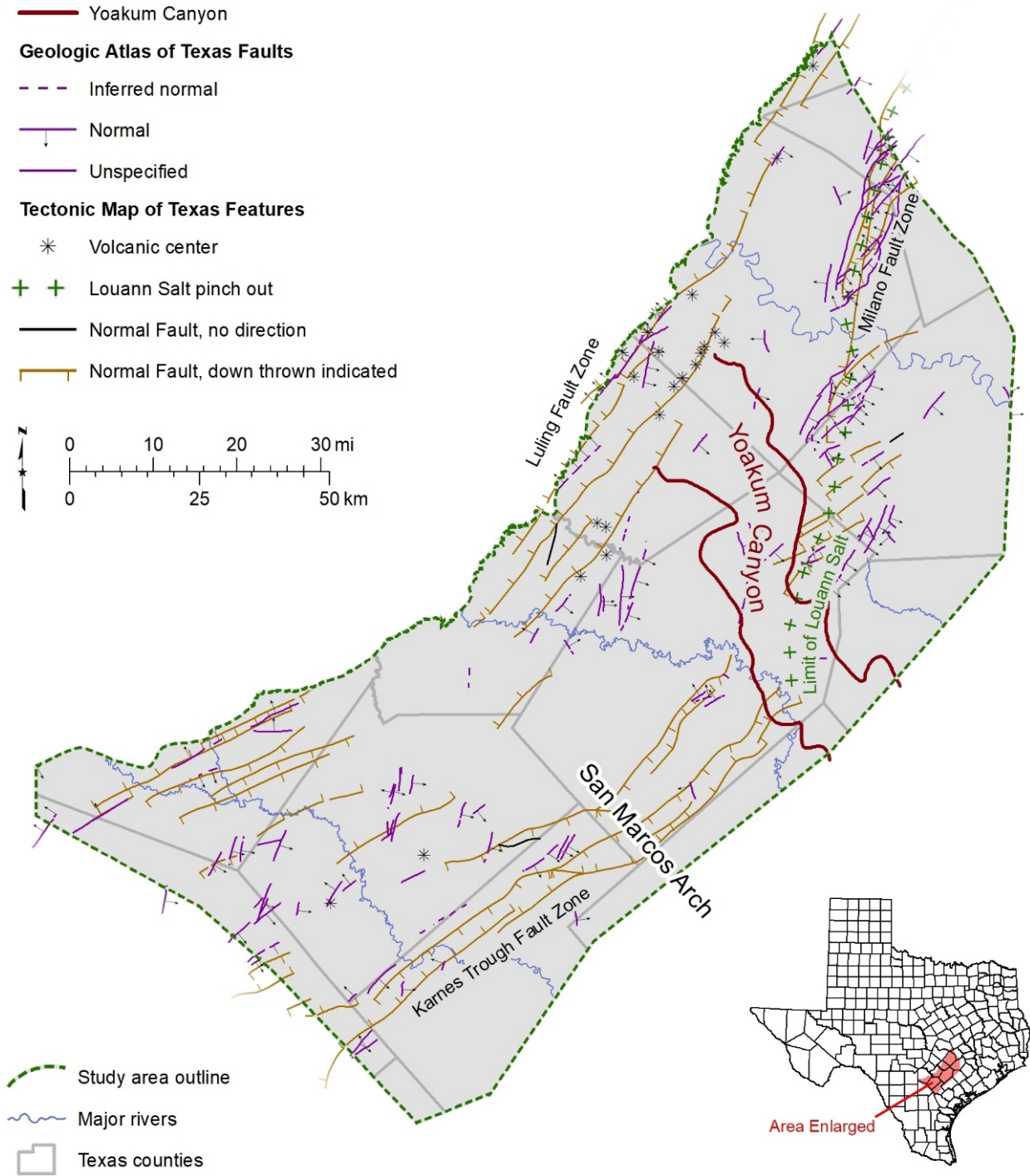


Figure 5.2-1. Regional geologic structure map showing surficial faults from the digital Geologic Atlas of Texas (TWDB, 2007b) and faults and other features from the Tectonic Map of Texas (Breton, 2013; Ewing, 1991). The extent of the Yoakum Canyon is based on mapping from this study and Dingus and Galloway (1990).

Thick Wilcox Group fluvial and deltaic strata are significant in the Houston Embayment and lap onto the San Marcos Arch (Fisher and McGowan, 1967). It is postulated that the fluvial system then shifted locus southwest into the Rio Grande Embayment where greater accumulations of Carrizo Sand sediment occur as compared to areas overlying the San Marcos Arch and Houston Embayment (Ayers and Lewis, 1985; Galloway and others, 2011). As deposition of Paleogene strata began to load basin sediment gulfward from the Cretaceous reef edges (Stuart City and Sligo), the Wilcox Fault Zone was established with normal, listric (a normal fault whose dip decreases with depth), down-to-basin growth faults.

Normal faults (faults whose hanging wall has moved downward relative to the footwall), antithetic (a minor, secondary normal fault whose displacement is opposite to that of the major fault), synthetic (a minor, secondary normal fault whose displacement is parallel to that of the major fault), and down-dropped graben structures in the Milano Fault Zone and Karnes Trough were formed at the updip limit of Jurassic Louann Formation salt deposition (Jackson and others, 2003). As sediment loaded the ductile halite, salt movement began in Jurassic and may continue to present time (Ewing, 1991). Salt movement created the extensional fault systems, with strata generally northwest of the faults locked in place and the detached strata overlying the salt moved generally to the southeast. The surface expressions of these faults are displayed and were extracted from the digital Geologic Atlas of Texas (TWDB, 2007b). The faults mapped on these maps represent a fraction of the faults within the study area. Many faults that were not recognized during surficial mapping are covered by surficial deposits or occur at depth.

The Milano Fault Zone in the study area includes the Paige Graben, the Kovar Complex, and an unnamed zone straddling the Gonzales–Fayette county line (Figure 5.2-2). The Milano Fault Zone consists of normal faults that are down to the northwest or down to the southeast and may be oriented parallel or subparallel to outcrop strike. Faults appear to die out between the two zones (Paige Graben and Kovar Complex), which are offset by approximately 6.7 miles (Young and others, 2018). Mapped faults in northeast Bastrop County occur in the Queen City Sand outcrop and progressively shift to younger formation outcrops in a left-stepping sequence to the southwest in the Yegua Formation outcrop in Gonzales and Wilson counties.

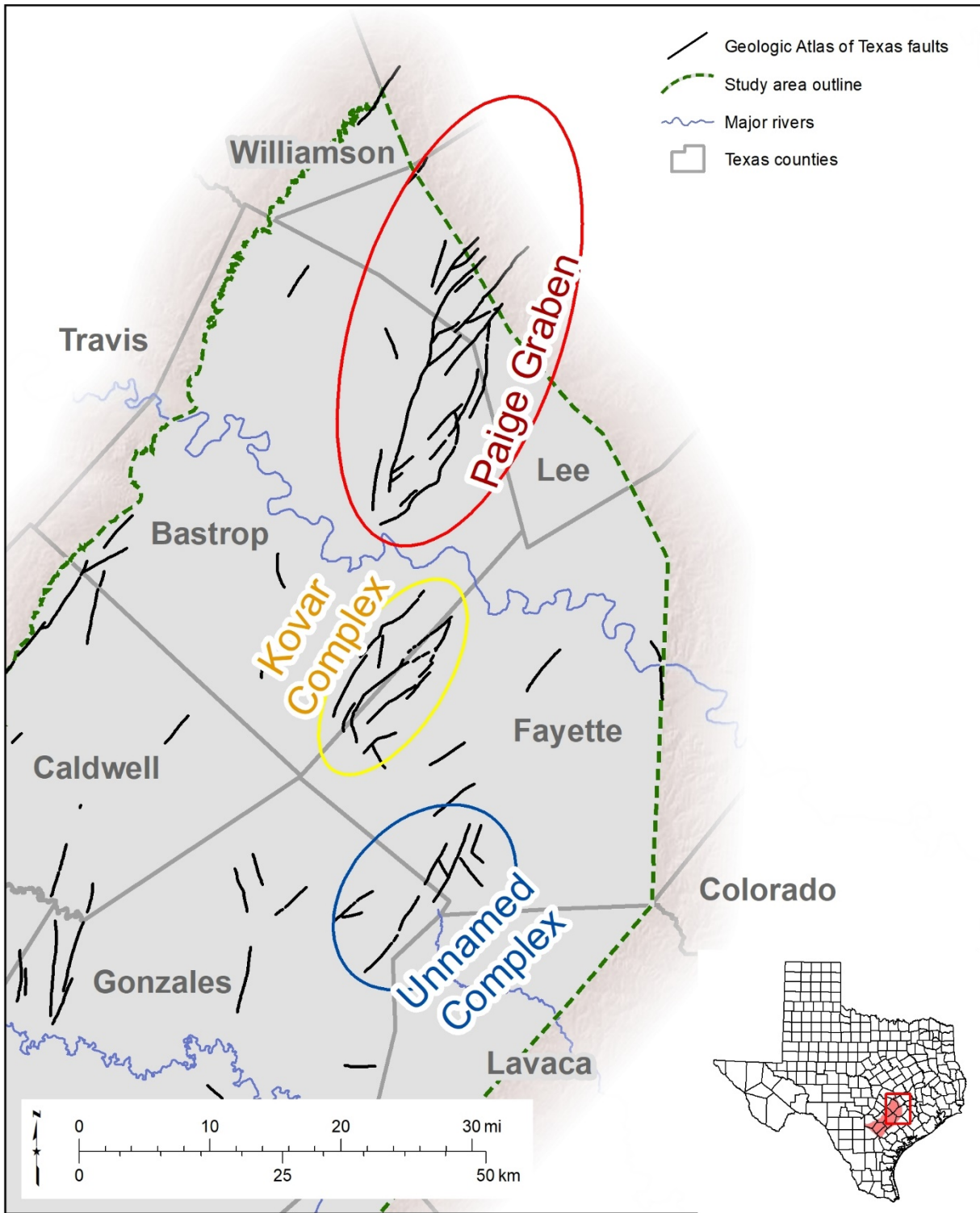


Figure 5.2-2. Fault zones within the Milano Fault Zone (surficial faults from the Geologic Atlas of Texas, TWDB, 2007b).

The Paige Graben strikes approximately north 20° east with maximum fault offsets approximately 700 feet. These faults cut both Cretaceous and Paleogene strata based on offset stratigraphic markers at the Navarro Group top and Wilcox Group bottom. The strike of this zone is parallel to the Paleogene outcrop. The zone is particularly complex, and we discovered discrepancies between surface geology on the Austin geologic atlas map (Proctor and others, 1974a) and our stratigraphic picks from geophysical well log analysis. There are additional antithetic and synthetic faults not mapped.

The Kovar Complex strikes approximately north 45° east with fault offsets from 100 to 500 feet. These faults cut both Cretaceous and Paleogene strata based on offset stratigraphic markers at the Navarro Group top and Wilcox Group bottom. The strike of this zone is 20° east of the Paleogene outcrop. There are additional antithetic (dipping opposite to the major fault) and synthetic (dipping in the same direction as the major fault) faults not mapped. Some of the wells in this area are cut by faults; we entered this information into the geology table in the BRACS Database.

An unnamed fault zone straddling the Gonzales-Fayette county line strikes north 60° east with a series of en echelon normal faults and a graben structure (Ewing, 1991). Graben fault offsets in east central Gonzales County along the (1) updip fault are approximately 286 to 362 feet based on offset stratigraphic markers at the Wilcox Group bottom and (2) downdip faults are approximately 175 to 242 feet based on offset of stratigraphic markers at the Wilcox Group bottom (Figure 5.2-3). The strike of this zone is 35° degrees east of the Paleogene outcrop. These faults are mapped on the Tectonic Map of Texas (Ewing, 1991) and it is not known if the other normal faults offset Paleogene strata.

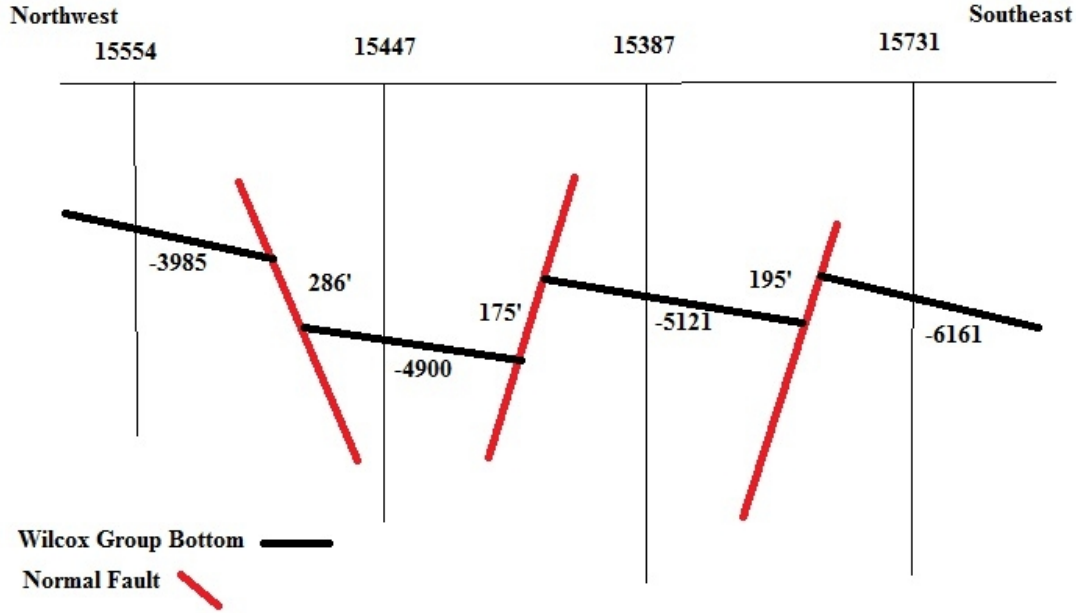


Figure 5.2-3. Diagrammatic cross-section across an unnamed fault zone along the Gonzales-Fayette county line. Wilcox Group bottom is offset by several normal faults (fault offset shown next to fault in black numbers in units of feet). The fault dip angle is unknown and the figure symbol is diagrammatic only. Fault block rotation is not known, and the orientation of the geological formation surface approximates regional dip. BRACS Database well identification number listed at the top of the well, elevation of the Wilcox Group bottom is displayed relative to mean sea level. Approximate fault offsets are corrected for relative structural dip of the Wilcox Group in this area and distance between wells.

The Karnes Trough graben structure strikes approximately north 60° east with the updip fault dipping to the southeast and the downdip fault dipping to the northwest. The strike of the zone is approximately 20° north of the Paleogene outcrop. Fault offsets in south central Gonzales County along the (1) updip fault are approximately 305 feet based on offset stratigraphic markers at the Wilcox Group bottom and (2) downdip fault are approximately 20 feet based on offset of stratigraphic markers at the Sparta Sand top.

Fault offsets in southeast Wilson and adjacent Karnes counties along the (1) two updip faults are approximately 257 and 26 feet based on offset stratigraphic markers at the Wilcox Group bottom and (2) downdip fault are approximately 90 feet based on offset stratigraphic markers at the Wilcox Group bottom (Figure 5.2-4).

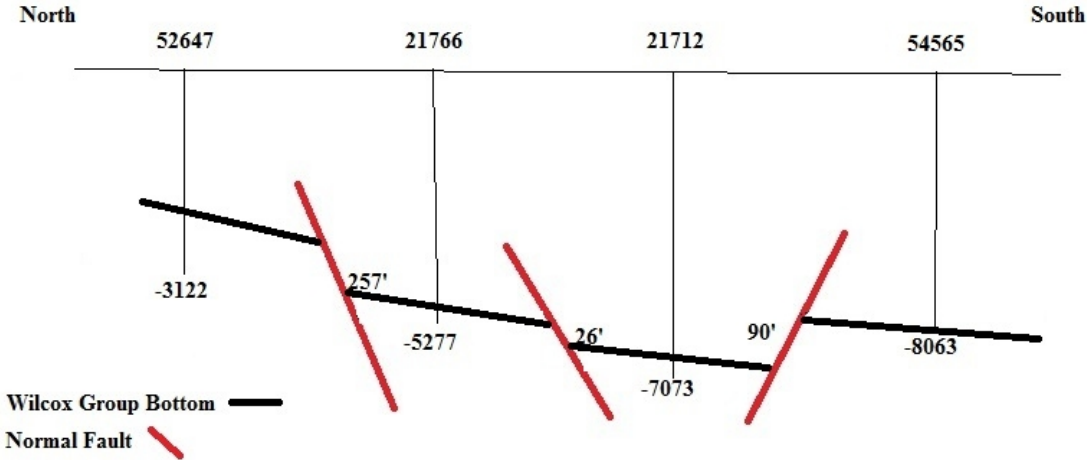


Figure 5.2-4. Diagrammatic cross-section across the Karnes Trough in eastern Wilson and Karnes counties. Wilcox Group bottom is offset by several normal faults (fault offset shown next to fault in black numbers in units of feet). The fault dip angle is unknown and the figure symbol is diagrammatic only. Fault block rotation is not known, and the orientation of the geological formation surface approximates regional dip. BRACS Database well identification number listed at the top of the well, elevation of the Wilcox Group bottom is displayed relative to mean sea level. Approximate fault offsets are corrected for relative structural dip of the Wilcox Group in this area and distance between wells.

Fault offsets in south central Wilson and adjacent Karnes counties along the (1) updip fault is approximately 132 feet based on offset stratigraphic markers at the Wilcox Group bottom and (2) downdip fault are approximately 112 feet based on offset stratigraphic markers at the Wilcox Group bottom.

The Luling Fault Zone consists of normal faults with the hanging wall down to the northwest. Fault strike changes from north 25° east (northeast part of the study area) to north 45° east (southwest part of the study area) (Figure 5.2-5). These faults cut Cretaceous and Wilcox Group strata and occur within the Wilcox Group outcrop in Bastrop, Caldwell, and Guadalupe counties. Estimated fault offsets in southwestern Bastrop County are 230 to 249 feet at the Wilcox Group bottom and Navarro Group top stratigraphic picks. Sands within the Wilcox Group outcrop are relatively thin (10 to 30 feet thick, as opposed to thicker sands downdip) and estimated fault offsets imply groundwater flow across the fault zone is impeded. Timing of fault movement is complex, with Ewing (1991) reporting that there is evidence of Cretaceous extension in the Luling Fault Zone concomitant with volcanism. Miocene regional uplift of the western United States includes movement along the Luling Fault Zone and the Balcones Fault Zone (normal fault orientation mostly down to the southeast, Ewing, 1991).

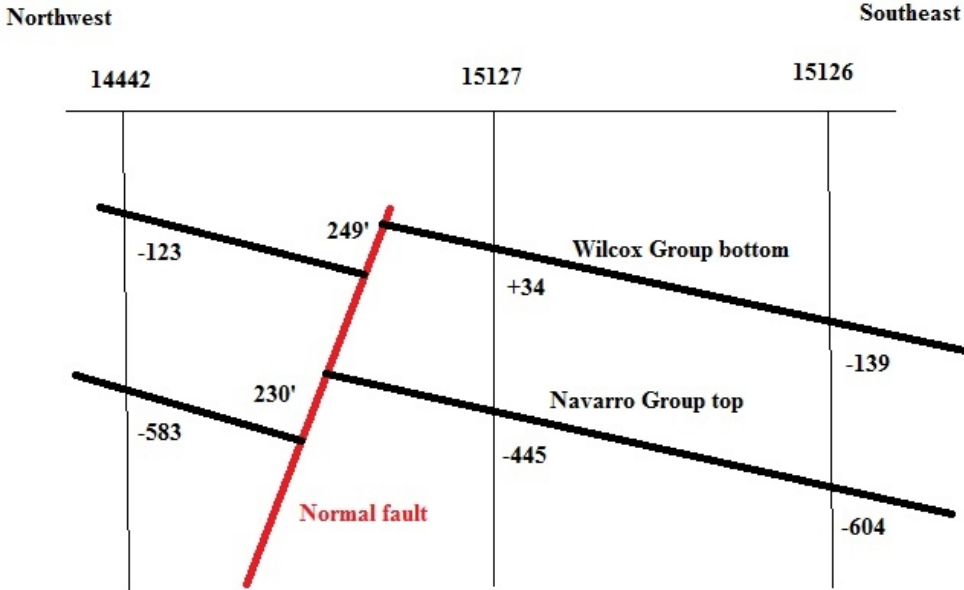


Figure 5.2-5. Diagrammatic cross-section across the Luling Fault Zone in southwest Bastrop County. Wilcox Group bottom and Navarro Group top is offset by a normal fault dipping to the northwest (fault offset shown next to fault in black numbers in units of feet). The fault dip angle is unknown and the figure symbol is diagrammatic only. Fault block rotation is not known, and the orientation of the geological formation surface approximates regional dip. BRACS Database well identification number listed at the top of the well, elevation of the Wilcox Group bottom and Navarro Group top is displayed relative to mean sea level. Approximate fault offsets are corrected for relative structural dip of the Wilcox Group in this area and distance between wells.

The Wilcox Fault Zone is southeast of the Late Cretaceous reef trends (Sligo and Stuart City), downdip of the study area, and was created by syndepositional growth faulting due to sediment loading over unstable fine-grained sediment.

Fault zone effect on groundwater flow is to be expected when fault offsets are greater than individual sand thickness. Fault offsets juxtaposing sand against shale will impede groundwater flow and sand against another sand will retard groundwater flow if fault gouge or fine-grained material is smeared through the fault zone. The presence of synthetic and antithetic faults may incrementally offset sand units across the fault zone, further impeding or retarding groundwater flow.

It appears that the recognized fault zones are not continuous along strike. If this is the case, then groundwater has the opportunity to flow downdip between the fault zones if dip-oriented sand units are present in a geological formation.

Finally, the location and orientation of the fault zone with respect to a geological formation strike has a significant effect on groundwater flow. For example, the Luling Fault Zone has no effect on post-Wilcox Group formations since it occurs within the Wilcox Group outcrop. The orientation of faults with respect to geological formation strike may also control groundwater flow. Faults striking at an angle to a geological formation strike may permit groundwater to flow

obliquely and downdip as opposed to faults that strike parallel to geological formation strike which will have a downdip flow impact.

Post-Cretaceous extensional fault zones offset study area formations. We did not have the time and well control necessary to determine fault offsets and identify unmapped faults. Missing section (strata not present at a fault-cut well) was identified using geophysical well logs in some wells, and the information was recorded in the BRACS Database. It is recommended that once potential brackish groundwater zones are identified for potential development, detailed geophysical well log lithofacies and fault mapping should be conducted prior to selecting test well sites. Test well pumping with monitor wells could show potential aquifer boundary conditions due to faulted sands. Several hydrogeological consulting firms have identified this situation when developing municipal and mine dewatering/depressurization well fields in study area aquifers.

6. Methodology

One of the objectives of the BRACS reports is to provide detailed information about the sources of data used for the study (well control and report references) and the methods employed to study the aquifers. This report serves as a technology transfer of applied interpretation techniques for the individual tasks. One of our fundamental goals is to provide all information to the stakeholder, including (1) original well control, (2) interpreted data, (3) techniques of analysis, (4) GIS data, (5) BRACS Database well control, and (6) a peer-reviewed report. We believe that this serves as a solid foundation for future work in the area.

The methodology section is organized into a sequence of tasks in the order they were performed, although some tasks such as data collection occurred throughout the project as each task sometimes required specific or additional data collected and analyzed.

6.1 Previous investigations

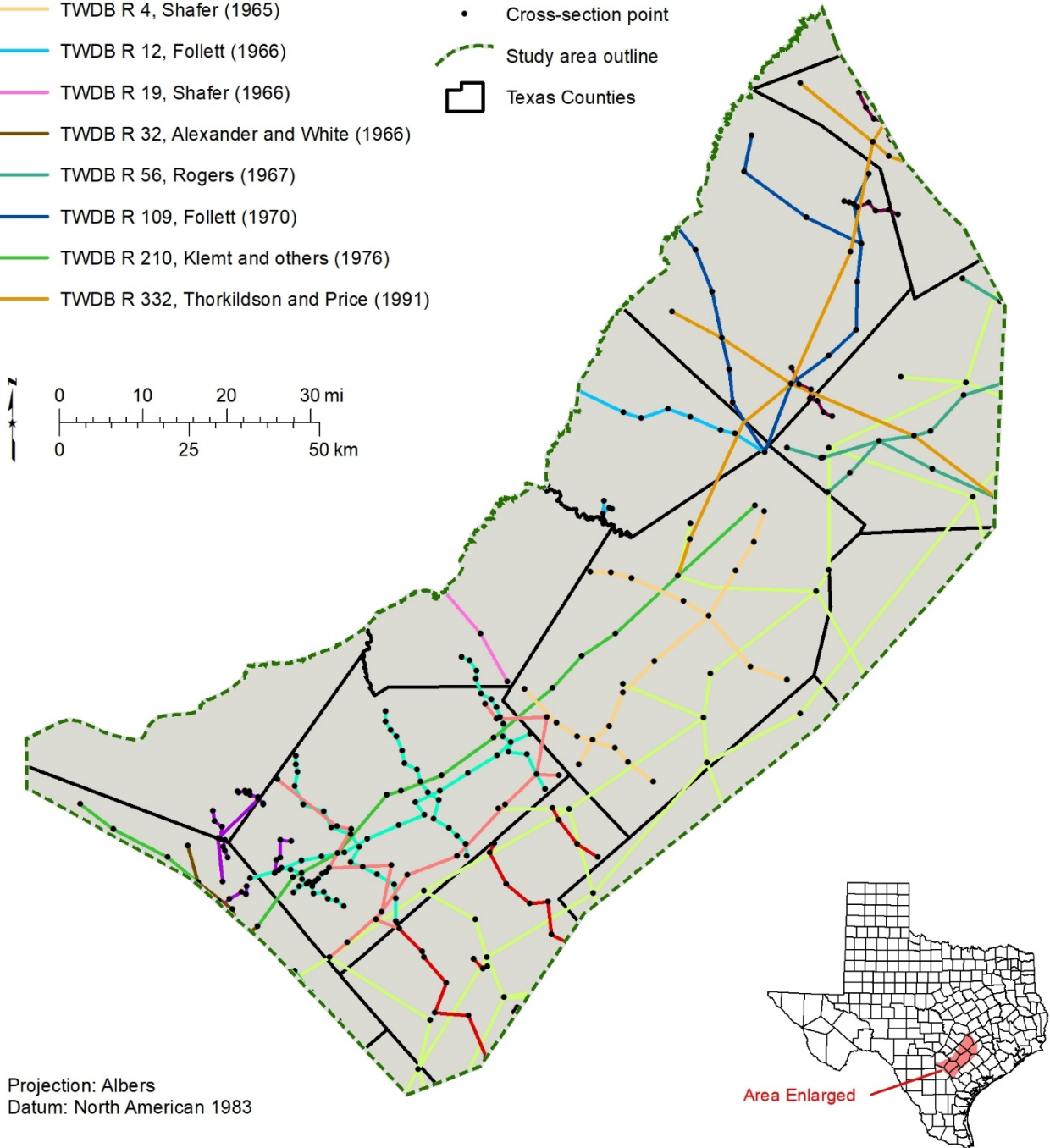
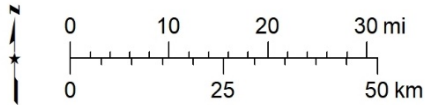
The first step in the project was to assemble existing information on the geological formations within the study area. We compiled publicly available reports, articles, and cross-sections. BRACS studies typically extend the three-dimensional mapping of the aquifers beyond the TWDB-defined major and minor aquifer extents (George and others, 2011; TWDB, 2007a). As such, we rely on data that was originally prepared for oil and gas exploration, as water well data is insufficient in the down-dip extent of our study area. Lists of county-wide hydrological studies, the development of groundwater models in the area, groundwater resource studies, formation-based studies, and cross-sections are provided in Appendix 13.3.

The well control points and cross-section lines from these studies were appended to one of two sets of GIS files in the study area (Figures 6.1-1 and 6.1-2). The GIS files include point and polyline shapefiles for cross-sections and estimated cross-sections, the latter used when an accurate location of the well was not determined. Where possible, cross-section wells and their geophysical well logs were added to the BRACS Database with the cross-section name, well identification, and report reference listed as a Foreign Key table record.

Cross-section line

- TBWE B 5710, Anders (1957)
- TBWE B 6007, Anders (1960)
- TWC B 6520, Harris (1965)
- TWDB R 4, Shafer (1965)
- TWDB R 12, Follett (1966)
- TWDB R 19, Shafer (1966)
- TWDB R 32, Alexander and White (1966)
- TWDB R 56, Rogers (1967)
- TWDB R 109, Follett (1970)
- TWDB R 210, Klemt and others (1976)
- TWDB R 332, Thorkildson and Price (1991)







- SAWS Brackish Site Selection, LBG-Guyton (2006)
- Yegua-Jackson Aquifer Structure Report, Knox and others (2007)
- Study on Wilcox Group, Hargis (2009)
- GMA 12 Faulting Study, Young and others (2018)
- Cross-section point
- - - Study area outline
- Texas Counties



Projection: Albers
Datum: North American 1983

Figure 6.1-1. Cross-section lines and points reviewed for the study. The location of cross-section points and lines is well constrained.

Estimated cross-section line

-  TBWE B 5911, Arnow (1959)
-  Dodge and Posey (1981)
-  Ayers and Lewis (1985)
-  Estimated cross-section point
-  Study area outline
-  Texas counties

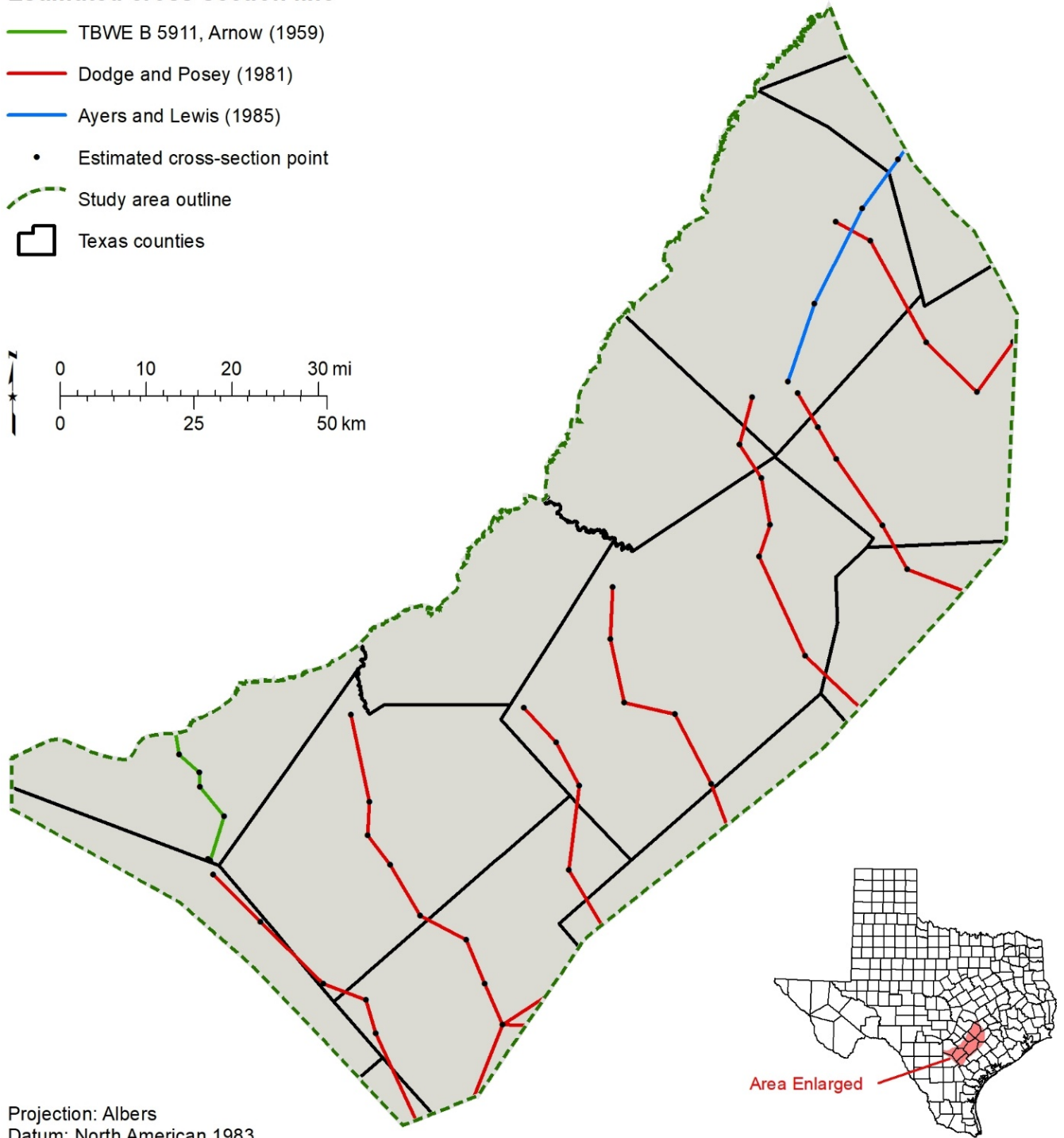
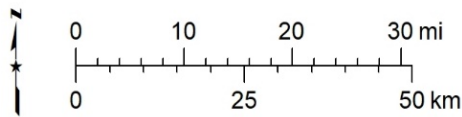















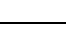












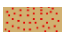





Figure 6.1-2. Estimated cross-section lines and points reviewed for the study. The location of points and lines is estimated for many, but not all, of the features based on information and maps in the original reports.

The University of Texas at Austin Bureau of Economic Geology has published the Geologic Atlas of Texas map sheets at a scale of 1:250,000 using the Universal Transverse Mercator projection (various zones) using an Army Map Service topographic base map. The five map sheets covering the study area include (1) Austin (Proctor and others, 1974a), (2) Beeville – Bay City (Aronow and others, 1975), (3) Crystal City – Eagle Pass (Brown and others, 1976), (4) San Antonio (Brown and others, 1974), and (5) Seguin (Proctor and others, 1974b). We utilized the digitized vector version of these maps created by the United States Geological Survey, in cooperation with the TWDB Texas Natural Resources Information System (TWDB, 2007b) to generate the surface geology map (Table 6.1-1 and Figure 6.1-3).

Table 6.1-1. Geological formation map-unit symbol labels for Figure 6.1-3.

Symbol	Map-unit symbol	Geological formation name
	Qal	Alluvium
	Qt	Terrace deposits
	Qhg	High gravel deposits
	Qle	Leona Formation
	Qw	Willis Formation
	T-Qu	Uvalde Gravel
	Pg or Mg	Goliad Formation
	Mf	Fleming Formation
	Mfo	Fleming Formation and Oakville Sandstone
	Mo	Oakville Sandstone
	Mc or Oc	Catahoula Formation
	Of	Frio Formation
	EOw	Whitsett Formation
	EOdd or OEdd	Dubose and Deweesville Sandstone Members of the Whitsett Formation
	Edd	Fashing Clay, Calliham Sandstone, Dubose Clay, and Deweesville Sandstone Members of the Whitsett Formation
	Ecd	Conquista Clay and Dilworth Sandstone Members of the Whitsett Formation
	Em	Manning Formation
	Ewb	Wellborn Formation
	Eca	Caddell Formation
	Ey	Yegua Formation
	Ecm	Cook Mountain Formation
	Es	Sparta Sand
	Ew	Weches Formation
	Eqc	Queen City Sand
	Er	Reklaw Formation
	Ec	Carrizo Sand
	Ewi	Wilcox Group
	Ecb	Calvert Bluff Formation

Symbol	Map-unit symbol	Geological formation name
	Esb	Simsboro Formation
	Eh	Hooper Formation
	Emi	Midway Group
	Wa	Water

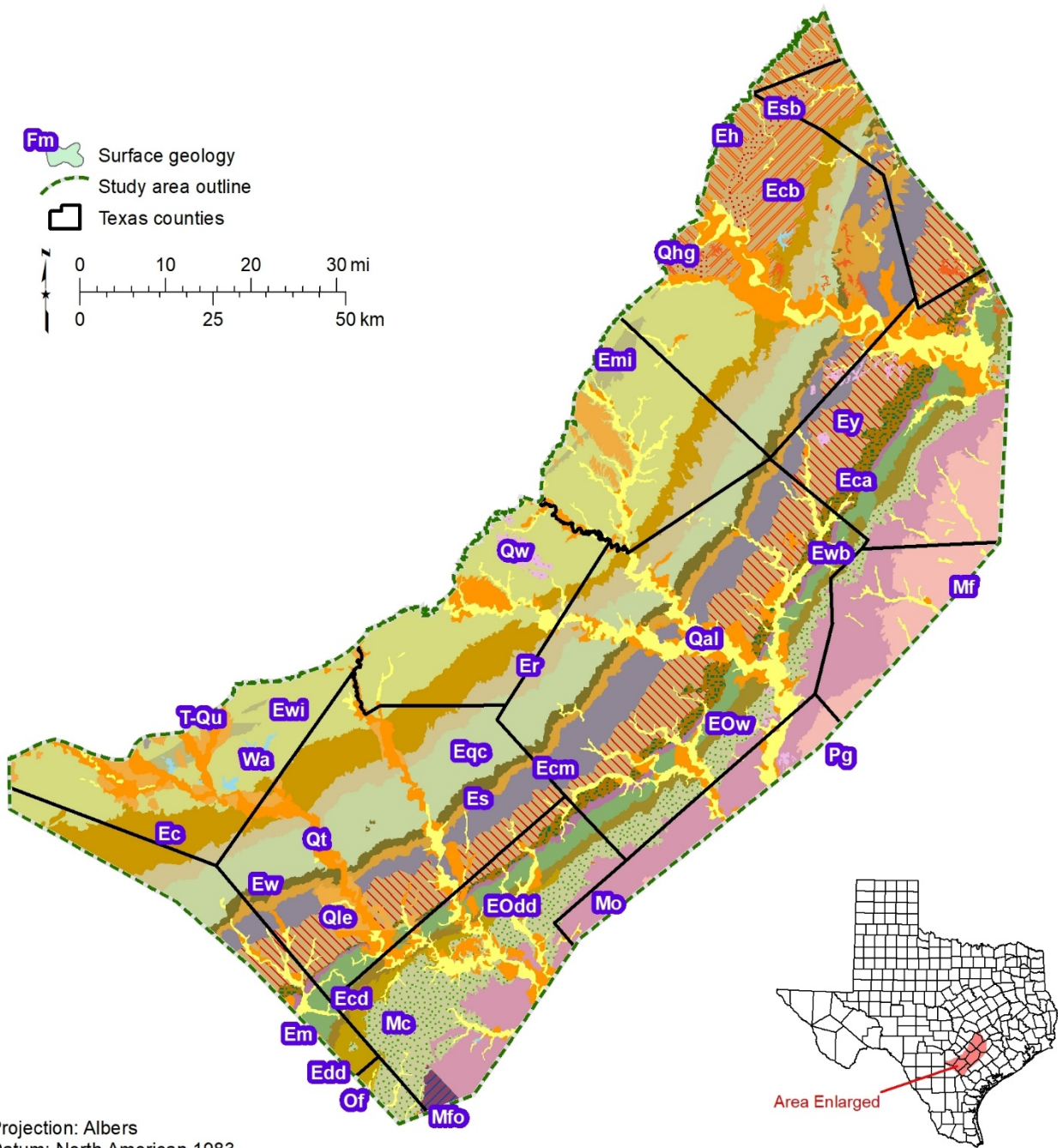


Figure 6.1-3. Geological formations outcropping within the study area based on the Geologic Atlas of Texas (TWDB 2007b). Refer to Table 6.1-1 for map-unit symbols.

6.2 Data collection and analysis

One of the primary objectives of the study is to gather available well data from existing water well reports, geophysical well logs, water chemistry samples, and aquifer tests. This information augments information in the TWDB Groundwater Database (TWDB, 2019b). No single agency has complete information on all water wells or oil and gas wells in Texas. Therefore, we evaluated existing collections that contain publicly available paper and digital information. The information was loaded into the BRACS Database. Each well that was added to the BRACS Database references the source of the information and all applicable well identification numbers.

Another equally important objective is to make the information and datasets gathered for the study readily available to the public. Therefore, all information collected is non-confidential. The information includes raw data such as water well reports and digital geophysical well logs, processed data such as lithology, simplified lithologic descriptions, stratigraphic picks, water chemistry, and interpreted results in the form of GIS datasets.

With these objectives in mind, we appended 5,284 wells located in the study area to the BRACS Database; 1,594 of these well records have a state well number with additional information in the Groundwater Database. An additional 2,846 well records are within the study area and in the Groundwater Database, resulting in a total of 8,130 well records. The 8,130 wells were appended to the study aquifer determination table described in Section 6.5. These included 4,978 water wells, 2,941 oil and/or gas wells, and 211 other types of wells (Figure 6.2-1). This represents only a fraction of all the wells completed in the study area. Information about many other wells was either unavailable, incomplete, limited in scope, of poor quality, confidential, or did not meet the requirements of the study.

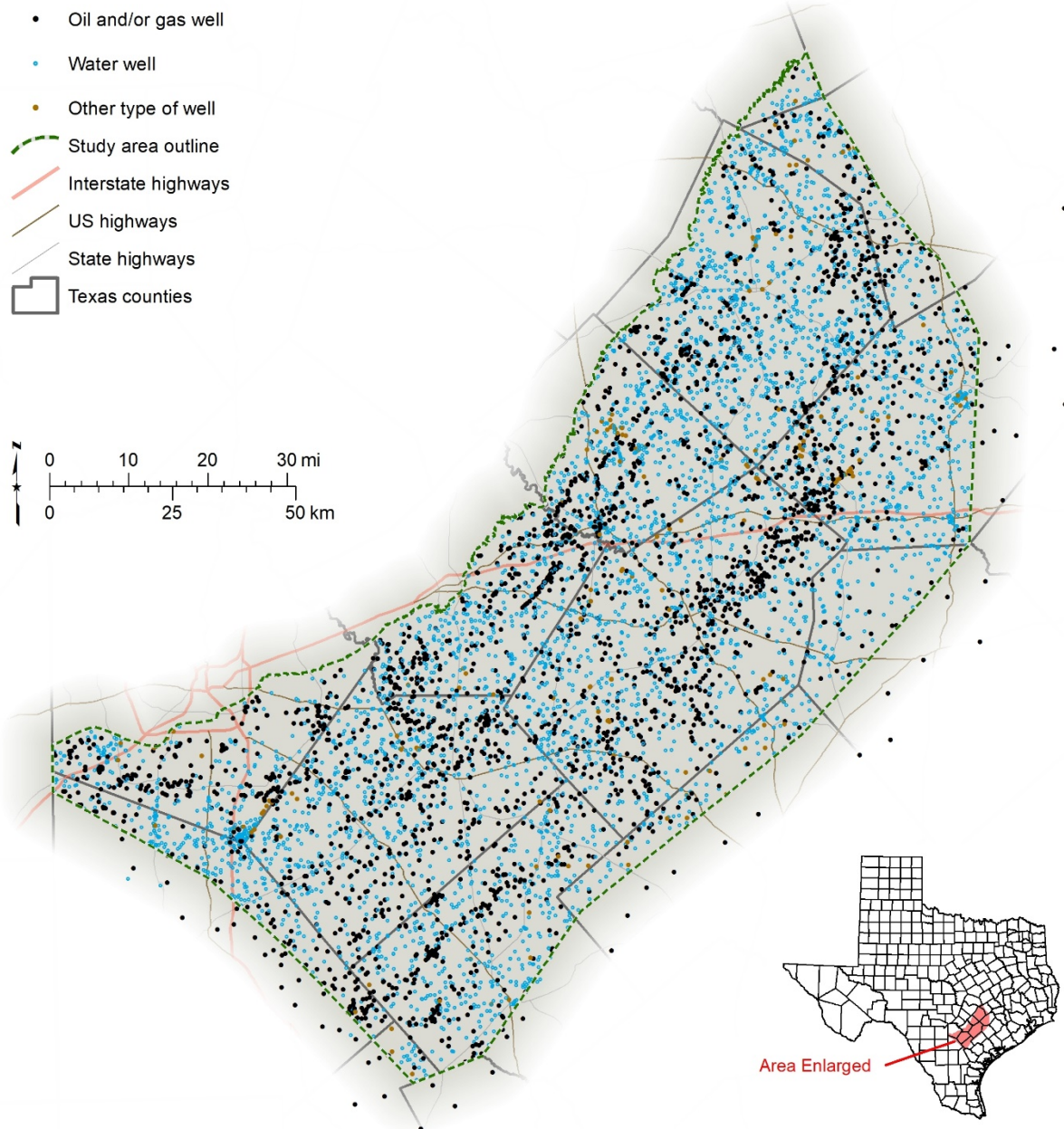


Figure 6.2-1. Study well control consists of 8,130 wells: 4,978 water wells, 2,941 oil and gas wells, and 211 wells classified as other.

Additional information in the study area is available from public and private sources:

- additional water quality data in the Groundwater Database
- Submitted Driller's Report Database for well reports younger than 2001
- Water Well Report Viewer (www.tceq.texas.gov/gis/waterwellview.html) on the Texas Commission on Environmental Quality website for well reports older than 2001
- digital geophysical well logs available on the Railroad Commission of Texas website (gis.rrc.texas.gov/GISViewer/)
- paper and digital geophysical well logs and miscellaneous records at the Bureau of Economic Geology
- well records at the groundwater conservation districts

We obtained 1,643 wells (Q-logs) from the Groundwater Advisory Unit of the Railroad Commission of Texas (Railroad Commission of Texas, 2018a) and added this invaluable information to the BRACS Database and geophysical well log collection. Many of these well logs were used to prepare cross-sections in the first water resource reports of the TWDB and predecessor agencies. In addition, many of the older wells had shallow casing allowing logging of near-surface portion of the geological formations. This facilitated interpretation of geology and water quality in those near-surface areas.

We did not verify the location of every well that was obtained from other agency datasets unless there appeared to be a problem, such as a mismatch in the geology. When locations had to be verified or digital locations were not available, the Original Texas Land Survey GIS files and georeferenced, county linen maps from the Railroad Commission of Texas, Groundwater Advisory Unit were used as a base map. The location legal description noted on the log header was used to plot the wells in GIS to determine the latitude and longitude coordinates. Users of our study data should be aware that well locations may need verification. Some well locations appended to the BRACS Database could not be accurately located; we applied zero to the latitude and longitude coordinates.

We used the following sources of well data in this study (Table 6.2-1):

- Bureau of Economic Geology Geophysical Log Facility
- Texas Commission on Environmental Quality State of Texas Well Report image files (plotted wells, non-plotted wells, wells with assigned state well numbers), digital geophysical well log files, and public drinking water program well files and database (TCEQ, 2010)
- Texas Department of Licensing and Regulation Submitted Driller's Report Database (TWDB, 2019c)
- Railroad Commission of Texas paper and digital geophysical well logs (Railroad Commission of Texas, 2018a) and the Underground Injection Control Database (Railroad Commission of Texas, 2018b)
- TWDB Groundwater Database (TWDB, 2019b), BRACS Database (TWDB 2019a), state well numbered water well reports, geophysical log collection, groundwater availability model studies, miscellaneous contracted projects, and published reports

- U.S. Geological Survey published reports; geophysical well log collection at the Texas Water Science Center; and the Produced Water Database, version 2.2 (Blondes and others, 2016)
- San Antonio Water System well reports from the H₂Oaks facility including aquifer storage and recovery Carrizo Aquifer wells, and the lower Wilcox Aquifer brackish groundwater well field in southern Bexar County
- Gonzales County Underground Water Conservation District selected well reports, water quality data, and geophysical well logs
- Evergreen Underground Water Conservation District, Hargis (2010) study evaluating the Carrizo and Wilcox Aquifers in Wilson and Guadalupe counties, and digital geophysical well log files

Table 6.2-1. Study area well control and use.

Well control and use	Count
Total well control in study area	8,130
Total BRACS Database wells	5,284
Total Groundwater Database wells	4,440
Wells in both BRACS and Groundwater databases	1,594
Wells with geophysical well logs	2,960
Wells with lithology (from driller well reports)	1,834
Number of lithology records (from driller well reports)	27,818
Wells used for interpreting lithology from geophysical well logs	635
Number of lithology records interpreted from geophysical well logs	82,012
Wells used for stratigraphic interpretation	1,207
Number of stratigraphic picks	4,652
Wells with aquifer hydraulic properties	2,325
Wells with water quality samples	1,984
Number of water quality of samples	3,862
Wells used for estimating TDS from geophysical well logs	911
Number of TDS estimates from geophysical well logs	5,139

Note: TDS = total dissolved solids

We included all wells from the Groundwater Database (TWDB, 2019b), some wells in the Submitted Driller’s Report Database (TWDB, 2019c), and all wells in the BRACS Database located in our study area for our study well control. These wells contain information that is essential to understanding the geology of the region. Some wells were used for many different purposes, such as lithology, net sand, stratigraphic picks, and salinity calculations. However, most of the well control could only be used for one or two purposes (Figure 6.2-2). Because the Groundwater Database and the Submitted Driller’s Report Database are updated daily, users should be aware that in the future there will be new information available in these databases in addition to that present in the BRACS Database. We will continue to add new well control to the BRACS Database from the study area, especially if wells are drilled for brackish groundwater development.

Based on information obtained from the Railroad Commission of Texas Oil and Gas Well Database, the study area contains approximately 45,370 oil and gas wells (Railroad Commission of Texas, 2018c) and 1,962 Class II injection wells (Railroad Commission of Texas, 2018b) in the study area.



Figure 6.2-2. Symbolic Venn diagram of geologic evaluation well control overlap for the study. Only a small subset of the wells will have all three types of geologic picks: stratigraphy, lithology, and salinity. Many more wells will only have a combination of two or only one type of pick depending on mapping needs.

6.3 Stratigraphic interpretation

Water well reports, geophysical well logs, and published reports were the most important sources used to define the stratigraphic top and bottom of each geological formation in the study area. Existing publicly available stratigraphic GIS surface data contained significant errors especially in the downdip extent of the study area. We decided to interpret well control to define a regionally consistent set of stratigraphic depths to ensure that all subsequent analysis was assigned to the correct geological formation. Regional geologic maps and cross-sections were used as a reference, although inconsistent stratigraphic mapping of these geological formations is common. An iterative process was used for correlating logs and defining stratigraphic picks based on regional lithologic geophysical log signatures; picks were revised several times as we became more familiar with the area and new well control was added to the study. Stratigraphic information for each geological formation and figures showing typical geophysical well log signatures is presented in Section 7.

Generally, there is less geophysical well log control near the geological formation outcrops due to the presence of well surface casing. Shallow geological formation contacts are not represented and recorded on the logs. There was also less well control at the downdip extent of the study area (southeast) due to fewer publicly available well logs, shallow well depths, and in many cases the deeper sections of well logs were physically removed before they were submitted to the state. We used well control outside of the study area boundary to interpolate the geological formation raster surfaces to reduce edge-effect distortion and artifacts. A significant number of wells southwest of the study area were used from the Queen City and Sparta aquifer study (Wise, 2014). Since the Wise (2014) study was limited to the Queen City and Sparta formations,

additional stratigraphic picks were interpreted in these wells for the Yegua, Cook Mountain, Reklaw, and Carrizo formations and the Wilcox Group where possible.

The stratigraphic top and bottom depths were appended to the geology table in the BRACS Database. The top and bottom depths are based on the measured depth below the measuring datum for the geophysical well log, typically the kelly bushing or rig floor. We did this to maintain a one-to-one correlation between the log and the geology table. If a stratigraphic pick was not possible using information present on a well log (or not present due to a cased section), no value for that pick was added to the geology table. If a well did not fully penetrate a geological formation, no bottom depth was recorded and a “>” character was added to the table to designate partial penetration.

The stratigraphic picks were exported to a stratigraphic GIS shapefile using a study table (gBRACS_ST_PE_sTx) populated with set of custom queries that corrected the depth and elevation values with the kelly bushing height and site elevation based on a statewide seamless 30-meter digital elevation model. The stratigraphic GIS table was used to develop the three-dimensional geological formation surface and thickness rasters described in more detail in Section 13.6.1. The stratigraphic information was locked down on February 8, 2017, so we could proceed with geological surface preparation. Additional stratigraphic picks were appended to the geology table to support net sand and total dissolved solids interpretations using geophysical well logs. Stratigraphic records in the geology table contain the date of interpretation, so the user will know if a pick was appended post-geological surface preparation.

The database table (gBRACS_ST_PE_sTx) is provided as a study deliverable in the public version of the BRACS Database and a table description is provided in the data dictionary (Meyer, 2020). The stratigraphic GIS shapefile is provided as a study deliverable with metadata (Appendix, Section 13.5, Table 13.5.2-4).

We prepared figures for each geological formation showing the GIS raster files for (1) top and bottom elevation, (2) top and bottom depth below ground surface, and (3) thickness (isochore). Each type of map has a consistent GIS color ramp for each geological formation for ease of comparison. These figures are organized by geological formation (Section 7).

6.4 Net sand analysis

The geological formations within the study area consist primarily of interbedded layers of sand and clay. Although both types of lithologies contain groundwater, sands can produce groundwater more economically and clay layers contain water that could leak into adjacent sands. We calculated net sand and sand percent for selected wells with lithology and prepared maps of net sand (the cumulative thickness of sand) for each geological formation. The net sand thickness at a well was generated from either an existing description of formations by water well drillers (also referred to as driller’s lithology or description) or our interpretation of geophysical well logs. The thickness of net sand was used with other parameters to estimate the saturated thickness of formation for calculating volume of brackish groundwater.

We appended driller’s formation descriptions on water well reports to the geology table either manually from scanned PDFs or by digital parsing records in the Submitted Driller’s Report Database (TWDB, 2019c). The geology table in the BRACS Database includes the following information for each lithologic unit: top and bottom depths, thickness, lithologic description, a simplified lithologic description, and the source of information (Meyer, 2020).

Because well drillers frequently use non-geological terms (for example, gumbo), misapply terms (for example, soapstone in an alluvial deposit), and typically do not describe the rocks and geological formations in a uniform and systematic manner, we developed a process to methodically translate the drillers' descriptions of formations into simple and consistent terminology. Our simplified description consists of a short list of terms based on mineralogy and grain size. A database lookup table was prepared relating the driller's lithologic name to the simplified lithologic description to accommodate the numerous variations present on well reports. Presently, the database lookup table contains more than 27,000 unique records and 120 simplified lithologic terms.

The simplified lithologic terms represent either one predominant type of material (for example, sand), or a mixture of two materials (for example, sand and gravel). Each term representing a mixture assumes that each component of the mixture approximates a 50-50 mix. The creation of the database table relating lithologic name to simplified lithologic name presented challenges and necessitated simplifications. Formation descriptions that contained more than two terms as part of a mixture (for example, sand, clay, and limestone) were converted to only the first two terms or the two most relevant terms based on percentage (if provided by the driller). Formation descriptions that included percentages of material within the 35-65 percent range were categorized as a 50-50 mixture. The simplified lithologic description was applied from ground surface to the total depth of the hole for water wells.

Geophysical well log lithology was evaluated using a four-tier method using the terms sand, clay, sand with clay, and clay with sand. The log was interpreted from 50 feet above the Yegua Formation top depth to 50 feet below the Wilcox Group bottom depth where possible. We included strata above and below the formations of interest to (1) document low permeability materials and (2) to ensure the net sand analysis Visual Basic for Applications[®] code will perform adequately using well site geological formation top and bottom depths based on interpolated raster surfaces.

We used deep investigative resistivity tools in the shallow sections (fresher aquifer sections) because the spontaneous potential tool may be ineffective in this zone. In the deeper portions of the aquifers, where the resistivity of the drilling mud filtrate is greater than the resistivity of groundwater, we used spontaneous potential tools in conjunction with deep resistivity tools. These zones typically produce a negative (or left) shift of the spontaneous potential log with respect to the shale baseline within permeable sands. The spontaneous potential and resistivity logs are affected by the presence of hydrocarbons (the spontaneous potential log is depressed and the resistivity is increased [Hilchie, 1978]). Where available, gamma ray tools were interpreted because of its suitability for discriminating sand and clay sequences and, where present, were used in conjunction with the spontaneous potential and resistivity tools to identify lithology.

We also used well lithology from selected wells provided in the Banerji and others (2019) study. Data from these logs was supplemented with additional lithologic interpretation and corrected to ensure all geological formations present on the log were represented.

We used two techniques to append lithology data from geophysical well log analysis to the BRACS Database. One technique involved marking the digital log with the four-tier lithology and manually entering lithology and top/bottom unit depths into the database. The second technique, used late in the study after the software was purchased, involved marking the lithology using IHS Kingdom[®] software and appending the data to the BRACS Database using

an open database connection between the Microsoft® SQL Server® project and the Microsoft® Access® BRACS Database. Visual Basic for Applications® code was used to evaluate every record and a gap analysis routine was used to ensure the top/bottom of a lithologic unit corresponded to the top/bottom of adjacent units. Corrections were made and missing intervals, if any, were flagged for manual correction.

The well geology table contains all well lithology, including clay units. Although we did not prepare net clay or clay percent maps, the information can be of interest for at least two reasons. The presence of clay units and their thickness should be considered when locating groundwater wells for a desalination plant, especially if a well screen is going to be placed in an aquifer that is adjacent to a significant salinity class boundary (zones of different salinity). Evaluation for potential up-coning of higher salinity groundwater into a production well is important. Equally important is an evaluation of clay units separating saline from fresh groundwater to evaluate fresh groundwater impact.

If the water well report or geophysical well log is missing information because of the presence of well casing or lost circulation (no drill cuttings returned to surface), “No Record” is listed in the geology table for this depth interval. If a portion of the well report or geophysical well log is missing because the log is incomplete (only part of the log was scanned as a digital image), “Geology Not Processed–Log Image Cut Off” is listed in the geology table for this depth interval. If a portion of the geophysical log was not interpreted, “Geology Not Described, But Available on Log” is listed in the geology table for this depth interval. Recording missing information with these terms is required during net sand and sand percent calculations.

Net sand and sand percent values for wells penetrating the geological formations in the study area were generated from the simplified lithologic description using structured query language in the BRACS Database. If a well only partially penetrated a geological formation, this is noted in the net sand table and a net sand value is calculated, but not the sand percent.

The table listing all simplified lithologic names contains a field for sand percent. Values of 0, 35, 50, 65, or 100 were chosen based on the presence of sand or coarser material. For example, a value of 50 would be applied to a lithologic unit containing a mixture of sand and clay. This table is used in subsequent database queries to process well records.

Because database queries must address lithologic units that are not completely contained within one geological formation (the unit may straddle the formation top, bottom, or both), we wrote specific queries to evaluate each of these scenarios to assign the correct thickness of a lithologic unit to the correct formation. We ran a separate query to assemble the information into a table for export into GIS for spatial analysis. We also developed queries to determine (1) if the geological formation is present at a well site, (2) if the well partially penetrates the geological formation and the percent penetration, (3) if the lithologic description partially describes the entire geological formation, (4) the percent of partial lithologic description due to situations such as a cased hole (recorded as a “no record”), and (5) the percent of the partial analysis of the well log (recorded as a “partial geologic description”). Well records that do not fully describe a geological formation are used based on best professional judgement, for example if the percent of lithologic description is high (90 percent or more).

We created three tables in the BRACS Database containing net sand information for the study area: (1) a table of individual records for each layer containing sand, (2) a table with one record per well with net sand and sand percent for each geological formation encountered, and (3) a

table with a decision to use or not use a well for net sand analysis for a specified geological formation. These tables were exported into GIS for display and analysis. The database tables can also be queried to develop custom approaches to analysis. The design of the geology and net sand tables and the methods used to capture this data afford the user a tremendous degree of flexibility in data analysis. These tables are provided as a study deliverable in the public version of the BRACS Database and a table description is provided in the data dictionary (Meyer, 2020). The GIS shapefiles are provided as a study deliverable with metadata (Appendix, Section 13.5.2, Table 13.5.2-2).

A series of net sand maps were prepared for each aquifer in the study area. We evaluated data points for each geological formation and added control where needed and culled well control if the information did not support the regional trend. The later was especially true for water well driller descriptions of lithology. Total well control and well control used to prepare aquifer net sand maps are summarized in Table 6.4-1. Different raster color ramps were used on each figure for each geological formation due to the significant differences in net sand values between the formations.

Table 6.4-1. Summary of study area well control for geological formation net sand maps.

Geologic formation	Number of wells used for net sand maps
Yegua Formation	195
Sparta Sand	335
Queen City Sand	384
Carrizo Sand	526
Wilcox Group	499

Each data point was compared to geological formation top and bottom depths to determine a net sand and sand percent value using sequential queries compiled in Visual Basic for Applications®. The points were exported to ArcGIS® as a point file using the Groundwater Availability Model projection with a 1983 North American Datum horizontal datum. We prepared the net sand maps using ArcGIS® 10.2 software with the Spatial Analyst® extension (Appendix, Section 13.6.2) and extracted a subset of data points for each geological formation for analysis. Net sand maps of geological formations present at the ground surface (within the outcrop) generally reflect a lower value of net sand due to (1) erosional thinning, (2) cover by Quaternary deposits, (3) wells drilled less than total thickness of the formation, (4) inaccurate well driller descriptions, and (5) presence of surface casing, which precluded evaluation with geophysical well logs.

6.5 Aquifer determination

We employed a technique to consistently assign the correct aquifer(s) to wells drilled in the study area so that information from these wells, specifically aquifer hydraulic properties, lithology, and water quality, could be meaningfully compared and extrapolated across the study area. The BRACS Database aquifer determination table (tblAquiferDetermination_PaleoceneEocene_sTx) was designed for this task. This table is provided as a study deliverable in the public version of the BRACS Database and a table description is provided in the data dictionary. The GIS shapefile is provided as a study deliverable with metadata (Appendix, Section 13.5, Table 13.5.2-5).

The hydrostratigraphic framework for the study area aquifers was used to meet this objective. Each well in the study area (all BRACS Database and all Groundwater Database wells; a total of 8,130 wells) was assigned a stratigraphic top and bottom depth based on the GIS surfaces created for the eight geological formations within the study area, with a few exceptions described later. Each well was also assigned a one-digit region code, with each region representing a unique stratigraphic column of geologic formations in the study area (Table 6.5-1). The surficial geographic area for each region represents the outcrop area of a geological formation and, if present, overlying Quaternary age sedimentary deposits (Figure 6.5-1).

Table 6.5-1. The study area was divided into regions 1 through 11 based on the geological formation outcropping at ground surface (formation listed at the top of each column) and a unique stratigraphic sequence of geologic formations below. Light gray cells represent aquifers, and dark gray cells are not aquifers. Colors in the region cells coordinate with Figure 6.5-1.

System	Region 1	Region 2	Region 3	Region 4	Region 5	Region 6
Oligocene						
Eocene						Sparta
					Weches	Weches
				Queen City	Queen City	Queen City
			Reklaw	Reklaw	Reklaw	Reklaw
		Carrizo	Carrizo	Carrizo	Carrizo	Carrizo
Paleocene	Wilcox	Wilcox	Wilcox	Wilcox	Wilcox	Wilcox
	Midway	Midway	Midway	Midway	Midway	Midway

System	Region 7	Region 8	Region 9	Region 10	Region 11
Oligocene					Gulf Coast
				Frio	Catahoula
Eocene			Jackson	Jackson	Jackson
		Yegua	Yegua	Yegua	Yegua
	Cook Mountain	Cook Mountain	Cook Mountain	Cook Mountain	Cook Mountain
	Sparta	Sparta	Sparta	Sparta	Sparta
	Weches	Weches	Weches	Weches	Weches
	Queen City	Queen City	Queen City	Queen City	Queen City
	Reklaw	Reklaw	Reklaw	Reklaw	Reklaw
	Carrizo	Carrizo	Carrizo	Carrizo	Carrizo
Paleocene	Wilcox	Wilcox	Wilcox	Wilcox	Wilcox
	Midway	Midway	Midway	Midway	Midway

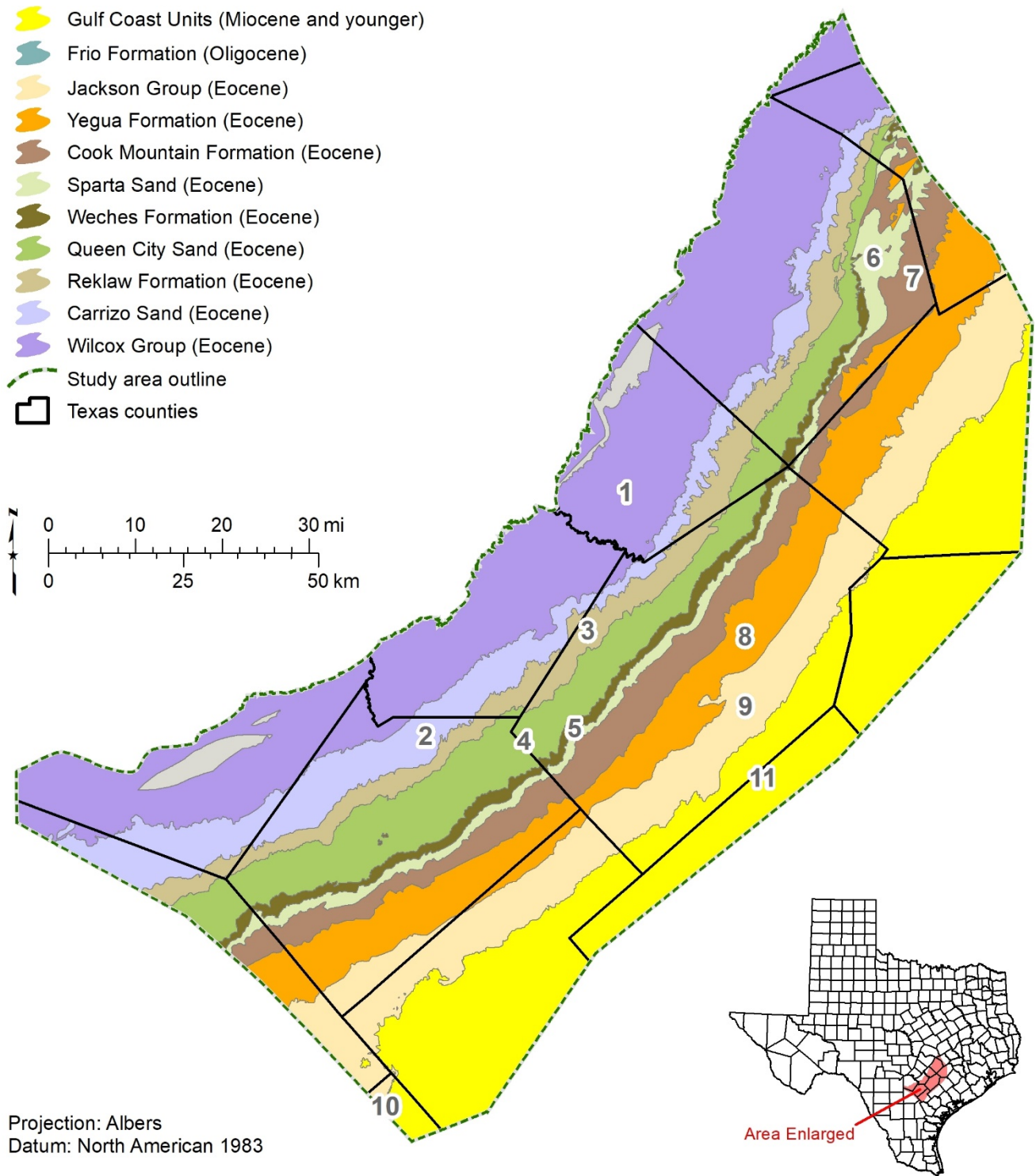


Figure 6.5-1. Modified geological formation outcrops with region codes (Table 6.5-1) interpreted from the Geologic Atlas of Texas. The surficial Quaternary formations have been removed. Figure 6.1-3 shows Geologic Atlas of Texas surficial geology.

The region code permitted automated aquifer determination analysis using sequential queries compiled in Visual Basic for Applications® within the BRACS Database. Well-screen information was compared with geological formation top and bottom depths to determine the aquifer(s) used by the water well. If well-screen information was not available, we used the total depth of the well or borehole and all aquifers present at the well site were selected from the total depth to surface. The aquifer determination technique also facilitated the assignment of sand layers to specific geological formations, allowing the tabulation and mapping of net sand and sand percent information.

Water wells in the Groundwater Database have aquifer codes assigned to them. Over the 30 years that the database has been in existence, different staff using a variety of information has assigned aquifer codes in the database. The complex stratigraphic nomenclature, changes in stratigraphic interpretation by different authors, and discontinuity of lithologic units within geological formations in the study area have led to inconsistencies in the application of aquifer codes. Wells appended to the BRACS Database from sources other than the Groundwater Database do not have aquifer codes. The aquifer determination technique solves these problems.

The stratigraphic top and bottom depths obtained from the GIS geological formation raster surfaces in the aquifer determination table were compared with the values in the geology table for quality control. We evaluated the differences between the two depth values and concluded there were a few errors, subsequently corrected, and five cases where we decided to assign the depths from the geology table (noted in the remarks field). These cases include

- 1) wells added to the project after February 2017 when the stratigraphic data was locked for GIS raster preparation,
- 2) wells where the geological formation was known to be structurally faulted,
- 3) wells where Quaternary alluvium overlies a geological formation in the outcrop area,
- 4) wells within fault zones where the raster surface could not replicate the complex geology, and
- 5) wells where the location was verified but the stratigraphic interpretation using a geophysical well log did not match the surficial mapped geology.

We received a dataset of additional geophysical well logs submitted with the Young and others (2018) draft report after the GIS surface preparation began and interpreted many of these logs to support this study and to evaluate the author's conclusions. Cases 1, 2 and 4 included many of the new wells evaluated in March 2017. The geological formation raster surfaces do not replicate the complex geology in the fault zones because of limited software capabilities and insufficient well control to adequately map the major faults, synthetic faults, and antithetic faults and determine fault offsets for each of the geological formations along the entire fault length.

6.6 Water Quality

We obtained water quality data from the Groundwater Database (TWDB, 2019b), San Antonio Water System, Gonzales Underground Water Conservation District, U.S. Geological Survey Produced Water Database (Blondes and others, 2016), published reports, raw-water sample reports from the Texas Commission on Environmental Quality public drinking water system program, and other sources. The new samples were entered into the BRACS Database.

All water quality data obtained for the study was combined into one master water quality table that contained 3,862 water quality samples from 1,971 wells. Radionuclide sample data were combined into a separate table, which included 652 water quality samples from 198 wells. Additional water quality data (for example, metals) is present in the Groundwater Database. We assigned an updated aquifer assignment for each well based on the aquifer determination task described in Section 6.5, allowing us to organize the data for each aquifer.

The master water quality table (tblBRACS_PE_sTx_MasterWaterQuality) was combined with location coordinates and exported into GIS as a point file. The water quality tables are provided as a study deliverable in the public version of the BRACS Database and table descriptions are provided in the data dictionary. Water quality data organized by aquifer as GIS files with metadata are available as deliverables in this study (Appendix, Section 13.5.2, Table 13.5.2-3).

6.6.1 Sources of dissolved minerals

Groundwater quality in an aquifer can vary greatly due to factors such as mineral composition of aquifer materials, recharge rates, spatial distribution, chemical composition of recharge waters and original connate water, historical changes with time, geochemical processes, natural and man-made discharge rates and spatial distribution, residence time, groundwater flow velocity, and anthropogenic sources.

Kreitler and others (2013) provide a good discussion of the evolution of groundwater chemistry from outcrop to downdip. Within the study area, the Wilcox and Carrizo aquifers originate as a calcium-magnesium-sulfate-chloride type groundwater in the outcrop recharge zone and evolve into a sodium-bicarbonate water downdip. The lower Wilcox Group in Bexar and Atascosa counties, however, is a sodium-sulfate type groundwater similar to the Yegua and Jackson aquifers (Kreitler and others, 2013). The Queen City and Sparta aquifers do not evolve into a sodium-bicarbonate type groundwater downdip, although the two aquifers are underlain by the Carrizo Aquifer. The water chemistry does not support the concept of significant leakage from the Carrizo into the Queen City and Sparta aquifers (Kreitler and others, 2013). The Yegua and Jackson aquifers are predominantly sodium-chloride-sulfate type groundwater. Generally, the Yegua and Jackson aquifers have higher total dissolved solids content than underlying aquifers, implying that leakage from underlying aquifers is not occurring (Kreitler and others, 2013). Kreitler and others (2013) note that their conclusions of inter-aquifer flow do not account for water chemistry changes that could occur during leakage through aquitards. Groundwater in all aquifers eventually changes into a sodium-chloride type downdip, although the distance downdip is variable.

Salinity sources can include rock-water interaction along downdip flow paths, brine upwelling from geopressured zones along growth faults (Dutton, 2016), sea salt spray, connate water, natural deposits of evaporite minerals (salts derived from evaporation of sea water), salt water intrusion, and oil and gas development.

The study area aquifers have two primary types of groundwater: meteoric and connate water. Meteoric water is sourced from precipitation and connate water is water that was trapped in the sediments during deposition. Saline water has been assumed to represent original connate water or seawater flooding during marine transgressions. A deep geopressured regime has greater than hydrostatic pressure due to compartmentalized coarser sediments encased in low-permeability clay. Faults are likely pathways for migration of deep basin brines into overlying aquifers,

providing a significant source of sodium and chloride in groundwater (Dutton, 2016; Dutton and Nicot, 2006).

6.6.2 Parameters of concern for desalination

If used for potable purposes, brackish groundwater needs to be treated (desalinated). Without treatment, brackish water can cause scaling and corrosion problems in water wells and treatment equipment and cannot be used in many industrial processes. The Texas Commission on Environmental Quality has established a secondary standard of 1,000 milligrams per liter of total dissolved solids for public water supply systems (TCEQ, 2015). Groundwater containing total dissolved solids at concentrations greater than 3,000 milligrams per liter is not suitable for irrigation without dilution or desalination and, although considered satisfactory for most poultry and livestock watering, can cause health problems at increasingly higher concentrations (Kalaswad and Arroyo, 2006).

The physical and chemical parameters of concern to desalination facilities that use reverse osmosis—the predominant desalination technology in Texas—are listed in Table 6.6.2-1. While the Groundwater Database contains sample results for most of these parameters, the amount of information available from a well can vary greatly. The TWDB does not maintain information on silt density index or turbidity from groundwater samples. If the turbidity or silt density index is high, pretreatment of the feedwater is required to avoid plugging the membranes in a reverse osmosis treatment system.

Table 6.6.2-1. Parameters of concern for desalination. The integers with a positive or negative sign indicate ion valence.

Physical parameters	Chemical parameters			
	Cations		Anions	Other
Conductivity	Al ⁺³	K ⁺¹	Cl ⁻¹	Alkalinity
pH	As ⁺³	Mg ⁺²	CO ₃ ⁻²	Boron
Silt density index	As ⁺⁵	Mn ⁺²	F ⁻¹	Dissolved oxygen
Temperature	Ba ⁺²	Na ⁺¹	HCO ₃ ⁻¹	H ₂ S
Turbidity	Ca ⁺²	NH ₄ ⁺¹	NO ₂ ⁻¹	Hardness
	Cu ⁺²	Ni ⁺²	NO ₃ ⁻¹	Pesticides
	Fe ⁺²	Si ⁺²	OH ⁻¹	Radionuclides
	Fe ⁺³	Zn ⁺²	SO ₄ ⁻²	Silica
				Total dissolved solids

6.7 Aquifer hydraulic properties

The hydraulic properties of an aquifer refer to characteristics that allow water to flow through the aquifer. Hydraulic properties include transmissivity, hydraulic conductivity, specific yield, specific capacity, drawdown, pumping rate (well yield), and storage coefficient. Lithology, porosity, cementation, fracturing, structural framework, and juxtaposition of adjacent formations all influence the flow of water within and between aquifers.

Sources of aquifer test information include TWDB aquifer test spreadsheet, the remarks table in the former Groundwater Database, TWDB and U.S. Geological Survey well schedules in the TWDB state well numbered water well records, Texas Commission on Environmental Quality

State of Texas Well Reports and public drinking water system well files, Submitted Driller’s Report Database, and selected consultant well reports. Reports with hydraulic property data incorporated into the BRACS Database include the following:

- Anders (1960): Karnes County
- Christian and Wuerch (2012): Texas
- Follett (1966; 1970): Caldwell County; Bastrop County
- HDR Engineering (2004): Gonzales County
- LBG-Guyton Associates (2013): Bexar County
- Myers (1969): Texas
- Rogers (1967): Fayette County
- Shafer (1965): Gonzales County
- Thompson (1966): Lee County

Additional information (for example, time drawdown pumping tests) is available in the Groundwater Database water well records. Specific yield data for wells located within the study area was not available.

We compiled 2,441 hydraulic property measurements from 2,293 wells in the study area and added this information to the BRACS Database table (tblBRACS_AquiferTestInformation). The aquifer determination process was used (Section 6.5) to select the aquifer(s) for each well.

We summarized records from wells that are exclusively completed in one of the five aquifers (Yegua, Sparta, Queen City, Carrizo, and Wilcox) in the study area and excluded wells screened across more than one aquifer. This led to a total of 1,600 wells with 1,714 hydraulic property measurements (Table 6.7-1). Aquifer hydraulic data for the study area is displayed in Figure 6.7-1. Aquifer properties for individual aquifers are summarized in Section 7.

Table 6.7-1. Study area aquifer hydraulic property records.

Geological formation	Number of wells	Number of records
Yegua Formation	146	148
Sparta Sand	50	50
Queen City Sand	190	191
Carrizo Sand	550	632
Wilcox Group	664	693
Total	1,600	1,714

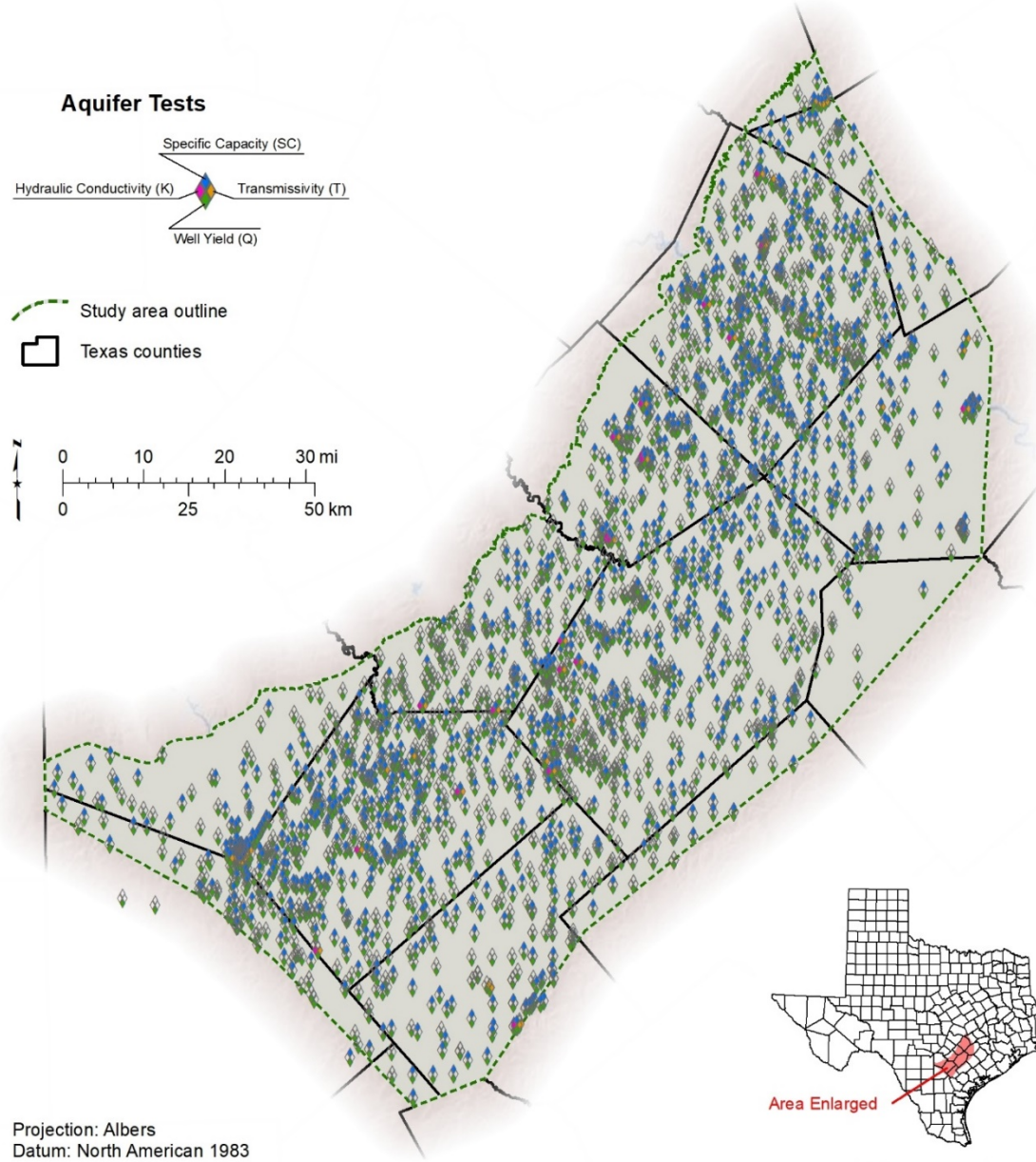


Figure 6.7-1. Study area wells with aquifer hydraulic data regardless of aquifer or combination of aquifers. Aquifer specific maps are presented in Section 7, Results.

We obtained many of the well yields from tests conducted decades ago and many well yields are from domestic, small capacity wells that may not be indicative of what a properly designed, large capacity well may be capable of producing. Users of the hydraulic property data presented in our study should evaluate the data in the proper context.

6.8 Formation porosity

Porosity is a required parameter in calculations of groundwater volume and interpreted total dissolved solids concentration. We calculated estimated total porosity of the water-bearing geological formations in the study area from geophysical well log porosity tools (density,

neutron, and sonic). Porosity used for interpreting total dissolved solids concentration should be interconnected porosity and in siliciclastic rocks total porosity equals interconnected porosity for most cases (Torres-Verdín, 2017).

Porosity information was appended to the BRACS Database table (tblGeophysicalLog_Porosity) consisting of all input and output parameters. Porosity geophysical well logs in the study area are limited in number, depth range, spatial distribution, and tool type, which affected the number of wells and depth ranges that could be interpreted. The estimated total porosity should be considered an upper limit for sands within the geological formations since clean, thick sands were preferentially selected for interpretation.

There are three types of porosity in the Tertiary siliciclastic rocks: primary pores, secondary pores, and micropores. Primary porosity is the most important control in groundwater flow within an aquifer because primary pores are connected by larger pore throats than secondary pores or micropores. Primary porosity decreases with increasing depth and temperature due to compaction and cementation (Dutton and Loucks, 2014). Primary pores are the dominant pore type in Wilcox Group sandstones at low temperatures, but at higher temperatures (greater than 250 degrees Fahrenheit) porosity consists of a mixture of all three types with secondary porosity exceeding primary porosity (Dutton and Loucks, 2014). Porosity determined using log analysis does not discriminate between the different types of pores, hence we reported estimated total porosity as opposed to measured porosity using cores or thin section analysis.

We used geophysical well logs from 34 wells and interpreted the estimated total porosity from 116 depth intervals in the Wilcox Group and the Carrizo, Queen City, Sparta, and Yegua formations (Table 6.8-1) for use in estimating salinity using geophysical well logs. We discovered and interpreted additional porosity well control during later phases of the study; this information was also appended to the BRACS Database.

Table 6.8-1. Summary of well control used for porosity versus depth correlations in the study area geological formations.

Geological formation	Number of wells	Number of measurements	R ² correlation coefficient	Linear equation
Yegua Formation	6	9	0.1468	$y = -0.0008x + 41.401$
Sparta Sand	9	11	0.0324	$y = -0.0007x + 37.592$
Queen City Sand	15	20	0.3454	$y = -0.0023x + 41.657$
Carrizo Sand	26	36	0.4445	$y = -0.0015x + 38.465$
Wilcox Group	24	40	0.6584	$y = -0.0019x + 39.839$

We selected clay- and hydrocarbon-free sand units with good caliper curves (no washouts) and, with respect to density tools, a density correction factor of less than +/- 0.2 grams per cubic centimeter (indicating logging technicians applied a minor correction for mud cake thickness). We used five techniques to interpret porosity, each technique dependent upon the type of log data available. Only geophysical well logs calibrated in sandstone units were used.

We calculated 66 neutron-density porosity measurements in the formations of interest using a concentration of shale correction. The following calculations used equations in Torres-Verdín (2017):

1. Read the apparent neutron and density in porosity units directly from the geophysical well log.
2. Calculate the shale index using gamma ray values from the sand being evaluated and a “pure” sand and “pure” shale in the same geological formation with the equation:

$$I_{sh} = \frac{\gamma_{formation} - \gamma_{sand}}{\gamma_{shale} - \gamma_{sand}}$$

where: I_{sh} = shale index

$\gamma_{formation}$ = formation sand unit gamma ray value in API units

γ_{sand} = “pure” sand unit gamma ray value in API units

γ_{shale} = “pure” shale unit gamma ray value in API units

3. Calculate the concentration of shale using the Larionov I method used for Tertiary siliciclastic rocks with the equation:

$$C_{sh} = 0.083 \cdot (2^{3.7 \cdot I_{sh}} - 1)$$

where: C_{sh} = concentration of shale

I_{sh} = shale index

4. Calculate corrected apparent neutron and density porosity values with the concentration of shale with the equations:

$$\text{cor } \phi_D = \frac{(\phi_D - C_{sh}) \cdot \phi_{D sh}}{1 - C_{sh}}$$

$$\text{cor } \phi_N = \frac{(\phi_N - C_{sh}) \cdot \phi_{N sh}}{1 - C_{sh}}$$

where: $\text{cor } \phi_D$ = corrected apparent density porosity

$\text{cor } \phi_N$ = corrected apparent neutron porosity

ϕ_D = apparent density porosity, read from geophysical well log

ϕ_N = apparent neutron porosity, read from geophysical well log

$\phi_{D sh}$ = apparent density porosity of a “pure” shale unit, read from geophysical well log

$\phi_{N sh}$ = apparent neutron porosity of a “pure” shale unit, read from geophysical well log

C_{sh} = concentration of shale

5. Calculated corrected neutron-density estimated total porosity using corrected apparent density and neutron porosity with the equation:

$$\text{cor } \phi_{N-D} = \sqrt{\frac{\text{cor } \phi_N^2 + \text{cor } \phi_D^2}{2}}$$

where: $\text{cor } \phi_{N-D}$ = corrected neutron-density porosity

$\text{cor } \phi_D$ = corrected apparent density porosity

$\text{cor } \phi_N$ = corrected apparent neutron porosity

We calculated 19 neutron-density porosity measurements in the formations of interest without using a concentration of shale correction. Five apparent density porosity measurements were read directly from the density geophysical well log. The following calculations used the equation in Torres-Verdín (2017):

1. Read the apparent neutron and density in porosity units directly from the geophysical well log.
2. Calculate neutron-density estimated total porosity using the apparent neutron and density porosity with the equation:

$$\phi_{N-D} = \sqrt{\frac{\phi_N^2 + \phi_D^2}{2}}$$

where: ϕ_{N-D} = neutron-density porosity

ϕ_D = apparent density porosity

ϕ_N = apparent neutron porosity

We calculated six porosity estimates using the density tool in units of grams per cubic centimeter and the Asquith (1982) equation:

1. Read the apparent density in units of grams per cubic centimeter directly from the geophysical well log.
2. A density total porosity was calculated using the apparent density with the equation:

$$\phi_D = \frac{\rho_m - \rho_{fm}}{\rho_m - \rho_{fl}}$$

where: ϕ_D = density porosity

ρ_m = density of the matrix, sandstone (2.65 grams per cubic centimeter)

ρ_{fl} = density of the borehole fluid is fresh mud (1 gram per cubic centimeter)

ρ_{fm} = density of the formation, read from the geophysical well log (grams per cubic centimeter)

We calculated 20 porosity estimates using the sonic (acoustic) tool interval transit time in units of microseconds per foot and the Asquith (1982) equation:

1. Read the sonic interval transit time in units of microseconds per foot directly from the geophysical well log.
2. A sonic total porosity was calculated using the sonic interval transit time with the equation:

$$\phi_s = \frac{1}{C} \cdot \frac{\Delta_{Tfm} - \Delta_{Tm}}{\Delta_{Tfl} - \Delta_{Tm}}$$

where: ϕ_s = sonic porosity

Δ_{Tfm} = time of formation is read from the geophysical well log in microseconds per foot

Δ_{Tm} = time of matrix in sandstone (55.5 microseconds per foot)

Δ_{Tfl} = time of borehole fluid in fresh mud (189 microseconds per foot)

C = compaction factor = $\frac{\Delta_{Tsh} \cdot C_n}{100}$

Δ_{Tsh} = time of adjacent shale unit in microseconds per foot

C_n = constant which is normally 1 (Hilchie, 1978)

The neutron – density estimated porosity values are more reliable than the individual density tool or sonic tool estimates. The sonic tool is less reliable in unconsolidated sediment and required a compaction correction factor based on an adjacent shale unit. The estimated sonic porosity compared favorably with neutron – density porosity values in the same or nearby wells, however these should be used with caution.

Concentration of shale calculations were especially useful in selecting the cleanest (clay free) sands possible for interpretation. Sands selected for interpretation may appear to meet initial criteria until a “clean” sand and “pure” shale was located within the same geological formation. We discovered that clean, clay-free sands are relatively uncommon and most sands have small to large amounts of interbedded clay. The presence of clay will affect porosity calculations and cause the resistivity to decrease. It was assumed most of the sands contained interbedded clay. We did not have detailed petrographic analysis of core to support the identification of and correction for grain-coating (pore-filling) clay that is a product of diagenesis. This type of clay has a significant impact on calculations using resistivity logs (Torres-Verdín, 2017) and is known to occur in the Tertiary clastic sequences at deep depth (for example, Dutton and others, 2016). Its occurrence in the shallower parts of aquifers in the study area is not known.

We plotted porosity with depth using scatter plots for the Wilcox Group, Carrizo Sand, and Queen City Sand (Figures 6.8-1 through 6.8-3). Porosity estimates for the Sparta Sand and Yegua Formation are extremely limited and the poor correlation coefficients reflect the limited number of samples in the scatter plots. We calculated an average porosity value for the Sparta and Queen City formations (34 and 39 percent, respectively) due to limited porosity values and poor regressions. Total porosity was used in the calculations for total dissolved solids concentration as described in Section 6.9.

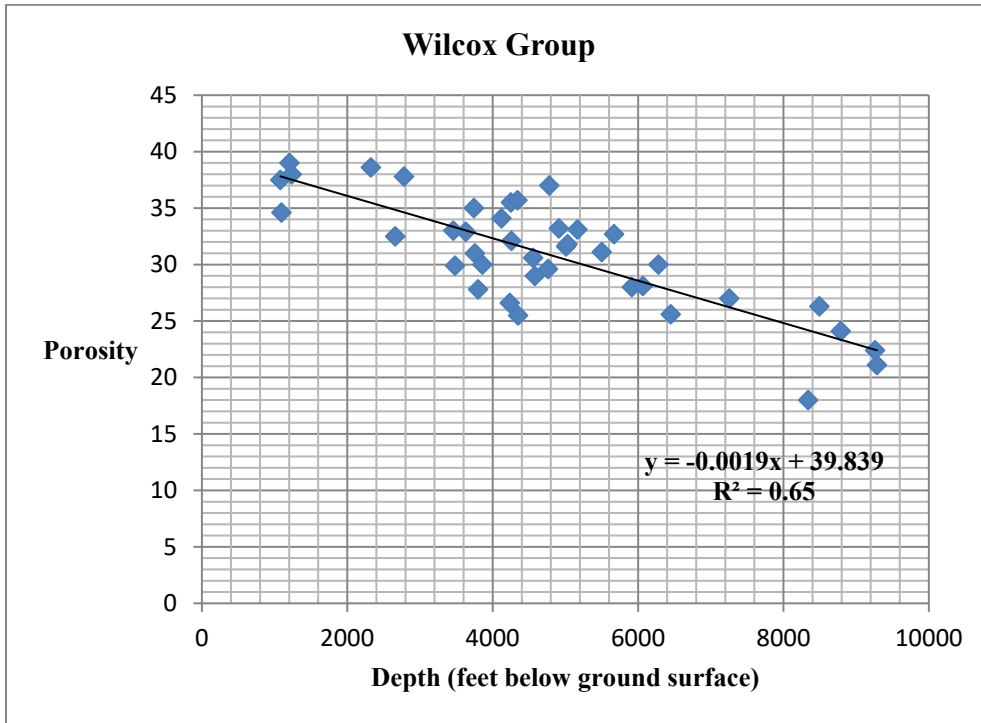


Figure 6.8-1. Wilcox Group estimated total porosity versus depth plotted on a scatter plot. The correlation produced a linear trend line with a regression R^2 of 0.65 and the equation $y = -0.0019x + 39.839$ to convert depth (x) to porosity (y). Data consists of 40 measurements from 24 wells.

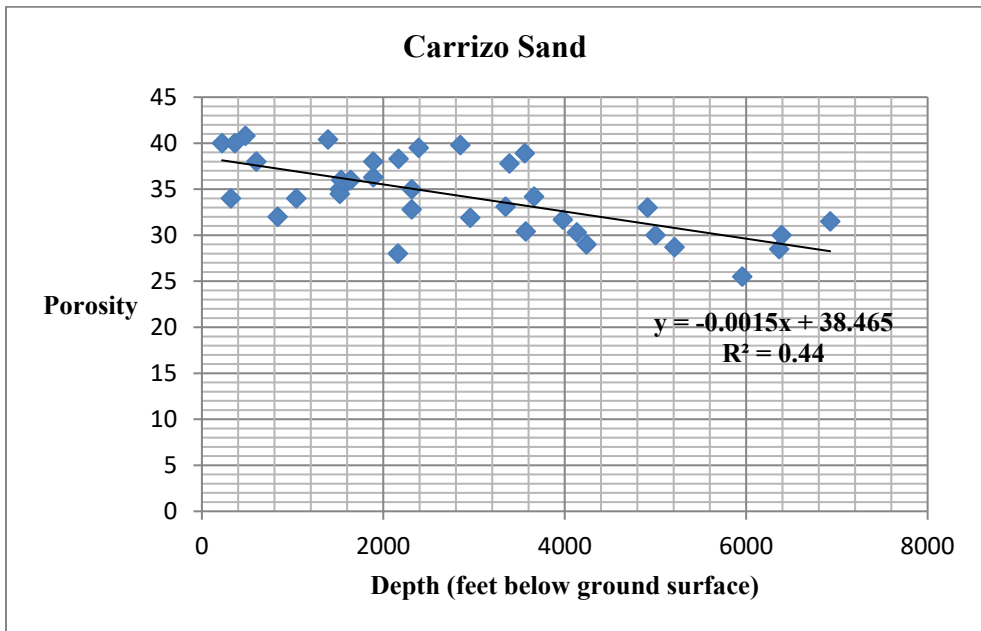


Figure 6.8-2. Carrizo Sand estimated total porosity versus depth plotted on a scatter plot. The correlation produced a linear trend line with a regression R^2 of 0.44 and the equation $y = -0.0015x + 38.465$ to convert depth (x) to porosity (y). Data consists of 36 measurements from 25 wells.

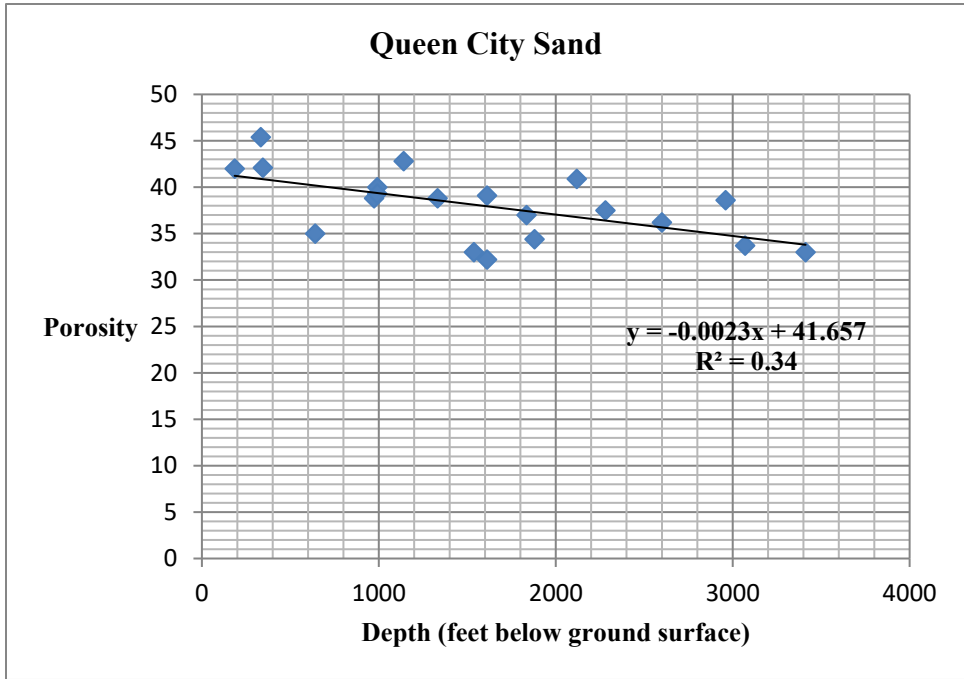


Figure 6.8-3. Queen City Sand estimated total porosity versus depth plotted on a scatter plot. The correlation produced a linear trend line with a regression R^2 of 0.34 and the equation $y = -0.0023x + 41.657$ to convert depth (x) to porosity (y). Data consists of 20 measurements from 15 wells.

We also plotted Wilcox Group porosity with formation temperature (Figure 6.8-4) to compare the results with those determined in Dutton and Loucks (2014). Wilcox Group porosity in this study area is less than 250 degrees Fahrenheit, whereas Dutton and Loucks (2014) have data exceeding 400 degrees Fahrenheit. Our data are similar to that of Dutton and Loucks (2014) for their upper Texas coast region data. The power law curve generated using our data does not trend at the higher temperatures, however, because we lack the deep, high temperature data. Dutton and Loucks (2014) also used point counts of porosity (primary, secondary, and micro pores) using thin sections and porosity and permeability data from cores in their study as compared to ours using log analysis.

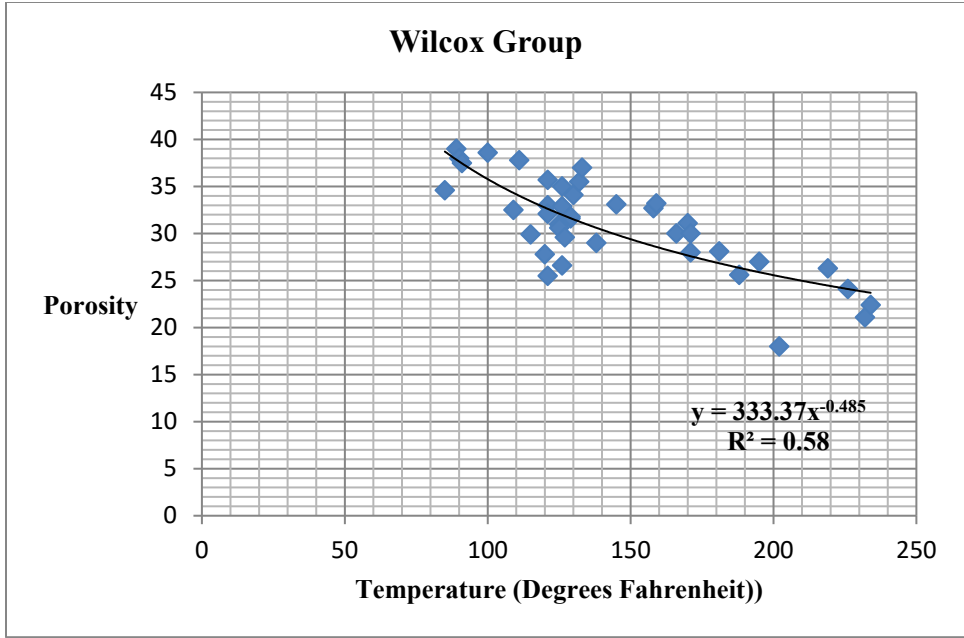


Figure 6.8-4. Wilcox Group estimated total porosity versus temperature plotted on a scatter plot. The correlation produced a power law trend line with a regression R^2 of 0.58 and the equation $y = 333.37x^{-0.485}$ to convert temperature (x) to porosity (y). Data consists of 40 measurements from 24 wells.

Formation porosity data was compiled from Core Laboratories (1972, volume 3) for geological formations within the study area and appended to a BRACS Database table (tblBracs_Formation_Porosity_R157). The porosity data was acquired from many sources associated with oil and gas exploration and production well fields. The data cannot be back-referenced to a specific well or series of wells and was often averaged by depth and porosity to reduce the number of data points.

Use of this porosity data is therefore limited to the following qualitative evaluation: Porosity data from the Carrizo Sand (11 of 35 records) indicates the porosity from Core Laboratories averages 5 percent lower than that calculated by the linear equation for the Carrizo Sand. Porosity data from the Wilcox Group (24 of 35 records) indicates the porosity from Core Laboratories averages 7 percent lower than that calculated by the linear equation for the Wilcox Group.

The differences can be attributed to factors including the uncertainty of the exact depth, location, lithology, stratigraphy, and porosity, and method of measurement.

6.9 Geophysical well log analysis for interpreted total dissolved solids concentration

We used geophysical well logs to calculate an interpreted total dissolved solids concentration across the entire depth range of the study area aquifers. We used existing groundwater quality data to determine groundwater quality correction factors.

Estepp (1998, 2010) provided six methods for interpreting total dissolved solids concentration in a formation using geophysical well logs. Each of the methods has advantages and disadvantages with respect to the type of logging tool, input parameters, assumptions, geological formations

being assessed, and expected range of groundwater salinity. Calculating groundwater total dissolved solids concentration is complicated because the geologic environment is complex and the majority of the existing geophysical well logs were developed for petroleum exploration and production where the groundwater is dominated by sodium and chloride ions. Application of these logging tools and techniques for fresh and brackish aquifers poses problems that are addressed in different ways by each of the six methods. We selected the R_{WA} (resistivity water apparent) Minimum Method for this project because it performed reasonably well with the available data and assumptions.

The R_{WA} Minimum Method is based on Archie’s equation (1942):

$$R_o = R_w \cdot \frac{a}{\phi^m} \cdot \frac{1}{S_w^n}$$

- where:
- R_o = resistivity of the formation in ohm-meter
 - R_w = resistivity of water in ohm-meter
 - a = Winsauer factor (dimensionless)
 - ϕ = porosity in percent
 - m = cementation exponent (dimensionless)
 - S_w = water saturation
 - n = saturation exponent

In a 100 percent water saturated formation ($S_w = 100$ percent), as would be expected in a fresh or brackish aquifer, the water saturation factor (n) is one (1) so this factor can be eliminated from the equation. The Winsauer factor (a ; Archie’s original equation did not contain this factor) is often reported as one (Estep, 1998; Torres-Verdín, 2017), further simplifying the equation. Rearranging the equation and solving for R_w :

$$R_w = R_o \cdot \phi^m$$

The resistivity of the formation is determined with a deep investigation resistivity logging tool and is a combination of formation rock matrix resistivity and groundwater resistivity. The resistivity of the formation is the result of several parameters: resistivity of the formation minerals, resistivity of groundwater and its composition, porosity, cementation of sediment grains, sediment grain size, and surface conductance on mineral grains (Alger, 1966). Obtaining some of these parameters is not possible using only a geophysical well log. Hence, some information for the parameters, such as the cementation exponent (m), are not available in the study area. To solve the calculations, we estimated some of these parameters based on similar geologic conditions existing elsewhere or using best professional judgment.

Relatively thick, granular, clay-free, hydrocarbon-free, clean sand units can be used for interpretation. Most formation rock matrix, when dry, will have infinitely high resistivity (this does not include formations containing metal ore deposits). Clay within a sand unit, however, contributes to lower resistivity because it contains interstitial water containing ions. Clay can occur in the form of laminar, grain coating or pore filling, and structural (original mineral grains diagenetically replaced with clay). The effect of clay on a resistivity log depends on the mineralogy, amount, and form. Hydrocarbons do not conduct electrical current. The presence of

hydrocarbons in sand will show elevated resistivity and a decrease in spontaneous potential response (Hilchie, 1978; Schlumberger, 1987).

Electric current will only flow through the interstitial water within the interconnected pore structure, and then only if the water contains dissolved minerals (Schlumberger, 1987). To conduct a current the ion must move through the solution to transfer the charge (Hem, 1985). Groundwater resistivity is a function of ion concentration, charge, size, interaction and interference, mobility, and the way it interacts with the water (solvent) (Hem, 1985; Jones and Buford, 1951). Ionic mobility is decreased as the concentration increases due to interference and interaction among the ions (Hem, 1985). Groundwater resistivity varies inversely with dissolved mineral concentration, but this is not a linear (straight line) relationship when graphed. Resistivity decreases with increasing ion concentrations although the change in resistivity varies between the ions (Hem, 1985).

6.9.1 R_{WA} Minimum Method input parameters

The R_{WA} Minimum Method requires several input parameters to calculate an interpreted total dissolved solids value (Table 6.9.1-1).

Table 6.9.1-1. Input parameters for the R_{WA} Minimum Method.

Parameter	Symbol	Units
Depth total	Dt	Feet
Depth formation	Df	Feet
Temperature surface	Ts	Degrees Fahrenheit
Temperature bottom hole	Tbh	Degrees Fahrenheit
Deep resistivity	Ro	Ohm-meter
Porosity	φ	Percent
ct conversion factor	ct	dimensionless
Cementation exponent	m	dimensionless
Water quality correction factor	R _{wcRw}	dimensionless

R_{WA} Minimum Method parameters are described in detail in the following sections. If a parameter could not be measured, we made a reasonable assumption based on the geology of the formation being investigated. Each of these parameter values is recorded in the BRACS Database for each well analysis.

Depth total

The total measured depth of the well is required to calculate the formation temperature at the depth of formation. If a well was logged during multiple runs, with each run representing a different depth range, the total depth of the logging run applicable to the depth of investigation must be used.

Depth formation

Typically, the measured depth of the middle of the thick, shale-free, water-saturated sand unit is obtained from the geophysical well log and recorded in the BRACS Database table (tblGeophysicalLog_WQ). The reference datum is the kelly bushing height, if known. The depth is not corrected for kelly bushing height in the database table (kelly bushing depth corrections

are made prior to GIS analysis of well points when mapping the three-dimensional limits of the salinity classes). The depth of the formation that is being investigated is required to calculate the formation temperature. The thickness of the evaluated sand unit and geologic formation are also recorded in the BRACS Database.

Temperature surface

Well site surface temperature is required to calculate the formation temperature at the depth of investigation. Mean annual surface temperature data is used for geothermal gradient calculations (Doveton, 1999; Dutton and Loucks, 2014; Forrest and others, 2005). Temperature records from 1951-1980 compiled by Larkin and Bomar (1983) indicate mean annual surface temperature in the study area ranged from 68 to 70 degrees Fahrenheit. The use of the Larkin and Bomar (1983) data works well with logging performed during this same time period. Most of the interpreted total dissolved solids calculations in this study used a surface temperature value of 69 degrees Fahrenheit.

Temperature bottom hole

Bottom hole temperature is required to calculate the formation temperature at the depth of investigation. The bottom hole temperature, along with surface temperature, are critical inputs and have an impact on the calculated formation temperature, resistivity correction at the depth of investigation, and subsequent calculation of interpreted total dissolved solids.

Bottom hole temperature is usually found on the geophysical well log header (bottom hole temperature, BHT; maximum temperature; maximum recorded temperature, MRT) either as a separate value or associated with a mud resistivity temperature and is collected with a maximum temperature recorder. If a well was logged during multiple runs, with each run representing a different depth range, the bottom hole temperature of the logging run applicable to the depth of investigation must be used for log analysis of the geological formations in this depth range. Bottom hole temperatures are valid if the temperature recorded during logging was measured after the drilling fluids in the bottom of the hole equilibrated with the deepest geological formation (Blackwell and others, 2010; Forrest and others, 2005). Drilling mud circulated during the drilling of the well is used to cool and lubricate the drill bit, stabilize the borehole wall, and carry formation cuttings to the surface. The formation can return to equilibrium with the mud after circulation has ceased based on a number of factors including (1) thermal conductivity of the formation, (2) pore fluid movement, (3) drilling fluid invasion, (4) drilling conditions, (5) mud temperature, and (6) time since mud circulation. The drilling mud can impact the formation temperature by cooling the formation at deep depths and possibly warm the formation at shallow depths. Bottom hole temperatures on geophysical well log headers are commonly cooler than equilibrium formation temperatures.

Corrections to the bottom hole temperature can be performed using a variety of techniques. The correction technique chosen for this study was a modification of the Harrison correction by Southern Methodist University (SMU-Harrison correction) reported in Blackwell and others (2010) and is based on a depth correction. Their study evaluated geothermal gradients east of the Interstate 35 corridor in Texas. Temperature correction is not made for wells with a total depth of less than 3,000 feet. Between 3,000 and 12,900 feet in depth, the following formula is used:

$$C_{cf} = (-16.51213476 + (0.01826842109 * D_t)) - (0.000002344936959 * D_t^2)$$

where:

C_{cf} = correction factor in degrees Centigrade

D_t = depth total in meters below ground surface

The correction factor is added to the bottom hole temperature from the geophysical log header (converted to units of degrees Centigrade) and then the final temperature is converted to degrees Fahrenheit for use in log analysis. Wells drilled deeper than 12,900 feet have an additional correction factor of 0.05 degrees Fahrenheit per 500 feet of depth added to the maximum correction value of 34.3 degrees Fahrenheit at 12,900.

If the bottom hole temperature is missing from the log header, a bottom hole temperature can be calculated using the well's surface temperature and well depth (or depth of logging run) with a geothermal gradient calculated from the log of a nearby well. Calculated bottom hole temperatures are noted in the BRACS Database table (tblGeophysicalLog_Header_LogRuns) with supporting information.

Deep resistivity

The resistivity of the geological formation being investigated is determined with a deep investigative logging tool. Two logging tools were utilized for deep resistivity measurement: the induction log and the deep normal resistivity log. The type of tool used is recorded in the BRACS Database.

The resistivity value is selected from clean, shale-free sand that is greater than 10 feet thick. Thin beds or units containing shale will not provide a meaningful resistivity value. Care must be exercised in determining the correct resistivity value by checking the tool scale, over-range scale, potential scale changes with depth or logging run, and line symbol(s) for the appropriate tool. Older logs and logs of poor quality present particular challenges.

Porosity

The porosity variable has a significant impact on the interpreted total dissolved solids calculations. Porosity data from interpretation of geophysical well logs is discussed in Section 6.8.

We used the total porosity data in our calculations from a well or adjacent well if it had porosity tools. The remainder of the wells used the porosity – depth regression equations prepared for the Wilcox Group, Carrizo Sand, and the Queen City Sand. Sparta and Yegua formation interpretation could not use the regression equations due to poor results, so an average total porosity was determined across the study area depth ranges for these formations (Table 6.9.1-2).

Table 6.9.1-2. Estimated total porosity for each study area geological formation used for total dissolved solids calculations and groundwater volume calculations. Porosity = y and depth below ground surface = x in the regression equations.

Geological formation	Total porosity
Yegua Formation	39
Sparta Sand	34
Queen City Sand	$y = -0.0023x + 41.657$
Carrizo Sand	$y = -0.0015x + 38.465$
Wilcox Group	$y = -0.0019x + 39.839$

CT conversion factor

The conversion factor *ct* represents total dissolved solids concentration divided by specific conductance and is determined empirically from water quality samples. The *ct* factor is used in the *R_{WA}* Minimum Method to convert conductivity to interpreted total dissolved solids concentration. The *ct* factor has a range of 0.55 to 0.75 for waters of ordinary composition up to total dissolved solids concentration of a few thousand milligrams per liter (Hem, 1985). Water with anions dominated by bicarbonate and chloride will be near the lower end of this range and water with anions dominated by sulfate will have water near the high end of or even beyond this range (Hem, 1985). Waters saturated with gypsum or having high concentrations of silica may have a *ct* factor as high as 1 (Hem, 1985). Because groundwater quality can vary between aquifers and within an aquifer as the ion concentrations evolve, the *ct* factor should be considered valid for a specific aquifer in a specific area.

The *ct* factor used for interpreting geophysical well logs can be derived with three different approaches. First, *ct* factors for a given geological formation in a specific area (for example, a county) can be collected and averaged for a representative *ct*. Second, water quality samples can be averaged and organized per geological formation, per area, per range of total dissolved solids concentration to develop representative water quality parameters. We used this approach to extrapolate water quality parameters for geological formations without a nearby water quality sample. Third, one can use the *ct* factor from the nearest well with water quality data for a given geological formation. We used this approach to calibrate geophysical well logs with water quality data for a specific geological formation. Refer to Tables 6.9.1-4 through 6.9.1-8 for *ct* factors used in this study.

Cementation exponent

The cementation exponent (*m*) is a dimensionless parameter that is estimated from detailed core analysis (Torres-Verdín, 2017) or can be determined empirically if all the other parameters are known with certainty (Estepp, 1998). We did not have this type of information in the study area, so we used a constant value of *m* = 1.75. The cementation exponent is a function of grain size, grain size distribution, grain sorting, pore tortuosity, and grain lithology. The importance of the cementation exponent is based on the path an electric current takes through the geological formation. Cemented sands have a higher cementation exponent relative to unconsolidated sands. Tables of cementation exponents have been produced in studies across the country (Carothers, 1968; Carothers and Porter, 1970; Kwader, 1986) and the range of values for clean sand with varying degrees of cementation is quite large. The value of 1.75 is within the range of slightly to moderately cemented sandstones (Torres-Verdín, 2017).

Water quality correction factor

Geophysical well logs were developed originally for oil and gas exploration. Typical geophysical well log analysis assumes the formation water is dominated by sodium and chloride ions. Evaluating geophysical well logs in fresh and brackish aquifers requires a water quality correction factor applied. Individual groundwater ions have different resistivity values. For example, bicarbonate contributes more resistivity than an equal weight of chloride in a solution (Alger, 1966; Jones and Buford, 1951; Schlumberger, 1979, 1985). This means that a sand unit containing groundwater with a high bicarbonate concentration will have a larger deep resistivity value on a geophysical well log than the same sand unit containing an equivalent concentration of chloride. This sand unit would need to have a water quality correction factor applied to adjust the resistivity value to provide a more realistic interpreted total dissolved solids concentration. Estep (1998) proposed fixed correction factors (for example, 1.75 for high bicarbonate groundwater) when using the R_{WA} Minimum Method, based on a value obtained from Alger (1966). There are two problems with using fixed correction factors for groundwater interpretation. First, this may work satisfactorily for water with high bicarbonate concentration but does not address groundwater with intermediate bicarbonate concentration or waters with mixed constituents, including sulfate. Second, Alger (1966) provided the following explanation but did not provide supporting documentation of how the value of 1.75 was determined:

“The HCO_3 ion contributes only 27 percent as much conductivity as an equal weight of Cl^- ion. Or, in other words, the R_w of an $NaHCO_3$ solution is 1.75 times greater than R_w of an Cl^- solution having the same Na^+ concentration.”

Further complicating the use of fixed correction factors (and estimating salinity in general) may be the presence of ion complexes in groundwater. Miller and others (1988) state:

“Ion associations or complexes form in natural waters (Stumm and Morgan, 1981) particularly between the alkaline-earth cations (Ca^{2+} , Mg^{2+} , and Sr^{2+}) and the sulfate (SO_4^{2-}), carbonate (CO_3^{2-}), and bicarbonate (HCO_3^-) anions. The conductivity of a solution is reduced by this effect, because the complexes are uncharged or less charged than the parent ions and contribute little or nothing to the conductivity of the solution. Complexes between alkaline-earth cations and the bicarbonate anion (HCO_3^-) predominantly form compounds with a single plus charge, which contributes to solution conductivity. The reduction in free forms of the parent ions by complexation needs to be considered. For most dilute natural waters, however, the conductivity of the complex can be ignored because the relative amount of complex formed is small and the mobility of the complex is low compared to that of the free ions.”

We modified a technique first used in Meyer and others (2014) for this study using a correction factor based on mixed ion groundwater. A method to adjust cation and anion concentrations to obtain an equivalent sodium chloride concentration has been used in oilfield log analysis applications. Cation and anion concentrations are multiplied with a weighting multiplier specific to the ion and total dissolved solids concentration of the water sample and added together to obtain an equivalent sodium chloride concentration. Weighting multipliers from Chart Gen-8, Resistivities of Solutions (Schlumberger, 1979; 1985) were used.

Water quality sample total dissolved solids concentration is divided by the equivalent sodium chloride concentration to determine the water quality correction factor (R_{wcRw}). This method has

five drawbacks. First, weighting multipliers are not available for fluoride, strontium, and nitrate, which are used to calculate total dissolved solids concentration. Therefore, the equivalent sodium chloride concentration is lower than it should be if these constituents are present and the resulting resistivity correction factor is slightly larger than it should be. Second, many older water quality analyses have a combined sodium and potassium concentration so the correction for potassium is not possible. Potassium tends to have a very small concentration in groundwater (except for groundwater containing dissolved potassium-bearing evaporite), so this should not pose a significant problem. Third, many water quality analyses prior to 1960 had sodium and potassium calculated rather than measured (Hem, 1985). This can cause errors if other species were not identified or inaccuracies of other analyses were made. Fourth, many older water quality analyses failed to measure each constituent such as sodium. These samples are noted in the master water quality table for the study. The total dissolved solids concentration was obtained by drying the sample and sodium was back-calculated as the missing constituent. Fifth, Chart Gen-8 (Schlumberger, 1979; 1985) consists of separate, complex curves for each constituent. To support automated processing in this study, the Chart Gen-8 weighting multipliers were manually extracted from the midpoint between distinct intervals of total dissolved solids concentration and loaded into a BRACS Database table (tblLkCf_NaClWeightingMultiplier). This simplification was made to support automated calculations and may introduce slight errors in the calculations, however manually determining values from the chart and calculating a correction factor for each chemical sample was considered impractical.

We applied these correction factors to pre-defined intervals of total dissolved solids concentration based on the assumption that individual ion constituent concentrations will vary as total dissolved solids concentration increases within a geological formation. All water quality samples within the project area were grouped by geological formation and each chemical constituent was averaged within defined intervals of total dissolved solids concentration. This data is presented for each geological formation (Wilcox Group; Carrizo, Queen City, Sparta and Yegua formations) in Tables 6.9.1-4 through 6.9.1-8. Empty cells in the tables represent null values.

During analysis of geophysical well logs, the formation deep resistivity value serves as a guide to selecting appropriate ct and sodium chloride correction factors based on an iterative approach. Since groundwater resistivity and total dissolved solids concentration are inversely related, a low deep resistivity value requires input parameters from a high total dissolved solids interval and vice versa. If the calculated interpreted total dissolved solids concentration does not match the input parameter total dissolved solids interval, input parameters of a lower or higher interval are tested until satisfactory results are obtained. Because the tables are based on actual water quality data in the study area, each interval of total dissolved solids concentration may not have data – this is especially true as salinity increases. If a defined total dissolved solids concentration interval is lacking values, the next appropriate interval of values may be selected. We assume this is reasonable since water quality changes as groundwater flows from outcrop to downdip and the concentration of different constituents may be different for each geologic formation.

Limitations of this method include (1) nonexistence of water quality data for many geological formations with elevated total dissolved solids concentration; (2) some intervals of total dissolved solids are represented by one to a few samples, some of which may not occur in the same geologic setting being investigated; (3) water quality samples with elevated salinity are

difficult to analyze in the lab; (4) water quality data from many wells lacked well screen information, making it difficult or impossible to determine the correct aquifer so it was not used; and (5) many wells were completed in multiple aquifers and this data was not used.

We assigned the default ct parameter equal to 0.56 and the sodium chloride equivalent correction factor (R_{wcrw}) equal to 1 (Schlumberger, 1985, Chart GEN-8) when we encountered extremely low formation resistivity (elevated salinity) and we lacked water quality sample data in the area. A sodium chloride correction factor of one (1) at high total dissolved solids concentrations assumes the cations and anions are dominated by sodium and chloride (Schlumberger, 1985, Chart GEN-8).

Table 6.9.1-4. Wilcox Group groundwater quality data organized by selected intervals of total dissolved solids concentration.

TDS low	TDS high	Number records	TDS average	ct factor	R_{wcrw}	Ca	Mg	Na	HCO ₃	SO ₄	Cl
0	499	255	332	0.54	1.24	51	11	60	213	46	57
500	999	184	706	0.57	1.25	70	20	168	356	142	128
1,000	1,999	90	1,333	0.58	1.22	73	25	388	462	282	326
2,000	2,999	15	2,316	0.59	1.19	292	68	451	498	548	709
3,000	3,999	3	3,669	0.56	1.16	338	76	1,029	1013	330	1,397
4,000	4,999 ³	1	4,387	0.53	1.32	514	215	660	818	1788	808
5,000	5,999	0	-	-	-	-	-	-	-	-	-
6,000	6,999	0	-	-	-	-	-	-	-	-	-
7,000	7,999	0	-	-	-	-	-	-	-	-	-
8,000	8,999	0	-	-	-	-	-	-	-	-	-
9,000	9,999	1	9,006	-	1.09	33	30	3,499	2053	7	4,428
10,000	14,999	0	-	-	-	-	-	-	-	-	-
15,000	19,999	0	-	-	-	-	-	-	-	-	-
20,000	24,999	0	-	-	-	-	-	-	-	-	-
25,000	29,999	0	-	-	-	-	-	-	-	-	-
30,000	34,999	0	-	-	-	-	-	-	-	-	-
35,000	39,999	0	-	-	-	-	-	-	-	-	-
40,000	44,999	0	-	-	-	-	-	-	-	-	-
45,000	49,999	0	-	-	-	-	-	-	-	-	-

Notes:

All constituents are reported in milligram per liter, unless indicated.

Each constituent is averaged from all samples (number records) within this interval.

Empty cells in the table represent null values.

The factors in the 4,000 to 4,999 TDS interval were not used. The well is 20 feet deep with abnormally high sulfate.

TDS = Total dissolved solids interval

Number records = Number of water quality sample records

ct factor = Total dissolved solids / specific conductance, dimensionless

R_{wcrw} = Sodium chloride equivalent water quality correction factor, dimensionless

Ca = Calcium

Mg = Magnesium

Na = Sodium

K = Potassium

HCO₃ = Bicarbonate

SO₄ = Sulfate

Cl = Chloride

Table 6.9.1-5. Carrizo Sand groundwater quality data organized by selected intervals of total dissolved solids concentration.

TDS low	TDS high	Number records	TDS average	ct factor	R _{wcRw}	Ca	Mg	Na	HCO ₃	SO ₄	Cl
0	499	425	276	0.54	1.27	32	6	64	200	34	36
500	999	94	662	0.55	1.37	24	7	230	483	68	91
1,000	1,999	17	1,369	0.55	1.33	38	10	503	953	75	260
2,000	2,999	2	2,280	0.58	1.42	3	2	961	2,008	20	282
3,000	3,999	0	-	-	-	-	-	-	-	-	-
4,000	4,999	1	4,571	-	1.13	0	1	1,867	1,634	0	1,900
5,000	5,999	1	5,895	0.57	1.12	7	1	2,410	1,733	35	2,590
6,000	6,999	0	-	-	-	-	-	-	-	-	-
7,000	7,999	0	-	-	-	-	-	-	-	-	-
8,000	8,999	0	-	-	-	-	-	-	-	-	-
9,000	9,999	0	-	-	-	-	-	-	-	-	-
10,000	14,999	0	-	-	-	-	-	-	-	-	-
15,000	19,999	0	-	-	-	-	-	-	-	-	-
20,000	24,999	0	-	-	-	-	-	-	-	-	-
25,000	29,999	0	-	-	-	-	-	-	-	-	-
30,000	34,999	1	34,467	-	1.01	361	83	12,537	651	13	21,000
35,000	39,999	0	-	-	-	-	-	-	-	-	-
40,000	44,999	0	-	-	-	-	-	-	-	-	-
45,000	49,999	1	48,644	-	1.02	430	97	21,000	320	750	26,000

Notes:

- All constituents are reported in milligram per liter, unless indicated.
- Each constituent is averaged from all samples (number records) within this interval.
- Empty cells in the table represent null values.
- TDS = Total dissolved solids interval
- Number records = Number of water quality sample records
- ct factor = Total dissolved solids / specific conductance, dimensionless
- R_{wcRw} = Sodium chloride equivalent water quality correction factor, dimensionless
- Ca = Calcium
- Mg = Magnesium
- Na = Sodium
- K = Potassium
- HCO₃ = Bicarbonate
- SO₄ = Sulfate
- Cl = Chloride

Table 6.9.1-6. Queen City Sand groundwater quality data organized by selected intervals of total dissolved solids concentration.

TDS low	TDS high	Number records	TDS average	ct factor	R _{wcRw}	Ca	Mg	Na	HCO ₃	SO ₄	Cl
0	499	35	335	0.54	1.23	39	9	72	183	55	63
500	999	61	686	0.56	1.22	69	21	146	282	181	122
1,000	1,999	6	1,224	0.62	1.25	110	41	245	279	504	179
2,000	2,999	2	2,272	0.52	1.25	190	75	497	395	876	438
3,000	3,999	3	3,420	0.57	1.11	140	48	1,050	205	623	1,450
4,000	4,999	1	4,345	0.5	1.14	15	12	1,607	682	704	1,654
5,000	5,999	0	-	-	-	-	-	-	-	-	-
6,000	6,999	0	-	-	-	-	-	-	-	-	-
7,000	7,999	0	-	-	-	-	-	-	-	-	-
8,000	8,999	0	-	-	-	-	-	-	-	-	-
9,000	9,999	0	-	-	-	-	-	-	-	-	-
10,000	14,999	0	-	-	-	-	-	-	-	-	-
15,000	19,999	0	-	-	-	-	-	-	-	-	-
20,000	24,999	0	-	-	-	-	-	-	-	-	-
25,000	29,999	0	-	-	-	-	-	-	-	-	-
30,000	34,999	0	-	-	-	-	-	-	-	-	-
35,000	39,999	0	-	-	-	-	-	-	-	-	-
40,000	44,999	0	-	-	-	-	-	-	-	-	-
45,000	49,999	0	-	-	-	-	-	-	-	-	-

Notes:

All constituents are reported in milligram per liter, unless indicated.

Each constituent is averaged from all samples (number records) within this interval.

Empty cells in the table represent null values.

TDS = Total dissolved solids interval

Number records = Number of water quality sample records

ct factor = Total dissolved solids / specific conductance, dimensionless

R_{wcRw} = Sodium chloride equivalent water quality correction factor, dimensionless

Ca = Calcium

Mg = Magnesium

Na = Sodium

K = Potassium

HCO₃ = Bicarbonate

SO₄ = Sulfate

Cl = Chloride

Table 6.9.1-7. Sparta Sand groundwater quality data organized by selected intervals of total dissolved solids concentration.

TDS low	TDS high	Number records	TDS average	ct factor	R _{wcRw}	Ca	Mg	Na	HCO ₃	SO ₄	Cl
0	499	6	355	0.5	1.16	42	11	74	129	71	89
500	999	12	738	0.56	1.21	39	11	213	248	193	154
1,000	1,999	5	1,298	0.53	1.16	87	27	392	262	311	352
2,000	2,999	1	2,112	0.62	1.14	188	110	388	168	600	730
3,000	3,999	0	-	-	-	-	-	-	-	-	-
4,000	4,999	0	-	-	-	-	-	-	-	-	-
5,000	5,999	0	-	-	-	-	-	-	-	-	-
6,000	6,999	2	6,508	-	1.05	14.3	12.2	2465	937	0	3,543
7,000	7,999	0	-	-	-	-	-	-	-	-	-
8,000	8,999	0	-	-	-	-	-	-	-	-	-
9,000	9,999	0	-	-	-	-	-	-	-	-	-
10,000	14,999	0	-	-	-	-	-	-	-	-	-
15,000	19,999	0	-	-	-	-	-	-	-	-	-
20,000	24,999	0	-	-	-	-	-	-	-	-	-
25,000	29,999	0	-	-	-	-	-	-	-	-	-
30,000	34,999	0	-	-	-	-	-	-	-	-	-
35,000	39,999	0	-	-	-	-	-	-	-	-	-
40,000	44,999	0	-	-	-	-	-	-	-	-	-
45,000	49,999	0	-	-	-	-	-	-	-	-	-

Notes:

All constituents are reported in milligram per liter, unless indicated.

Each constituent is averaged from all samples (number records) within this interval.

Empty cells in the table represent null values.

TDS = Total dissolved solids interval

Number records = Number of water quality sample records

ct factor = Total dissolved solids / specific conductance, dimensionless

R_{wcRw} = Sodium chloride equivalent water quality correction factor, dimensionless

Ca = Calcium

Mg = Magnesium

Na = Sodium

K = Potassium

HCO₃ = Bicarbonate

SO₄ = Sulfate

Cl = Chloride

Table 6.9.1-8. Yegua Formation groundwater quality data organized by selected intervals of total dissolved solids concentration.

TDS low	TDS high	Number records	TDS average	ct factor	R _{wcRw}	Ca	Mg	Na	HCO ₃	SO ₄	Cl
0	499	17	353	0.53	1.24	50	10	70	214	49	65
500	999	20	774	0.53	1.21	73	19	182	280	181	175
1,000	1,999	18	1,402	0.57	1.2	111	23	361	338	389	345
2,000	2,999	13	2,421	0.58	1.21	164	48	615	315	851	584
3,000	3,999	2	3,194	0.56	1.17	16	3	1,205	698	522	1,100
4,000	4,999	1	4,323	0.74	1.27	382	182	804	211	1920	900
5,000	5,999	0	-	-	-	-	-	-	-	-	-
6,000	6,999	0	-	-	-	-	-	-	-	-	-
7,000	7,999	1	7,848	-	1.07	6	-	2,990	1,510	10	4,100
8,000	8,999	0	-	-	-	-	-	-	-	-	-
9,000	9,999	0	-	-	-	-	-	-	-	-	-
10,000	14,999	0	-	-	-	-	-	-	-	-	-
15,000	19,999	0	-	-	-	-	-	-	-	-	-
20,000	24,999	0	-	-	-	-	-	-	-	-	-
25,000	29,999	0	-	-	-	-	-	-	-	-	-
30,000	34,999	0	-	-	-	-	-	-	-	-	-
35,000	39,999	0	-	-	-	-	-	-	-	-	-
40,000	44,999	0	-	-	-	-	-	-	-	-	-
45,000	49,999	0	-	-	-	-	-	-	-	-	-

Notes:

- All constituents are reported in milligram per liter, unless indicated.
- Each constituent is averaged from all samples (number records) within this interval.
- Empty cells in the table represent null values.
- The factors in the 4,000 to 4,999 TDS interval were not used. The well is 35 feet deep with abnormally high sulfate.
- TDS = Total dissolved solids interval
- Number records = Number of water quality sample records
- ct factor = Total dissolved solids / specific conductance, dimensionless
- R_{wcRw} = Sodium chloride equivalent water quality correction factor, dimensionless
- Ca = Calcium
- Mg = Magnesium
- Na = Sodium
- K = Potassium
- HCO₃ = Bicarbonate
- SO₄ = Sulfate
- Cl = Chloride

6.9.2 R_{WA} Minimum Method formulas

We used equations from Estep (1998) to calculate interpreted total dissolved solids. Equations with similar parameter names were standardized and coded in Visual Basic for Applications[®] as a class object within the BRACS Database for automated calculation. Parameters were entered into a series of data entry forms linked to tables. Once we select the type of method, the calculations are performed and the outputs are written into tables. There are many advantages in performing this work in Microsoft[®] Access[®]. First, parameter performance can be evaluated when calibrating existing groundwater chemistry samples. Second, calculations are performed quickly and consistently. Third, all parameters, correction factors, intermediate, and final results are recorded for future review and use. In other words, staff can open an existing record and

modify the output without starting from scratch. Lastly, the software will only write completed analysis information to the tables once staff commit the save operation.

Steps to perform the R_{WA} Minimum Method for interpreted total dissolved solids:

1. Determine each parameter listed in Table 6.9.1-1.
2. Determine the temperature at the depth of the formation being investigated.

$$T_f = (G_g \cdot D_f) + T_s$$

where:

- T_f = temperature formation in degrees Fahrenheit
- D_f = depth formation in feet
- G_g = geothermal gradient in degrees Fahrenheit/foot
- T_s = temperature surface in degrees Fahrenheit

$$G_g = \frac{(T_{bh} - T_s)}{D_t}$$

where:

- G_g = geothermal gradient in degrees Fahrenheit/foot
- T_{bh} = temperature bottom hole in degrees Fahrenheit
- T_s = temperature surface in degrees Fahrenheit
- D_t = depth total in feet

3. Determine resistivity of water equivalent.

$$R_w = \phi^m \cdot R_o$$

where:

- R_w = resistivity of water equivalent in ohm-meter
- ϕ = total porosity of the formation evaluated dimensionless
- m = cementation exponent in dimensionless
- R_o = resistivity of formation from geophysical log in ohm-meter

4. Correct resistivity water based on groundwater type correction factor.

$$R_{wc} = \frac{R_w}{R_{wcRw}}$$

where:

- R_{wc} = resistivity water, corrected in ohm-meter
- R_w = resistivity water equivalent in ohm-meter
- R_{wcRw} = sodium chloride equivalent correction factor, dimensionless

- Convert resistivity water at formation temperature to 77°F using Arp’s Equation (Torres-Verdín, 2017).

$$R_{w77} = R_{wc} \cdot \frac{(T_f + 6.77)}{(77 + 6.77)}$$

where:

- T_f = temperature formation in degrees Fahrenheit
- R_{wc} = resistivity water, corrected in ohm-meter
- R_{w77} = resistivity water at 77°F in ohm-meter

- Convert resistivity water at 77°F to conductivity water at 77°F.

$$C_w = \frac{10,000}{R_{w77}}$$

where:

- C_w = conductivity water at 77°F in microsiemens-centimeter
- R_{w77} = resistivity water at 77°F in ohm-meter

- Calculate interpreted total dissolved solids.

$$TDS = ct \cdot C_w$$

where:

- TDS = interpreted total dissolved solids in milligrams per liter
- ct = ct conversion factor, dimensionless
- C_w = conductivity water at 77°F in microsiemens-centimeter

6.9.3 Geophysical well log tools

Interpretation of geophysical logs was used to: (1) calculate interpreted total dissolved solids concentration of groundwater at different depth zones, (2) determine the top and bottom of sand and clay layers, (3) determine total porosity, and (4) map stratigraphic markers for geological formation top and bottom.

Geophysical well logs are produced from tools that are lowered into a well bore with a wireline and retrieved back to the ground surface at a specific rate. Combinations of different tools can be assembled in standard “packages” to measure specific formation, fluid, borehole, casing, and cement properties. Tools are selected based on many factors including anticipated geology, information required from logging, cased or uncased bore holes, and the composition of the well bore fluid (air or drilling mud). The tools have progressively improved since they were first applied to oil field investigations in the 1930s. The geophysical well logs collected for this study were produced between 1935 and 2015. Interpretation of logs that were produced over such a long-time span with varying designs and accuracies presents challenges. As such, some of the older logs simply could not be used in all aspects of the study. The digital image quality of some logs also presented challenges. Geophysical well log tools available in the study area varied in age, type, and vertical depth ranges. Oil field wells are generally logged after a section of surface casing is installed. With the exception of the gamma ray tool, the section of the wellbore

containing surface casing cannot be logged. The amount of information that can be collected from ground surface to the bottom of the casing is limited, which can be hundreds or thousands of feet. Older wells generally had a shallower bottom depth of surface casing, making these important for near-surface interpretations.

The resistivity of a formation can be measured from geophysical logging tools that pass electricity into the formation and record voltages between measuring electrodes. The resistivity of dry rock is a good electrical insulator (except for metallic ores), so the only way electricity can pass through a formation is if the rock contains groundwater. The groundwater is contained either in the pores between mineral grains or adsorbed in interstitial clay. Tools with deep depths of investigation are needed to minimize the influence of borehole fluid, mud filter cake, and the groundwater invasion zone.

A normal resistivity log usually consists of multiple tools used to measure the resistivity of rocks and water surrounding the borehole at different depths of investigation. The spacing between the electrodes is directly proportional to the depth of investigation, with larger spacing offering deeper depth of investigation. Resistivity measurements are affected by the borehole, drilling fluids, mud filter cake, borehole fluid invasion zone, formation being investigated, surrounding formations, and formation groundwater. Resistivity tool measurements are presented on the right track of a geophysical well log in units of ohm-meter. A conductivity track may be present and is calculated from the inverse of a resistivity tool measurement. The tool must be run in an open borehole with a conductive drilling mud.

The induction log is a deep investigation tool used to measure the resistivity of rocks and water surrounding the borehole. This type of log uses focusing coils to direct the electricity into the formation and minimize the influence of the borehole, drilling fluids, surrounding formations, mud filter cake, and the invaded zone (Schlumberger, 1987). The tool must be run in an open borehole. Drilling mud conductivity is not an issue. Induction tool measurements are presented on the right track of a geophysical well log in units of ohm-meter.

The spontaneous potential log is a record of the direct current reading between a fixed electrode at the ground surface and a movable electrode (spontaneous potential tool) in the well bore. The tool must be run in an open borehole with a conductive drilling mud. Spontaneous potential is measured in millivolts, with a negative or positive value depending on the curve deflection of the measurement in a left or right direction, respectively, within a porous unit. The electrochemical factors that create the spontaneous potential response are based on the salinity difference between the borehole mud filtrate and the groundwater within permeable beds (Asquith, 1982). A negative deflection of the spontaneous potential response occurs when the mud filtrate is more resistive than groundwater. A positive deflection occurs when mud filtrate is less resistive than groundwater. When mud filtrate equals groundwater resistivity there is no deflection of the spontaneous potential response from the shale baseline. The spontaneous potential response of shale is relatively constant and is referred to as the shale baseline. The permeable bed boundaries are detected at the point of inflection of spontaneous potential response.

Spontaneous potential deflection is affected by the type of cation species (positive ions such as calcium, magnesium, potassium, or sodium) present in water. Oilfield analysis equations assume that the groundwater is dominated by sodium and chloride. Divalent cations (with a plus two charge, such as calcium and magnesium) in dilute groundwater have a larger impact on spontaneous potential deflection than sodium (Alger, 1966). The spontaneous potential response

of high calcium or magnesium waters indicates that the water is more saline than an analysis using resistivity tools. Alger (1966) described a method for correcting this effect; however, a complete water quality analysis is needed to apply the correction. Alger indicated that once a well is calibrated, the analysis can be extrapolated from one well to another assuming that water quality remains relatively constant.

The spontaneous potential response is affected by bed thickness; thin beds do not allow a full spontaneous potential response and must be corrected (Asquith, 1982; Estepp, 1998; Schlumberger, 1972). If a sand unit is less than 10 feet thick, the response curve tends to have a pointed shape, and requires a thickness correction. Spontaneous potential response is also affected by bed resistivity, adjacent bed properties, borehole invasion of drilling fluid, hydrocarbons, and shale content. Shale content reduces the spontaneous potential response. Spontaneous potential tools run in freshwater wells commonly use native mud when, prior to logging, the borehole fluid is essentially groundwater. In this situation, the resistivity of groundwater and borehole fluid is almost equal, and the spontaneous potential tool cannot be used to estimate total dissolved solids concentration (Keys, 1990).

Gamma ray logs normally reflect the clay content in sedimentary formations (Schlumberger, 1972). Clays such as illite and mica contain the radioactive potassium-40 isotope that produces gamma rays in clay or shale lithologies. Gamma ray tools encountering natural uranium or thorium will record the zone as an elevated measurement much higher than background clay response. Units exhibiting these spikes in gamma ray measurements are recorded in the well geology table with the top and bottom depths and the gamma ray measurement in American Petroleum Institute units.

There are several advantages of using a gamma ray logs. They are present on most logging runs for newer wells. Gamma ray logs can be recorded in cased holes. Unlike many tools, they generally start near ground surface, which is valuable when you are interested in groundwater. In many situations, their distinct responses to clay content can be used to recognize the boundaries of geologic units and facilitate the interpretation of depositional environments.

There are some challenges when using gamma ray logs. Though they can record useful readings in cased boreholes, there is attenuation of the overall log signature. This attenuation masks the more subtle changes in log response that occur, such as the transition from uncemented to cemented formations. When using gamma ray curves from the cased portion of the hole, there is an inability to evaluate borehole washouts if the caliper logs were not run prior to casing the well. Interpretation of gamma ray logs can also be undermined by the absence of important header information such as tool calibration or complete casing records. Older gamma tool types are especially challenging to use. The documentation of tool parameters is often limited or impossible to acquire. Older gamma ray logs may also have different units of measure compared with the modern standard American Petroleum Institute (API) units. Trying to compare measurements between tools with different units is problematic. Finally, there is an inability to differentiate clay-free sand, silt, and gravel using just the gamma ray tool.

6.10 Salinity class delineation

An iterative approach with multiple datasets was used to delineate salinity classes. The following information was used to define polylines separating the classes (1) the measured water quality total dissolved solids concentration, (2) the calculated total dissolved solids concentration from

geophysical well log analysis, (3) locations of structural faults from the tectonic map of Texas (Ewing, 1991), (4) structural faults and formation outcrop from the digital Geologic Atlas of Texas (TWDB, 2007b), (5) the formation net sand distribution, and (6) additional log analysis data points outside of the study area. The process for delineating salinity classes can be simplified into six steps. First, a GIS shapefile of all water quality sample results was prepared, and each geological formation was symbolized by salinity class using a GIS definition query. The GIS shapefile was made using the BRACS database master water quality table (tblBracs_PE_sTx_MasterWaterQuality) for this study. This table includes an aquifer code based on the aquifer determination task described in Section 6.5. Second, we selected geophysical well logs starting at the updip limit of the formation outcrop in a county and interpreted the logs while comparing log analysis results with water quality samples. Log analysis typically proceeded downdip from the formation outcrop. Third, we prepared three GIS shapefiles of all log analysis results using definition queries for each geological formation and each salinity class. The three files consisted of: (1) all estimated salinity calculations with depth per geological formation name, (2) salinity class (hydrochemical) records organized by geological formation name, and (3) the number of vertical salinity classes per geological formation per well. Fourth, we analyzed the available data to delineate the salinity classes. Displaying the combined water quality and log analysis results allowed us to look for data gaps for each geological formation. For transition zones where salinity was changing both horizontally and vertically within a geological formation, we attempted to fill in data gaps and updated the GIS files for further review. Once there was sufficient data density, we hand-contoured the salinity class divisions with polylines in GIS. Fifth, we compared mapped structural faults, net sand maps, and total dissolved solids contours interpolated in GIS with initial salinity class contours and refined class divisions. When placing salinity class lines, we tried to give preference to measured water quality samples over calculated total dissolved solids estimates. If the GIS-derived salinity class boundaries coincided with hand-contouring, the boundaries were approved. If the boundaries did not coincide, then best professional judgement using hand contouring was used to make or modify a boundary line. Lastly, we prepared salinity class maps. When mapping of a single class was not possible, we created mixed salinity class polygons. GIS files for points and polygons are listed in the Appendix, Section 13.5, Table 13.5.2-3.

6.11 Groundwater volumes

Volumes of brackish groundwater were calculated to aid in understanding the scale of this resource. The volume of in-place groundwater was estimated by using the following simple equation:

$$\text{Volume} = [\text{Area}] \times [\text{Saturated Thickness}] \times [\text{Specific Yield}]$$

Where:

Volume = in-place groundwater in acre-feet

Area = acres

Saturated Thickness = feet

Specific Yield = estimated volume ratio of water to rock

A snap grid shapefile of 250-foot by 250-foot grid cells was used to estimate area of the salinity classes. It was assumed that confined portions of the aquifers are fully saturated with

groundwater. Therefore, where the aquifers were confined, the net sand value (feet) was used for saturated thickness. Where the aquifers were unconfined, the saturated thickness of each grid cell was based on the static water level elevation, minus the formation bottom elevation, which was then multiplied by the percent sand to approximate a saturated net sand value (feet). Each aquifer was assigned a specific yield based on the literature review. Specific yield was used to estimate the ratio of waterfilled void spaces to sand in the aquifers. Volumes were prepared for fresh, slightly saline, moderately saline, very saline, and mixed classes of groundwater. A complete description of the volume methodology is presented in the Appendix, Section 13.2. We did not prepare a volumetric estimate for brine. Not all brackish groundwater can be produced or be economically developed, but the estimates provide an indication of the potential availability of this important resource.

We did not calculate the volume of groundwater from confined storage for the following reasons: (1) the volume was assumed to represent a small percentage of total groundwater volume for the study area (LBG-Guyton Associates, 2003), (2) the task would have been extremely complicated because each salinity class would require analysis of confined versus unconfined extent, (3) the storativity values available for the study area were insufficient, and (4) the head (potentiometric) values for the downdip portions of the brackish aquifers were insufficient.

Each formation in Section 7 contains a table listing groundwater volumes per salinity class. Tables listing all the volumes by districts and planning areas and a detailed methodology for calculating the groundwater volumes using grid shapefiles in ArcGIS are in Appendix 13.1. These volumes do not consider the effects of land surface subsidence, degradation of water quality, or any changes to surface water-groundwater interaction that may result from extracting groundwater from the aquifer. These volumes should not be used for joint groundwater planning or evaluation of achieving adopted desired future conditions because there is an established process in Texas Water Code §36.108. This process considers several factors, including calculating volumes using the total estimated recoverable storage (TERS) as determined by the TWDB Groundwater Availability Modeling (GAM) Program (Wade and Bradley, 2013; Wade and Shi, 2014). TERS is defined as the estimated amount of groundwater within an aquifer that accounts for recoverable storage scenarios that range between 25 percent and 75 percent of the porosity-adjusted aquifer volume (Texas Administrative Code Rule §356.10). Volumes calculated for brackish aquifer studies in the BRACS program differ from TERS volumes because of differences in the area, saturated thickness, and storage elements used in the calculations.

Differences in the area used to calculate volumes arise due to: (1) differences in the areal extent of the GAM models, as brackish groundwater often extends beyond the official TWDB boundaries for major and minor aquifers used to develop TERS, and (2) differences in the grid cell size and orientation of the GAM models used to estimate area.

Differences in the saturated thickness used to calculate volumes arise due to: (1) differences in aquifer top and bottom elevations and static water levels of the GAM models due to differences in interpretations and data availability during subsurface mapping and (2) whether bulk aquifer thickness (static water level or aquifer top minus aquifer bottom) or net sand, or percent sand, was used to estimate feet of saturated aquifer thickness.

Differences in the storage component used to calculate volumes include: (1) the value of specific yield (the ratio of drainable water in an aquifer, which is less than porosity), (2) whether volumes

calculated from specific yield are further reduced to “recoverable volumes,” and (3) whether confined storage is included, though this is generally a negligible volume.

Additionally, TERS does not take water quality into account and therefore cannot be directly compared to BRACS volumes which are divided by salinity class categories.

7. Results

This section will provide detailed information from our analysis for each geological formation: the Wilcox Group and the Carrizo, Reklaw, Queen City, Weches, Sparta, Cook Mountain, and Yegua formations.

We prepared nine structural strike and dip sections across the study area (Table 7-1; Figure 7-1) showing stratigraphic relationships, lithology, and interpreted salinity classes. These can be reviewed concurrently with the geological formation descriptions if needed. The three dip and six strike cross-sections are stand-alone, large-format, portable document format (pdf) documents (Plates 1 through 9). We selected this format because the amount of information presented on these plates could not be provided in a standard report figure of 6.5 by 8 inches. The plates include a portion of one marked digital geophysical log to graphically show the relationship between the spontaneous potential and resistivity response to lithology and salinity interpretation. Digital geophysical logs used on the cross-sections are available to the public and stratigraphic, lithologic, and salinity interpretations are recorded in the BRACS Database. Groundwater Database water wells with water quality samples are interspersed along the cross-section showing the salinity class of the total dissolved solids sample and screen depth (if known).

We also prepared a series of three figures (Figures 7-2, 7-3, and 7-4) that show the location of each structural dip cross-section and the plan-view salinity classes for each of the five aquifers in the study area. These figures demonstrate the tremendous spatial variability of aquifer salinity classes.

Table 7-1. Structural cross-section plate number, name, and type.

Plate number	Cross-section name	Cross-section type
1	A-A'	Strike
2	B-B'	Strike
3	C-C'	Strike
4	D-D'	Strike
5	E-E'	Strike
6	F-F'	Strike
7	X-X'	Dip
8	Y-Y'	Dip
9	Z-Z'	Dip

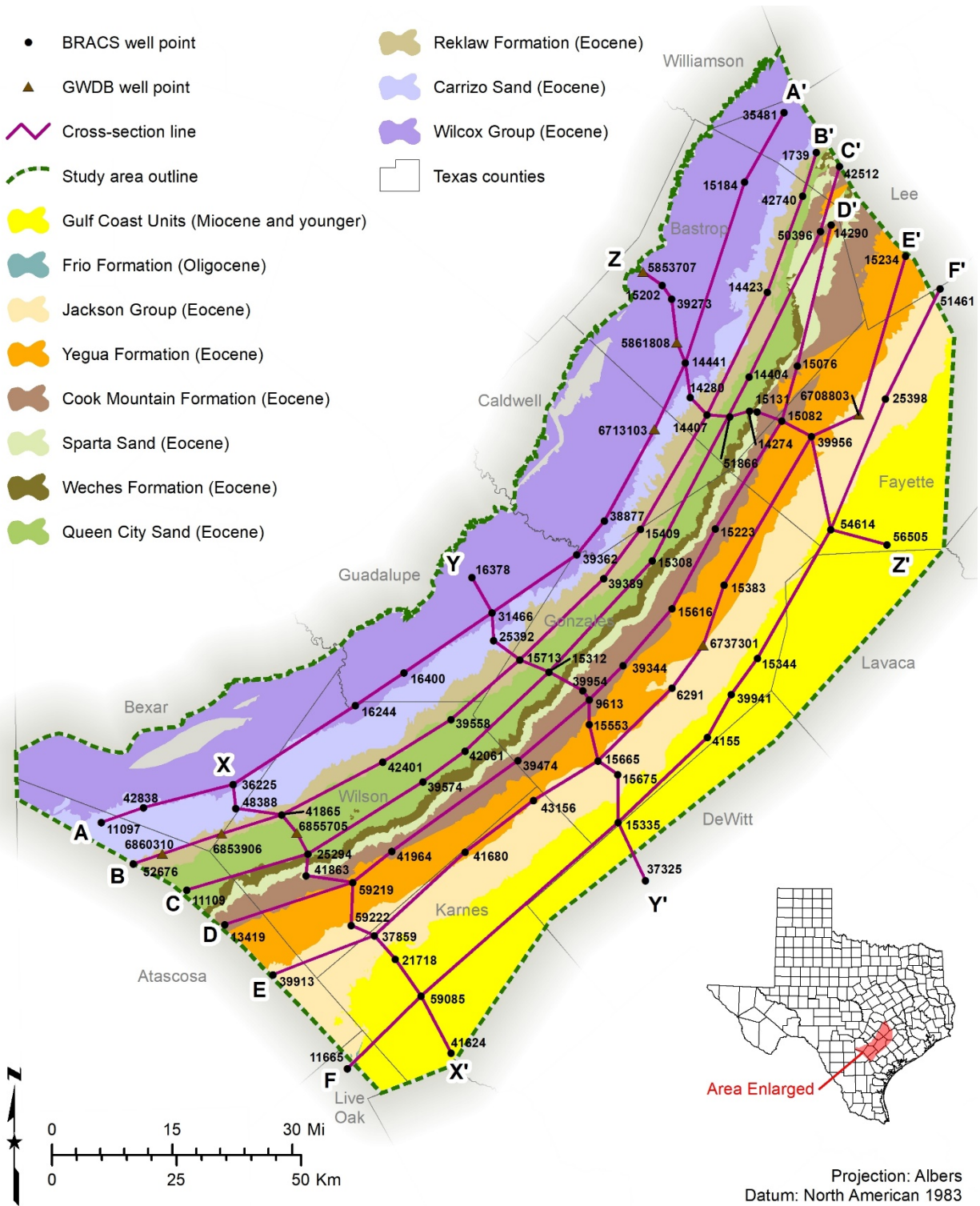


Figure 7-1. Structural strike and dip cross-section name and location relative to study area boundary, geological formation outcrops, and Texas counties. Well numbers refer to BRACS Database Well IDs (five digits) or Groundwater Database State Well Numbers (seven digits). Each cross-section was developed as a stand-alone, large-format, pdf (Plates 1 through 9) in this report (Table 7-1).

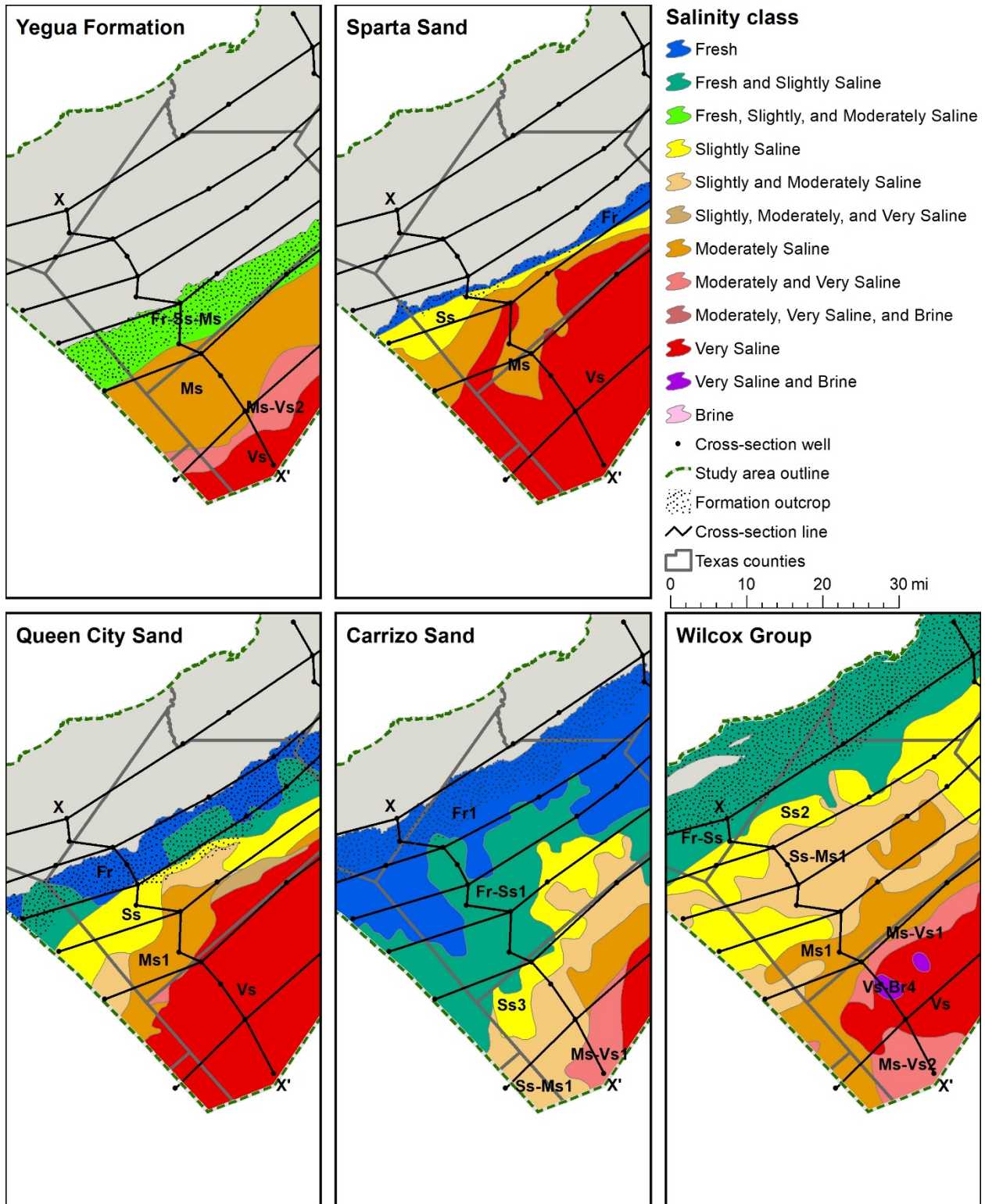


Figure 7-2. Aquifer salinity classes along structural dip cross-section X-X', Plate 7. The stipple pattern in each figure represents the outcrop of each geological formation. Refer to Figure 7-1 for the location of the cross-section line in relation to the study area. Refer to Table 2-1 for salinity class, color, code, and total dissolved solids concentration range.

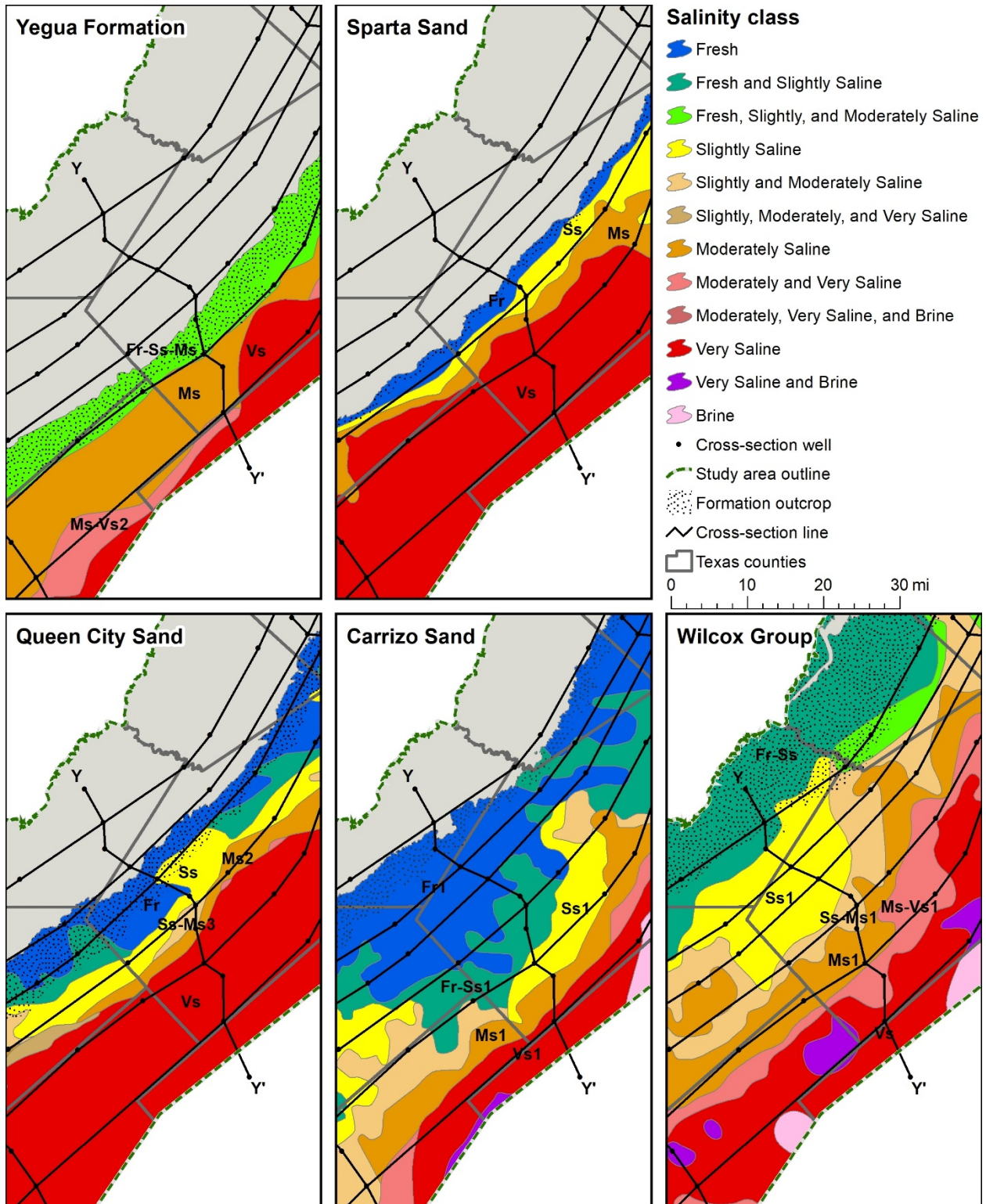


Figure 7-3. Aquifer salinity classes along structural dip cross-section Y-Y', Plate 8. The stipple pattern in each figure represents the outcrop of each geological formation. Refer to Figure 7-1 for the location of the cross-section line in relation to the study area. Refer to Table 2-1 for salinity class, color, code, and total dissolved solids concentration range.

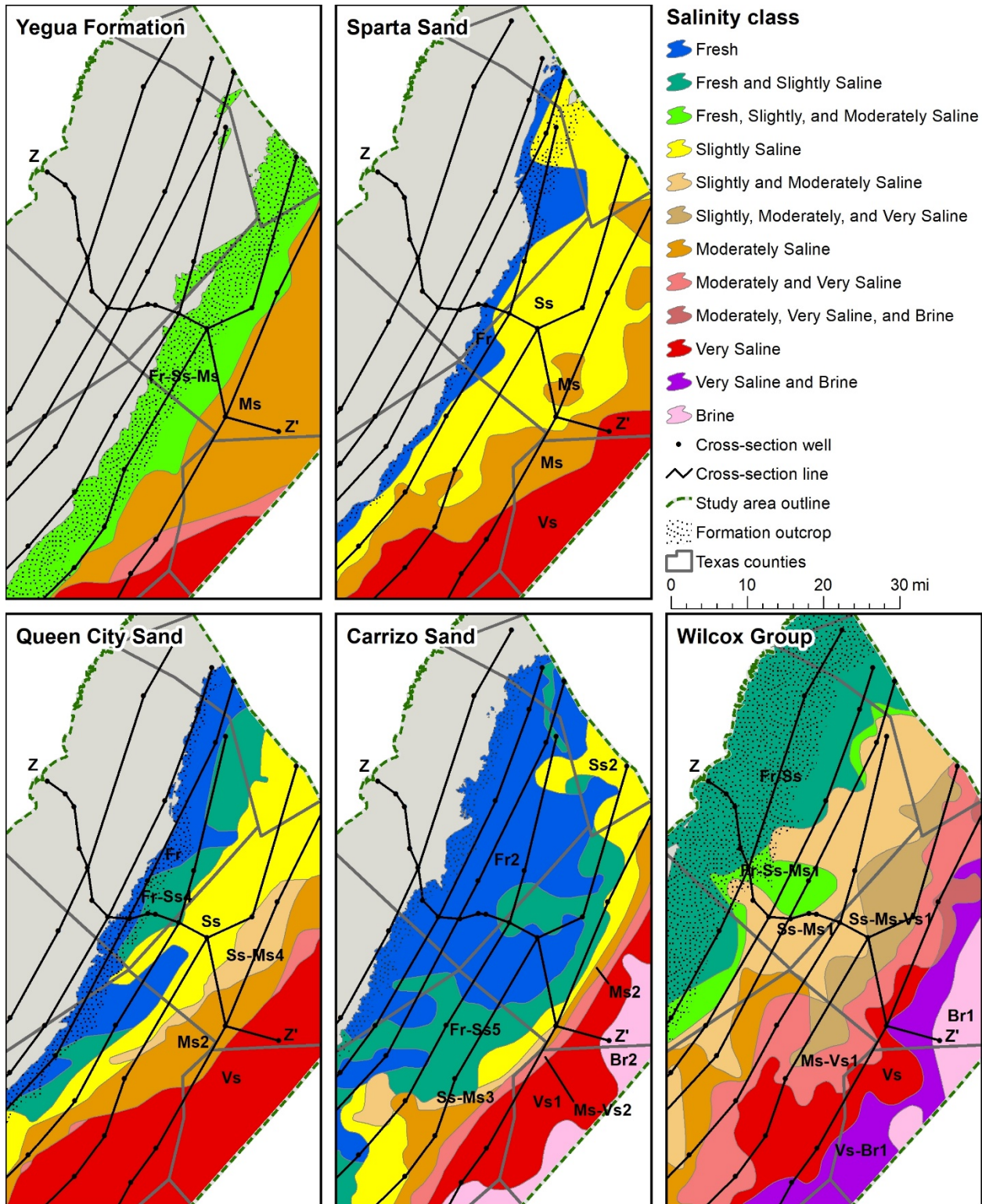


Figure 7-4. Aquifer salinity classes along structural dip cross-section Z-Z', Plate 9. The stipple pattern in each figure represents the outcrop of each geological formation. Refer to Figure 7-1 for the location of the cross-section line in relation to the study area. Refer to Table 2-1 for salinity class, color, code, and total dissolved solids concentration range.

7.1 Wilcox Group

We mapped the Wilcox Group and Carrizo Sand as separate units without subdivisions for this brackish groundwater study. The Carrizo-Wilcox Aquifer, wholly comprised of the Wilcox Group and Carrizo Sand, is a TWDB-designated major aquifer in Texas (George and others, 2011) that produces large amounts of water over a large geographic area. Wilcox stratigraphic nomenclature is quite confusing in the literature, and subsurface mapping is challenging. The following discussion will address some of the stratigraphic and lithologic challenges that are pertinent to our evaluation of brackish groundwater in the Wilcox Group.

The Wilcox Group is formally subdivided into the Hooper, Simsboro, and Calvert Bluff formations (from oldest to youngest) in the region between the Colorado and Trinity Rivers and informally subdivided into the lower, middle, and upper Wilcox south of the Colorado River. Although for this study we mapped the Carrizo Sand and the Wilcox Group separately, the Carrizo Sand is equivalent to the Upper Wilcox in the deep subsurface and was mapped by Hamlin (1988) and Banerji and others (2019) as one unit (Carrizo-Upper Wilcox). The Wilcox Group unconformably underlies the Carrizo Sand and conformably overlies the Midway Group. Upper Midway strata are considered Wilcox prodelta marine facies (Bebout and others, 1982).

In the area of Bastrop and Lee counties we attempted to identify the Hooper, Simsboro, and Calvert Bluff formations on some wells and included these stratigraphic picks in the geology table of the BRACS Database. In some areas these picks are relatively straightforward. However, where the Hooper and Calvert Bluff formations contain significant sand, the individual formation picks can become problematic and potentially subjective. This problem is exacerbated in areas within the Milano Fault Zone where fault-cut wells, possible errors in surface geologic mapping, and possible syndepositional faulting all add to the confusion.

As discussed in the Geologic setting section, the Yoakum Canyon (also known as the Yoakum channel, Hoyt, 1959) is a significant geologic feature in the Middle Wilcox. The significance of the Yoakum Canyon to this study is that (1) lateral continuity of sands is absent normal to the canyon axis, (2) deeper sands are progressively missing gulfward parallel to the canyon axis, and (3) Wilcox sands below the canyon base are not vertically connected to overlying Wilcox Group or Carrizo Sand sands above the canyon shale fill (Plate 6). Inferred slumping along the canyon margin (Dingus and Galloway, 1990) would isolate sands within the slump blocks from adjacent sands. Wells used for stratigraphic control within the canyon extent were evaluated for shale top, bottom, and thickness with notes placed in the remarks field of Wilcox Group stratigraphic records in the BRACS Database geology table, permitting query extraction and mapping within GIS.

7.1.1 Well control

Over 1,150 wells were used in defining aspects of the Wilcox Group stratigraphy, lithology, and water quality (Table 7.1.1-1). We only used wells for water quality and aquifer hydraulic properties based on the aquifer determination analysis. Undoubtedly there are many other wells completed in the Wilcox Group, but without detailed well screen information it is not possible to accurately assign the Wilcox Group as the discrete source of water produced from the wells.

Table 7.1.1-1. Wilcox Group well control data points.

Well control with this information:	Number of data points
Lithology	1,171
Top surface stratigraphic picks used for raster surface	840
Bottom surface stratigraphic picks used for raster surface	899
Top surface stratigraphic picks (database total*)	950
Bottom surface stratigraphic picks (database total*)	1,033
Net sand interpreted from wells	499
Aquifer hydraulic properties	664 wells with 693 measurements
Water quality: wells	488 wells with 899 measurements
TDS interpreted from geophysical well logs	439 wells with 1,145 depth intervals
Porosity	40

* Total number of stratigraphic picks in study counties

7.1.2 Stratigraphic analysis

The Wilcox Group stratigraphic top and bottom was evaluated using geophysical well logs and selected water well control, the latter primarily along the outcrop. The Wilcox stratigraphic base was selected as the base of the first significant sand-based, coarsening upward, progradational sequence superjacent to a regional marine shale marker equivalent to the Midway Group Poth Shale core of Hargis (2010). In the absence of the Poth Sands north of the San Marcos Arch, the base of Wilcox coincided with the erosive base of Wilcox Group sands. In places north of the San Marcos Arch there are one or more thin coarsening upward sequences subjacent to the base of the first significant Wilcox Group sand that could be temporally equivalent to the Poth sands. At the extreme downdip limit of our study area the basal Wilcox Group pick is problematic when the basal Wilcox consists of thick mudstone-dominated deltaic successions (Olariu and Zeng, 2018) and the Poth Shale core is difficult to discern. This contact is based on lithostratigraphic correlation using geophysical log signatures without paleontology control for dating. We strived for regional consistency, but Wilcox Group stratigraphy is one of the most controversial within Texas (Brown and Loucks, 2009).

The Wilcox Group stratigraphic top was selected as the top of a regional shale subjacent to the lowest significant sharp-based sand of the Carrizo Sand. Usually this is the base of the Carrizo Sand massive sand complex, however in some areas the lowermost Carrizo Sand may consist of interbedded sand and shale units. This contact is a regional unconformity. Hamlin (1988) included what he termed progradational sand and shale units in his lower Carrizo Sand, but in many locations it was difficult to distinguish lower Carrizo Sand from Upper Wilcox Group interbedded units; in this situation we defaulted to selecting the base of the largest Carrizo sand and ensured our formation thicknesses were regionally consistent.

Geophysical well log signature for the Wilcox Group top depth in Wilson County is displayed in Figure 7.1.2-1. The top depth is 1,878 feet below ground surface (yellow line). The geophysical well log includes: the spontaneous potential (solid line) and gamma ray (dotted line) are recorded in the left track, depth below ground surface (feet) in the center track (each depth increment represents 10 feet), and induction (dotted line) and shallow normal resistivity (solid line) tools in the right track. This log is from BRACS well id 42363 in southern Wilson County, Texas. The log was performed by Schlumberger in 1981 with a kelly bushing height of 15 feet.

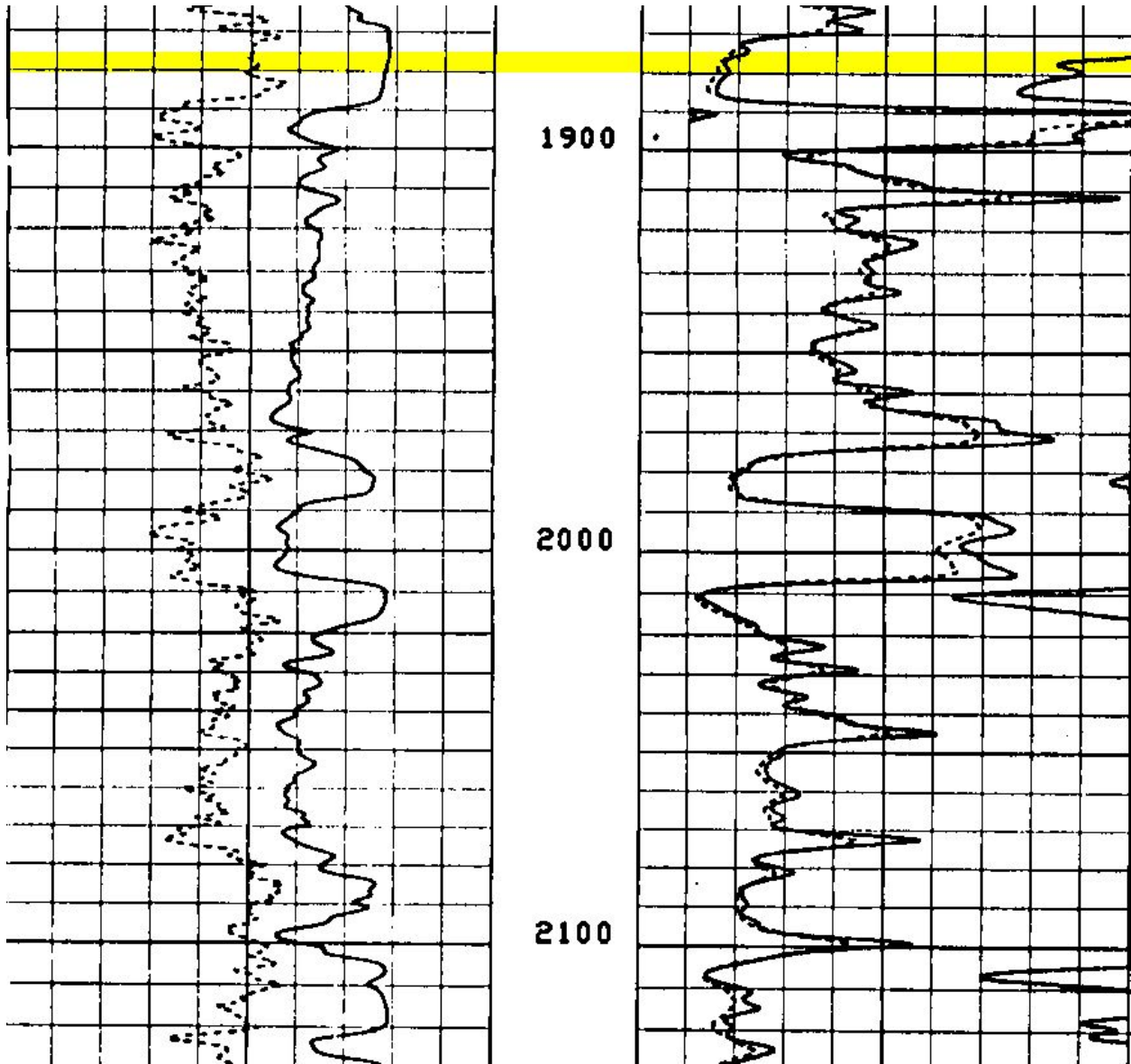


Figure 7.1.2-1. Wilcox Group top depth interpreted on a geophysical well log in Wilson County, Texas.

Geophysical well log signature for the Wilcox Group bottom depth in Wilson County is displayed in Figure 7.1.2-2. The Wilcox Group bottom depth is 3,520 feet below ground surface (yellow line). Several thin Midway Group Poth sands are seen below the Wilcox. The geophysical well log includes: the spontaneous potential (solid line) and gamma ray (dotted line) are recorded in the left track, depth below ground surface (feet) in the center track (each depth increment represents 10 feet), and induction (dotted line) and shallow normal resistivity (solid line) tools in the right track. This log is from BRACS well id 42363 in southern Wilson County, Texas. The log was performed by Schlumberger in 1981 with a kelly bushing height of 15 feet.

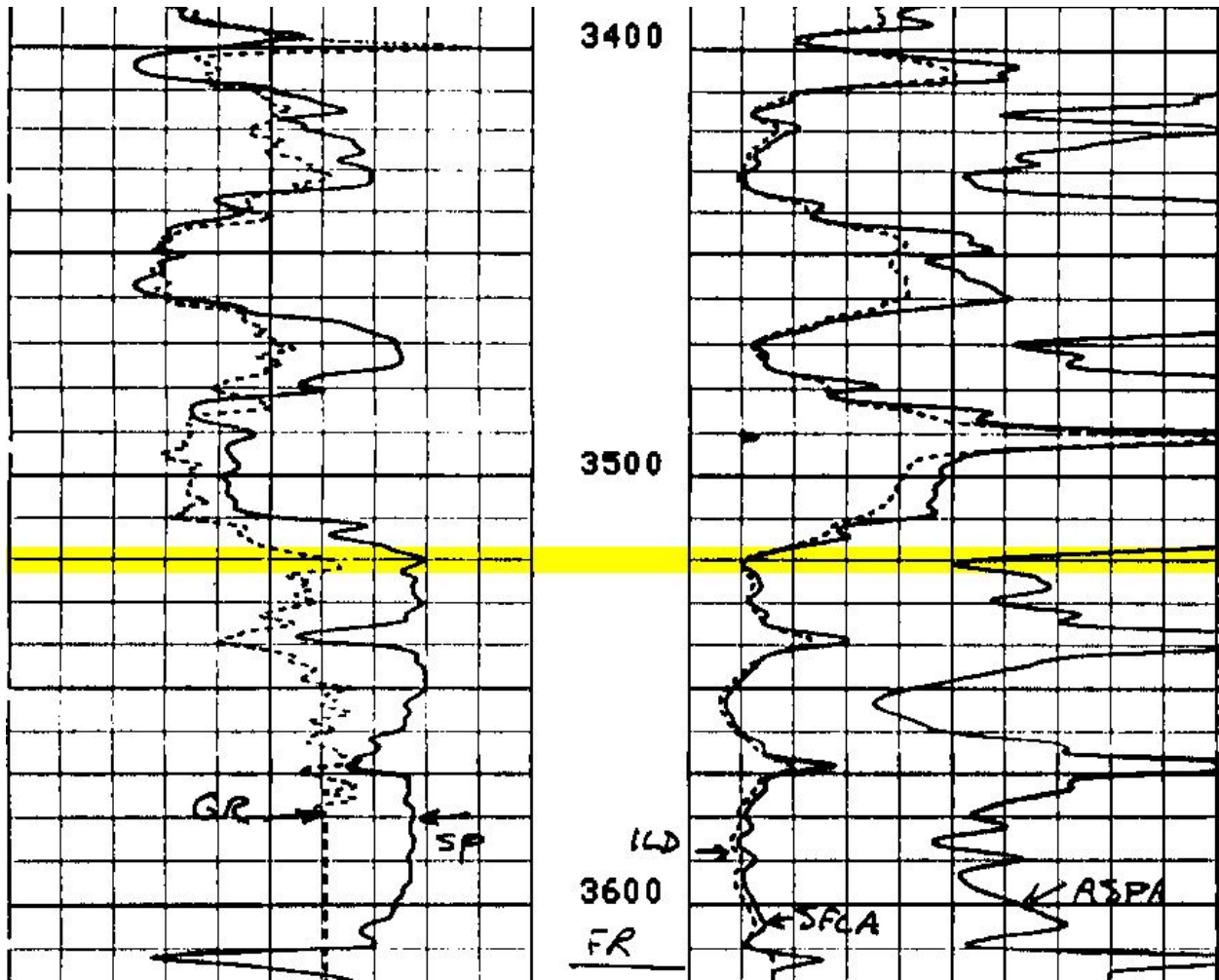


Figure 7.1.2-2. Wilcox Group bottom depth interpreted on a geophysical well log in Wilson County, Texas.

Geophysical well log signature for the Wilcox Group top depth in Gonzales County is displayed in Figure 7.1.2-3. The Wilcox Group top depth is 2,336 feet below ground surface (yellow line). Shale of the Yoakum Canyon is present from 2,400 to 2,970 feet below ground surface at this well site. The geophysical well log includes: the spontaneous potential is recorded in the left track, depth below ground surface (feet) in the center track (each depth increment represents 10 feet), and induction (dotted line) and short normal resistivity (solid line) tools in the right track. This log is from BRACS well id 15399 in northeastern Gonzales County, Texas. The log was performed by Lane Wells in 1966 with a kelly bushing height of 10 feet.

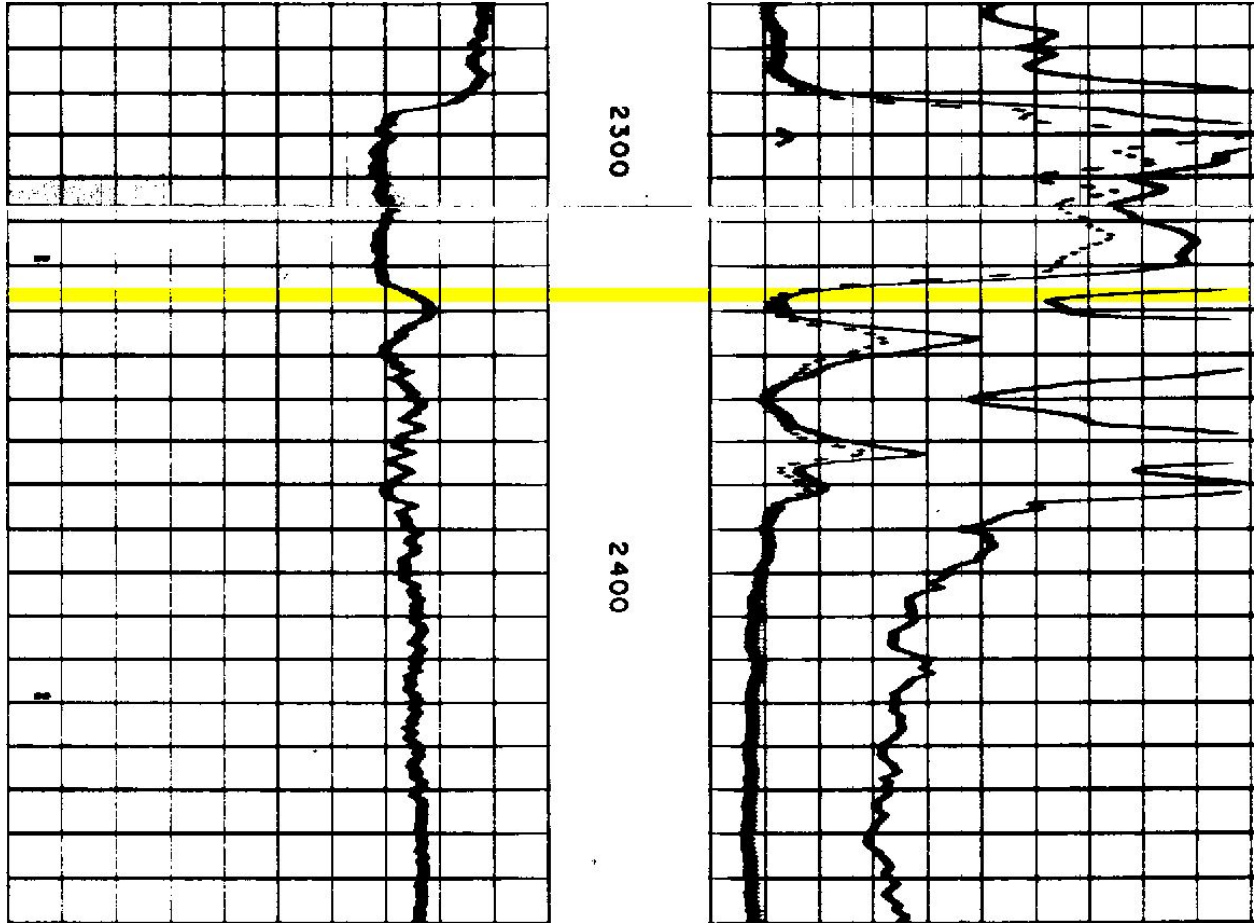


Figure 7.1.2-3. Wilcox Group top depth interpreted on a geophysical well log in Gonzales County, Texas.

Geophysical well log signature for the Wilcox Group bottom depth in Gonzales County is displayed in Figure 7.1.2-4. Bottom depth is 4,750 feet below ground surface (yellow line). The geophysical well log includes: the spontaneous potential is recorded in the left track, depth below ground surface (feet) in the center track (each depth increment represents 10 feet), and induction (dotted line) and short normal resistivity (solid line) tools in the right track. This log is from BRACS well id 15399 in northeastern Gonzales County, Texas. The log was performed by Lane Wells in 1966 with a kelly bushing height of 10 feet.

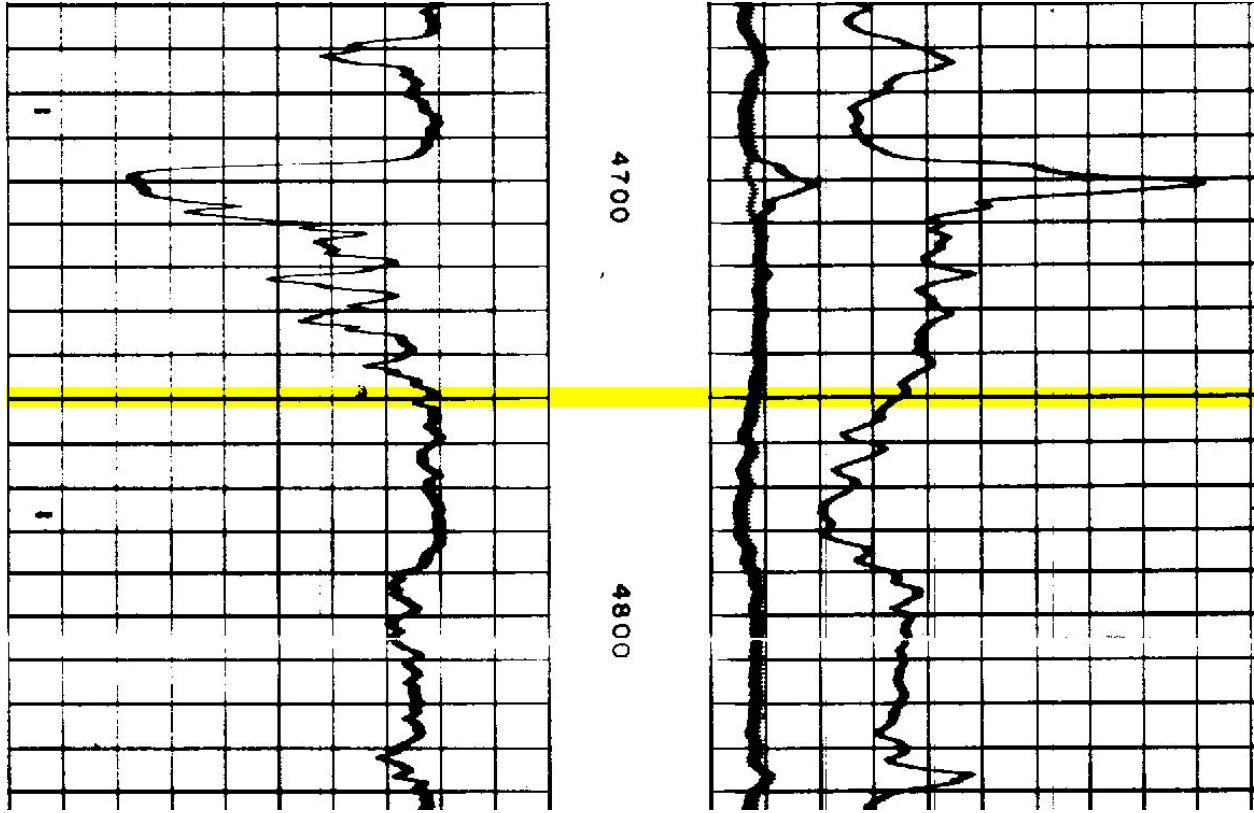


Figure 7.1.2-4. Wilcox Group bottom depth interpreted on a geophysical well log.

7.1.3 Formation top, bottom, and thickness

Wilcox Group top and bottom elevation maps (Figures 7.1.3-1 and 7.1.3-2) were prepared using 840 and 899 stratigraphic picks respectively from wells within the study area in addition to some wells immediately outside of the study area to control GIS raster edge effects. Wilcox Group top and bottom depth maps (Figures 7.1.3-3 and 7.1.3-4) were prepared using elevation GIS rasters subtracted from the study area digital elevation model (refer to Appendix, Section 13.6.1 raster interpolation documentation).

The Wilcox Group thickness was prepared by subtracting the bottom elevation GIS raster from the top elevation GIS raster. The Wilcox Group thickness is 0 at the updip outcrop edge and over 3,200 feet at the downdip limit of the study area in the southeast (east of the San Marcos Arch, Plate 9) and over 2,200 feet in the southwest part of the study area (Figure 7.1.3-5, Plate 7). The Wilcox Group thickens dramatically within the Wilcox Fault Zone, a series of growth-faults gulfward of the study area.

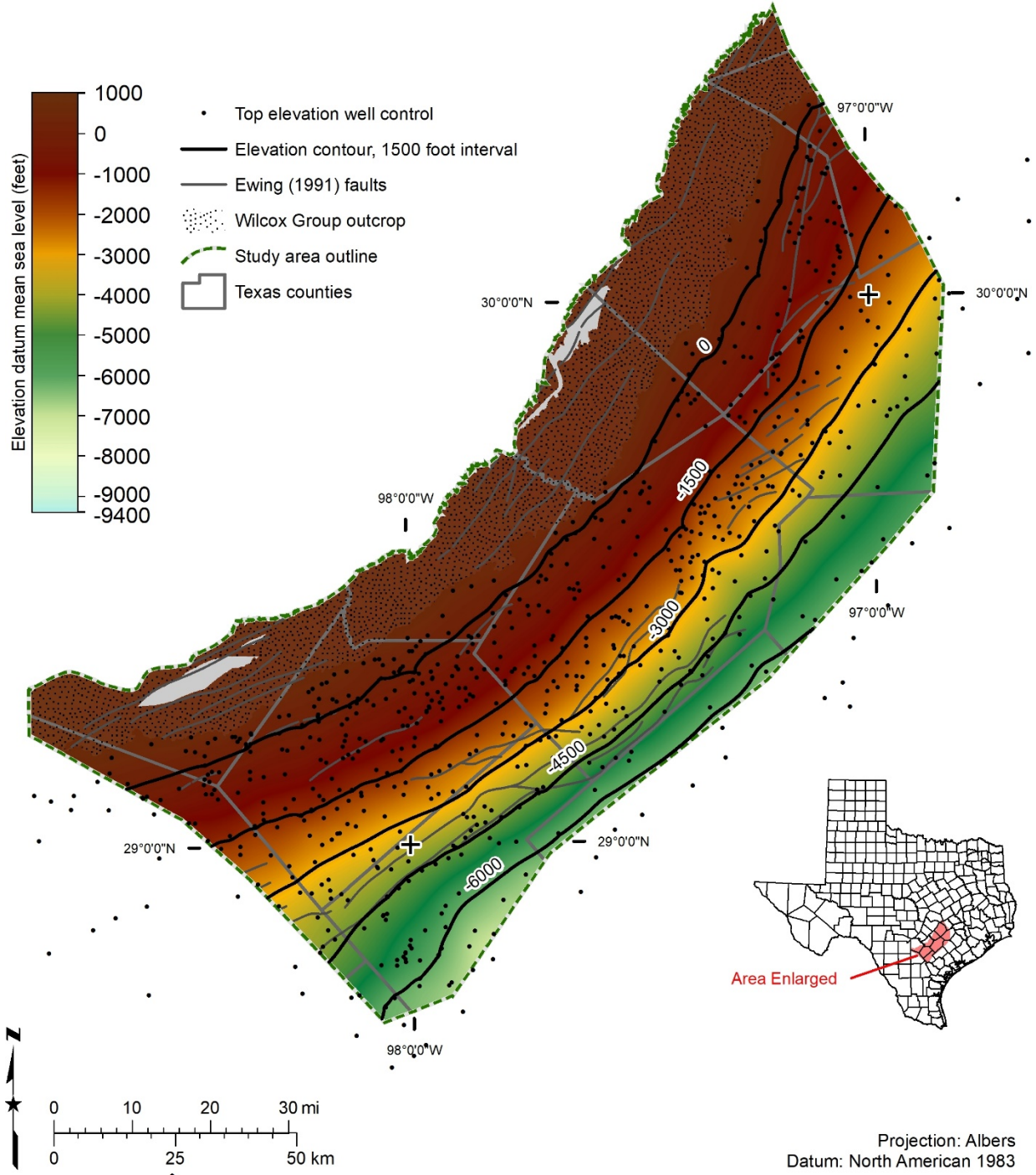


Figure 7.1.3-1. Wilcox Group top elevation surface (feet above mean sea level), which was prepared using 840 wells for stratigraphic control (black dots).

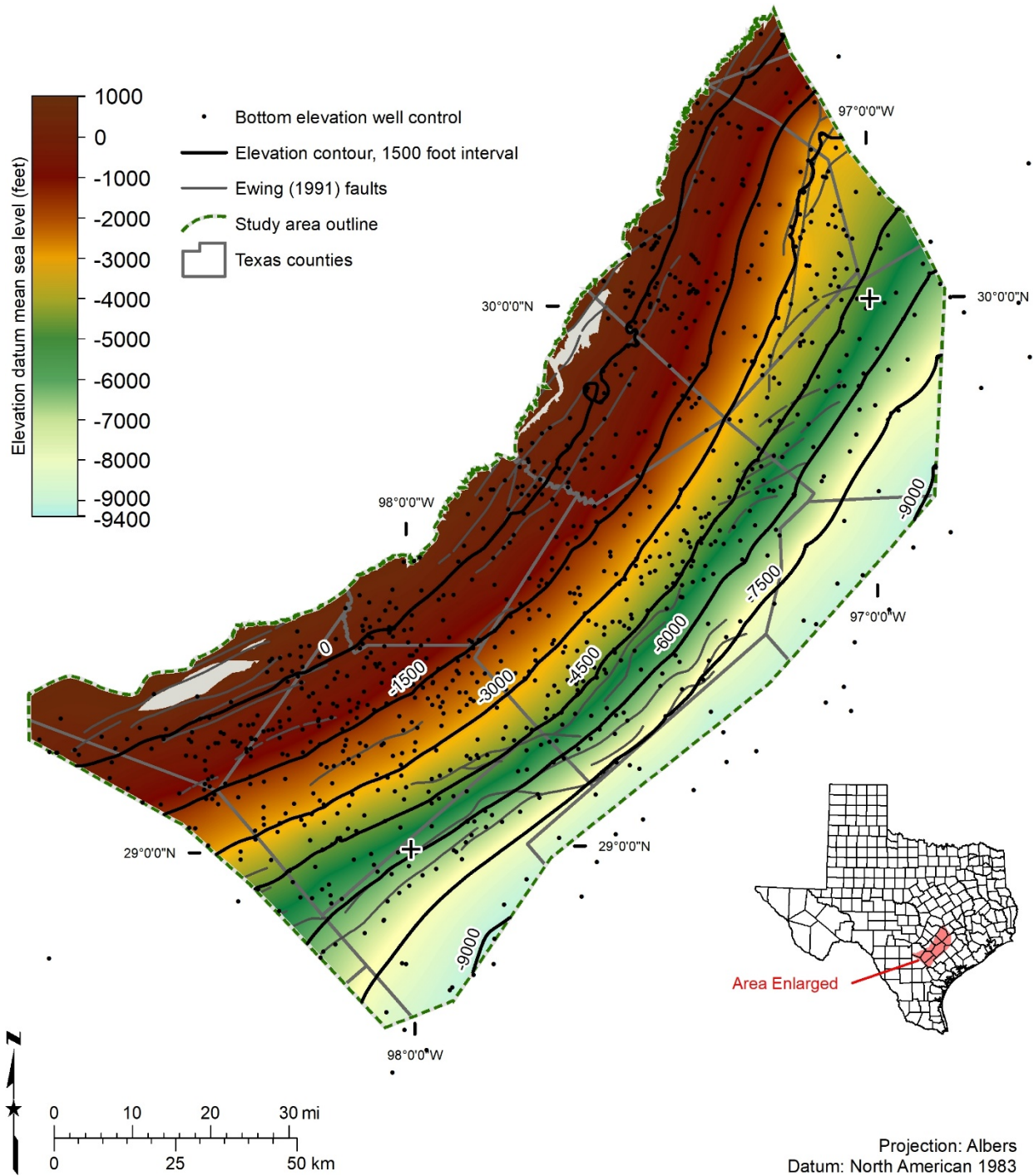


Figure 7.1.3-2. Wilcox Group bottom elevation surface (feet above mean sea level), which was prepared using 899 wells for stratigraphic control (black dots).

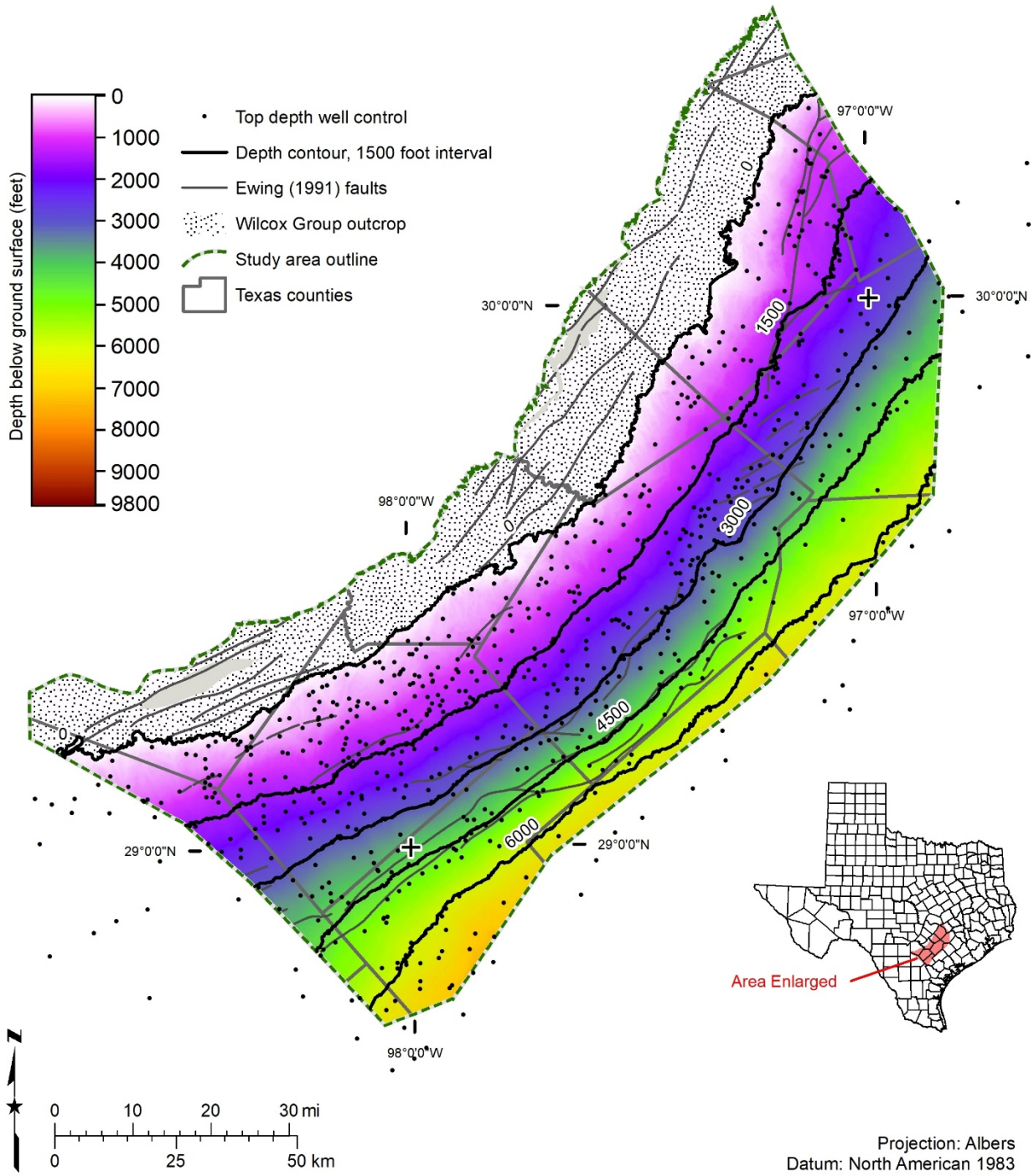


Figure 7.1.3-3. Wilcox Group top depth surface (feet below ground surface), which was prepared using 840 wells for stratigraphic control (black dots).

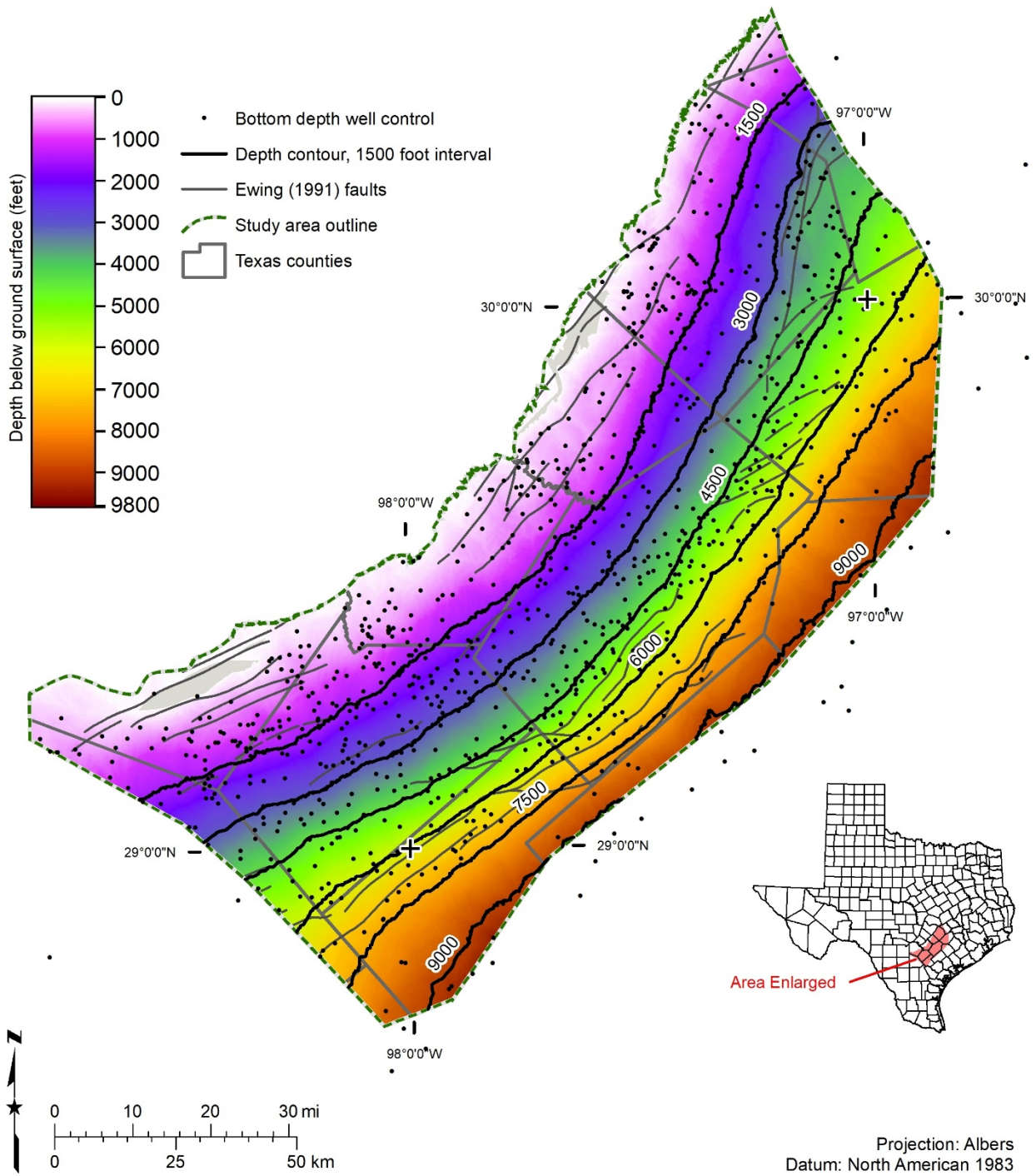


Figure 7.1.3-4. Wilcox Group bottom depth surface (feet below ground surface), which was prepared using 899 wells for stratigraphic control (black dots).

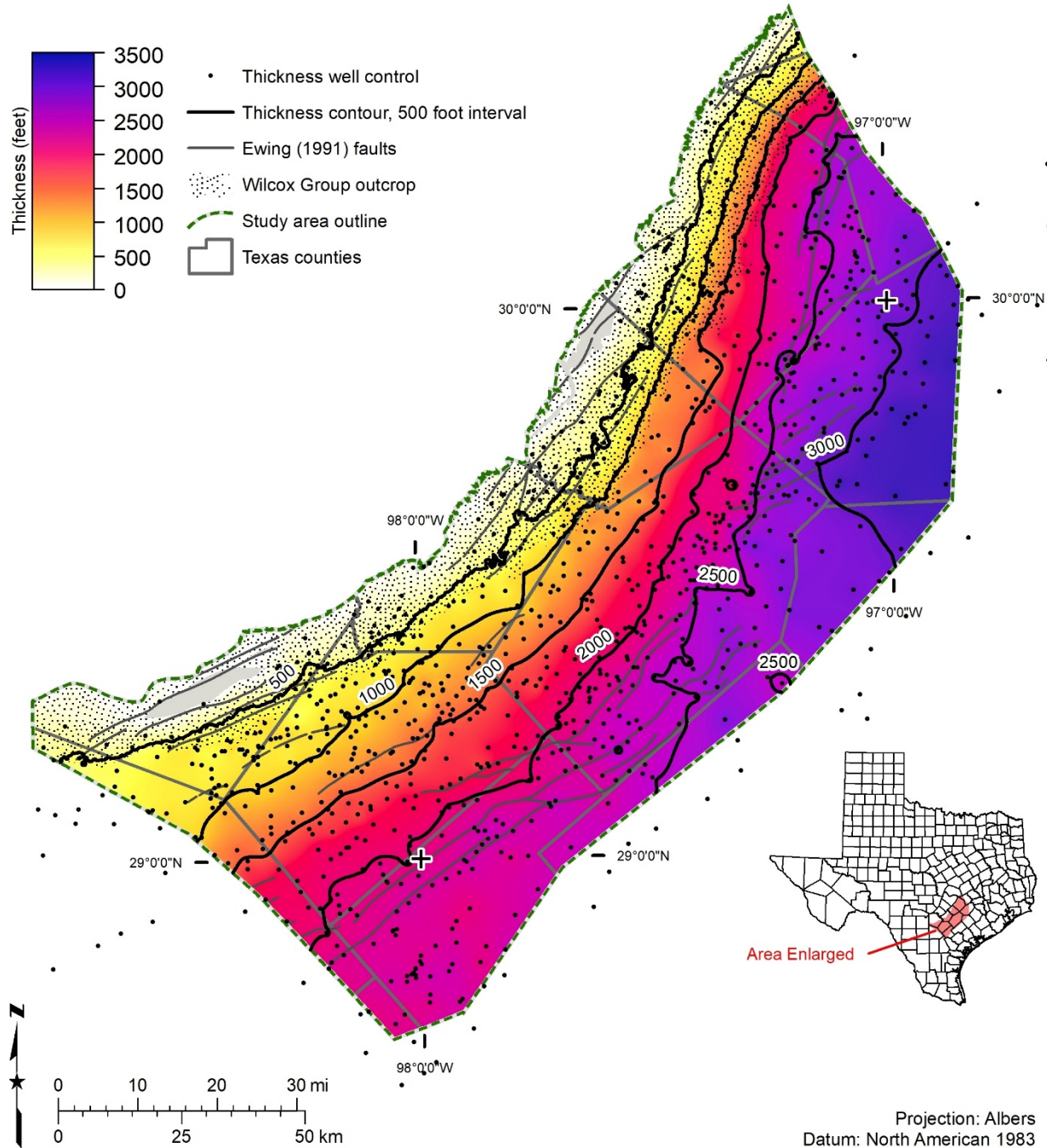


Figure 7.1.3-5. Wilcox Group thickness in units of feet, which was prepared using 840 wells for stratigraphic control (black dots).

7.1.4 Net sand

We used 499 wells to prepare the Wilcox Group net sand GIS raster (Figure 7.1.4-1). Oil and gas wells represent 356 wells, water wells represent 136 wells, and the remaining seven wells are classified as other. We used geophysical well logs for 366 wells and drillers' descriptions of lithology for the remaining 133 wells. The shale-filled Yoakum Canyon is a prominent feature

on the net sand map. Net sand values range from 0 at the updip outcrop edge to over 2,000 feet in Fayette County.

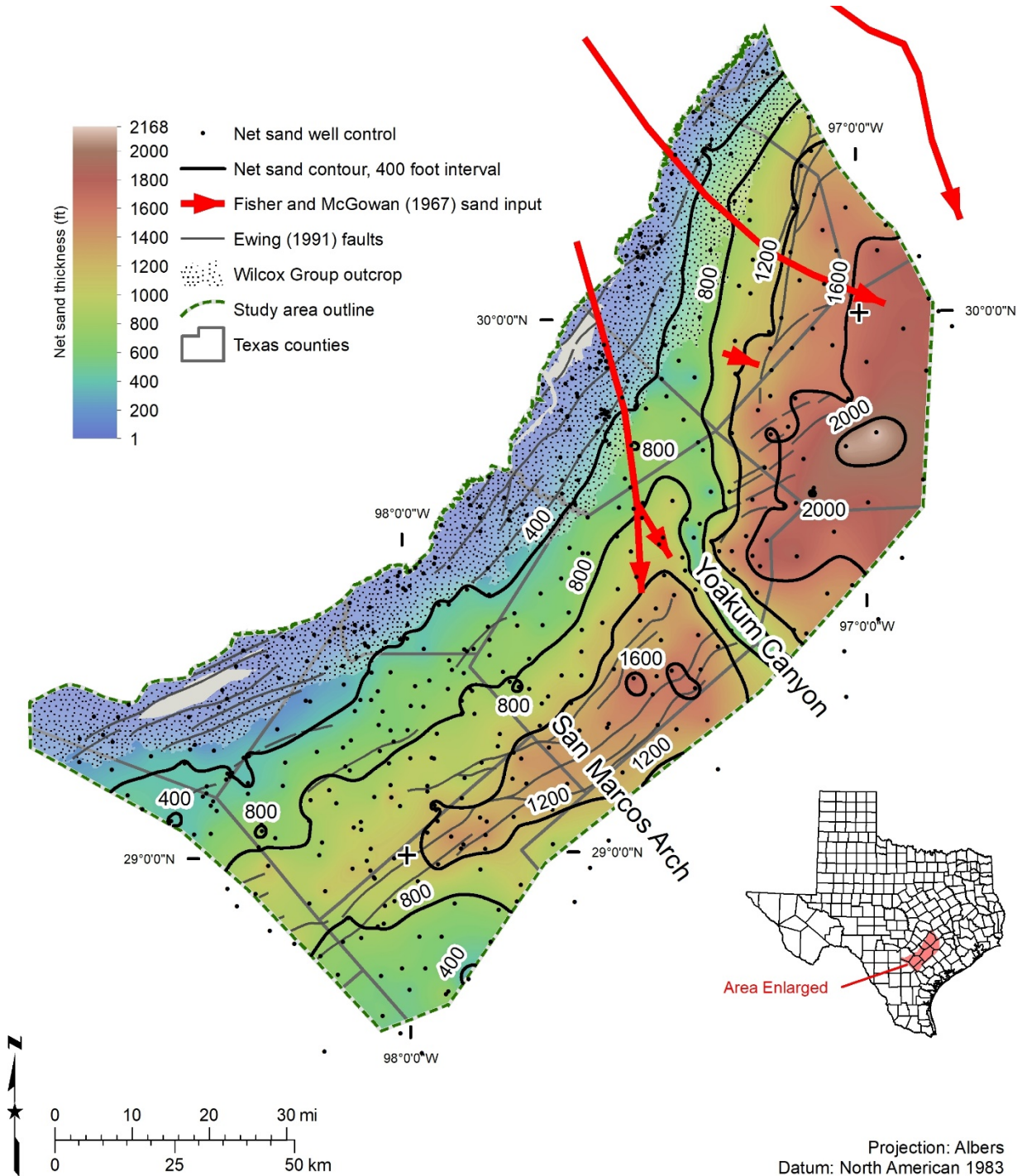


Figure 7.1.4-1. Wilcox Group net sand thickness (feet), which was prepared using 499 wells for net sand control (black dots). Axes of significant sand input to the basin from Fisher and McGowan (1967) are shown in red arrows. Area of low net sand from southwestern Bastrop through Gonzales County is due to the Yoakum Canyon.

7.1.5 Salinity classes

The Wilcox Group was mapped into defined salinity classes (1) mixed fresh and slightly saline, (2) mixed fresh, slightly saline, and moderately saline, (3) slightly saline, (4) mixed slightly saline and moderately saline, (5) mixed slightly saline, moderately saline, and very saline, (6) moderately saline, (7) mixed moderately saline and very saline, (8) mixed moderately saline, very saline, and brine, (9) very saline, (10) mixed very saline and brine, and (11) brine (Figures 7.1.5-1 and 7.1.5-2). Mapping was based on water quality samples from wells and estimated total dissolved solids calculations based on geophysical well logs. After performing aquifer determination, there were 384 Wilcox Group wells with water quality samples: 286 fresh, 92 slightly saline, and 6 moderately saline. There were 618 wells with estimated total dissolved solids calculations for the Wilcox Group. These calculations were performed on 1,867 depth intervals. This led to the creation of 952 salinity class intervals in 612 wells for the Wilcox Group: 36 fresh, 302 slightly saline, 345 moderately saline, 222 very saline, and 47 brine. Two hundred and ninety-two wells contain multiple salinity classes within the Wilcox Group ranging from two to five vertical zones per well.

Distribution of salinity within the Wilcox Group is quite complex with large areas mapped as mixed classes consisting of multiple stacked salinity zones. These areas could not be easily subdivided into individual, unmixed salinity classes. If we had subdivided the Wilcox Group (north of the Colorado River into the Hooper, Simsboro, and Calvert Bluff formations and south of the Colorado River informally into the upper, middle, and lower Wilcox) this may have allowed us to create fewer mixed class polygons in parts of the study area. An example of this is shown on Figure 7.1.7-3 for the Simsboro Formation. However, the multiple stacked salinity classes within the Wilcox Group do not necessarily follow formation boundaries and this extra effort to stratigraphically subdivide the Wilcox Group would have required data density more akin to a site-specific study than a regional study. Mapping the complex salinity classes is also complicated by limited water quality data, limited sampling across the entire thickness of the Wilcox Group, missing well screen data, water quality samples may include mixtures from more than one salinity zone, and anthropogenic contamination affecting native water quality (especially in and downdip from the outcrop zone). The evolution of salinity with depth is also affected by water-rock interaction, geologic faulting, recharge rates, and connectivity of sands resulting from original depositional environments and subsequent post-deposition Yoakum Canyon erosion and later filling.

The moderately saline class in the southwest corner of the study area is interesting since it is so far downdip. There are many wells showing this resistivity signature, however there are other causes that could increase the resistivity signature not related to total dissolved solids, for example, bicarbonate. It would be advisable for any exploration of brackish groundwater in this area to first perform additional analysis of actual water quality samples to confirm these results before proceeding further.

The outcrop area is particularly challenging since most water wells do not fully penetrate the aquifer and there are fewer geophysical logs available. If groundwater of different salinity classes is produced from wells, it is not apparent that the water quality sample represents a mix of the producing zones.

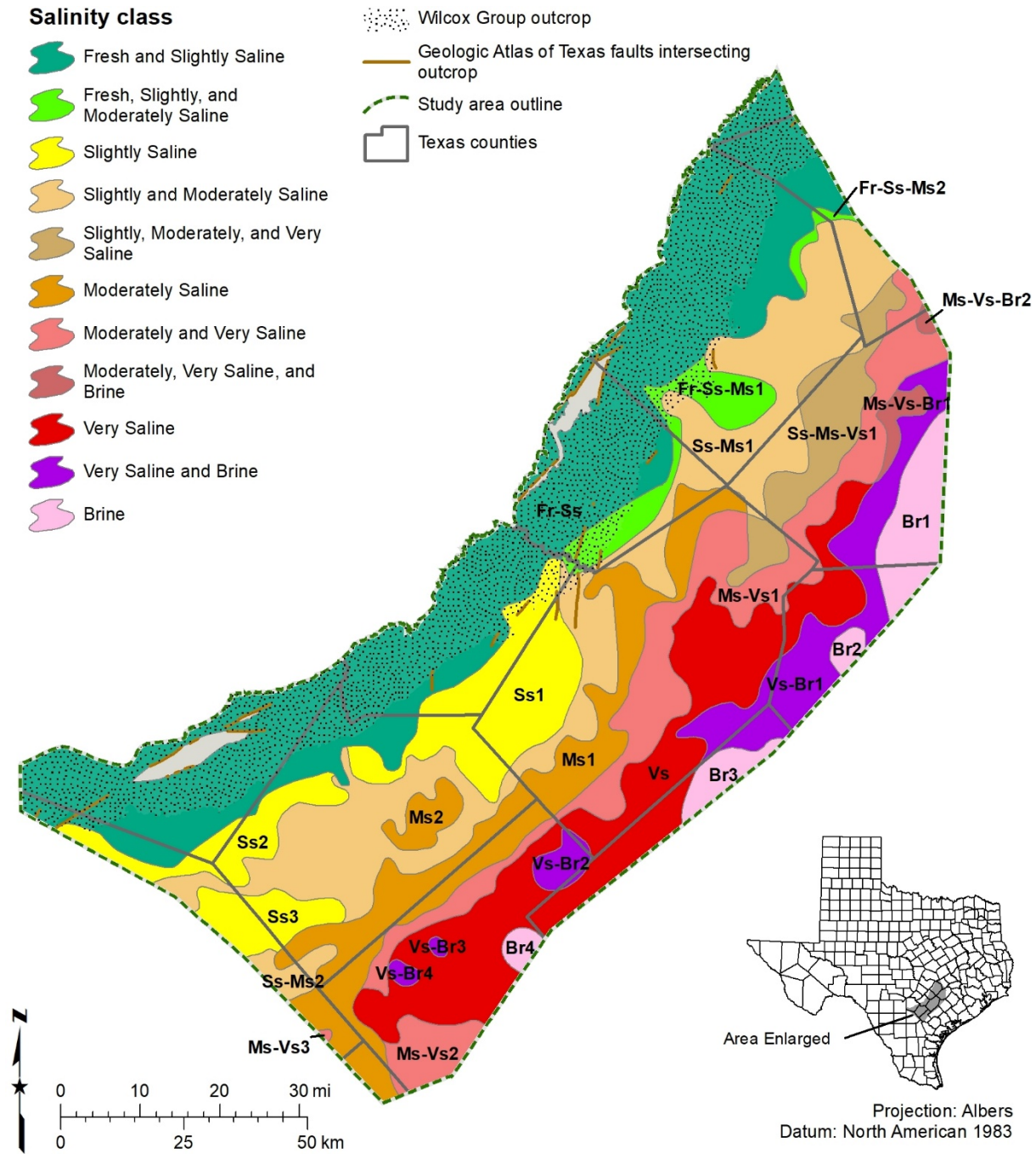


Figure 7.1.5-1. Wilcox Group salinity classes and identification names. Refer to Table 2-1 for salinity class definition.

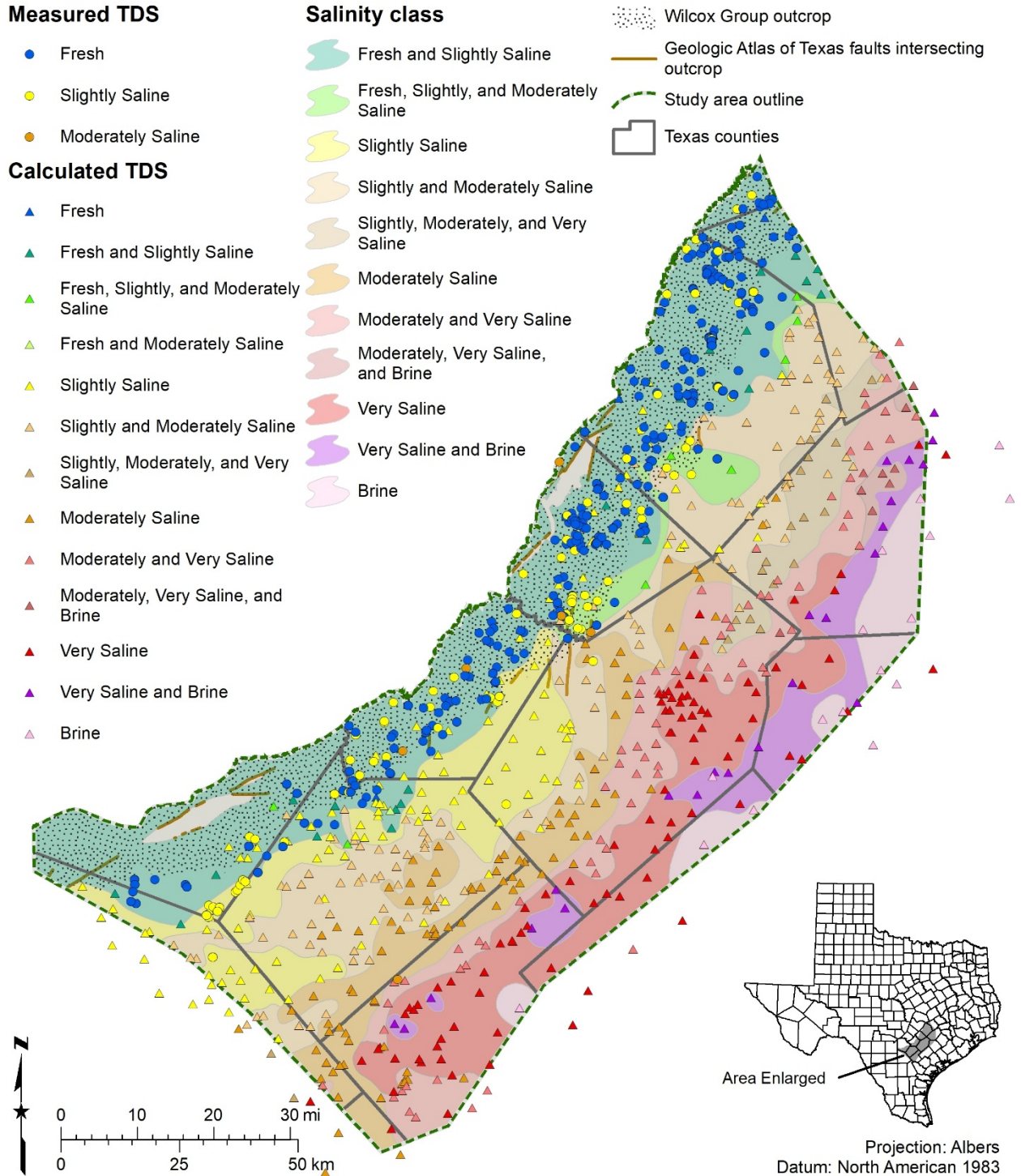


Figure 7.1.5-2. Wilcox Group salinity classes and well control consisting of water well quality data (circles) and interpreted geophysical well logs (triangles). Refer to Table 2-1 for salinity class definition. TDS = total dissolved solids.

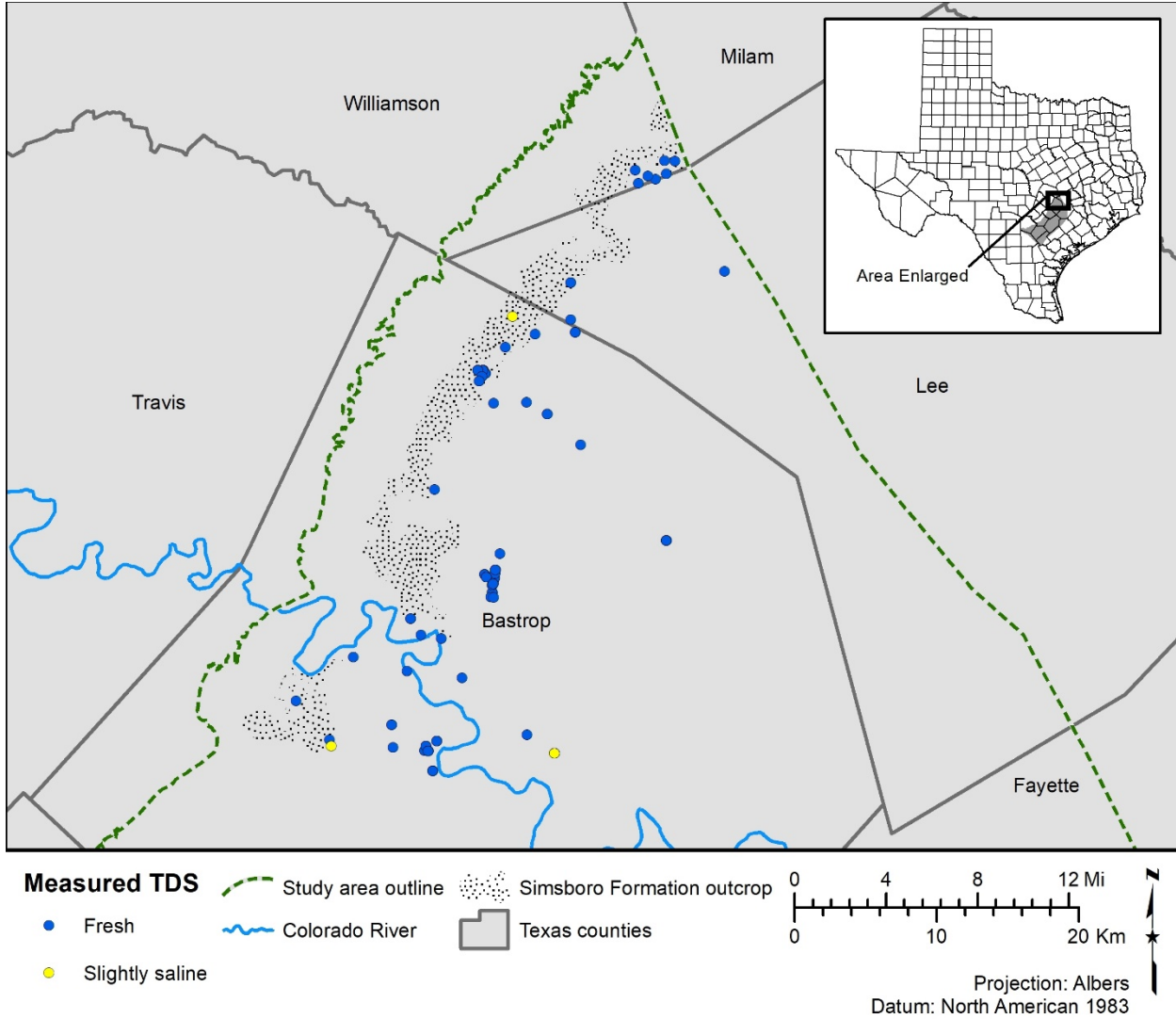


Figure 7.1.5-3. Wells with water quality data from the Simsboro Formation of the Wilcox Group in the northeastern portion of the study area. The Simsboro Formation is used by several public water systems in the area (Aqua Water Supply Corporation, City of Elgin, and others). TDS = total dissolved solids.

7.1.6 Volume of brackish groundwater

We calculated the volume of in-place groundwater for the Wilcox Group based on salinity classes (Table 7.1.6-1). The Wilcox Group contains more than 112 million acre-feet of in-place brackish groundwater and additional significant brackish groundwater in mixed classes within the study area. The Wilcox Group contains a total of more than 321 million acre-feet of in-place groundwater of all salinity ranges within the study area.

Table 7.1.6-1. Total volume (acre-feet) of in-place groundwater in the Wilcox Group based on salinity class. Values summarized from Table 13.1.1-1. Volume values rounded to the nearest 10,000 acre-feet. Refer to Figure 7.1.5-1 for location of each salinity class.

Salinity class	Identification name	Volume groundwater (per salinity subclass) (acre-feet)	Volume groundwater (per salinity class) (acre-feet)
Fr - Ss	Fr-Ss	27,950,000	27,950,000
Fr - Ss - Ms	Fr-Ss-Ms1	6,000,000	7,330,000
	Fr-Ss-Ms2	1,330,000	
Slightly saline	Ss1	12,750,000	21,520,000
	Ss2	3,520,000	
	Ss3	5,250,000	
Ss - Ms	Ss-Ms1	54,340,000	56,620,000
	Ss-Ms2	2,280,000	
Ss - Ms - Vs	Ss-Ms-Vs	19,730,000	19,730,000
Moderately saline	Ms1	31,050,000	33,850,000
	Ms2	2,800,000	
Ms - Vs	Ms-Vs1	41,100,000	44,030,000
	Ms-Vs2	2,840,000	
	Ms-Vs3	90,000	
Ms - Vs - Br	Ms-Vs-Br1	3,310,000	4,060,000
	Ms-Vs-Br2	750,000	
Very saline	Vs	52,740,000	52,740,000
Vs - Br	Vs-Br1	26,180,000	29,940,000
	Vs-Br2	2,960,000	
	Vs-Br3	300,000	
	Vs-Br4	500,000	
Brine	Br1	16,300,000	23,470,000
	Br2	1,670,000	
	Br3	4,250,000	
	Br4	1,250,000	

Notes:

Fr - Ss is a mixed class of fresh and slightly saline.

Fr - Ss - Ms is a mixed class of fresh, slightly, and moderately saline.

Ss - Ms is a mixed class of slightly and moderately saline.

Ss - Ms - Vs is a mixed class of slightly, moderately, and very saline.

Ms - Vs is a mixed class of moderately and very saline;

Ms - Vs - Br is a mixed class of moderately saline, very saline, and brine.

Vs - Br is a mixed class of very saline and brine.

Additionally, we subdivided the volumes based on administrative boundaries (Appendix 13.1, Tables 13.1.1-1, 13.1.1-2, 13.1.1-3, and 13.1.1-4). Appendix 13, Section 13.2 contains a complete discussion of volume methodology. Once salinity class mapping for the Wilcox Group was completed, we noticed that the study area did not include the entire available resource affecting some groundwater volume calculations. Specifically, the study area does not include the entire extent of Wilcox Group moderately saline water in the southwest part of the study area. Calculation of groundwater volumes used aquifer-based study area boundaries and some administrative boundaries are not coincident with the study area boundary. This resulted in

partial volumes for some areas. Future evaluation of the Wilcox Group to the northeast and southwest of this study area will address some of these issues.

7.1.7 Aquifer hydraulic properties

We compiled 693 sets of aquifer hydraulic property data from 664 wells completed in the Wilcox Group. The data is organized by hydraulic property (Table 7.1.7-1) and recorded in a BRACS Database table (tblUCPC_AquiferTestInformation). Wilcox Group records are identified using the field aquifer_new = WX. A full discussion of this dataset is provided in Section 6.7. We prepared a map showing the spatial distribution of wells with well yield, specific capacity, transmissivity, and hydraulic conductivity (Figure 7.1.7-1).

Table 7.1.7-1. Hydraulic properties of the Wilcox Group within the study area. Refer to the BRACS Database table (tblUCPC_AquiferTestInformation) for detailed information about each well and data. Refer to Figure 7.1.7-1 for a map of these parameters.

	Transmissivity (gallons per day per foot)	Hydraulic conductivity (feet per day)	Storage coefficient (dimensionless)	Specific capacity (gallons per minute per foot)	Well yield (gallons per minute)
Number of values	31	16	12	380	688
Low	609	3	0.000099	0.02	2
High	105,000	1,520	0.0012	116.66	3,100
Average	23,349	251	0.00058	4.46	213

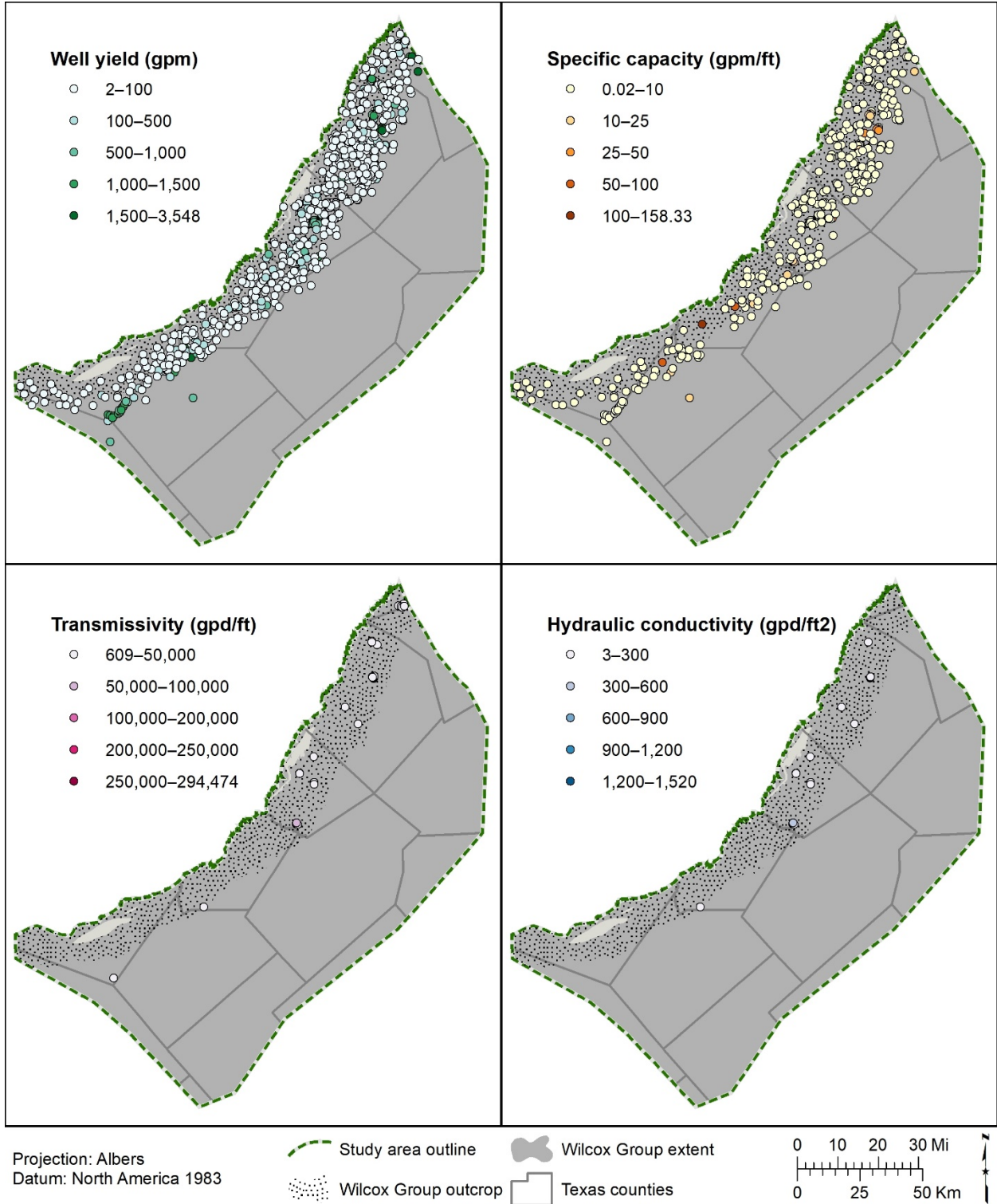


Figure 7.1.7-1. Wilcox Group hydraulic properties showing well yield (gallons per minute), specific capacity (gallons per minute per foot of drawdown), transmissivity (gallons per day per foot), and hydraulic conductivity (gallons per day per foot squared). Refer to Table 7.1.7-1 for a summary of these parameters.

7.2 Carrizo Sand

The Carrizo Sand of the Claiborne Group is also known as the Upper Wilcox in the region south of the San Marcos Arch and in the deep subsurface. The Carrizo Sand unconformably underlies the Reklaw Formation and unconformably overlies Middle Wilcox – Calvert Bluff Formation. The Carrizo-Wilcox Aquifer, wholly comprised of the Wilcox Group and Carrizo Sand, is a TWDB-designated major aquifer in Texas (George and others, 2011) that produces large amounts of water over a large geographic area.

7.2.1 Well control

More than 950 wells were used in defining aspects of the Carrizo Sand stratigraphy, lithology, and water quality (Table 7.2.1-1). We only used wells for water quality and aquifer hydraulic properties based on the aquifer determination analysis. Undoubtedly there are many other wells completed in the Carrizo Sand, but without detailed well screen information it is not possible to accurately assign the Carrizo Sand as the source of water produced from the wells.

Table 7.2.1-1. Carrizo Sand well control data points.

Well control with this information	Number of data points
Lithology	964
Top surface stratigraphic picks used for raster surface	645
Bottom surface stratigraphic picks used for raster surface	682
Top surface stratigraphic picks (database total*)	757
Bottom surface stratigraphic picks (database total*)	793
Net sand interpreted from wells	526
Aquifer hydraulic properties	550 wells with 632 measurements
Water quality: wells	250 wells with 708 measurements
TDS interpreted from geophysical well logs	404 wells with 864 depth intervals
Porosity	36

*Total number of stratigraphic picks in study counties

7.2.2 Stratigraphic analysis

The Carrizo Sand stratigraphic top and bottom was evaluated using geophysical well logs and selected water well control, the latter primarily along the outcrop. The Carrizo Sand stratigraphic base was selected as the base of the first significant sharp-based sand superjacent to a regional marine shale marker equivalent to the top of the Middle Wilcox (south of the San Marcos Arch) or top of the Calvert Bluff Formation (north of the San Marcos Arch). A regional unconformity exists at the base of the Carrizo Sand, and in some areas the base of Carrizo Sand has eroded into the underlying Wilcox sediments. In areas where there are several interbedded, sand-based, upward coarsening sequences in the Middle Wilcox, the Carrizo-Wilcox boundary is problematic, so we selected the base of Carrizo Sand at the base of the first major sand unit. Nearby well control was compared to formation thickness to ensure consistency. This contact is based on lithostratigraphic correlation using geophysical log signatures without paleontology control for dating.

The Carrizo Sand stratigraphic top was selected as the top of the massive sands. Usually sands occur within the overlying basal Reklaw Formation (known as the Newby Sand by Sellards and others, 1932; and as Mackhank, Luling, Slick, and Second Reklaw sands by Sams, 1990) that

represent re-worked sands of the underlying Carrizo Sand deposited during the Reklaw Formation marine transgression. In southwest Karnes and adjacent counties, some Reklaw sands may represent barrier island and associated depositional environments that may be difficult to distinguish from the underlying upper Carrizo Sand (Atkinson sand of Bulling and Breyer, 1989). These sands typically have a lower overall deep resistivity signature on geophysical well logs and limited areal extent. The Carrizo – Reklaw contact is based on lithostratigraphic correlation using geophysical log signatures without paleontology control for dating. Brown and Loucks (2009) include an unnamed transgressive systems tract overlain by a highstand systems tract between the top of the Carrizo Sand and base of the Reklaw Formation. We do not know if these sediments exist in the study area; if so, this may explain some of the uncertainty in stratigraphic assignment.

Geophysical well log signatures for the Carrizo Sand top depth in Wilson County are displayed in Figure 7.2.2-1. The Carrizo Sand top depth is 990 feet below ground surface (yellow line). The geophysical well log includes: the spontaneous potential (solid line) and gamma ray (dotted line) recorded in the left track, depth below ground surface (feet) in the center track (each depth increment represents 10 feet), and induction (dotted line) and shallow normal resistivity (solid line) tools in the right track. The induction tool is over-range below 1,105 in depth. This log is from BRACS well id 42363 in southern Wilson County, Texas. The log was performed by Schlumberger in 1981 with a kelly bushing height of 15 feet.

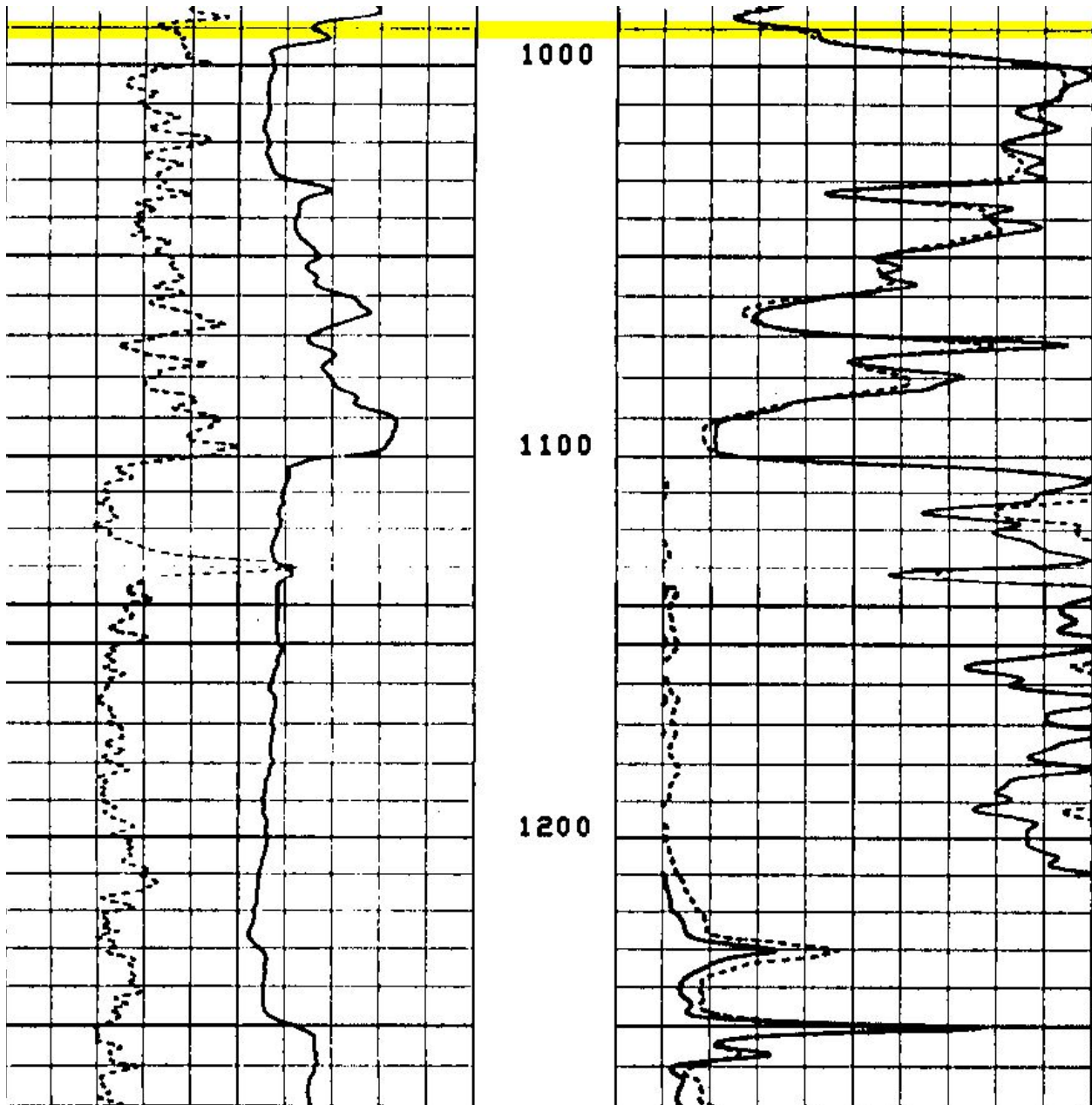


Figure 7.2.2-1. Carrizo Sand top depth interpreted on a geophysical well log in Wilson County, Texas.

Geophysical well log signatures for the Carrizo Sand bottom depth in Wilson County are displayed in Figure 7.2.2-2. The Carrizo Sand bottom depth is 1,878 feet below ground surface (yellow line). The geophysical well log includes: the spontaneous potential (solid line) and gamma ray (dotted line) recorded in the left track, depth below ground surface (feet) in the center track (each depth increment represents 10 feet), and induction (dotted line) and shallow normal resistivity (solid line) tools in the right track. This log is from BRACS well id 42363 in southern Wilson County, Texas. The log was performed by Schlumberger in 1981 with a kelly bushing height of 15 feet.

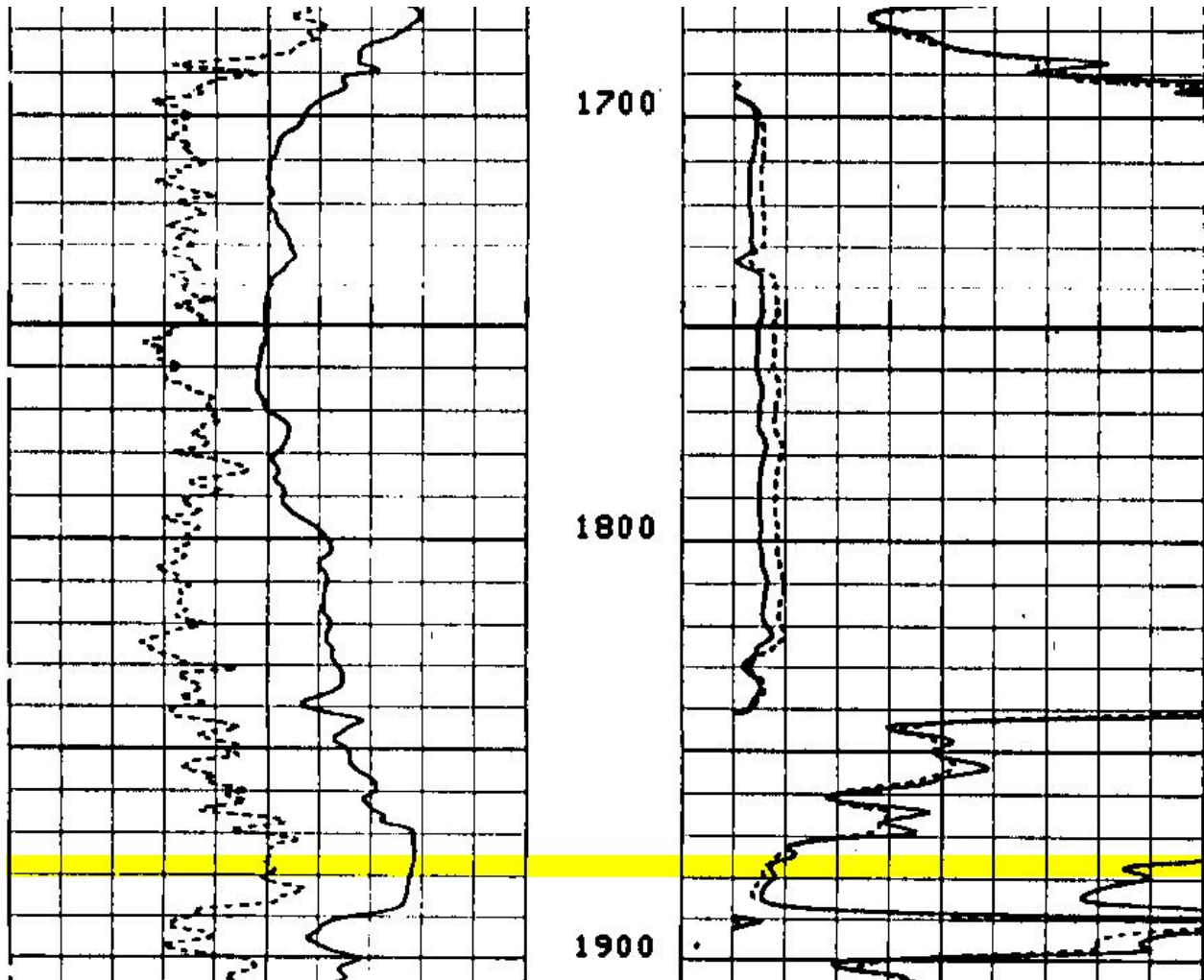


Figure 7.2.2-2. Carrizo Sand bottom depth interpreted on a geophysical well log in Wilson County, Texas.

Geophysical well log signatures for the Carrizo Sand top depth in Gonzales County are displayed in Figure 7.2.2-3. The Carrizo Sand top depth is 1,705 feet below ground surface (yellow line). The geophysical well log includes: the spontaneous potential recorded in the left track, depth below ground surface (feet) in the center track (each depth increment represents 10 feet), and induction (dotted line) and short normal resistivity (solid line) tools in the right track. This log is from BRACS well id 15399 in northeastern Gonzales County, Texas. The log was performed by Lane Wells in 1966 with a kelly bushing height of 10 feet.

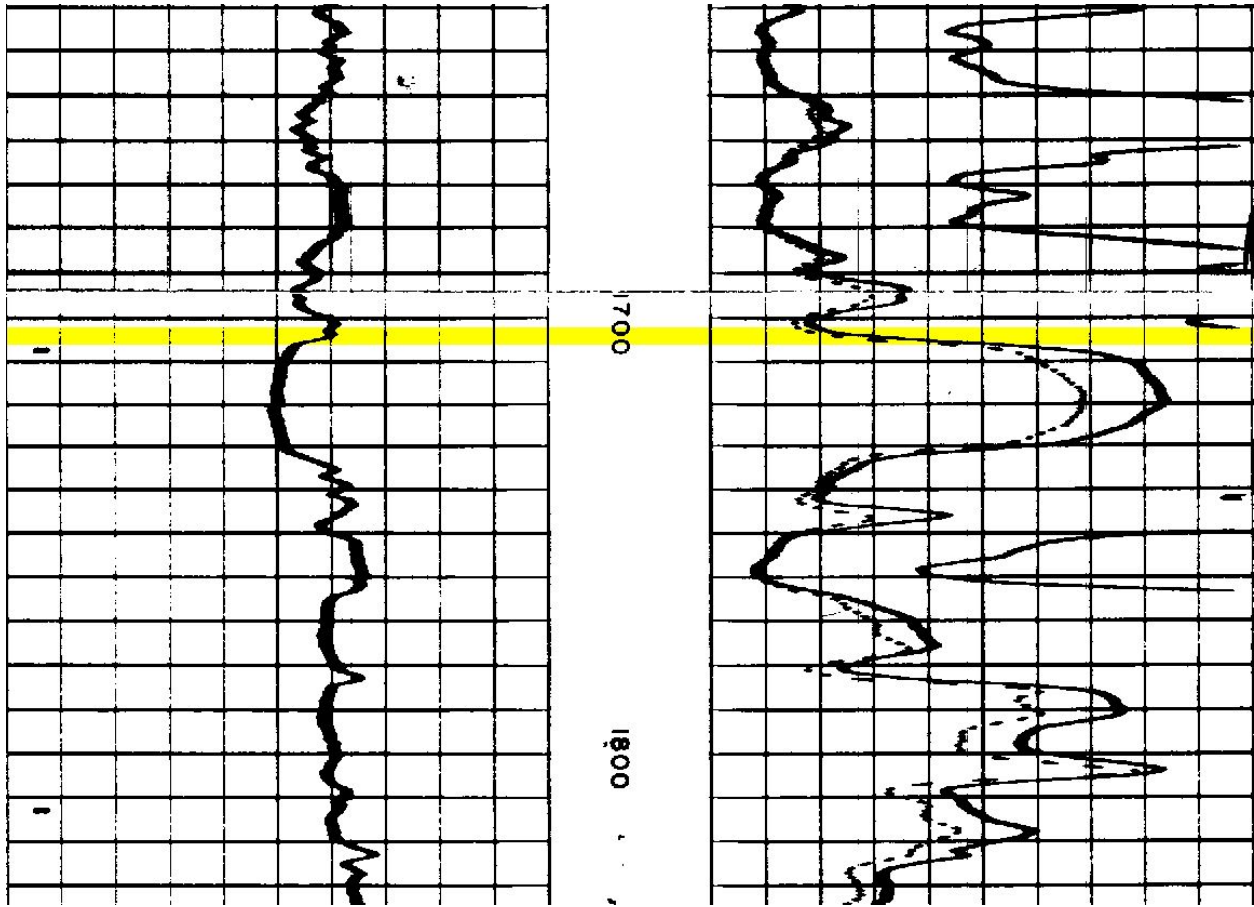


Figure 7.2.2-3. Carrizo Sand top depth interpreted on a geophysical well log in Gonzales County, Texas.

Geophysical well log signatures for the Carrizo Sand bottom depth in Gonzales County are displayed in Figure 7.2.2-4. The Carrizo Sand bottom depth is 2,336 feet below ground surface (yellow line). The geophysical well log includes: the spontaneous potential recorded in the left track, depth below ground surface (feet) in the center track (each depth increment represents 10 feet), and induction (dotted line) and short normal resistivity (solid line) tools in the right track. This log is from BRACS well id 15399 in northeastern Gonzales County, Texas. The log was performed by Lane Wells in 1966 with a kelly bushing height of 10 feet.

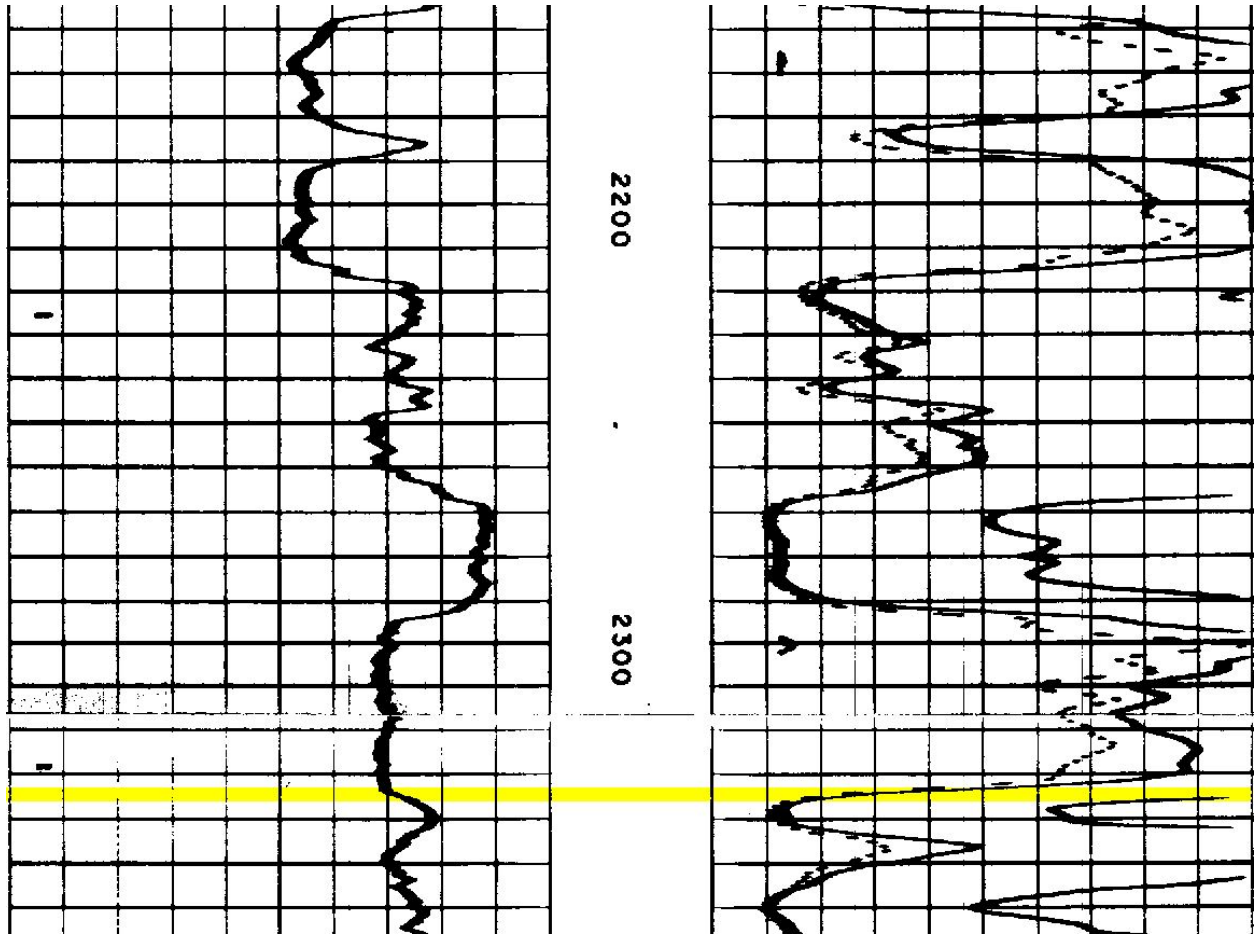


Figure 7.2.2-4. Carrizo Sand bottom depth interpreted on a geophysical well log in Gonzales County, Texas.

7.2.3 Formation top, bottom, thickness

Carrizo Sand top and bottom elevation maps (Figures 7.2.3-1 and 7.2.3-2) were prepared using 645 and 682 stratigraphic picks respectively from wells within the study area in addition to some wells immediately outside of the study area to control GIS raster edge effects. Carrizo Sand top and bottom depth maps (Figures 7.2.3-3 and 7.2.3-4) were prepared using elevation GIS rasters subtracted from the study area digital elevation model (refer to Appendix, Section 13.6 raster interpolation documentation).

The Carrizo Sand thickness was prepared by subtracting the bottom elevation GIS raster from the top elevation GIS raster. The Carrizo Sand thickness is 0 at the updip outcrop edge and over 1,500 feet at the downdip limit of the study area in Karnes County (Figure 7.2.3-5, Plate 7). The Carrizo Sand thickens dramatically within the Wilcox Fault Zone, a series of growth-faults gulfward of the study area.

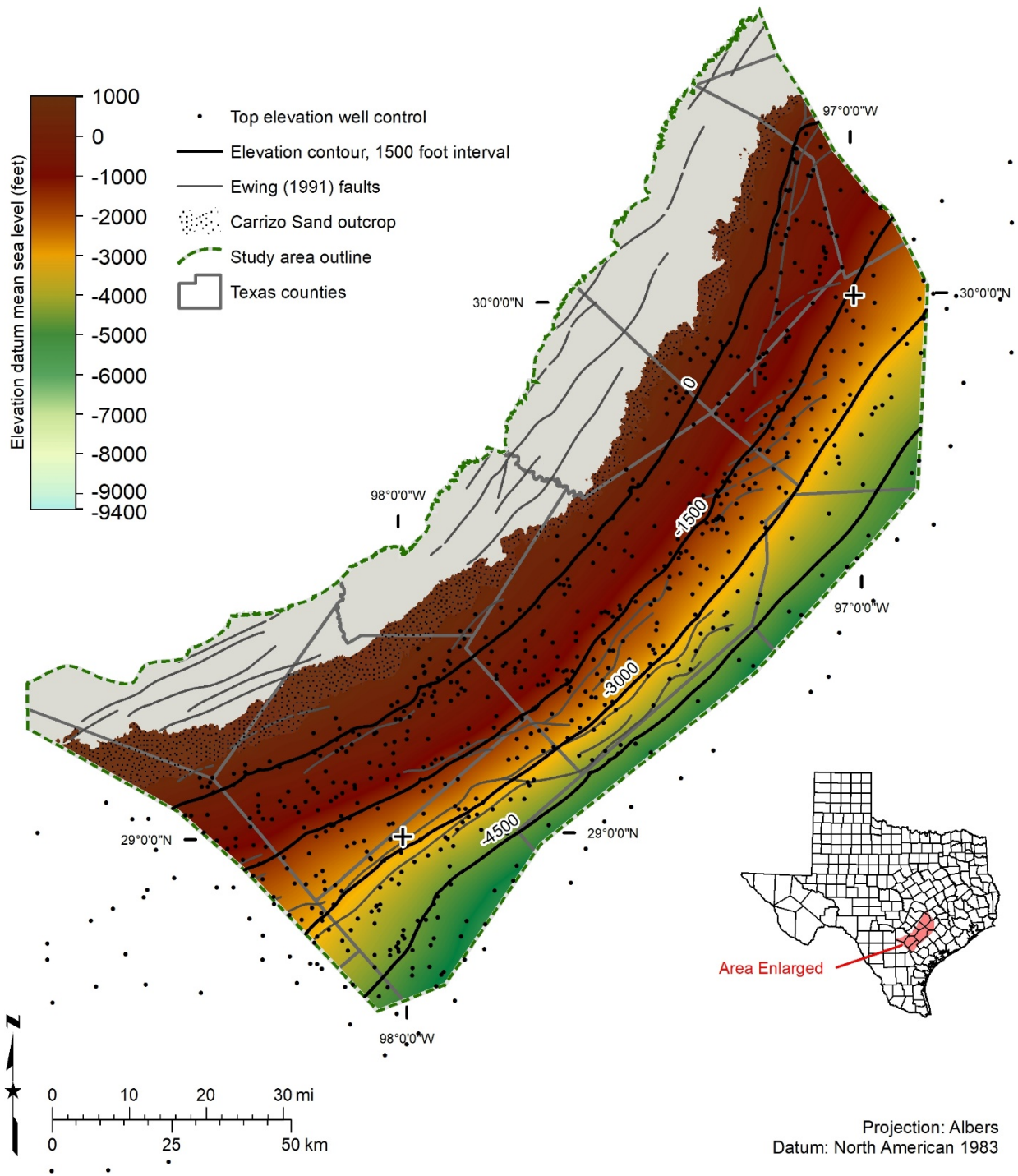


Figure 7.2.3-1. Carrizo Sand top elevation (feet above mean sea level), which was prepared using 645 wells for stratigraphic control (black dots).

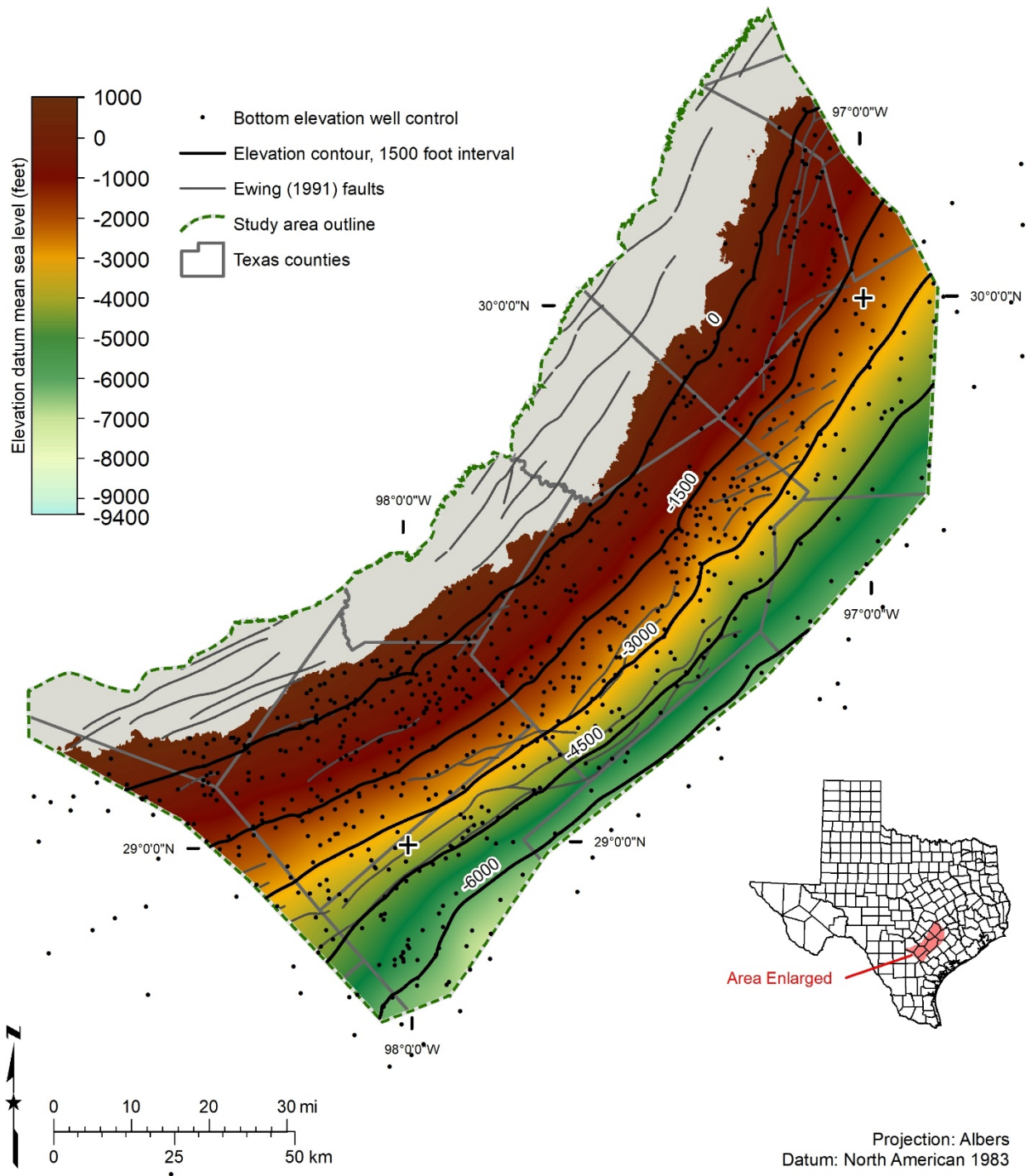


Figure 7.2.3-2. Carrizo Sand bottom elevation (feet above mean sea level), which was prepared using 682 wells for stratigraphic control (black dots).

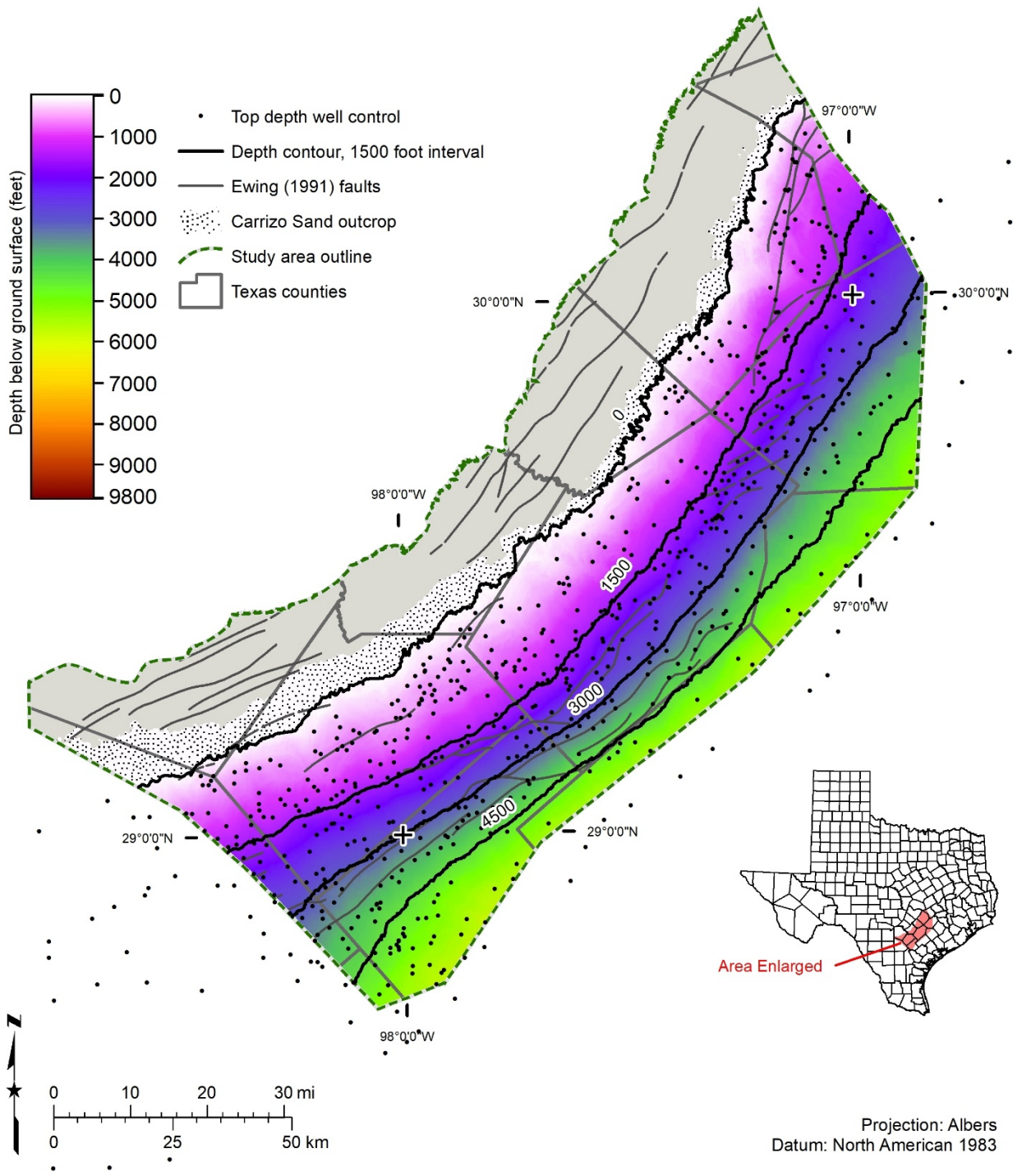


Figure 7.2.3-3. Carrizo Sand top depth (feet below ground surface), which was prepared using 645 wells for stratigraphic control (black dots).

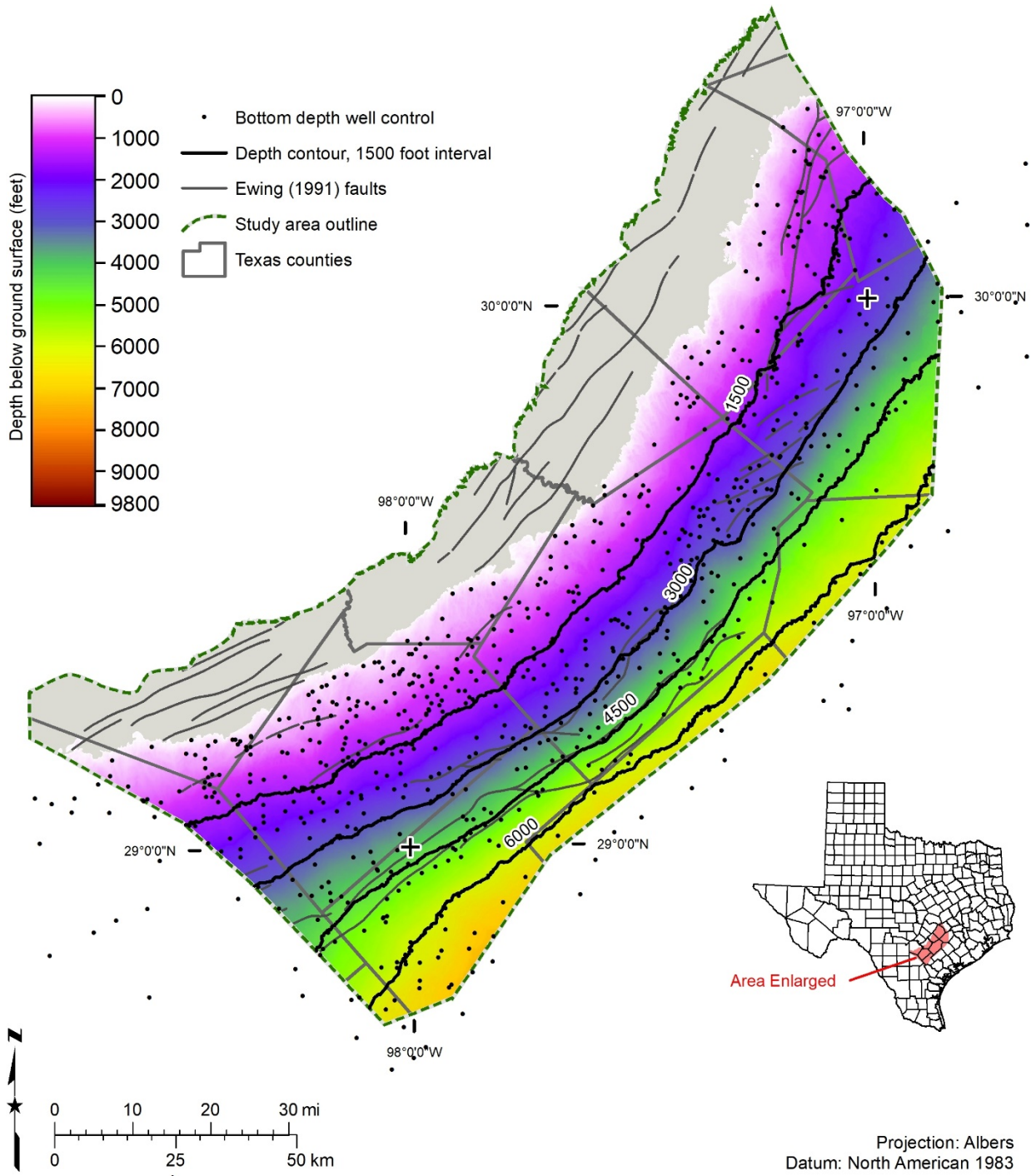


Figure 7.2.3-4. Carrizo Sand bottom depth (feet below ground surface), which was prepared using 682 wells for stratigraphic control (black dots).

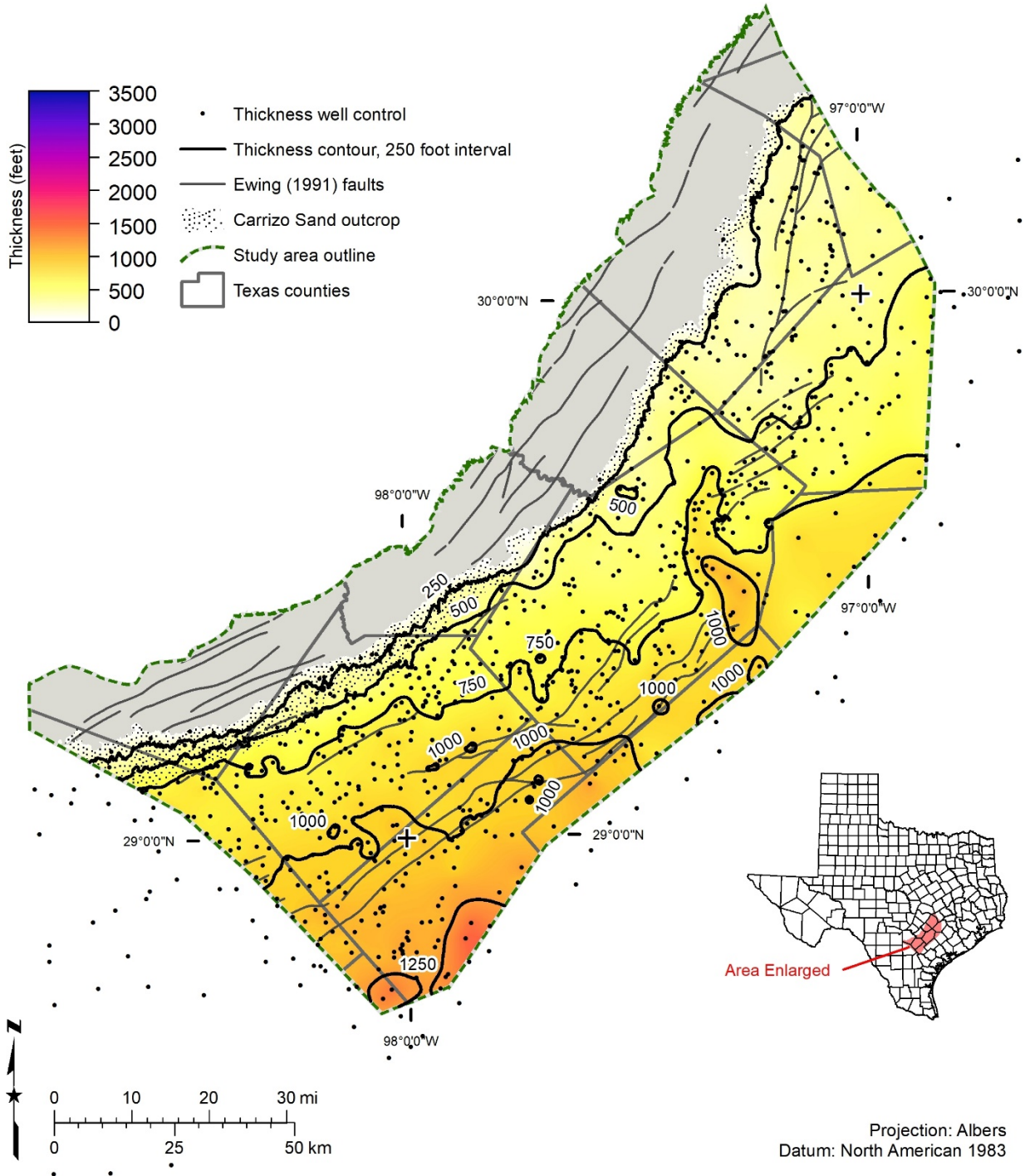


Figure 7.2.3-5. Carrizo Sand thickness in units of feet, which was prepared using 645 wells for stratigraphic control (black dots).

7.2.4 Net sand

We evaluated 526 wells, of which 202 are water wells, 302 are oil and gas wells, and 22 are wells classified as other (primarily test holes for water wells). We used geophysical well logs for 327 wells and drillers' descriptions of lithology for the remaining 199 wells. Net sand values

range from 0 at the updip outcrop edge to over 1,000 feet in Karnes County. One of the two primary fluvial sediment input axes in South Texas (Hamlin, 1988) is represented on this map (Figure 7.2.4-1). Our mapping shows significant accumulations of lower Wilcox Group sediment north of the San Marcos Arch and significant accumulation of Carrizo Sand sediment south of the San Marcos Arch that is also reflected in previous studies (Bebout and others, 1982).

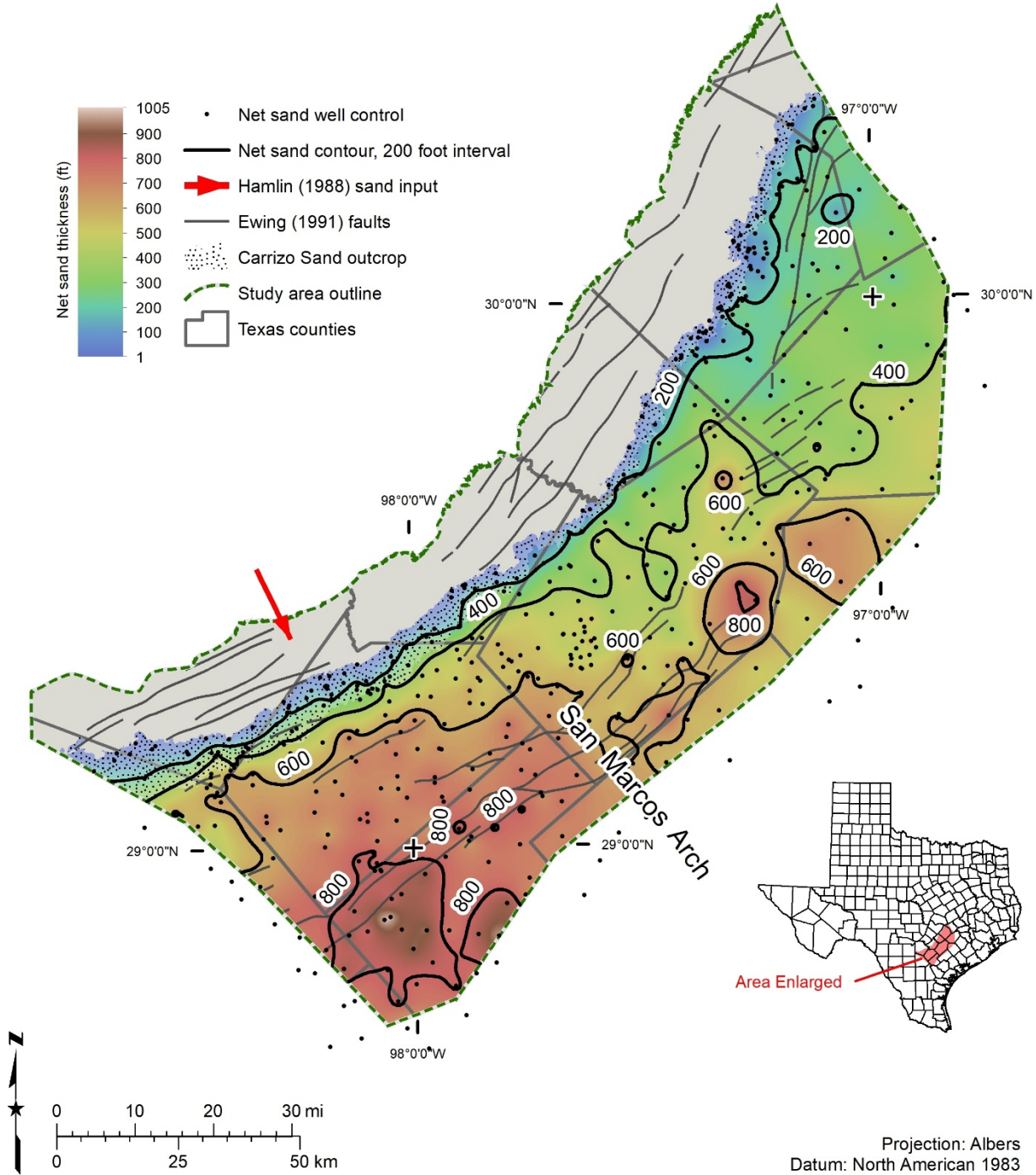


Figure 7.2.4-1. Carrizo Sand net sand thickness (feet), which was prepared using 526 wells for net sand control (black dots). A significant fluvial sand input to the basin by Hamlin (1988) is noted with the red arrow.

7.2.5 *Salinity classes*

The Carrizo Sand was mapped into defined salinity classes: (1) fresh, (2) mixed fresh and slightly saline, (3) slightly saline, (4) mixed slightly saline and moderately saline, (5) moderately saline, (6) mixed moderately saline and very saline, (7) very saline, (8) mixed very saline and brine, and (9) brine (Figures 7.2.5-1 and 7.2.5-2). Mapping was based on water quality samples (250 wells classified as: 229 fresh, 16 slightly saline, 1 very saline, and 1 brine; three wells had water quality samples in more than one salinity class) and estimated total dissolved solids calculations using geophysical well logs (590 wells with 1,283 depth intervals analyzed yielding 587 wells with 870 salinity class zones: 306 fresh, 297 slightly saline, 170 moderately saline, 72 very saline, and 25 brine). Two hundred and thirteen wells contain multiple salinity classes within the Carrizo Sand ranging from two to five vertical zones per well.

Distribution of salinity within the Carrizo Sand is quite complex with large areas mapped as mixed salinity classes consisting of multiple salinity zones. These areas could not be easily subdivided into unmixed salinity classes. Many geophysical well logs show differences in salinity with depth. The mixed salinity classes generally occur as transitions from one salinity class to another, for example from fresh to slightly saline. The study area is bisected with brackish groundwater mapped from the outcrop extending downdip in central Gonzales County. On either side of this brackish groundwater, lobes of fresh water extend 19 miles downdip from the outcrop in the northeast and the fresh groundwater and mixed fresh and slightly saline classes extend up to 27 miles downdip from the outcrop in the southwest. The lobe of mixed fresh and slightly saline groundwater in the southwest typically has a core of fresh water that may have brackish water at the top, bottom, or both positions in the Carrizo Sand. Very saline groundwater occurs about 24 miles downdip from the outcrop in the northeastern part of the study area, 17 miles downdip in the central part the study area, and 44 miles downdip in the extreme southwest corner of the study area.

The transition from one salinity class to another is not simple. We believe that initial depositional environments as illustrated by net sand distribution and the occurrence, displacement, orientation, and connectivity of normal faults all interact to control groundwater salinity distribution.

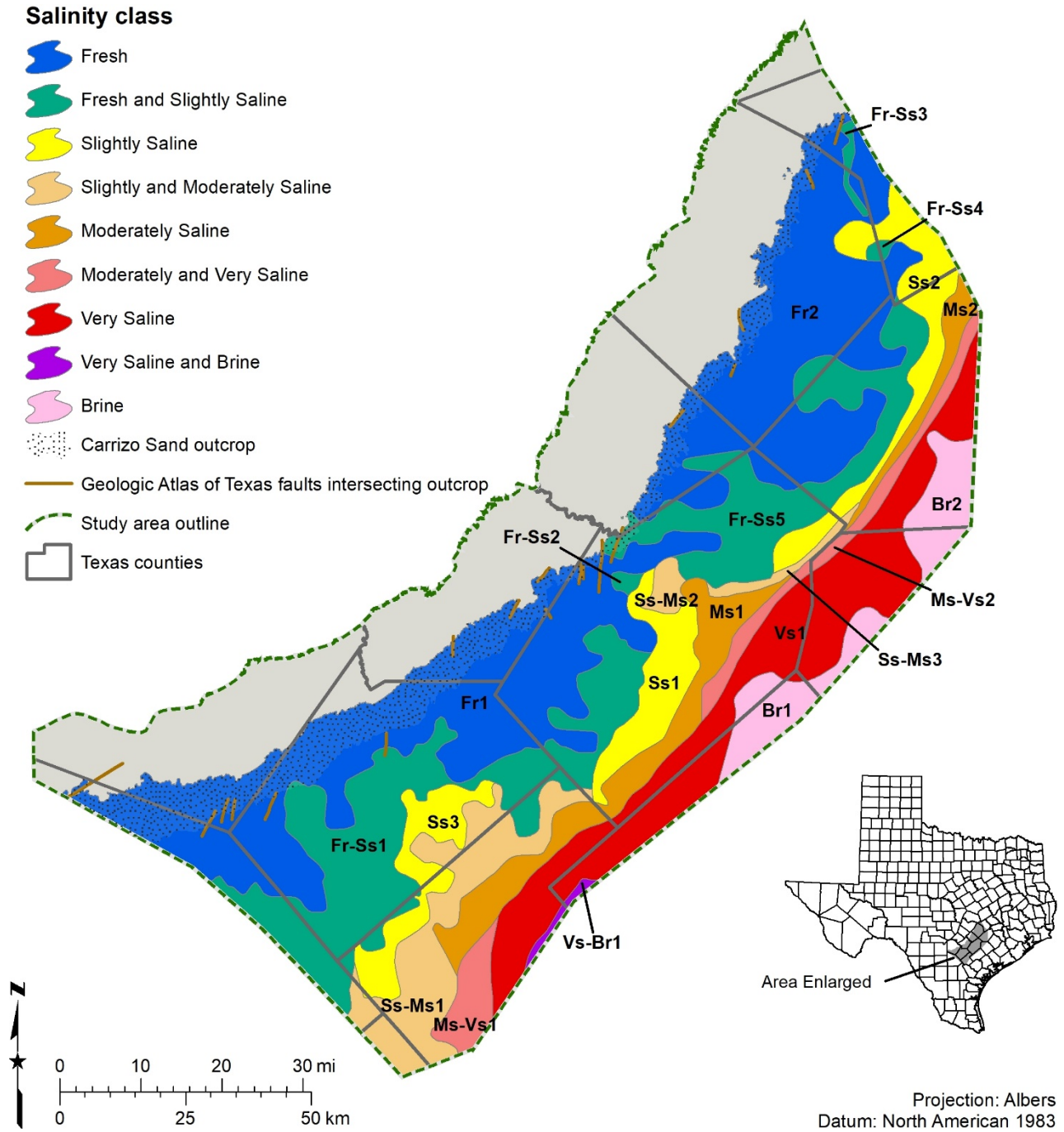


Figure 7.2.5-1. Carrizo Sand salinity classes and identification names. Refer to Table 2-1 for salinity class definition.

Measured TDS

- Fresh
- Slightly Saline
- Very Saline

Calculated TDS

- ▲ Fresh
- ▲ Fresh and Slightly Saline
- ▲ Fresh, Slightly, and Moderately Saline
- ▲ Slightly Saline
- ▲ Slightly and Moderately Saline
- ▲ Slightly, Moderately, and Very Saline
- ▲ Moderately Saline
- ▲ Moderately and Very Saline

- ▲ Very Saline
- ▲ Very Saline and Brine
- ▲ Brine

Salinity class

- Fresh
- Fresh and Slightly Saline
- Slightly Saline
- Slightly and Moderately Saline
- Moderately Saline
- Moderately and Very Saline
- Very Saline
- Very Saline and Brine
- Brine

- Carrizo Sand outcrop
- Geologic Atlas of Texas faults intersecting outcrop
- - - Study area outline
- Texas counties

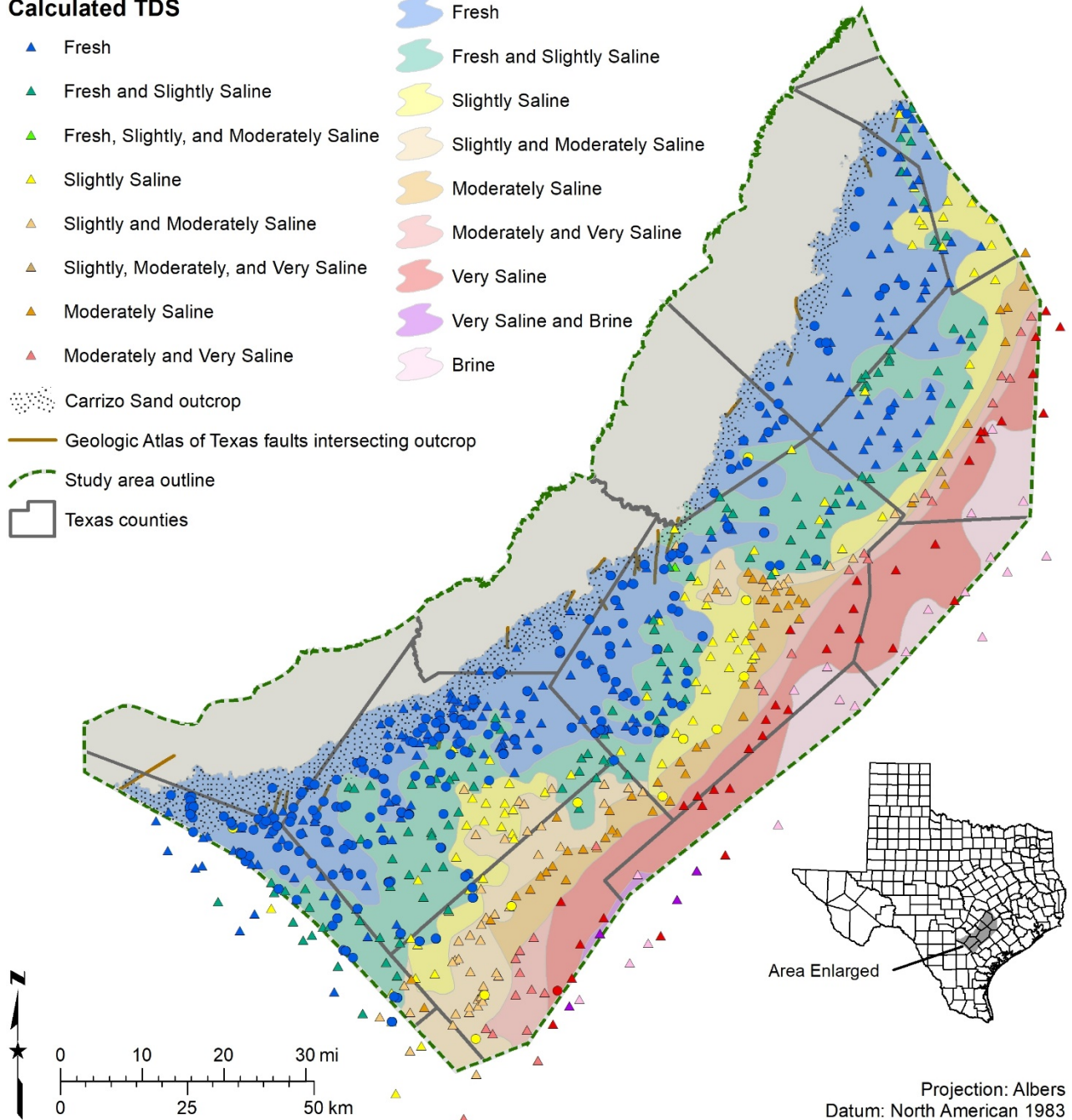


Figure 7.2.5-2. Carrizo Sand salinity classes and well control consisting of water well quality data (circles) and interpreted geophysical well logs (triangles). Refer to Table 2-1 for salinity class definition. TDS = total dissolved solids.

7.2.6 Volume of brackish groundwater

We calculated the volume of in-place groundwater for the Carrizo Sand based on salinity classes (Table 7.2.6-1). The Carrizo Sand contains more than 57 million acre-feet of in-place brackish groundwater and additional significant brackish groundwater in mixed classes within the study area. The Carrizo Sand contains a total of more than 204 million acre-feet of in-place groundwater of all salinity ranges within the study area.

Table 7.2.6-1. Total volume (acre-feet) of in-place groundwater in the Carrizo Sand based on salinity class. Values summarized from Table 13.1.2-1. Volume values rounded to the nearest 10,000 acre-feet. Refer to Figure 7.2.5-1 for location of each salinity class.

Salinity class	Identification name	Volume groundwater (per salinity subclass) (acre-feet)	Volume groundwater (per salinity class) (acre-feet)
Fresh	Fr1	31,140,000	46,370,000
	Fr2	15,230,000	
Fr - Ss	Fr-Ss1	34,040,000	46,690,000
	Fr-Ss2	320,000	
	Fr-Ss3	250,000	
	Fr-Ss4	160,000	
	Fr-Ss5	11,920,000	
Slightly saline	Ss1	6,100,000	20,400,000
	Ss2	5,160,000	
	Ss3	9,140,000	
Ss - Ms	Ss-Ms1	20,360,000	22,400,000
	Ss-Ms2	930,000	
	Ss-Ms3	1,110,000	
Moderately saline	Ms1	12,990,000	14,690,000
	Ms2	1,700,000	
Ms - Vs	Ms-Vs1	4,800,000	8,790,000
	Ms-Vs2	3,990,000	
Very saline	Vs1	33,370,000	33,370,000
Vs - Br	Vs-Br1	940,000	940,000
Brine	Br1	6,090,000	10,610,000
	Br2	4,520,000	

Notes:

Fr - Ss is a mixed class of fresh and slightly saline.

Ss - Ms is a mixed class of slightly and moderately saline.

Ms - Vs is a mixed class of moderately and very saline.

Vs - Br is a mixed class of very saline and brine.

Additionally, we subdivided the volumes based on administrative boundaries (Appendix 13, Tables 13.1.2-1, 13.1.2-2, 13.1.2-3, and 13.1.2-4). Appendix 13, Section 13.2 contains a complete discussion of volume methodology. Once salinity class mapping for the Carrizo Sand was completed, we noticed that the study area did not include the entire available resource affecting some groundwater volume calculations. Specifically, the study area does not include the entire extent of Carrizo Sand moderately saline water in the southwest part of the study area. The calculation of groundwater volumes used aquifer-based study area boundaries and some administrative boundaries are not coincident with the study area boundary. This resulted in

partial groundwater volumes for some counties, groundwater conservation districts, or regional water planning areas. Future evaluation of the Carrizo Sand to the northeast and southwest of this study area will address some of these issues.

7.2.7 Aquifer hydraulic properties

We compiled 630 sets of aquifer hydraulic property data from 550 wells completed in the Carrizo Sand. The data is organized by hydraulic property (Table 7.2.7-1) and recorded in the BRACS Database table (tblUCPC_AquiferTestInformation). Carrizo Sand records are identified using the field aquifer_new = CZ. A full discussion of this dataset is provided in Section 6.7. We prepared a map showing spatial distribution of wells with well yield, specific capacity, transmissivity, and hydraulic conductivity (Figure 7.2.7-1).

Table 7.2.7-1. Carrizo Sand hydraulic properties within the study area. Refer to the BRACS Database table (tblUCPC_AquiferTestInformation) for detailed information about each well and data. Refer to Figure 7.2.7-1 for a map of these parameters.

	Transmissivity (gallons per day per foot)	Hydraulic conductivity (feet per day)	Storage coefficient (dimensionless)	Specific capacity (gallons per minute per foot)	Well yield (gallons per minute)
Number of values	39	7	29	364	630
Low	23,802	145	0.0000843	0.05	2
High	294,474	734	0.0005	158.33	3,548
Average	148,467	360	0.00021	22.63	866

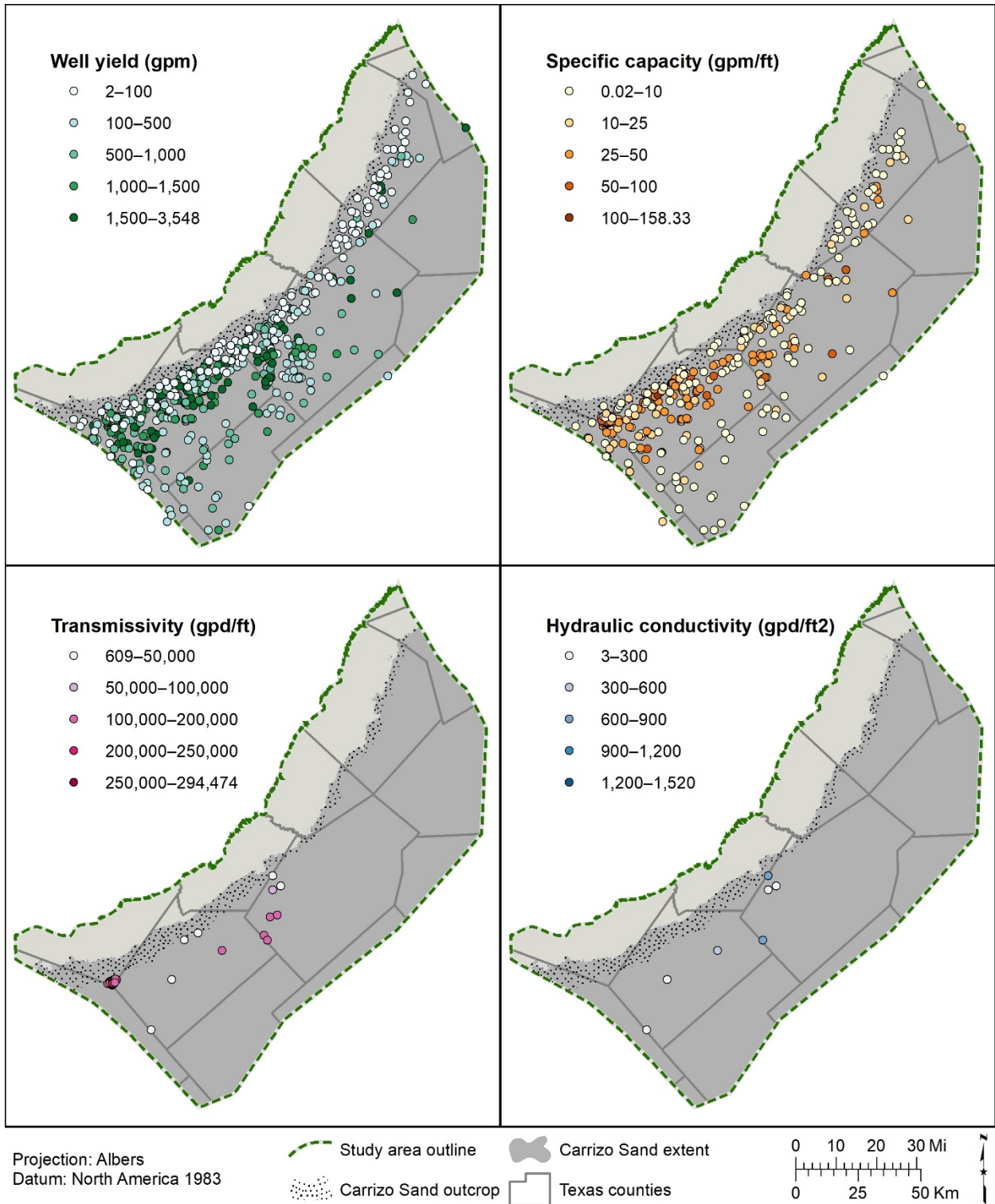


Figure 7.2.7-1. Hydraulic properties of the Carrizo Sand showing well yield (gallons per minute), specific capacity (gallons per minute per foot of drawdown), transmissivity (gallons per day per foot), and hydraulic conductivity (gallons per day per foot squared). Refer to Table 7.2.7-1 for a summary of these parameters.

7.3 Reklaw Formation

The Reklaw Formation of the Claiborne Group conformably underlies the Queen City Sand and unconformably overlies the Carrizo Sand. The Reklaw Formation consists of an upper Marquez Shale Member containing a marine condensed section representing maximum transgression and a lower Newby Sand Member in the region northeast of the San Marcos Arch. South of the arch, the lower Reklaw Formation contains an upper shale unit and several sands named after oilfield discoveries (Atkinson, Mackhank, Luling, Slick, and the First and Second Reklaw). Hamlin (1988) termed the sandy sediments transitional and assigned these to the Upper Wilcox of his usage (Carrizo Sand). Sams (1990) and Bulling and Breyer (1989) assume these sands are within the Reklaw Formation.

The Reklaw Formation is a regional aquitard with low permeability compared to the sand-rich Carrizo and Queen City formations and can hinder vertical water movement between the two aquifers. Isolated Reklaw Formation sands are generally encased in shale, offer limited potential for future production, and therefore, were not evaluated for groundwater potential.

7.3.1 Well control

More than 900 wells were used in defining aspects of the Reklaw Formation stratigraphy, lithology, and water quality (Table 7.3.1-1). We did not prepare net sand or salinity class maps, porosity, and volume calculations.

Table 7.3.1-1. Reklaw Formation well control data points.

Well control with this information	Number of data points
Lithology	706
Top surface stratigraphic picks used for raster surface	641
Bottom surface stratigraphic picks used for raster surface	634
Top surface stratigraphic picks (database total*)	902
Bottom surface stratigraphic picks (database total*)	755
Net sand interpreted from wells	596**
Aquifer hydraulic properties	47 wells with 47 measurements
Water quality: wells	26 wells with 32 measurements
TDS interpreted from geophysical well logs	0
Porosity	0

* Total number of stratigraphic picks in study counties

** Total number of wells with net sand values; however, these have not been verified for use

7.3.2 Stratigraphic analysis

Stratigraphic pick assignment of the upper contact of the Reklaw Formation was selected at the top of the shale subjacent to the base of the first progradational (coarsening upwards sequence) of the Queen City Sand. The bottom contact of the Reklaw Formation is at the base of a shale or sand marker above the massive sand signature of the Carrizo Sand. The bottom contact is problematic in places where significant apparent re-working of the upper Carrizo Sand sediments occurred during initial transgression. This problematic contact is exacerbated since it is based on lithostratigraphic correlations using geophysical log signatures without paleontology control for dating.

Geophysical well log signatures for the Reklaw Formation top and bottom depths in Wilson County are displayed in Figure 7.3.2-1. The Reklaw Formation top depth is 825 feet below ground surface (upper yellow line) and bottom depth is 990 feet below ground surface (bottom yellow line). The geophysical well log includes: the spontaneous potential (solid line) and gamma ray (dotted line) recorded in the left track, depth below ground surface (feet) in the center track (each depth increment represents 10 feet), and induction (dotted line) and shallow normal resistivity (solid line) tools in the right track. This log is from BRACS well id 42363 in southern Wilson County, Texas. The log was performed by Schlumberger in 1981 with a kelly bushing height of 15 feet.

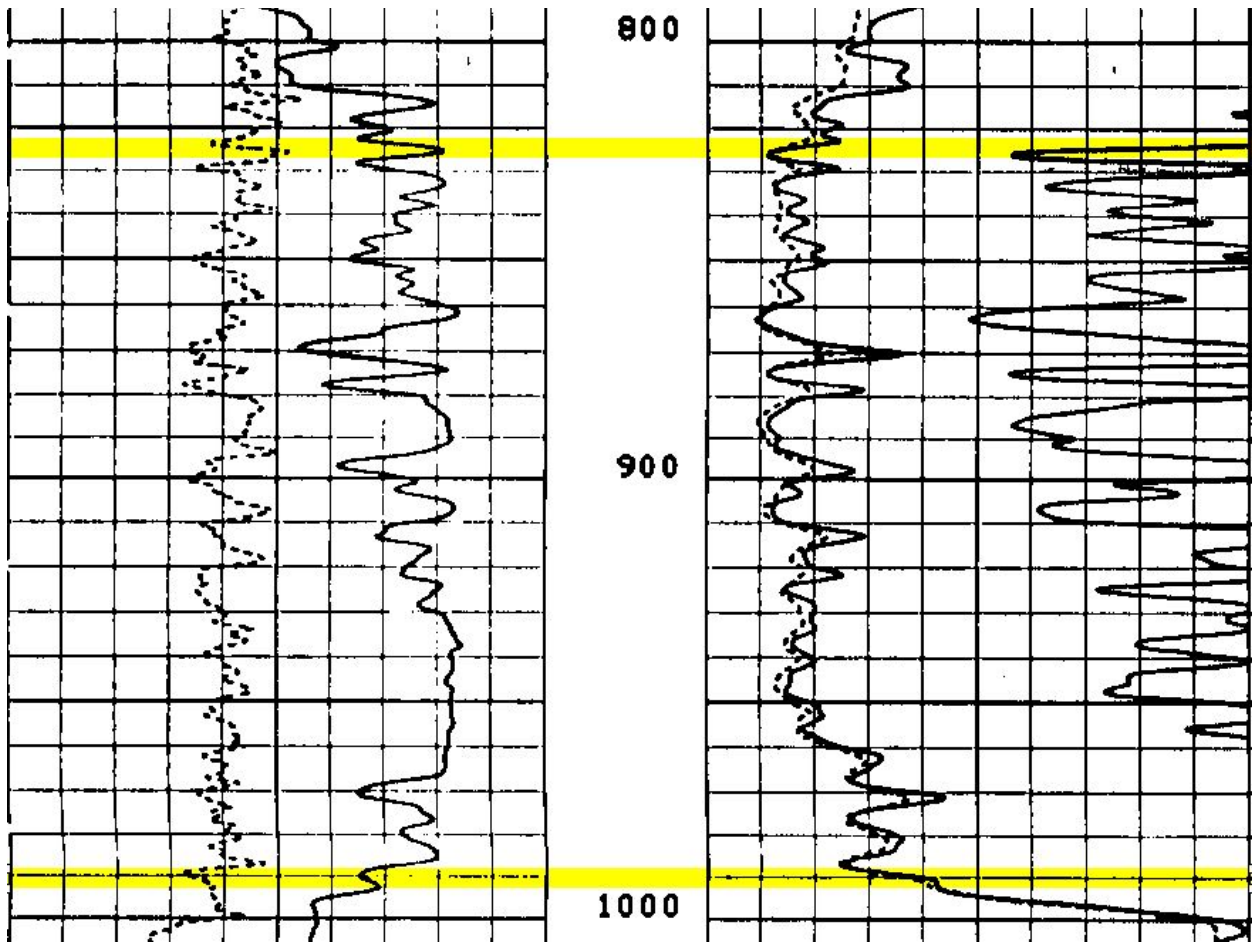


Figure 7.3.2-1. Reklaw Formation top and bottom depths interpreted on a geophysical well log in Wilson County, Texas.

Geophysical well log signatures for the Reklaw Formation top and bottom depths in Gonzales County are displayed in Figure 7.3.2-2. The Reklaw Formation top depth is 1,448 feet below ground surface (upper yellow line) and bottom depth is 1,705 feet below ground surface (bottom yellow line). The geophysical well log includes: the spontaneous potential recorded in the left track, depth below ground surface (feet) in the center track (each depth increment represents 10 feet), and induction (dotted line) and short normal resistivity (solid line) tools in the right track.

This log is from BRACS well id 15399 in northeastern Gonzales County, Texas. The log was performed by Lane Wells in 1966 with a kelly bushing height of 10 feet.

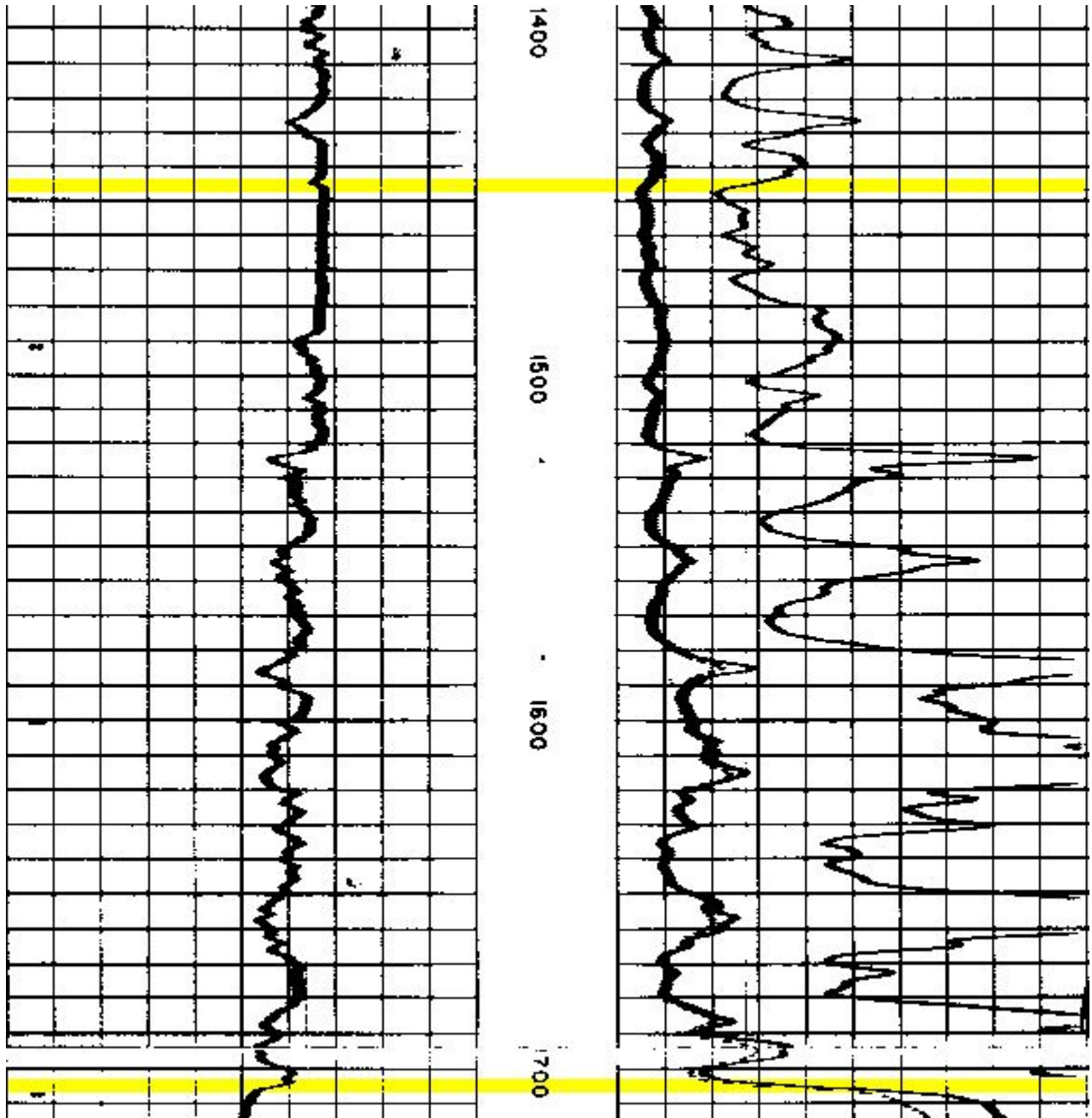


Figure 7.3.2-2. Reklaw Formation top and bottom depths interpreted on a geophysical well log in Gonzales County, Texas.

7.3.3 Formation top, bottom, thickness

Reklaw Formation top and bottom elevation maps (Figures 7.3.3-1 and 7.3.3-2) were prepared using 641 and 634 stratigraphic picks respectively from wells within the study area in addition to

some wells immediately outside of the study area to control GIS raster edge effects. Reklaw Formation top and bottom depth maps (Figures 7.3.3-3 and 7.3.3-4) were prepared using elevation GIS rasters subtracted from the study area digital elevation model (refer to Appendix, Section 13.6 raster interpolation documentation).

The Reklaw Formation thickness was prepared by subtracting the bottom elevation GIS raster from the top elevation GIS raster. The Reklaw Formation thickness is 0 at the updip outcrop edge and over 450 feet in southwestern Karnes County (Figure 7.3.3-5).

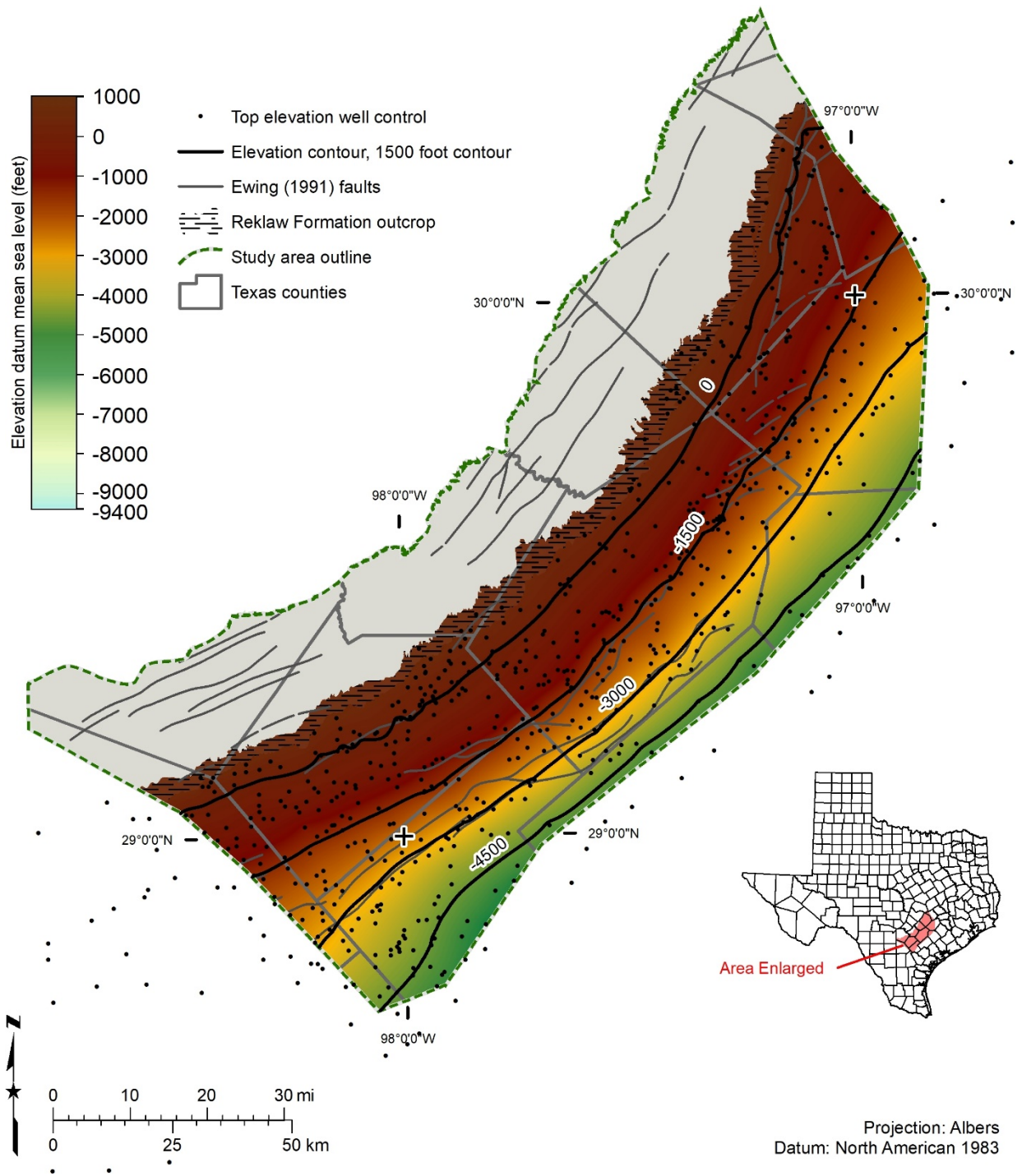


Figure 7.3.3-1. Reklaw Formation top elevation (feet above mean sea level), which was prepared using 641 wells for stratigraphic control (black dots).

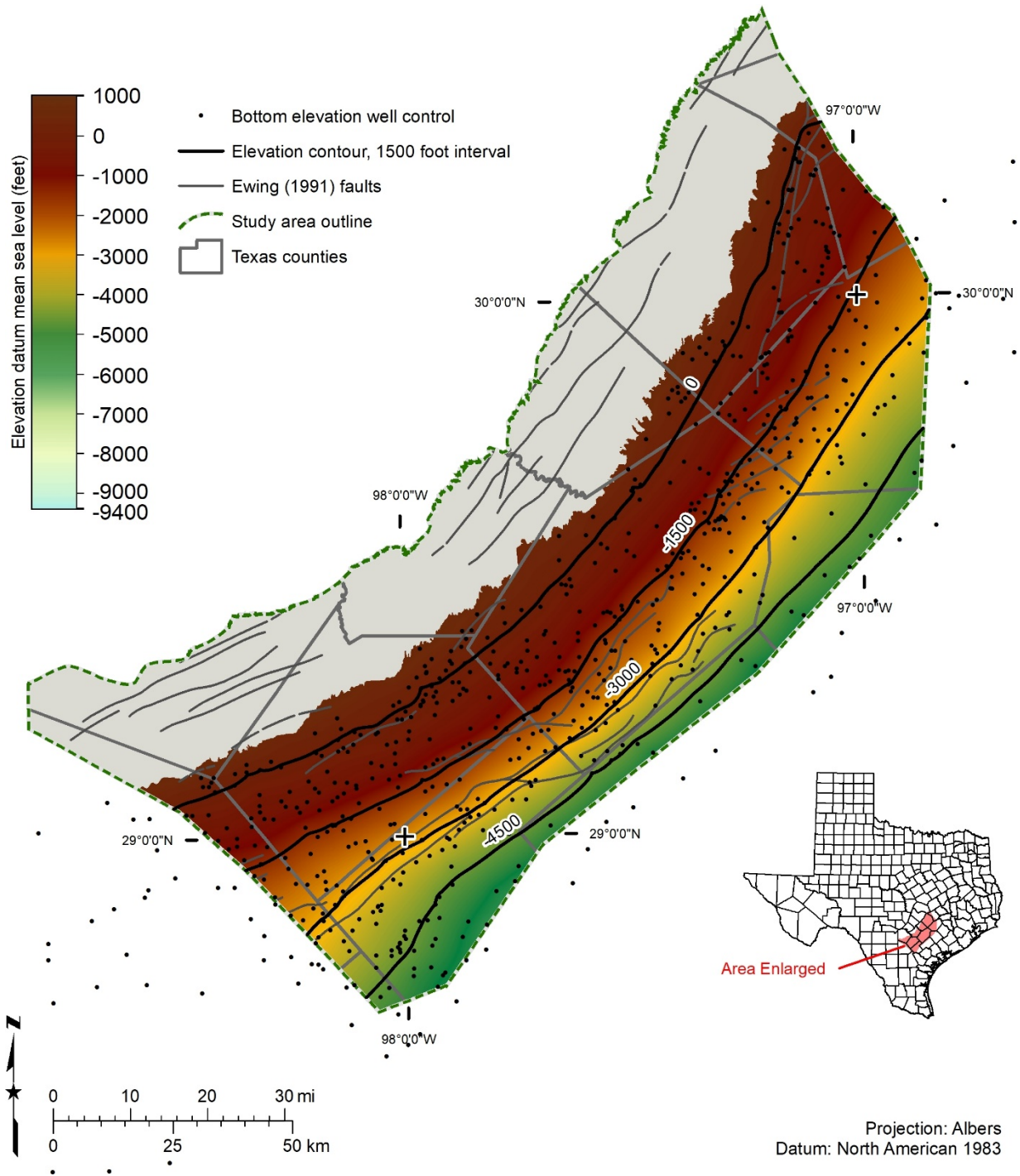


Figure 7.3.3-2. Reklaw Formation bottom elevation (feet above mean sea level), which was prepared using 634 wells for stratigraphic control (black dots).

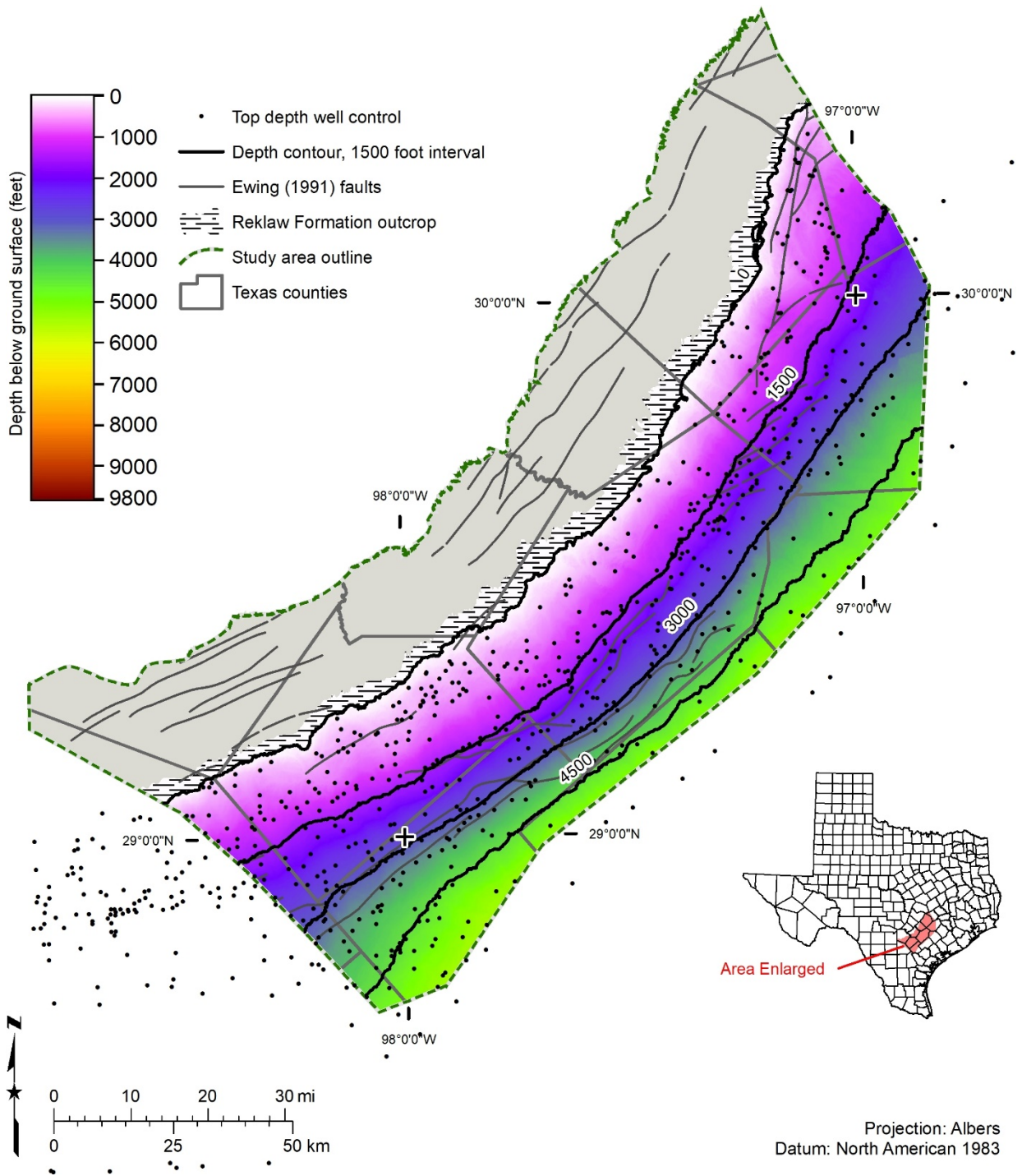


Figure 7.3.3-3. Reklaw Formation top depth (feet below ground surface), which was prepared using 641 wells for stratigraphic control (black dots).

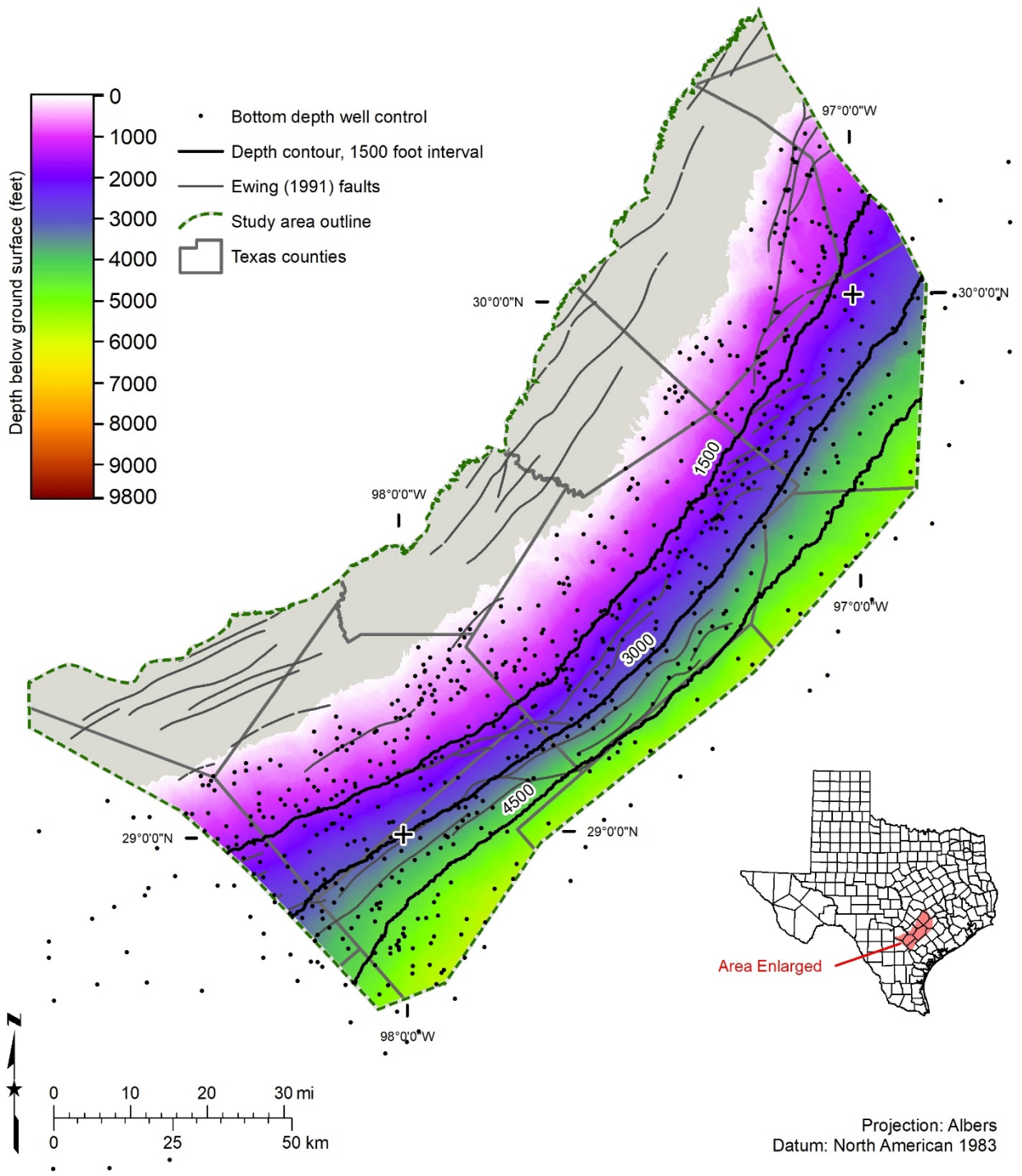


Figure 7.3.3-4. Reklaw Formation bottom depth (feet below ground surface), which was prepared using 634 wells for stratigraphic control (black dots).

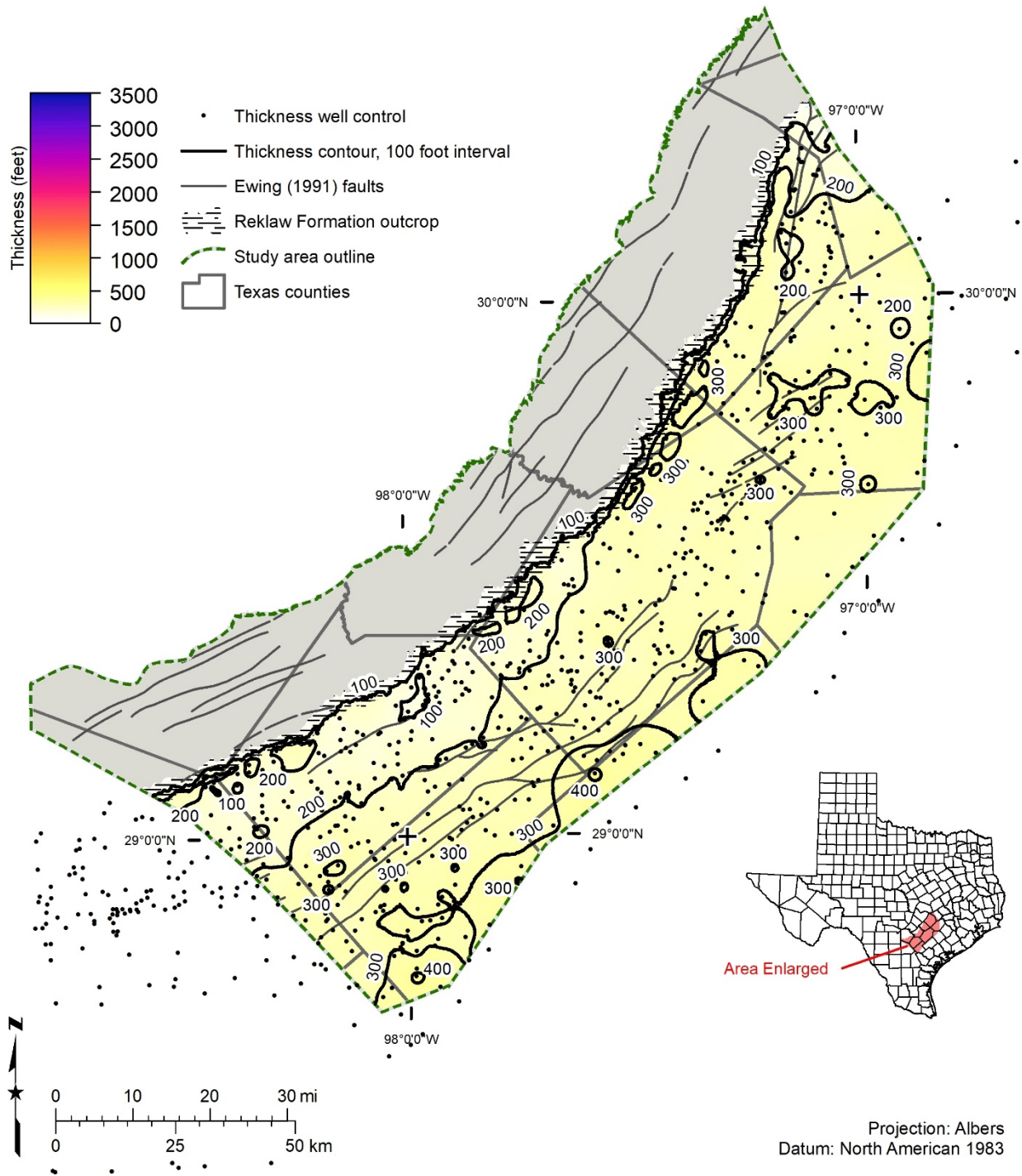


Figure 7.3.3-5. Reklaw Formation thickness in units of feet, which was prepared using 634 wells for stratigraphic control (black dots).

7.3.4 Net sand

Due to the limited production potential of the Reklaw Formation, we did not conduct a thorough analysis of the net sands in the formation. Draft Reklaw Formation net sand and sand percent calculations were performed and recorded in the BRACS Database. Maps were not prepared for this geological formation.

7.3.5 Salinity classes

Sands containing groundwater are limited and isolated in the Reklaw Formation. As such, salinity classes were not calculated using geophysical well logs or mapped.

7.3.6 Volume of brackish groundwater

Brackish groundwater volume was not calculated for the Reklaw Formation since this formation is considered an aquitard and not a major or minor aquifer in Texas.

7.4 Queen City Sand

The Queen City Sand of the Claiborne Group unconformably underlies the Weches Formation and conformably overlies the Reklaw Formation. The Queen City Aquifer, which is wholly comprised of the Queen City Sand, is a TWDB designated minor aquifer in Texas (George and others, 2011) that produces minor amounts of water over large geographic areas.

7.4.1 Well control

More than 800 wells were used in defining aspects of the Queen City Sand stratigraphy, lithology, and water quality (Table 7.4.1-1). We only used wells for water quality and aquifer hydraulic properties based on the aquifer determination analysis. Undoubtedly there are many other wells completed in the Queen City Sand, but without detailed well screen information it is not possible to accurately assign the Queen City Sand as the source of water produced from the wells.

Table 7.4.1-1. Queen City Sand well control data points.

Well control with this information	Number of data points
Lithology	752
Top surface stratigraphic picks used for raster surface	524
Bottom surface stratigraphic picks used for raster surface	578
Top surface stratigraphic picks (database total*)	755
Bottom surface stratigraphic picks (database total*)	837
Net sand interpreted from wells	384
Aquifer hydraulic properties	190 wells with 191 measurements
Water quality: wells	61 wells with 146 measurements
TDS interpreted from geophysical well logs	348 wells with 538 depth intervals
Porosity	20

* Total number of stratigraphic picks in study counties

7.4.2 Stratigraphic analysis

Stratigraphic pick assignment of the upper contact of the Queen City Sand was selected at the top of the shallowest sand subjacent to the base of the Weches Formation shale. The bottom contact of the Queen City Sand is at the base of the upward coarsening sand package above the

uppermost shale signature of the Reklaw Formation. The upper contact is uniform across the study area. The lower contact may be problematic if the upper Reklaw Formation contains thin sand packages. This problematic contact is exacerbated since it is based on lithostratigraphic correlations using geophysical log signatures without paleontology control for dating.

Geophysical well log signatures for the Queen City Sand top depth in Wilson County are displayed in Figure 7.4.2-1. The Queen City Sand top depth is 190 feet below ground surface (yellow line). The geophysical well log includes: the spontaneous potential (solid line) and gamma ray (dotted line) recorded in the left track, depth below ground surface (feet) in the center track (each depth increment represents 10 feet), and induction (dotted line) and shallow normal resistivity (solid line) tools in the right track. This log is from BRACS well id 42363 in southern Wilson County, Texas. The log was performed by Schlumberger in 1981 with a kelly bushing height of 15 feet.

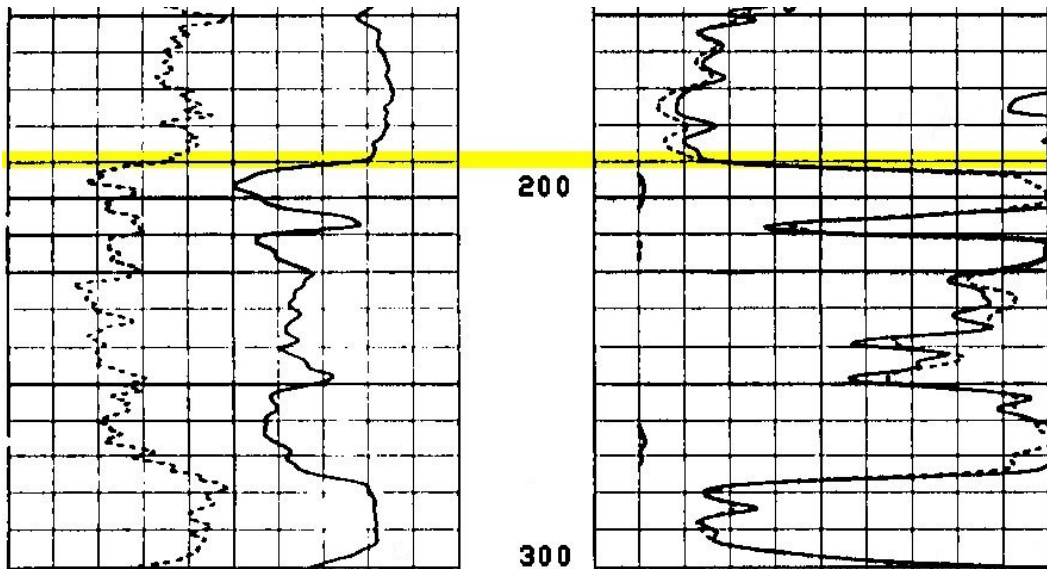


Figure 7.4.2-1. Queen City Sand top depth interpreted on a geophysical well log in Wilson County, Texas.

Geophysical well log signatures for the Queen City Sand bottom depth in Wilson County are displayed in Figure 7.4.2-2. The Queen City Sand bottom depth is 825 feet below ground surface (yellow line). The geophysical well log includes: the spontaneous potential (solid line) and gamma ray (dotted line) recorded in the left track, depth below ground surface (feet) in the center track (each depth increment represents 10 feet), and induction (dotted line) and shallow normal resistivity (solid line) tools in the right track. This log is from BRACS well id 42363 in southern Wilson County, Texas. The log was performed by Schlumberger in 1981 with a kelly bushing height of 15 feet.

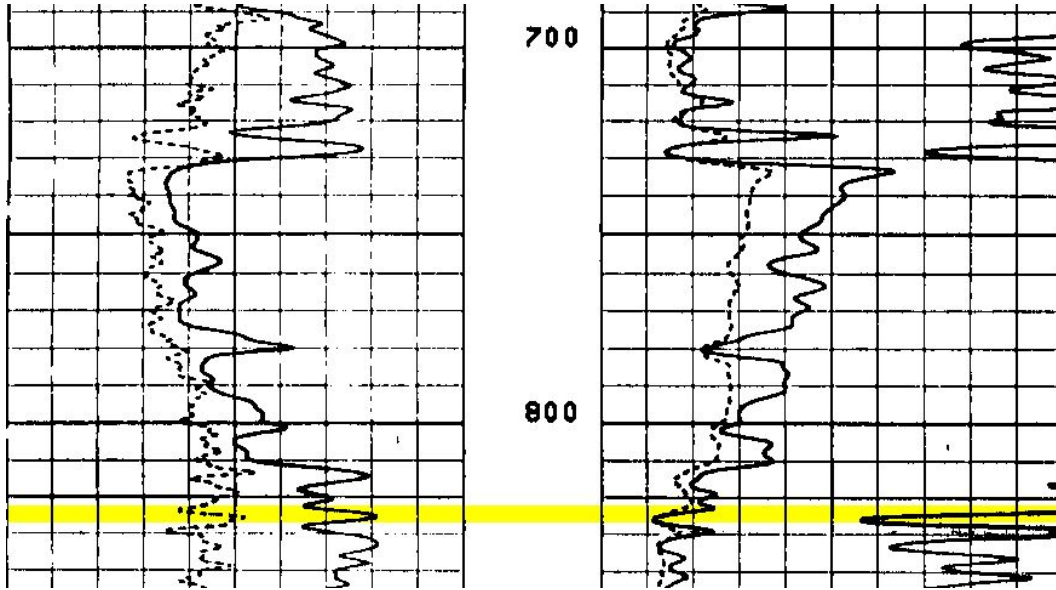


Figure 7.4.2-2. Queen City Sand bottom depth interpreted on a geophysical well log in Wilson County, Texas.

Geophysical well log signatures for the Queen City Sand top depth in Gonzales County are displayed in Figure 7.4.2-3. The Queen City Sand top depth is 1,020 feet below ground surface (yellow line). The geophysical well log includes: the spontaneous potential recorded in the left track, depth below ground surface (feet) in the center track (each depth increment represents 10 feet), and induction (dotted line) and short normal resistivity (solid line) tools in the right track. This log is from BRACS well id 15399 in northeastern Gonzales County, Texas. The log was performed by Lane Wells in 1966 with a kelly bushing height of 10 feet.

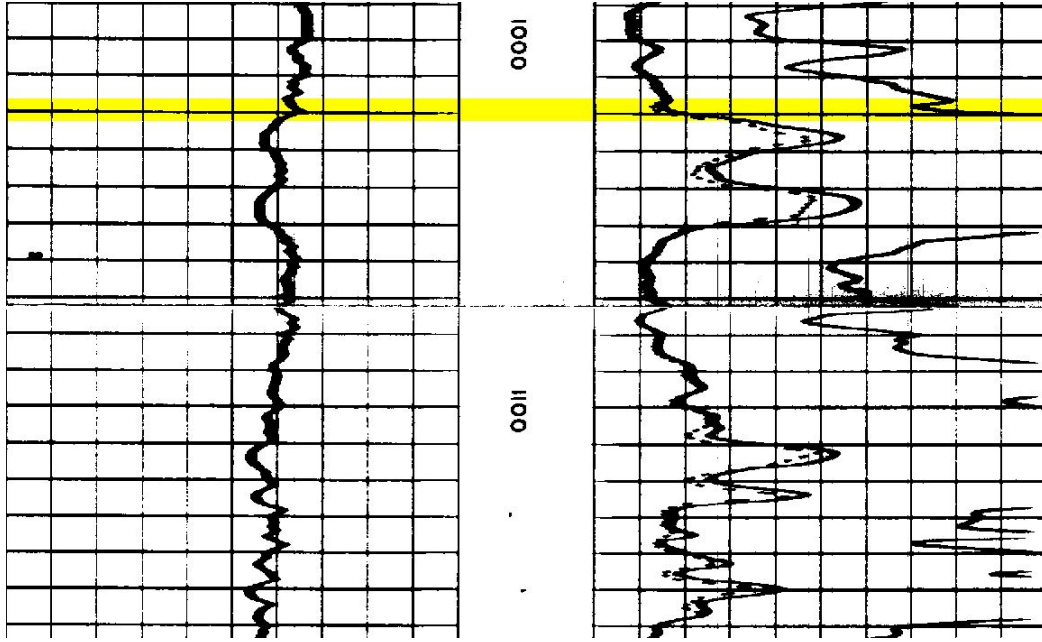


Figure 7.4.2-3. Queen City Sand top depth interpreted on a geophysical well log in Gonzales County, Texas.

Geophysical well log signatures for the Queen City Sand bottom depth in Gonzales County are displayed in Figure 7.4.2-4. The Queen City Sand bottom depth is 1,448 feet below ground surface (yellow line). The geophysical well log includes: the spontaneous potential recorded in the left track, depth below ground surface (feet) in the center track (each depth increment represents 10 feet), and induction (dotted line) and short normal resistivity (solid line) tools in the right track. This log is from BRACS well id 15399 in northeastern Gonzales County, Texas. The log was performed by Lane Wells in 1966 with a kelly bushing height of 10 feet.

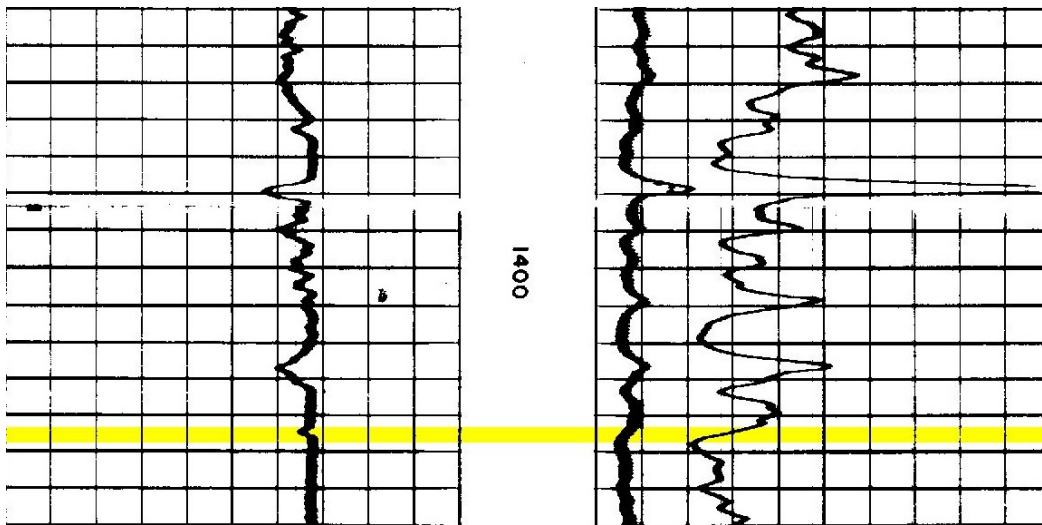


Figure 7.4.2-4. Queen City Sand bottom depth interpreted on a geophysical well log in Gonzales County, Texas.

7.4.3 Formation top, bottom, thickness

Queen City Sand top and bottom elevation maps (Figures 7.4.3-1 and 7.4.3-2) were prepared using 524 and 578 stratigraphic picks respectively from wells within the study area in addition to some wells immediately outside of the study area to control raster edge effects. Queen City Sand top and bottom depth maps (Figures 7.4.3-3 and 7.4.3-4) were prepared using elevation GIS rasters subtracted from the study area digital elevation model (refer to Appendix, Section 13.6 raster interpolation documentation).

The Queen City Sand thickness was prepared by subtracting the bottom elevation GIS raster from the top elevation GIS raster. The Queen City Sand thickness is 0 at the updip outcrop edge and over 700 feet at the downdip limit of the study area east of the San Marcos Arch and over 1,000 feet in eastern Atascosa County west of the arch (Figure 7.4.3-5, Plate 7).

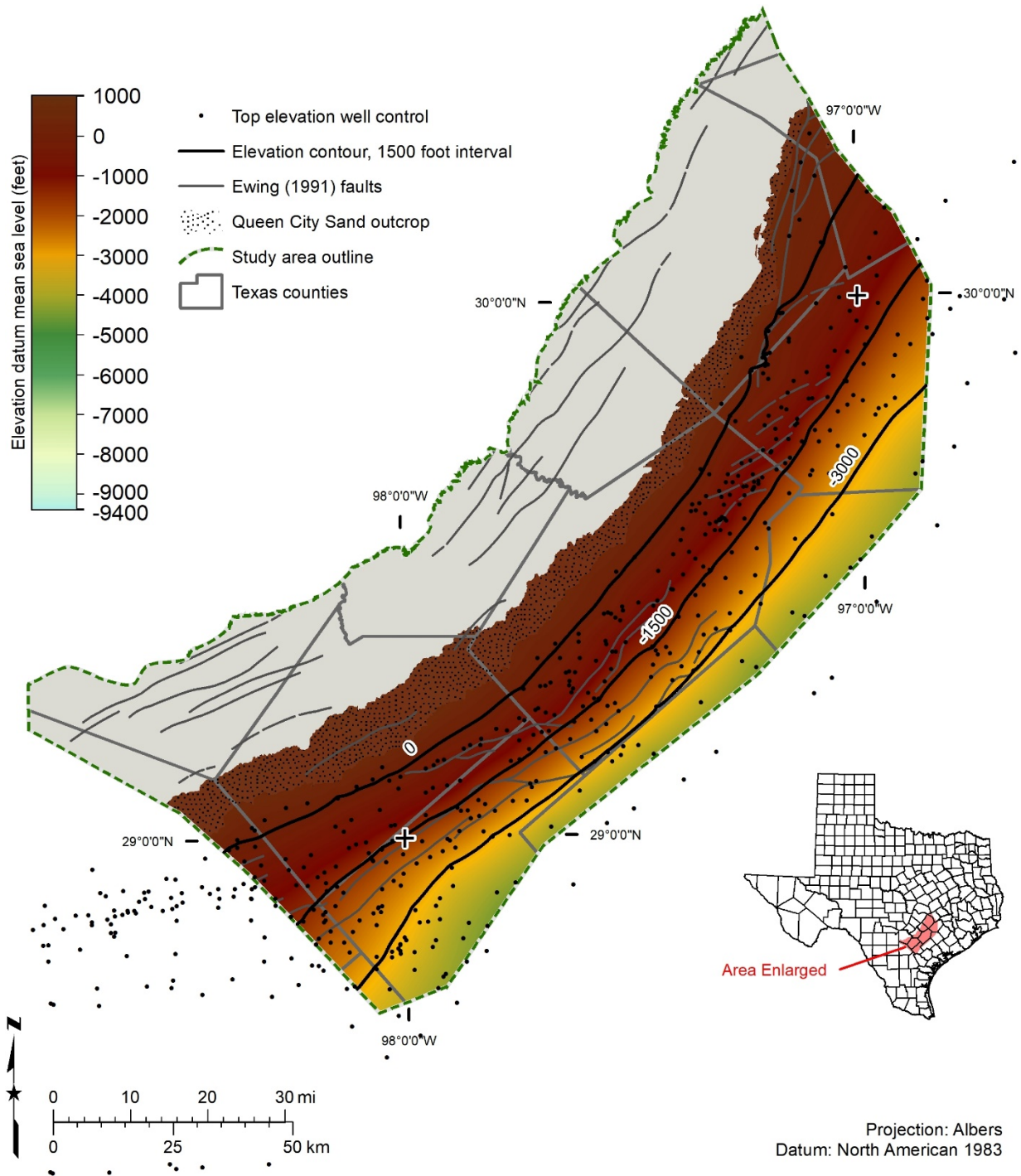


Figure 7.4.3-1. Queen City Sand top elevation (feet above mean sea level), which was prepared using 524 wells for stratigraphic control (black dots).

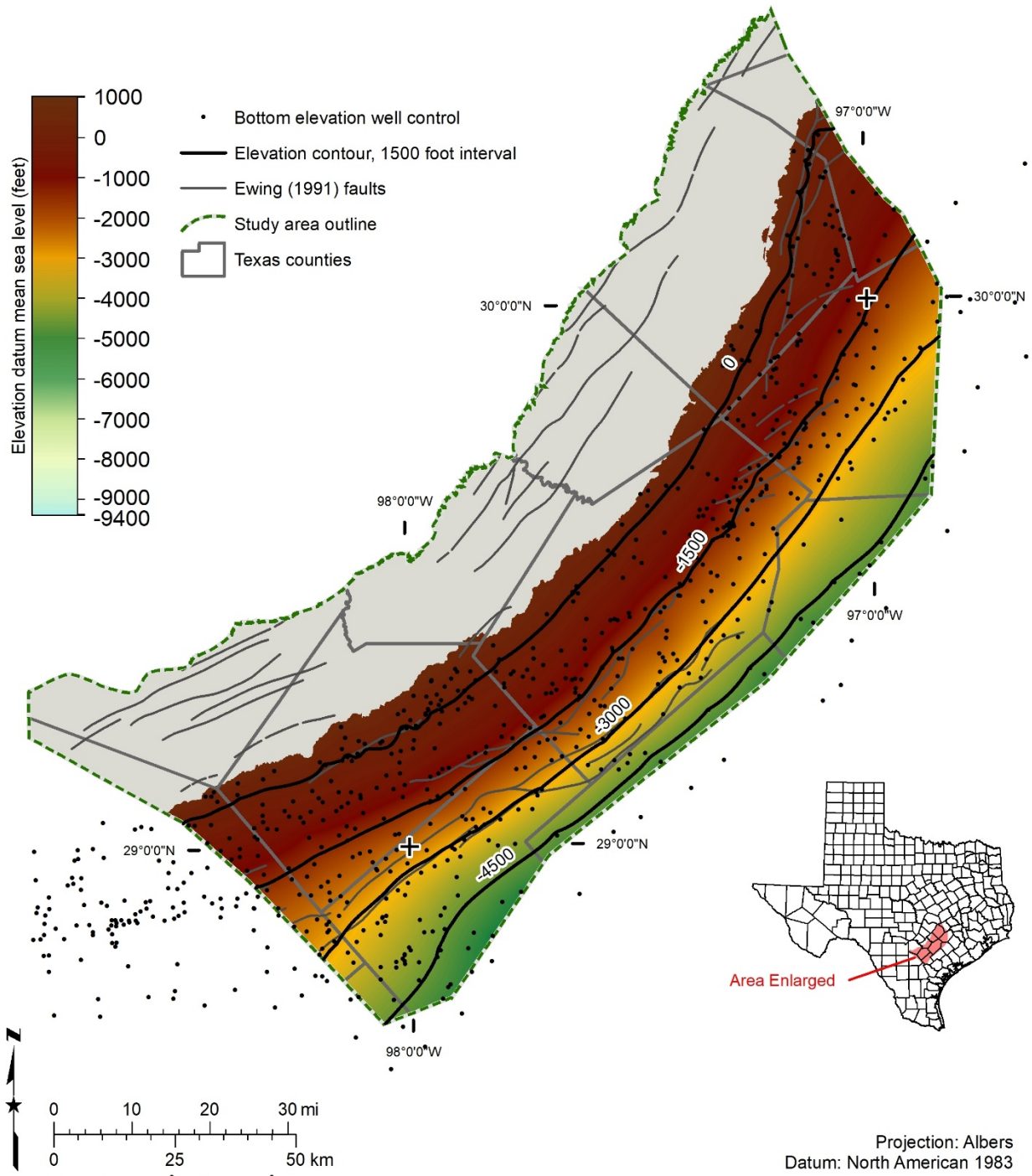


Figure 7.4.3-2. Queen City Sand bottom elevation (feet above mean sea level), which was prepared using 578 wells for stratigraphic control (black dots).

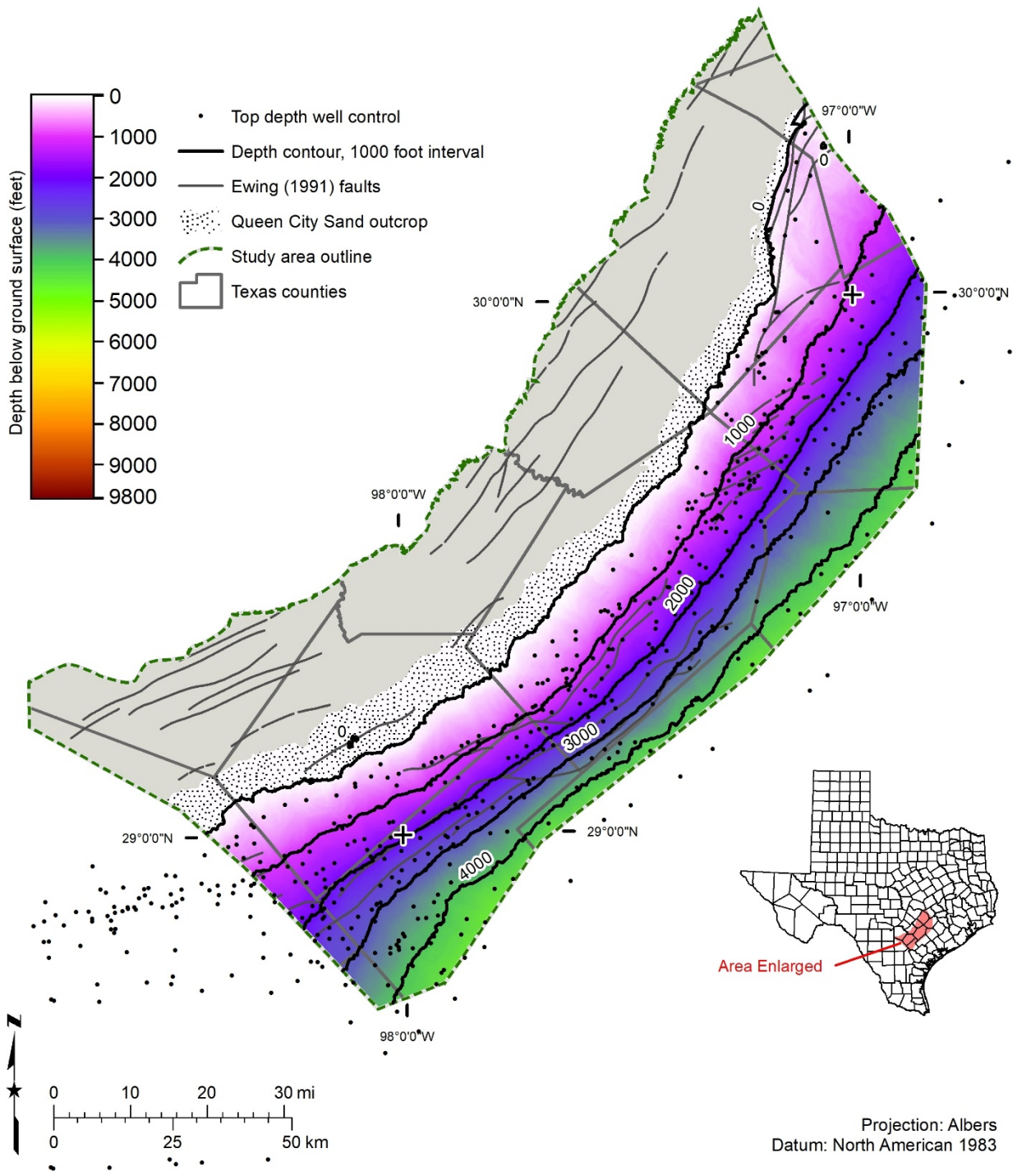


Figure 7.4.3-3. Queen City Sand top depth (feet below ground surface), which was prepared using 524 wells for stratigraphic control (black dots).

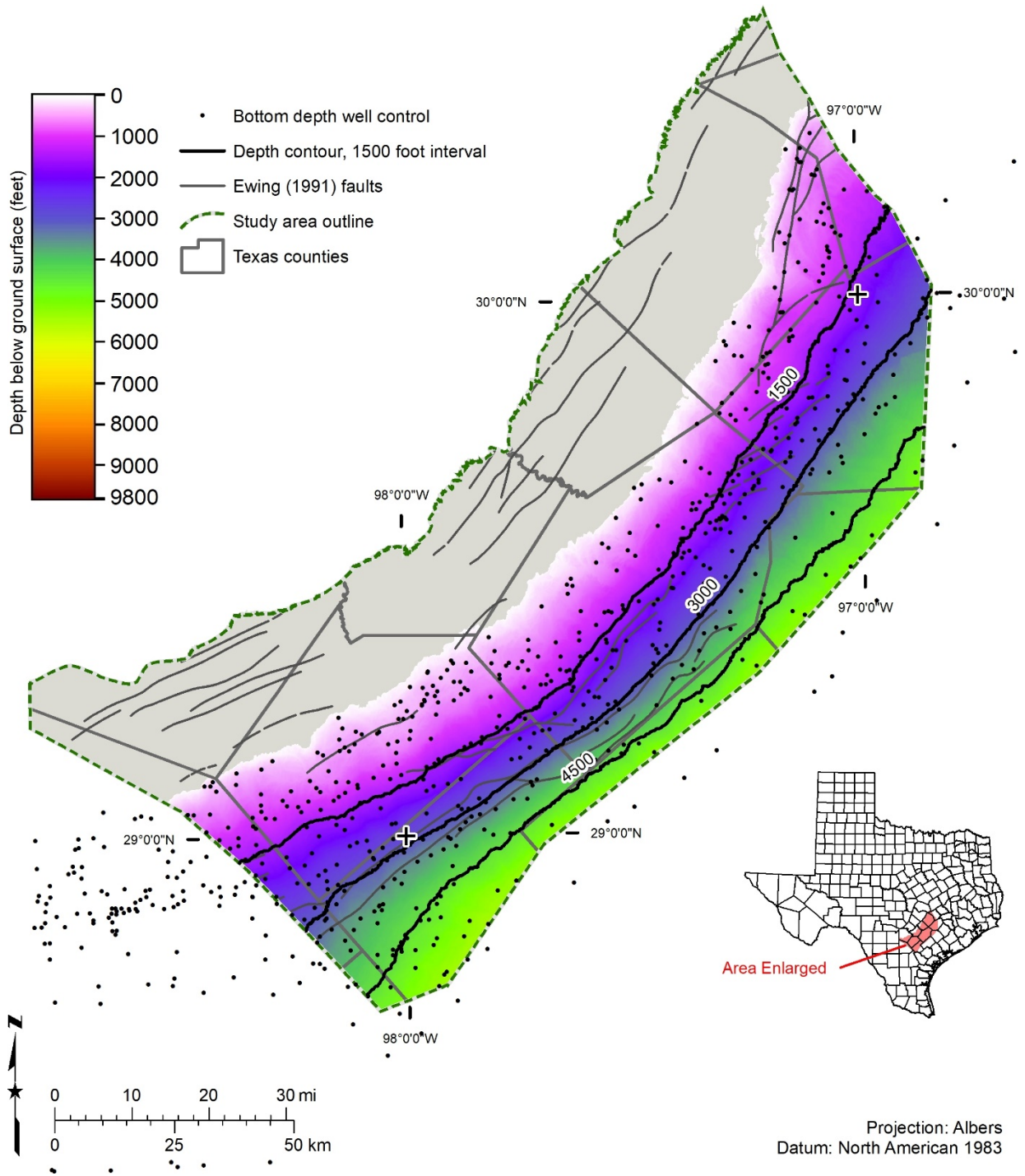


Figure 7.4.3-4. Queen City Sand bottom depth (feet below ground surface), which was prepared using 578 wells for stratigraphic control (black dots).

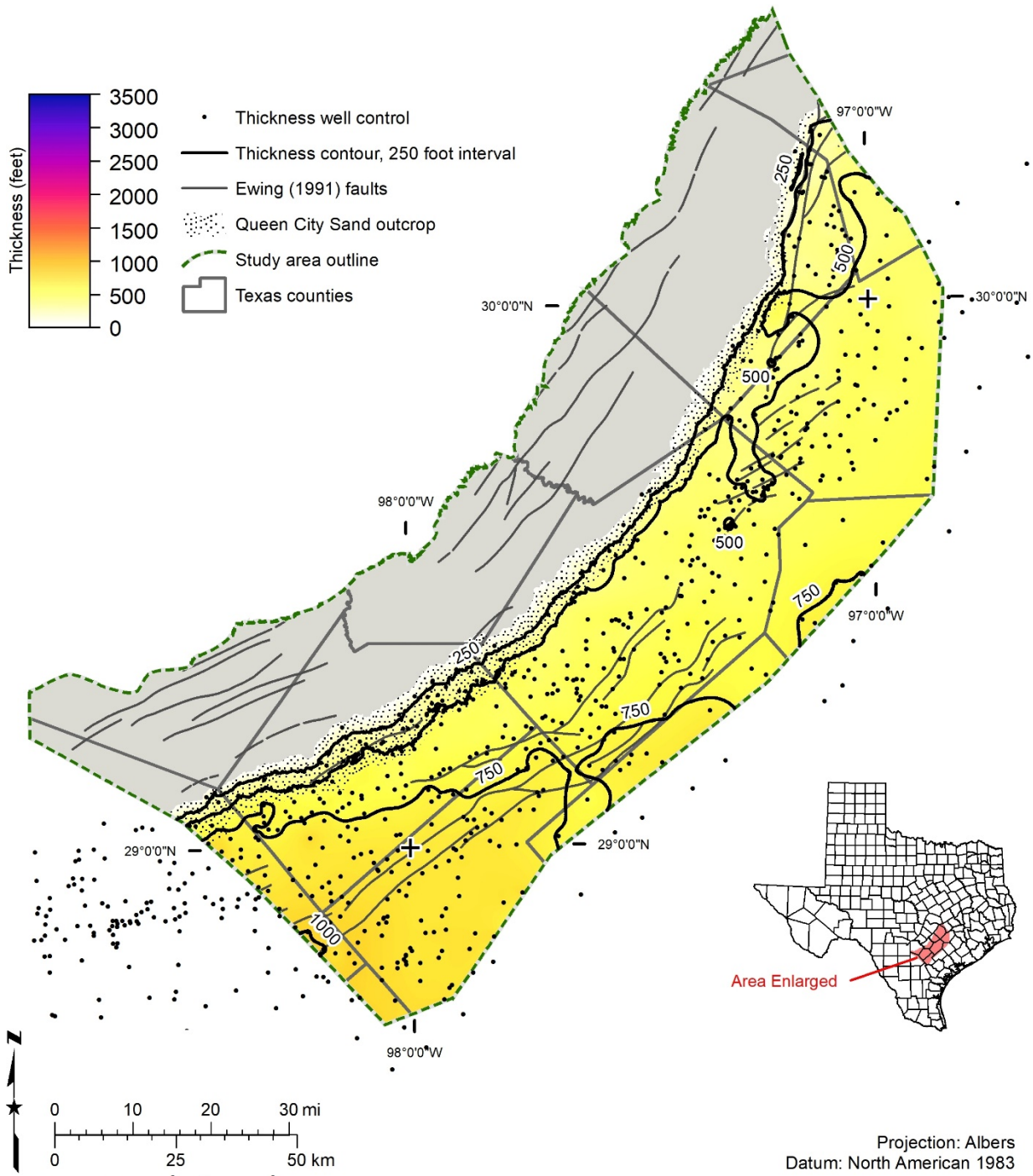


Figure 7.4.3-5. Queen City Sand thickness in units of feet, which was prepared using 524 wells for stratigraphic control (black dots).

7.4.4 Net sand

We used 384 wells to prepare the Queen City Sand net sand raster (Figure 7.4.4-1). Oil and gas wells represent 197 wells, water wells represent 180 wells, and the remaining seven wells are classified as other. We used geophysical well logs for 223 wells and drillers' descriptions of

lithology for the remaining 161 wells. Net sand values range from 0 at the updip outcrop edge to over 500 feet in eastern Atascosa County (Plate 4). There is a noticeable thinning in eastern Gonzales County with a gradual thickening to the west and to the northeast.

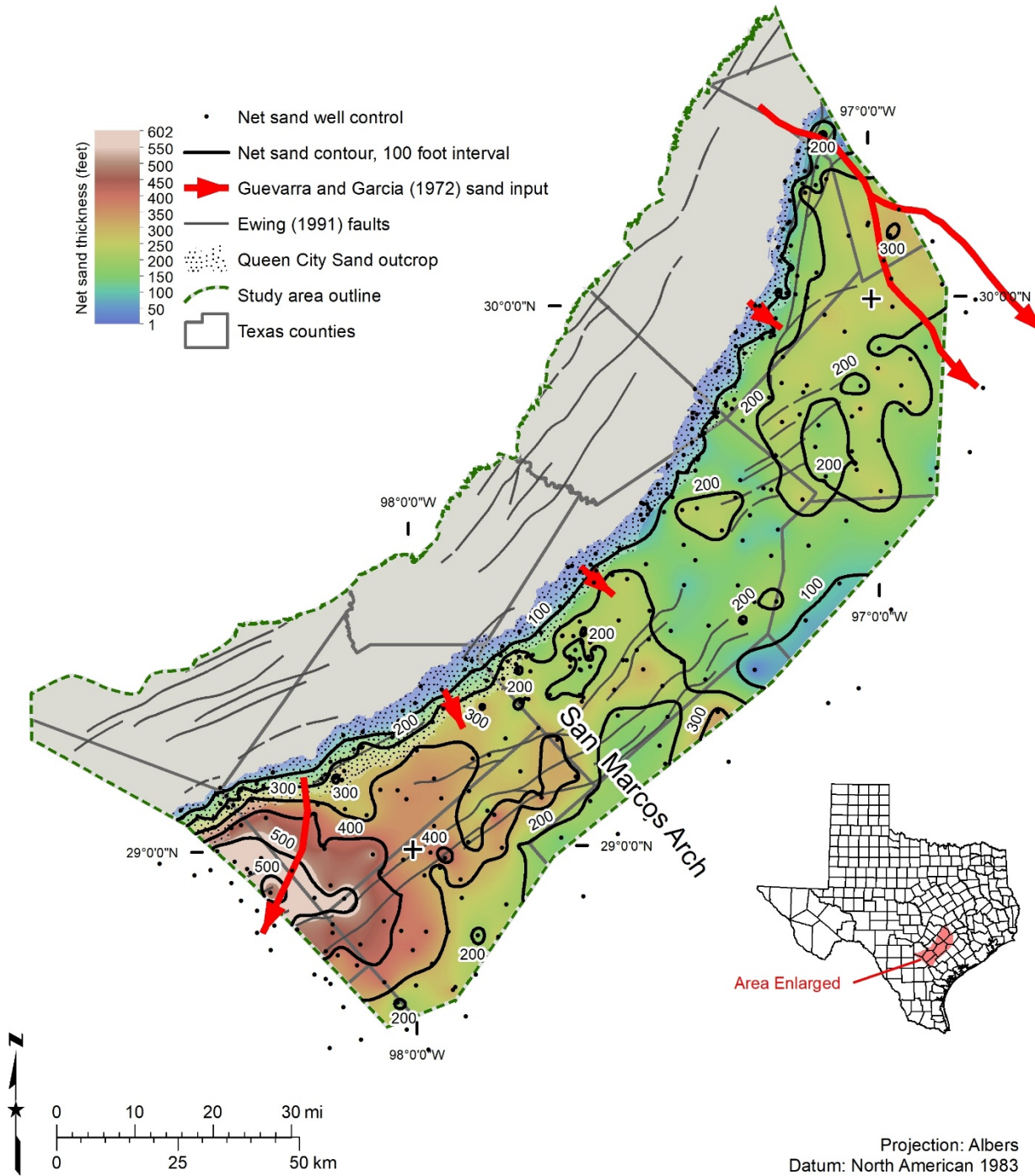


Figure 7.4.4-1. Queen City Sand net sand thickness (feet), which was prepared using 384 wells for net sand control (black dots). Axes of significant sand input into the basin from Guevara and Garcia (1972) are shown in red arrows.

Sand thickening in southwestern Lee and adjacent Fayette counties represents the westernmost main sediment input associated with the high-constructive delta system in East Texas. The region from Fayette to Wilson counties represents accumulation of reworked sediment transported via longshore currents into strandplain deposits (Guevara and Garcia, 1972). Western Wilson and adjacent Atascosa counties represent a main sand input into the basin.

7.4.5 Salinity classes

The Queen City Sand was mapped into defined salinity classes: (1) fresh, (2) mixed fresh and slightly saline, (3) slightly saline, (4) mixed slightly saline and moderately saline, (5) mixed slightly saline, moderately saline, and very saline, (6) moderately saline, (7) mixed moderately saline and very saline, and (8) very saline (Figures 7.4.5-1 and 7.4.5-2). Mapping was based on water quality samples (162 wells classified as: 139 fresh, 19 slightly saline, and 4 moderately saline) and estimated total dissolved solids calculations using geophysical well logs (519 wells with 951 depth intervals analyzed yielding 516 wells with 625 salinity class zones: 46 fresh, 225 slightly saline, 160 moderately saline, 193 very saline, and 1 brine). Forty-one wells contain mixed salinity classes within the Queen City Sand ranging from two to three vertical zones per well.

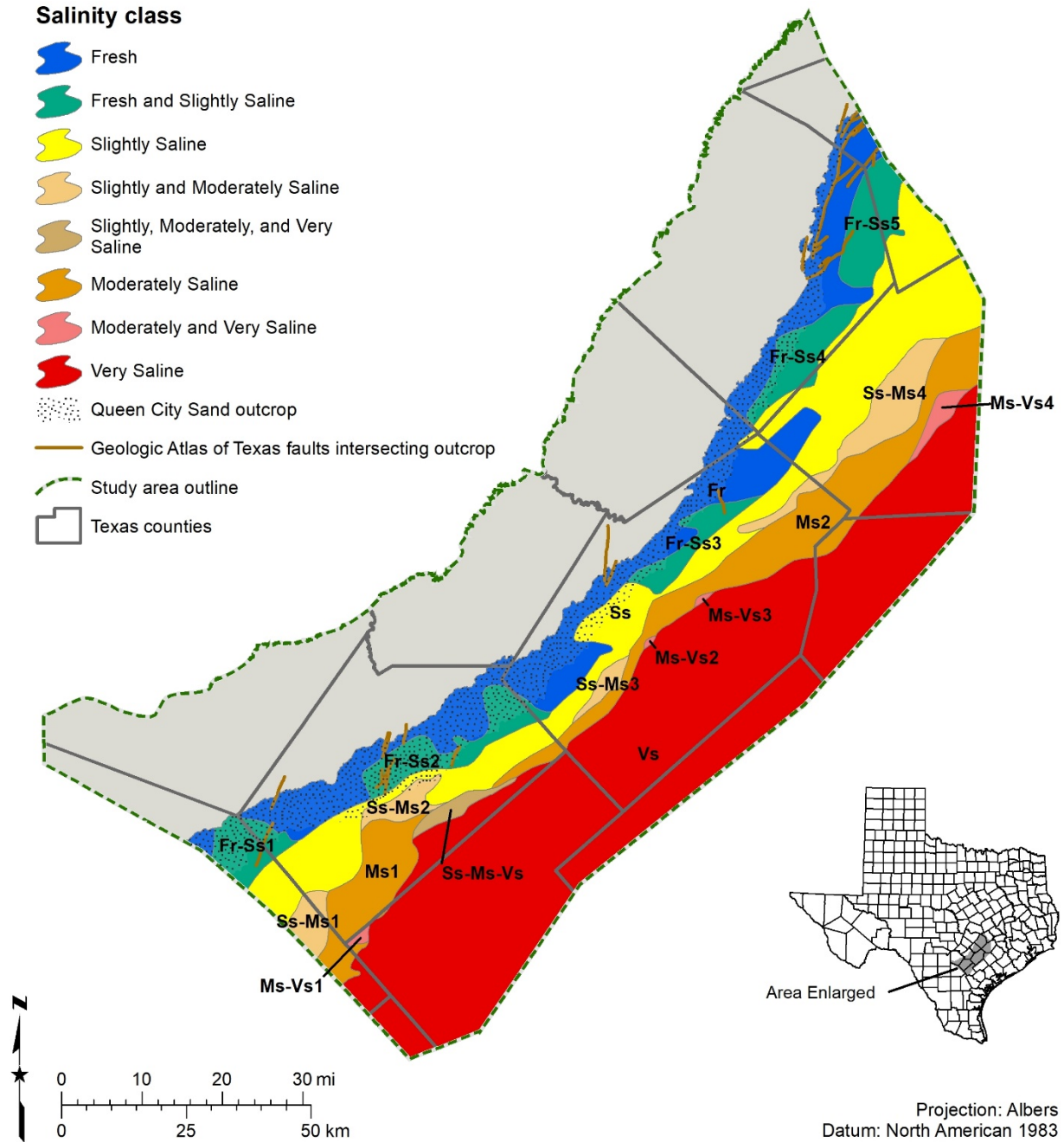


Figure 7.4.5-1. Queen City Sand salinity classes and identification names. Refer to Table 2-1 for salinity class definition.

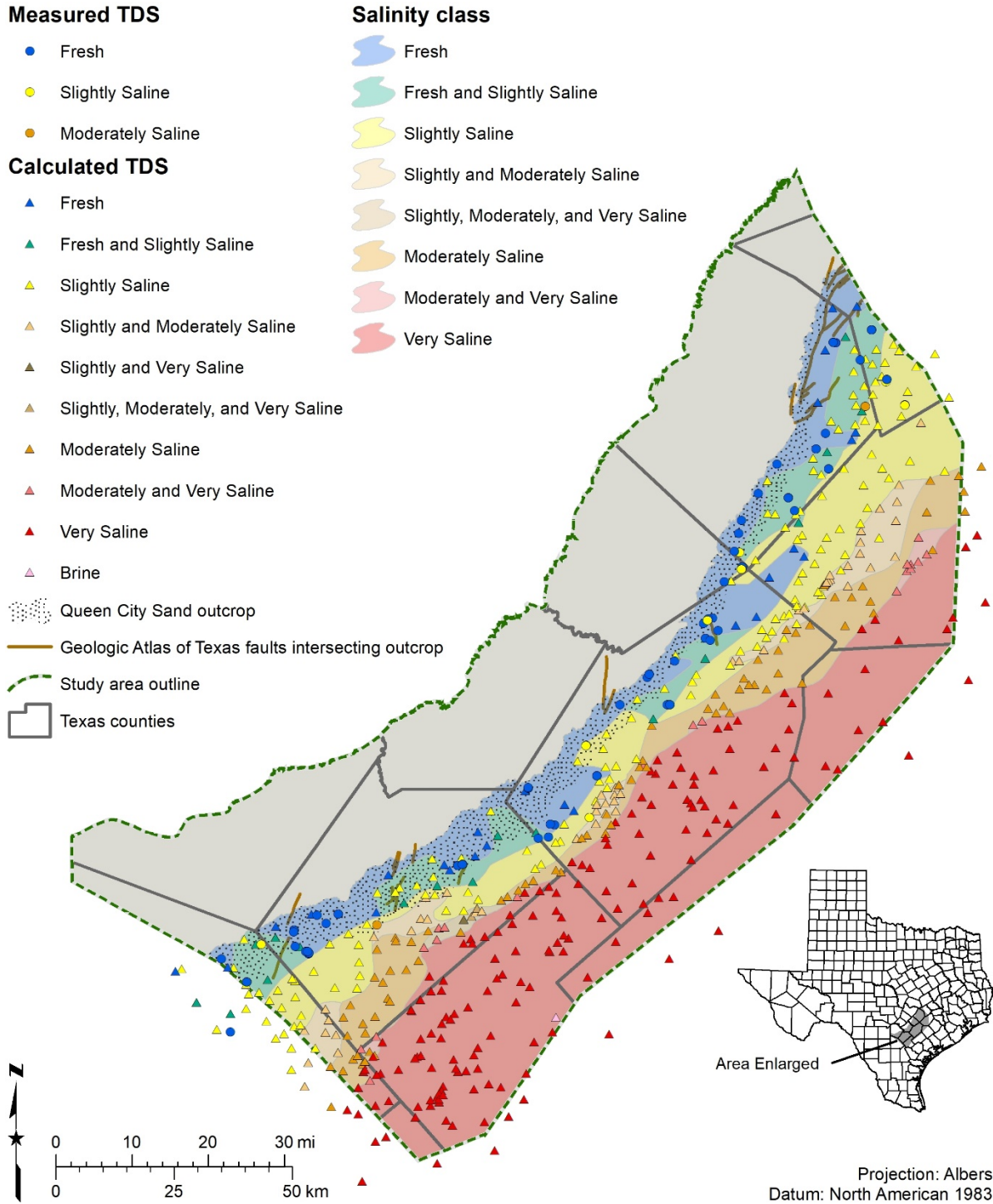


Figure 7.4.5-2. Queen City Sand salinity classes and well control consisting of water well quality data (circles) and interpreted geophysical well logs (triangles). Refer to Table 2-1 for salinity class definition. TDS = total dissolved solids.

The Queen City Sand exhibits vertical stacking of different salinity classes in multiple areas of the study area. The transition from fresh to very saline groundwater ranges from 4 to 7.4 miles of the outcrop in central Gonzales through central Wilson counties, in the area characterized as a strandplain system (Guevara and Garcia, 1972). In contrast, the slightly and moderately saline classes extend downdip from the fresh class (1) approximately 14 miles in west central Wilson County and to the southwest in the area of a high-destructive wave-dominated delta system (Guevara and Garcia, 1972) and (2) approximately 17 miles in eastern Fayette County and to the northeast in the area of a high-constructive lobate delta system (Guevara and Garcia, 1972).

We mapped multiple mixed salinity classes consisting of (1) both water quality and log analysis data points within and immediately downdip of the outcrop and (2) log analysis data points farther downdip. These mixed salinity classes represent a downdip transition from one dominant water quality class into another class, for example: slightly saline transitions into a mixed slightly/moderately saline class that transitions into a moderately saline class (Plates 7, 8, 9).

One curious mixed class (Ss-Ms-Vs) consisting of six mapped wells occurs immediately updip of a northwest-dipping normal fault in southwestern Wilson County where a lower Queen City sand approximately 40 feet thick is characterized as slightly saline (for example, refer to BRACS well id 20945). Overlying Queen City sands are moderately to very saline zones. We speculate that underlying slightly and moderately saline Carrizo Sand groundwater could be leaking upward into the Queen City Sand.

7.4.6 Volume of brackish groundwater

We calculated the volume of in-place groundwater for the Queen City Sand based on salinity classes (Table 7.4.6-1). The Queen City Sand contains more than 20 million acre-feet of in-place brackish groundwater and additional significant brackish groundwater in mixed classes within the study area. The Queen City Sand contains a total of almost 52 million acre-feet of in-place groundwater of all salinity ranges within the study area.

Table 7.4.6-1. Total volume (acre-feet) of in-place groundwater in the Queen City Sand based on salinity class. Values summarized from Table 13.1.3-1. Volume values rounded to the nearest 10,000 acre-feet. Refer to Figure 7.4.5-1 for location of each salinity class.

Salinity class	Identification names	Volume groundwater (per salinity subclass) (acre-feet)	Volume groundwater (per salinity class) (acre-feet)
Fresh	Fr	3,480,000	3,480,000
Fr - Ss	Fr-Ss1	1,110,000	4,220,000
	Fr-Ss2	960,000	
	Fr-Ss3	430,000	
	Fr-Ss4	630,000	
	Fr-Ss5	1,090,000	
Slightly saline	Ss	10,820,000	10,820,000
Ss - Ms	Ss-Ms1	960,000	2,870,000
	Ss-Ms2	520,000	
	Ss-Ms3	190,000	
	Ss-Ms4	1,200,000	
Ss - Ms - Vs	Ss-Ms-Vs	420,000	420,000
Moderately saline	Ms1	3,190,000	6,600,000
	Ms2	3,410,000	
Ms - Vs	Ms-Vs1	120,000	380,000
	Ms-Vs2	20,000	
	Ms-Vs3	10,000	
	Ms-Vs4	230,000	
Very saline	Vs	23,110,000	23,110,000

Notes:

Fr - Ss is a mixed class of fresh and slightly saline.

Ss - Ms is a mixed class of slightly and moderately saline.

Ss - Ms - Vs is a mixed class of slightly, moderately, and very saline.

Ms - Vs is a mixed class of moderately and very saline.

Additionally, we subdivided the volumes based on districts and planning areas (Appendix 13.1, Tables 13.1.3-1, 13.1.3-2, 13.1.3-3, and 13.1.3-4). Appendix 13, Section 13.2 contains a complete discussion of volume methodology. Once salinity class mapping for the Queen City Sand was completed, we noticed that the study area did not include the entire available resource affecting some groundwater volume calculations. Specifically, the study area does not include the entire extent of Queen City Sand moderately saline water in the eastern part of the study area. Calculation of groundwater volumes used aquifer-based study area boundaries and some administrative boundaries are not coincident with the study area boundary. This resulted in partial volumes for some counties, groundwater conservation districts, or regional water planning areas. Future evaluation of the Queen City Sand to the northeast of this study area will address this issue.

7.4.7 Aquifer hydraulic properties

We compiled 191 sets of aquifer hydraulic property data from 190 wells completed in the Queen City Sand. The data is organized by hydraulic property (Table 7.4.7-1) and recorded in the BRACS Database table (tblUCPC_AquiferTestInformation). Queen City Sand records are identified using the field aquifer_new = QC. A full discussion of this dataset is provided in

Section 6.7. We prepared a map showing spatial distribution of wells with well yield, specific capacity, transmissivity, and hydraulic conductivity (Figure 7.4.7-1).

Table 7.4.7-1. Hydraulic properties of the Queen City Sand within the study area. Refer to the BRACS Database table (tblUCPC_AquiferTestInformation) for detailed information about each well and data. Refer to Figure 7.4.7-1 for a map of these parameters.

	Transmissivity (gallons per day per foot)	Hydraulic conductivity (feet per day)	Storage coefficient (dimensionless)	Specific capacity (gallons per minute per foot)	Well yield (gallons per minute)
Number of values	1	0	0	111	191
Low	4,300	-	-	0.08	2
High	4,300	-	-	27.5	1,700
Average	4,300	-	-	3.90	161

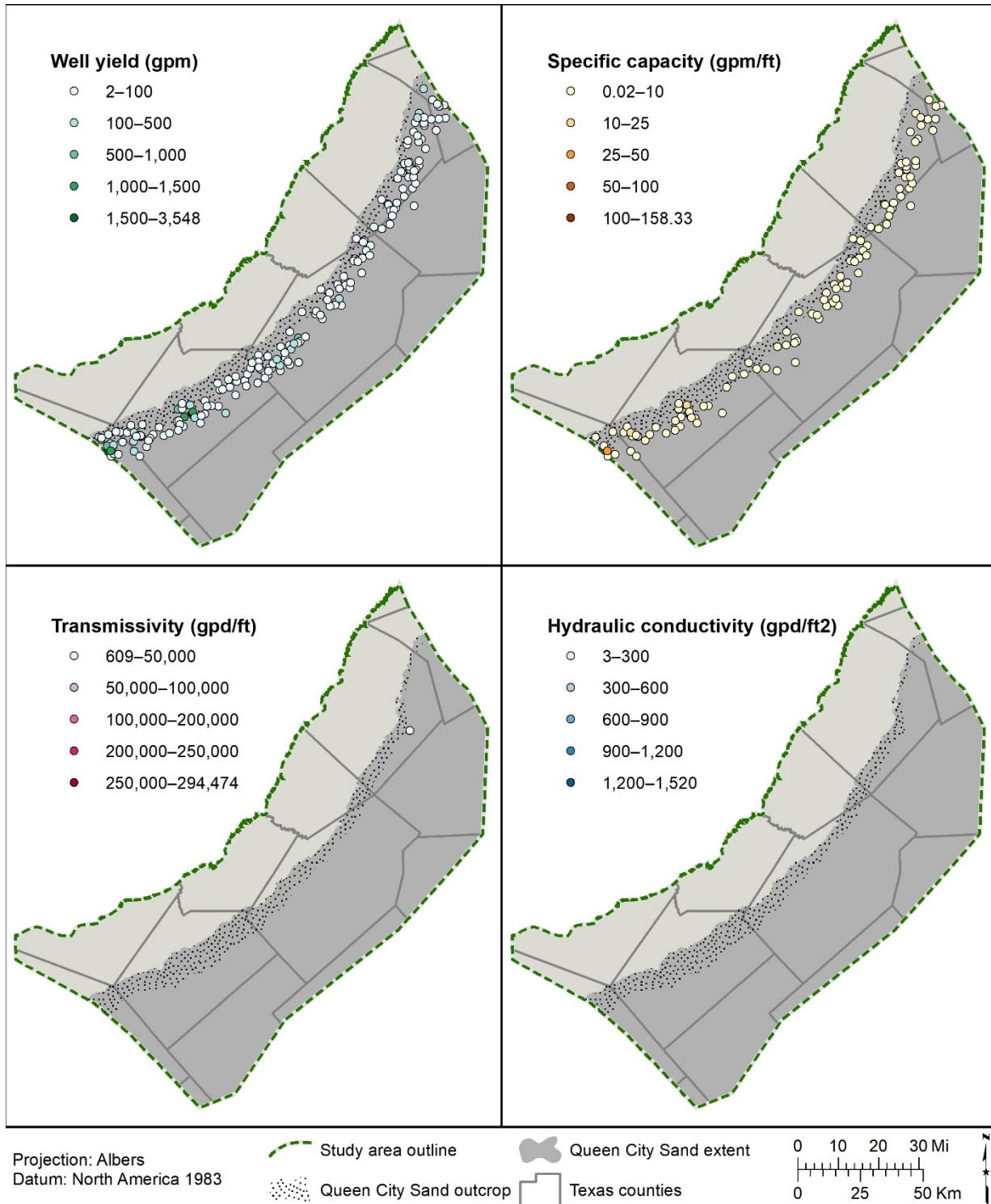


Figure 7.4.7-1. Queen City Sand hydraulic properties showing well yield (gallons per minute), specific capacity (gallons per minute per foot of drawdown), transmissivity (gallons per day per foot), and hydraulic conductivity (gallons per day per foot squared). Refer to Table 7.4.7-1 for a summary of these parameters.

7.5 Weches Formation

The Weches Formation of the Claiborne Group conformably underlies the Sparta Sand and unconformably overlies the Queen City Sand. The Weches Formation is a regional aquitard with low permeability compared to the sands of the Queen City Sand and Sparta Sand and can hinder vertical water movement between the two aquifers. For these reasons, the Weches Formation was not evaluated for groundwater potential.

7.5.1 Well control

More than 650 wells were used in defining aspects of the Weches Formation stratigraphy, lithology, and water quality (Table 7.5.1-1).

Table 7.5.1-1. Weches Formation well control data points.

Well control with this information	Number of data points
Lithology	378
Top surface stratigraphic picks used for raster surface	429
Bottom surface stratigraphic picks used for raster surface	415
Top surface stratigraphic picks (database total*)	654
Bottom surface stratigraphic picks (database total*)	628
Net sand interpreted from wells	348**
Aquifer hydraulic properties	7 wells with 7 measurements
Water quality: wells	1 well with 1 measurement
TDS interpreted from geophysical well logs	0
Porosity	0

* Total number of stratigraphic picks in study counties

** Total number of wells with net sand values; however, these have not been verified for use

7.5.2 Stratigraphic analysis

Stratigraphic pick assignment of the upper contact of the Weches Formation was selected at the top of the shale subjacent to the base of the first significant progradational (coarsening upwards sequence) of the Sparta Sand. The bottom contact of the Weches Formation is at the base of the shale marker above the uppermost sand signature of the Queen City Sand. The upper contact is problematic in places where there may be one or more progradational (upward coarsening) pulses of sediment below the major Sparta sand(s). This problematic contact is exacerbated since it is based on lithostratigraphic correlations using geophysical log signatures without paleontology control for dating.

Geophysical well log signatures for the Weches Formation top and bottom depths in Wilson Country are displayed in Figure 7.5.2-1. The Weches Formation top depth is 1,310 feet below ground surface (upper yellow line) and bottom depth is 1,390 feet below ground surface (bottom yellow line). The geophysical well log includes: the spontaneous potential recorded in the left track, depth below ground surface (feet) in the center track (each depth increment represents 10 feet), and induction (dotted line) and short normal resistivity (solid line) tools in the right track. This log is from BRACS well id 39995 in southern Wilson County, Texas. The log was performed by Gearhart-Owen Wireline Services in 1980 with a kelly bushing height of 7 feet.

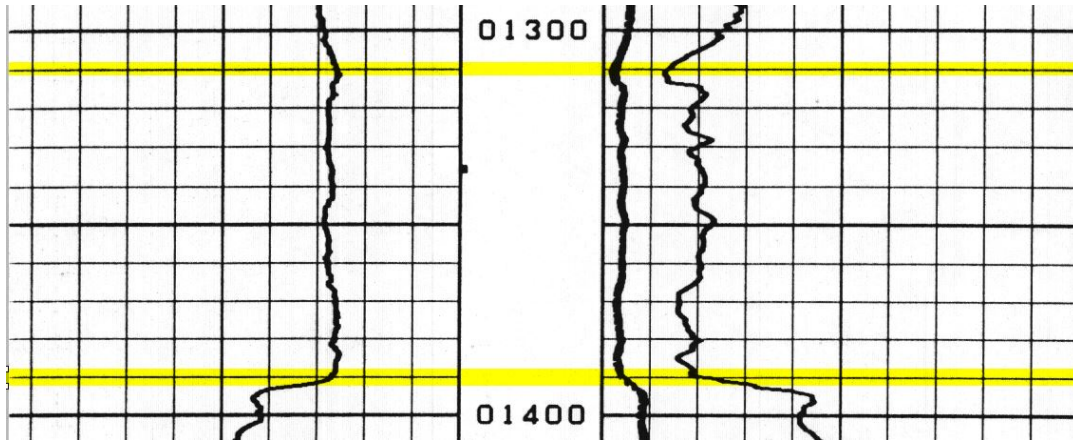


Figure 7.5.2-1. Weches Formation top and bottom depths interpreted on a geophysical well log in Wilson County, Texas.

Geophysical well log signatures for the Weches Formation top and bottom depths in Gonzales County are displayed in Figure 7.5.2-2. The Weches Formation top depth is 963 feet below ground surface (upper yellow line) and bottom depth is 1,020 feet below ground surface (bottom yellow line). Resistivity peaks at 985 and 1,003 feet may indicate glauconitic sands. The geophysical well log includes: the spontaneous potential recorded in the left track, depth below ground surface (feet) in the center track (each depth increment represents 10 feet), and induction (dotted line) and short normal resistivity (solid line) tools in the right track. This log is from BRACS well id 15399 in northeastern Gonzales County, Texas. The log was performed by Lane Wells in 1966 with a kelly bushing height of 10 feet.

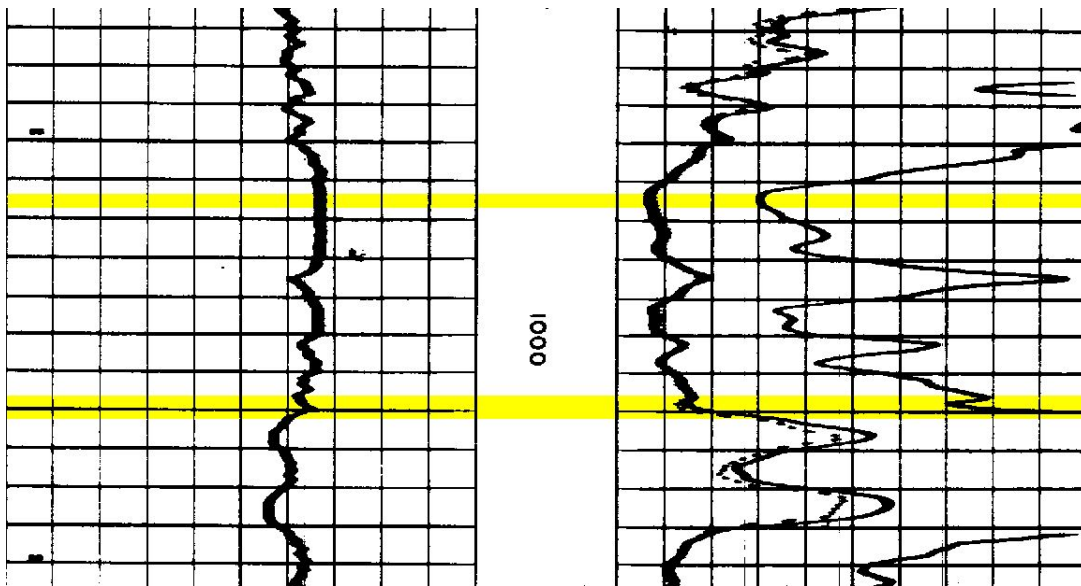


Figure 7.5.2-2. Weches Formation top and bottom depths interpreted on a geophysical well log in Gonzales County, Texas.

7.5.3 Formation top, bottom, thickness

Weches Formation top and bottom elevation maps (Figures 7.5.3-1 and 7.5.3-2) were prepared using 429 and 415 stratigraphic picks respectively from wells within the study area in addition to some wells immediately outside of the study area to control GIS raster edge effects. Weches Formation top and bottom depth maps (Figures 7.5.3-3 and 7.5.3-4) were prepared using elevation GIS rasters subtracted from the study area digital elevation model (refer to Appendix, Section 13.6 raster interpolation documentation).

The Weches Formation thickness was prepared by subtracting the bottom elevation GIS raster from the top elevation GIS raster. The Weches Formation thickness is 0 at the updip outcrop edge and over 170 feet in southwestern Karnes County (Figure 7.5.3-5).

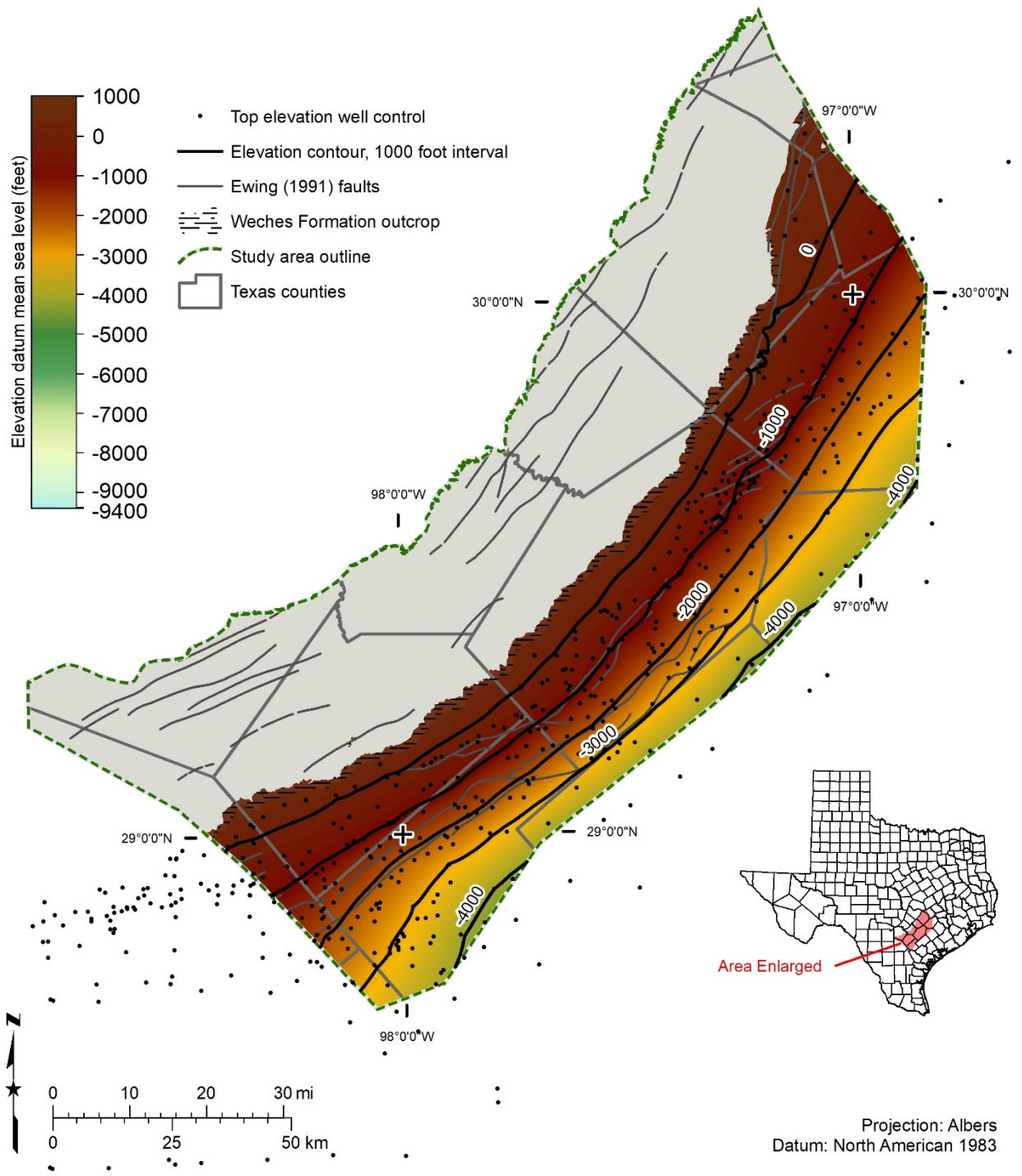


Figure 7.5.3-1. Weches Formation top elevation (feet above mean sea level), which was prepared using 429 wells for stratigraphic control (black dots).

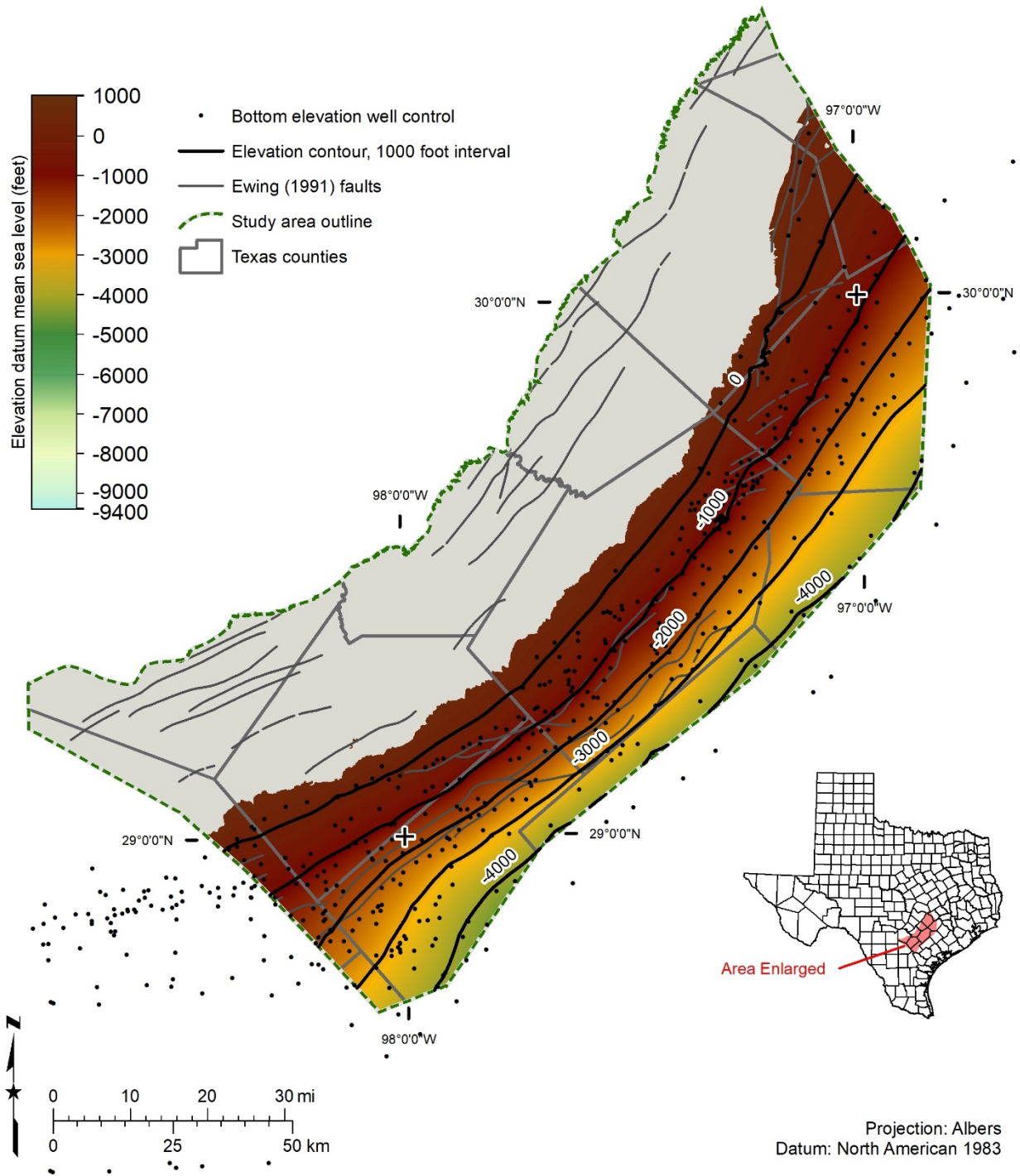


Figure 7.5.3-2. Weches Formation bottom elevation (feet above mean sea level), which was prepared using 415 wells for stratigraphic control (black dots).

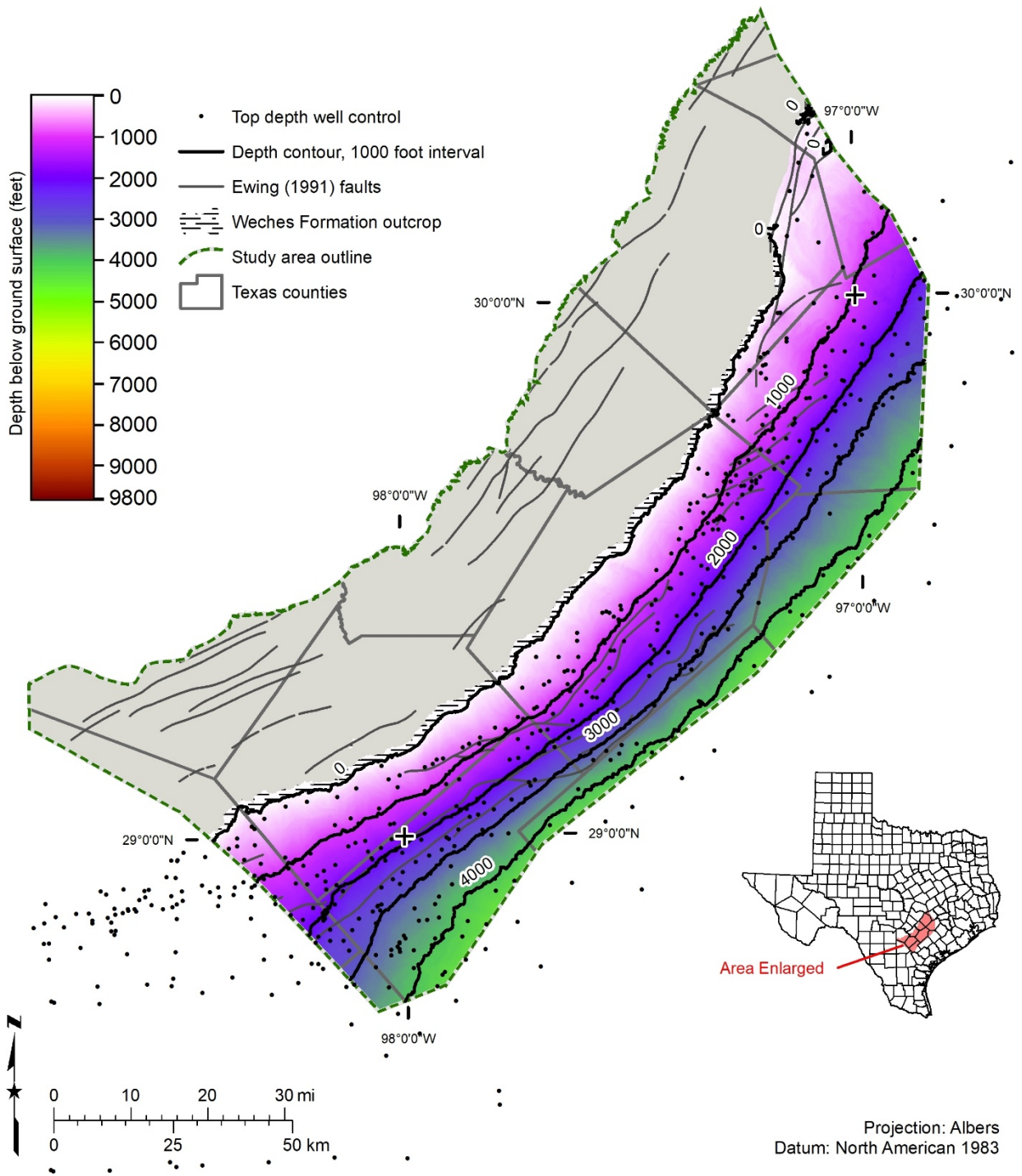


Figure 7.5.3-3. Weches Formation top depth (feet below ground surface), which was prepared using 429 wells for stratigraphic control (black dots).

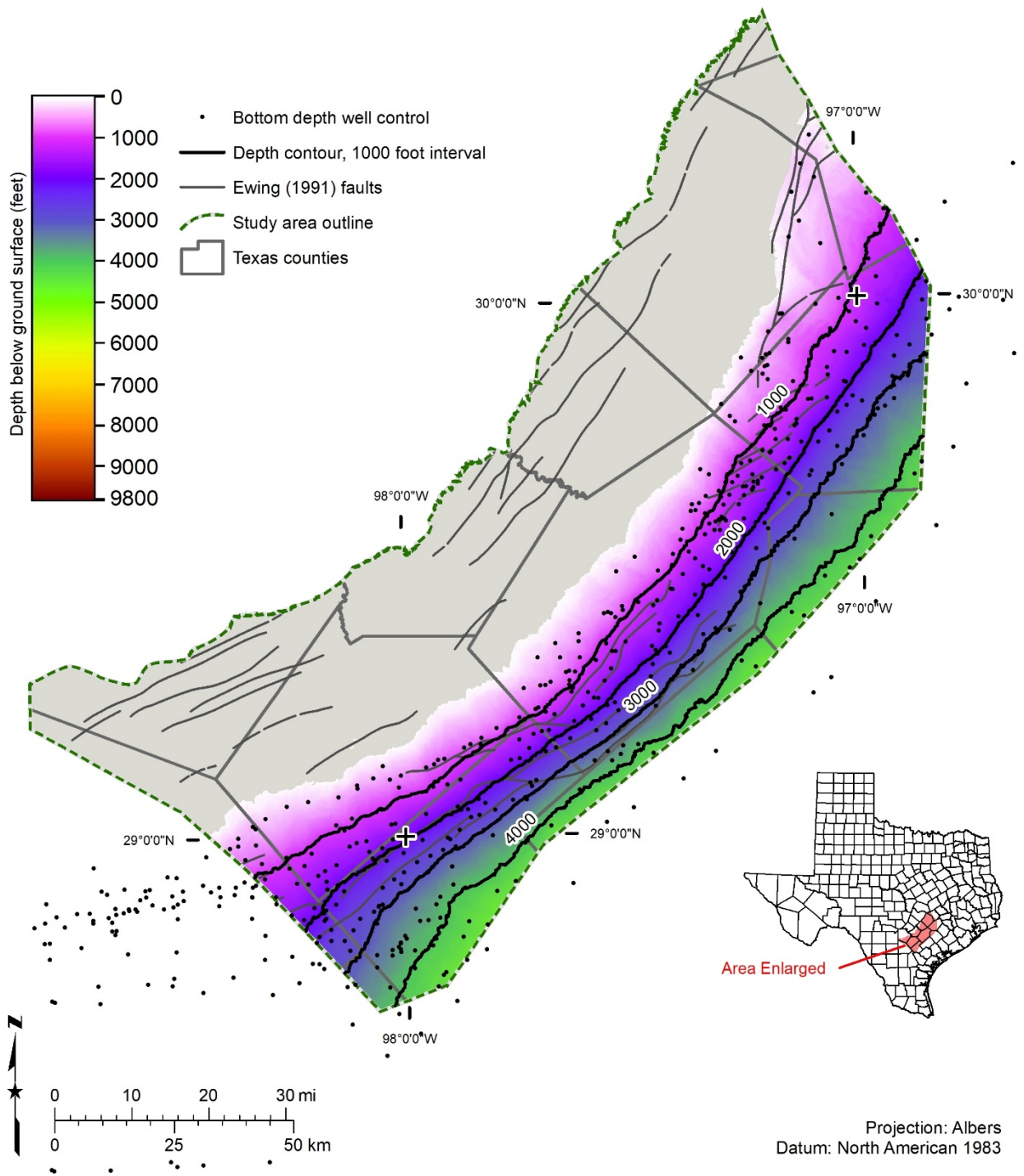


Figure 7.5.3-4. Weches Formation bottom depth (feet below ground surface), which was prepared using 415 wells for stratigraphic control (black dots).

7.5.4 Net sand

Due to the limited sand distribution and production potential of the Weches Formation, we did not conduct a thorough analysis of the net sands in the formation. Draft Weches Formation net sand and sand percent calculations were performed and recorded in the BRACS Database. Maps were not prepared.

7.5.5 Salinity classes

Sands containing groundwater are limited and isolated in the Weches Formation. As such, salinity classes were not calculated using geophysical well logs or mapped.

7.5.6 Volume of brackish groundwater

Brackish groundwater volume was not calculated for the Weches Formation since this formation is considered an aquitard and not a major or minor aquifer in Texas.

7.6 Sparta Sand

The Sparta Sand of the Claiborne Group unconformably underlies the Cook Mountain Formation and conformably overlies the Weches Formation. The Sparta Aquifer, wholly comprised of the Sparta Sand, is a TWDB designated minor aquifer in Texas (George and others, 2011) that produces minor amounts of water over large geographic areas.

7.6.1 Well control

More than 650 wells were used in defining aspects of the Sparta Sand stratigraphy, lithology, and water quality (Table 7.6.1-1). We only used wells for water quality and aquifer hydraulic properties based on the aquifer determination analysis. Undoubtedly there are many other wells completed in the Sparta Sand, but without detailed well screen information it is not possible to accurately assign the Sparta Sand as the source of water produced from the wells.

Table 7.6.1-1. Sparta Sand well control data points.

Well control with this information	Number of data points
Lithology	494
Top surface stratigraphic picks used for raster surface	426
Bottom surface stratigraphic picks used for raster surface	406
Top surface stratigraphic picks (database total*)	654
Bottom surface stratigraphic picks (database total*)	635
Net sand interpreted from wells	335
Aquifer hydraulic properties	50 wells with 50 measurements
Water quality: wells	23 wells with 39 measurements
TDS interpreted from geophysical well logs	423 wells with 432 depth intervals
Porosity	11

* Total number of stratigraphic picks in study counties

7.6.2 Stratigraphic analysis

Stratigraphic pick assignment of the upper contact of the Sparta Sand was selected at the top of the fining upwards sequence subjacent to the shale of the Cook Mountain Formation. The bottom

contact of the Sparta Sand is at the base of the first significant progradational (coarsening upwards sequence) of the Sparta Sand superjacent to the shales of the Weches Formation. The bottom contact is problematic in places where there may be one or more progradational (upward coarsening) sequences of sediment below the major Sparta sand(s). This problematic contact is exacerbated since it is based on lithostratigraphic correlations using geophysical log signatures without paleontology control for dating.

Geophysical well log signatures for the Sparta Sand top and bottom depths in Wilson County are displayed in Figure 7.6.2-1. The Sparta Sand top depth is 1,112 feet below ground surface (upper yellow line) and bottom depth is 1,310 feet below ground surface (bottom yellow line). The geophysical well log includes: the spontaneous potential recorded in the left track, depth below ground surface (feet) in the center track (each depth increment represents 10 feet), and induction (dotted line) and short normal resistivity (solid line) tools in the right track. This log is from BRACS well id 39995 in southern Wilson County, Texas. The log was performed by Gearhart-Owen Wireline Services in 1980 with a kelly bushing height of 7 feet.

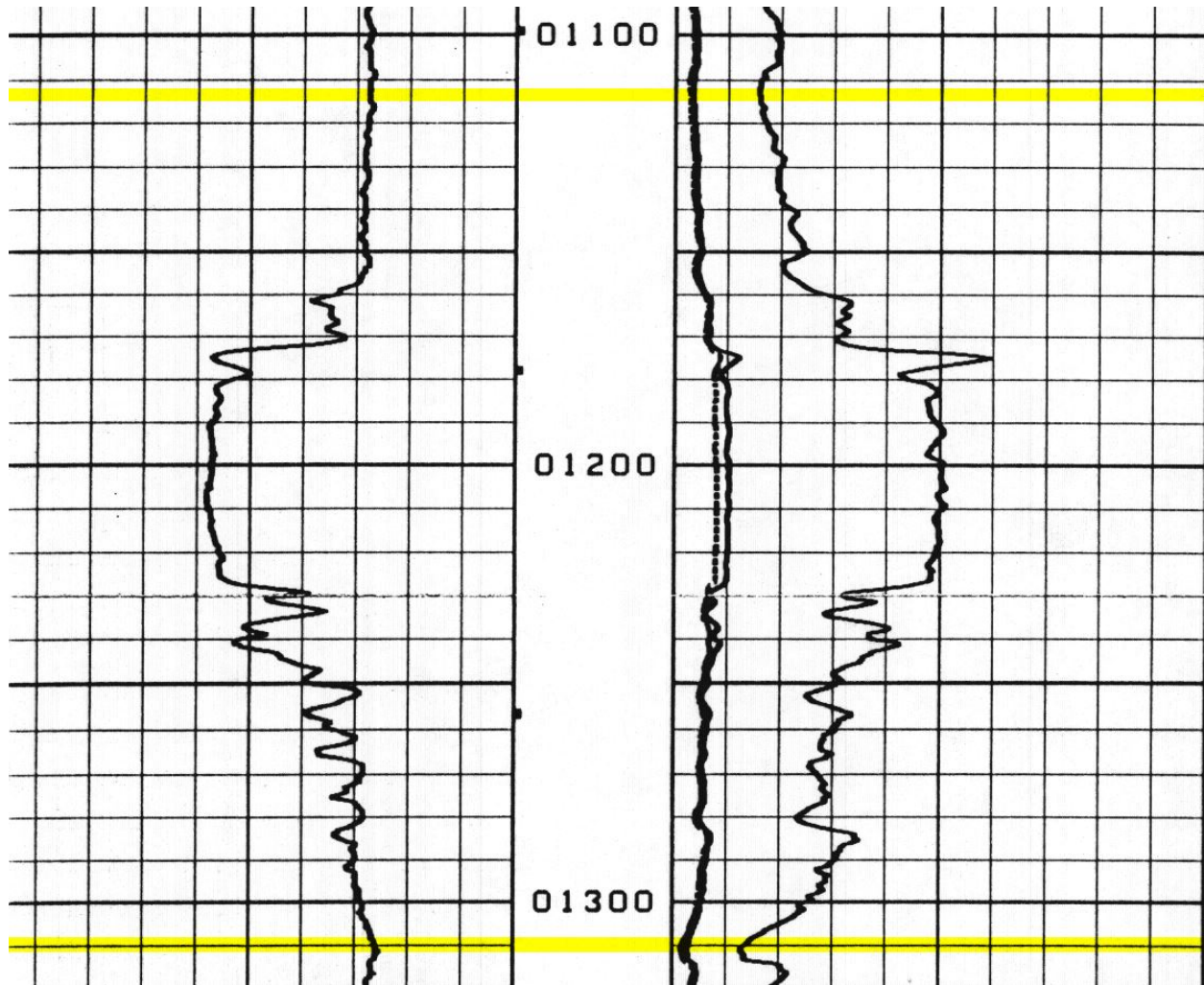


Figure 7.6.2-1. Sparta Sand top and bottom depths interpreted on a geophysical well log in Wilson County, Texas.

Geophysical well log signatures for the Sparta Sand top and bottom depths in Gonzales County are displayed in Figure 7.6.2-2. The Sparta Sand top depth is 763 feet below ground surface (upper yellow line) and bottom depth is 963 feet below ground surface (bottom yellow line). The geophysical well log includes: the spontaneous potential recorded in the left track, depth below ground surface (feet) in the center track (each depth increment represents 10 feet), and induction (dotted line) and short normal resistivity (solid line) tools in the right track. This log is from BRACS well id 15399 in northeastern Gonzales County, Texas. The log was performed by Lane Wells in 1966 with a kelly bushing height of 10 feet.

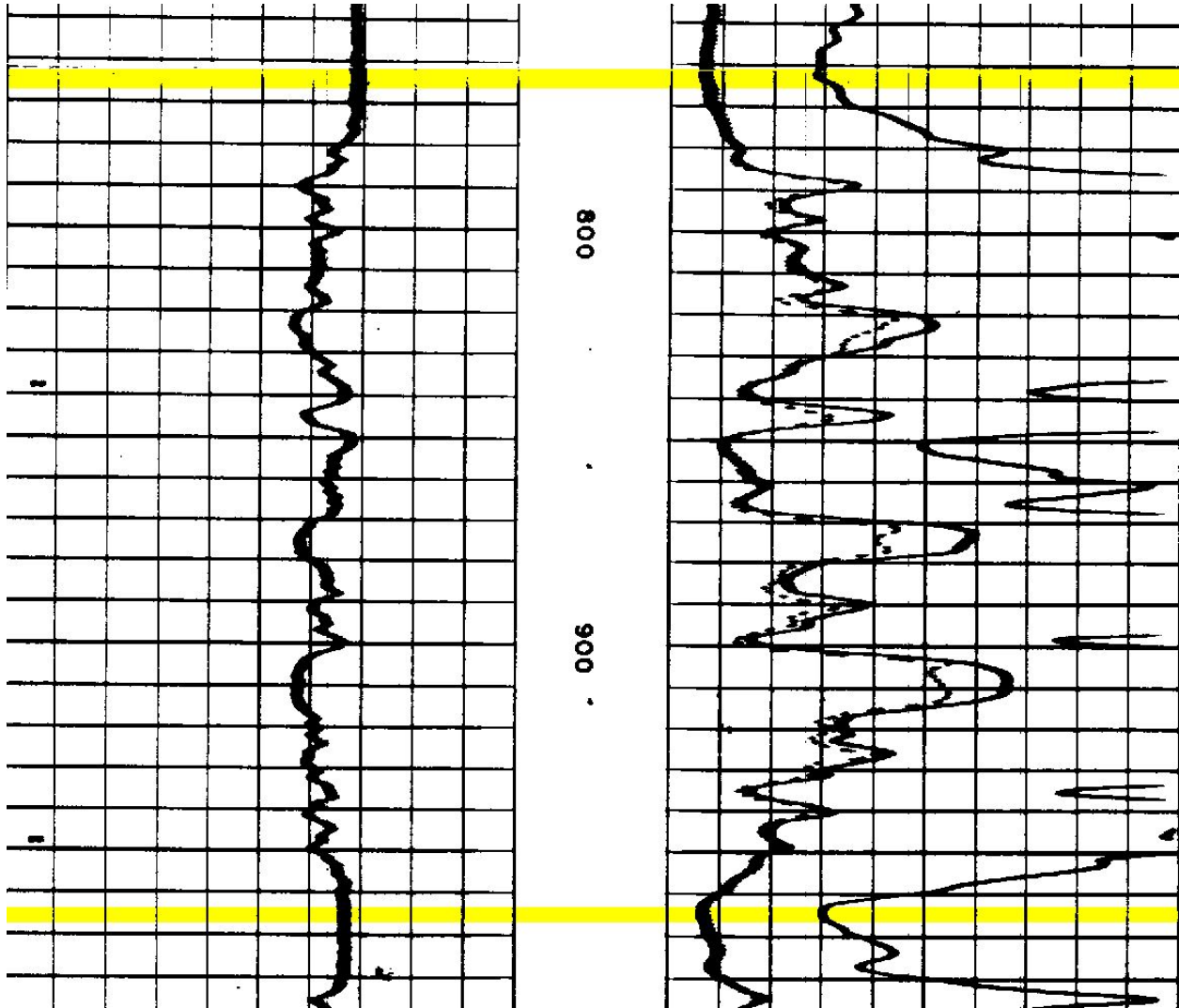


Figure 7.6.2-2. Sparta Sand top and bottom depths interpreted on a geophysical well log in Gonzales County, Texas.

7.6.3 Formation top, bottom, thickness

Sparta Sand top and bottom elevation maps (Figures 7.6.3-1 and 7.6.3-2) were prepared using 426 and 406 stratigraphic picks, respectively, from wells within the study area in addition to

some wells immediately outside of the study area to control GIS raster edge effects. Sparta Sand top and bottom depth maps (Figures 7.6.3-3 and 7.6.3-4) were prepared using elevation GIS rasters subtracted from the study area digital elevation model (refer to Appendix, Section 13.6 raster interpolation documentation).

The Sparta Sand thickness was prepared by subtracting the bottom elevation GIS raster from the top elevation GIS raster. The Sparta Sand thickness is 0 at the updip outcrop edge and over 300 feet in central Karnes County (Figure 7.6.3-5).

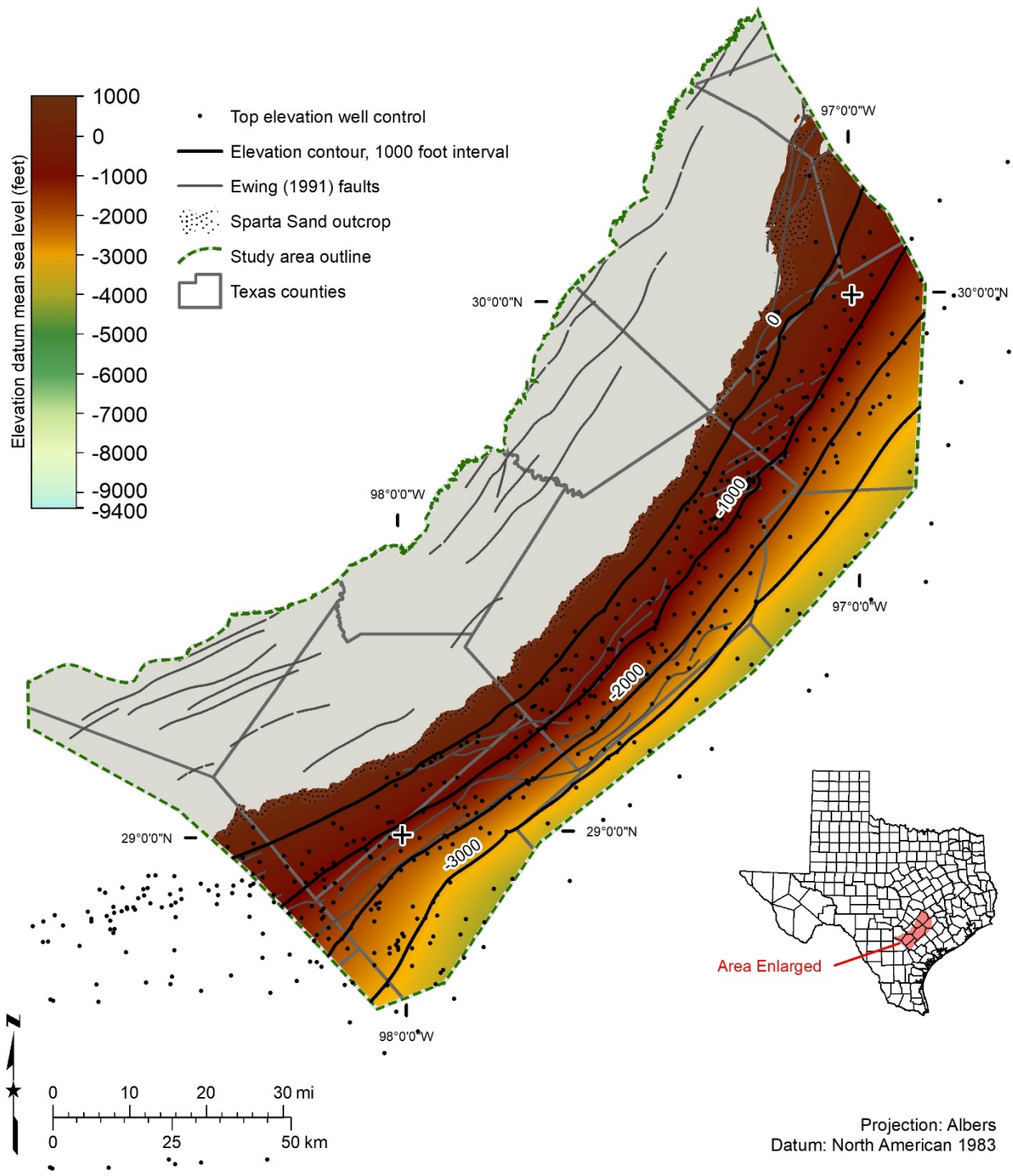


Figure 7.6.3-1. Sparta Sand top elevation (feet above mean sea level), which was prepared using 426 wells for stratigraphic control (black dots).

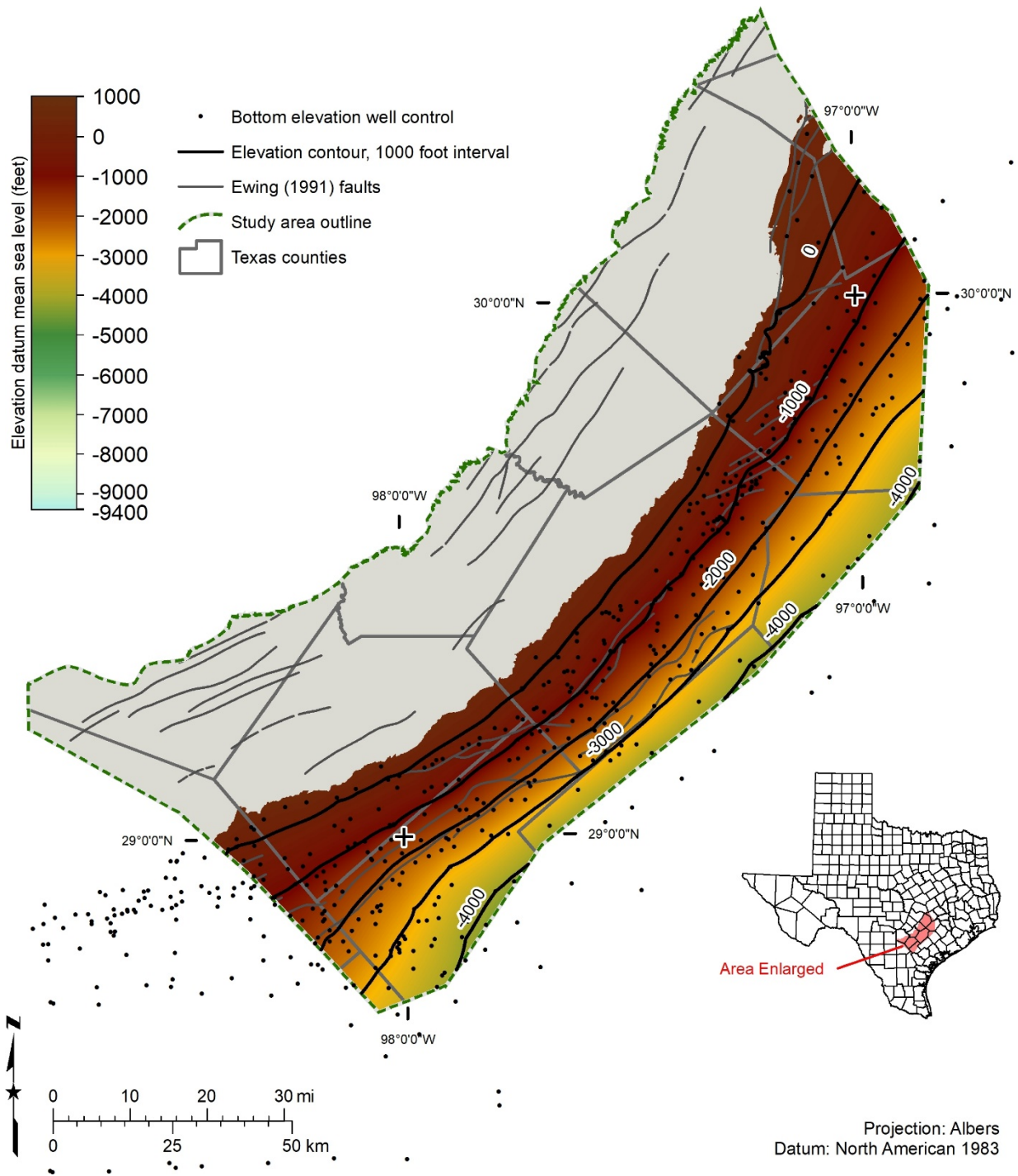


Figure 7.6.3-2. Sparta Sand bottom elevation (feet above mean sea level), which was prepared using 406 wells for stratigraphic control (black dots).

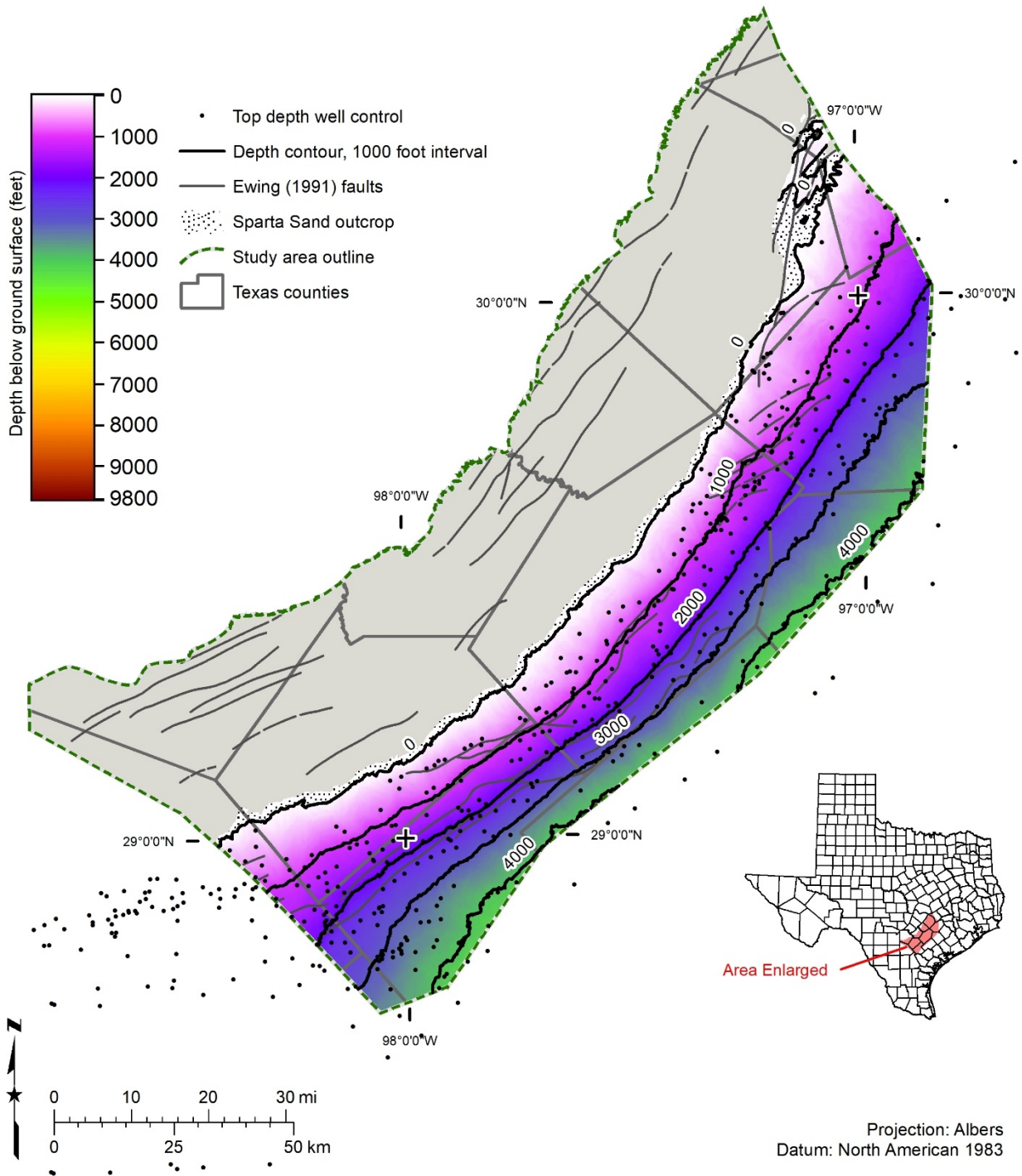


Figure 7.6.3-3. Sparta Sand top depth (feet below ground surface), which was prepared using 426 wells for stratigraphic control (black dots).

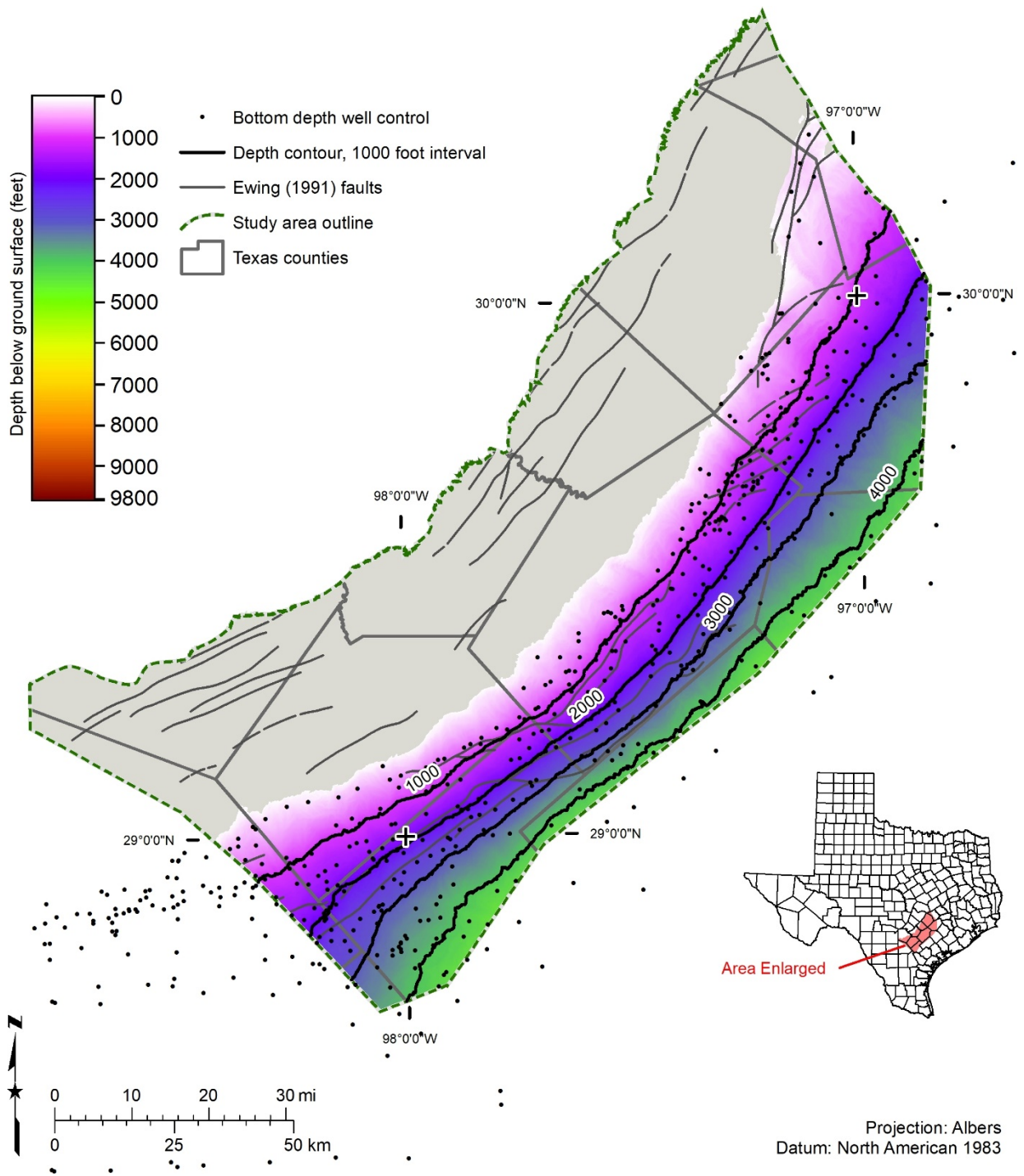


Figure 7.6.3-4. Sparta Sand bottom depth (feet below ground surface), which was prepared using 406 wells for stratigraphic control (black dots).

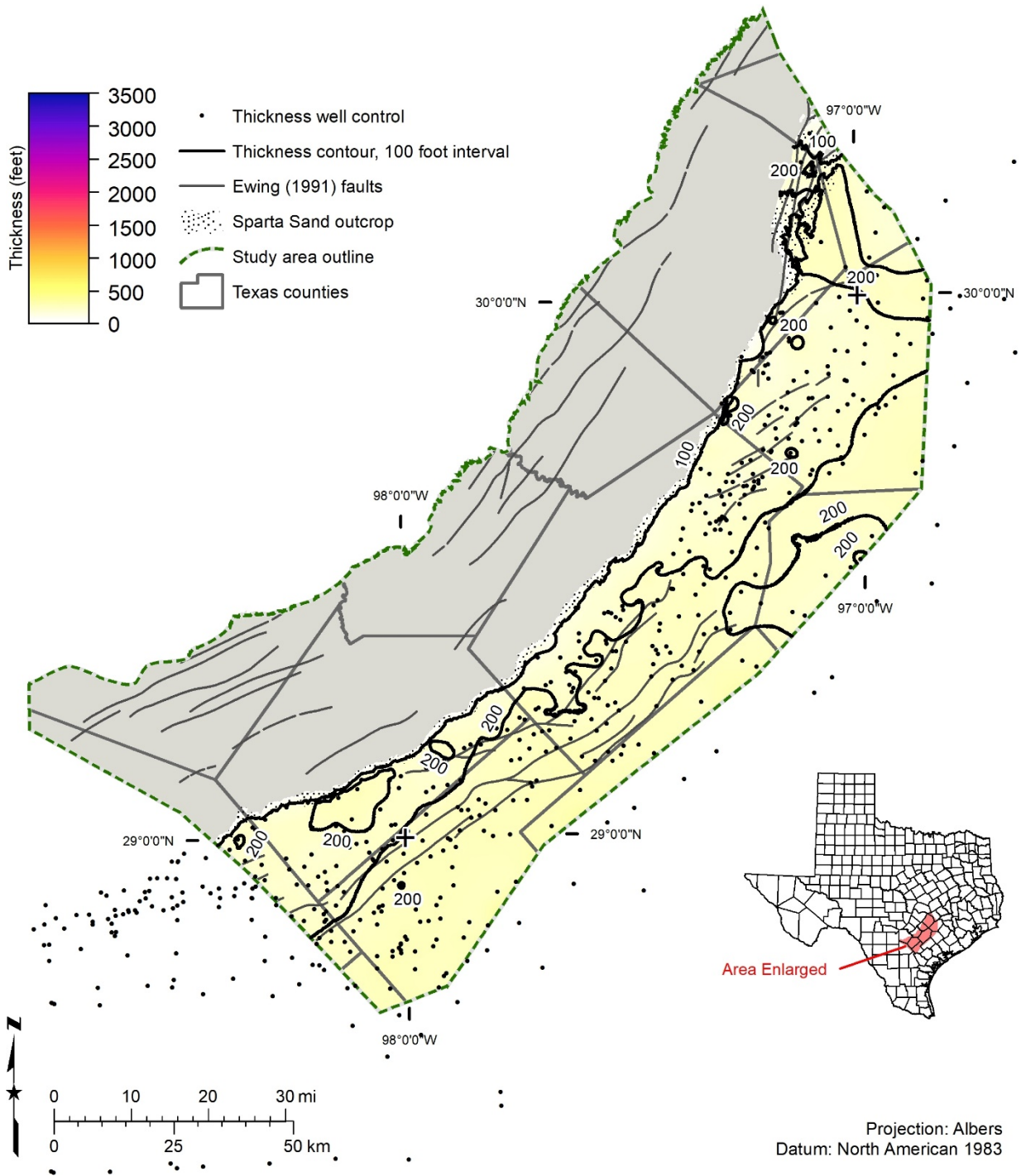


Figure 7.6.3-5. Sparta Sand thickness in units of feet, which was prepared using 406 wells for stratigraphic control (black dots).

7.6.4 Net sand

We evaluated 335 wells, of which 155 are water wells, 175 are oil and gas wells, and 5 are wells classified as other (primarily test holes for water wells). We used geophysical well logs for 197 wells and drillers' descriptions of lithology for the remaining 138 wells. Net sand values range from 0 at the updip outcrop edge to over 140 feet in northeastern Fayette County. The net sand map (Figure 7.6.4-1) shows the (1) westernmost lobe of the high-constructive delta in Fayette County, (2) transition to the strike-oriented strandplain/barrier bar sequence west of the delta, (3) first hint of the high-destructive delta facies evident along the Atascosa – Wilson county line, and (4) sand input axes shown as red arrows (Ricoy and Brown, 1977).

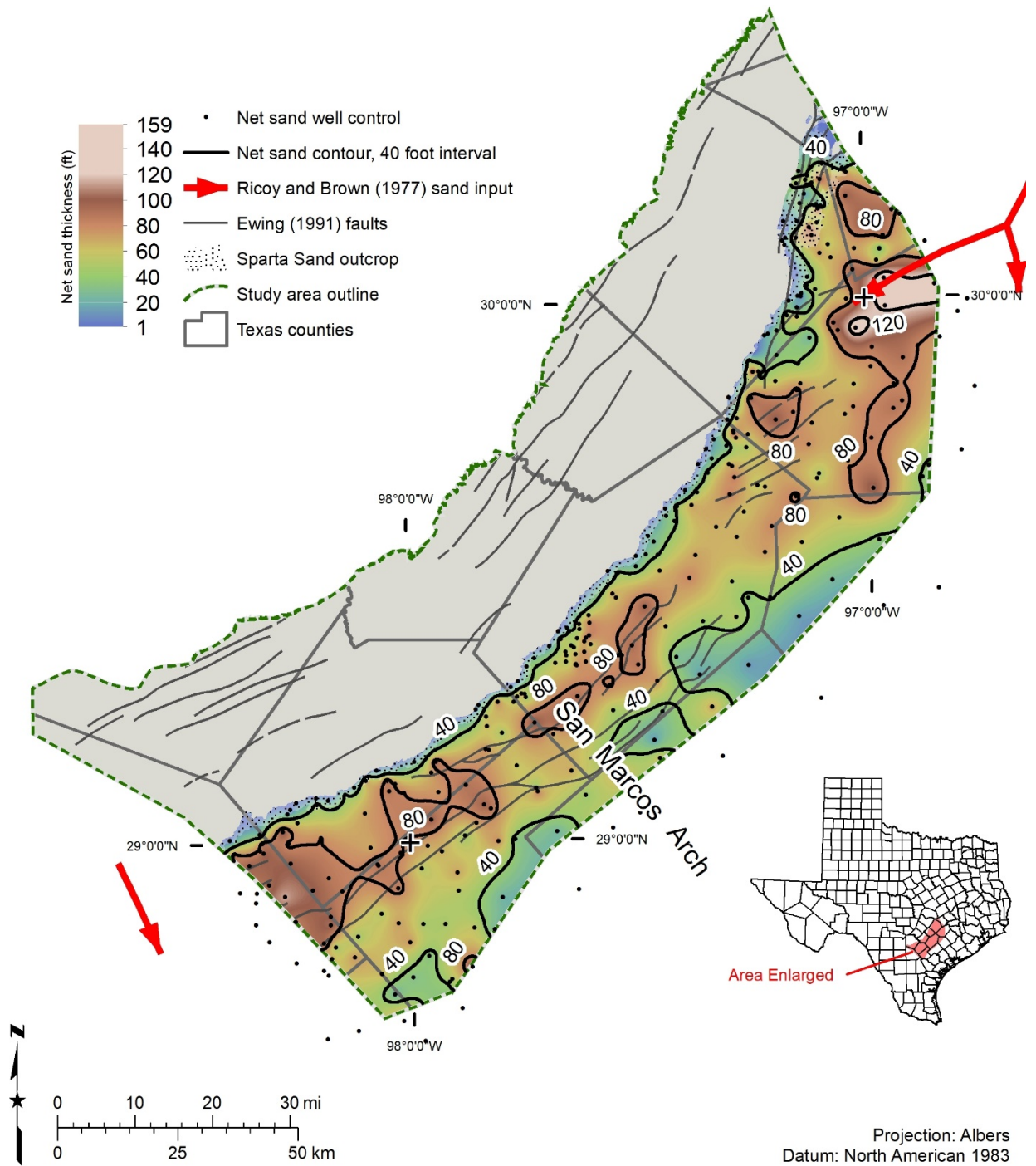


Figure 7.6.4-1. Sparta Sand net sand thickness (feet), which was prepared using 335 wells for net sand control (black dots). Axes of significant sand input into the basin modified from Ricoy and Brown (1977) are shown in red arrows.

7.6.5 Salinity classes

The Sparta Sand was mapped into defined salinity classes: (1) fresh, (2) slightly saline, (3) moderately saline, and (4) very saline (Figures 7.6.5-1 and 7.6.5-2). Mapping was based on water quality samples (31 wells classified as: 21 fresh, 9 slightly saline, and 1 moderately saline) and

estimated total dissolved solids calculations using geophysical well logs (427 wells with 427 depth intervals analyzed yielding salinity class zones: 4 fresh, 136 slightly saline, 112 moderately saline, 174 very saline, and 1 brine).

None of the wells reviewed contained mixed salinity classes within the Sparta Sand. The Sparta Sand does not exhibit vertical stacking of different salinity classes in contrast to the other formations evaluated in this study. The transition from fresh to very saline groundwater ranges from 2.6 to 7.4 miles of the outcrop in central Gonzales through central Wilson counties, in the area characterized as a strandplain/barrier bar system by Ricoy and Brown (1977). In contrast, the slightly and moderately saline classes extend downdip approximately 22 miles from central Gonzales County to the northeast where the high-constructive delta system of Ricoy and Brown (1977) has been mapped. Very saline water is only identified in the southern portion of Fayette County, nearly 22 miles from outcrop. A lobe of moderately saline groundwater extends from central Wilson County into Karnes County and the slightly saline and moderately saline class widens in western Wilson County extending into Atascosa County.

The transition from one salinity class to another is not simple, as Figure 7.6.5-2 demonstrates. We believe that initial depositional environments as illustrated by net sand distribution and the occurrence, displacement, orientation, and connectivity of normal faults all interact to control groundwater salinity distribution. Isolated pods of fresher or more saline water occur, as seen in Fayette County. Some are only represented by one well and were too small to map as a class.

Only one well was interpreted to have brine (eastern Karnes County) and the very saline to brine transition is downdip of the study area.

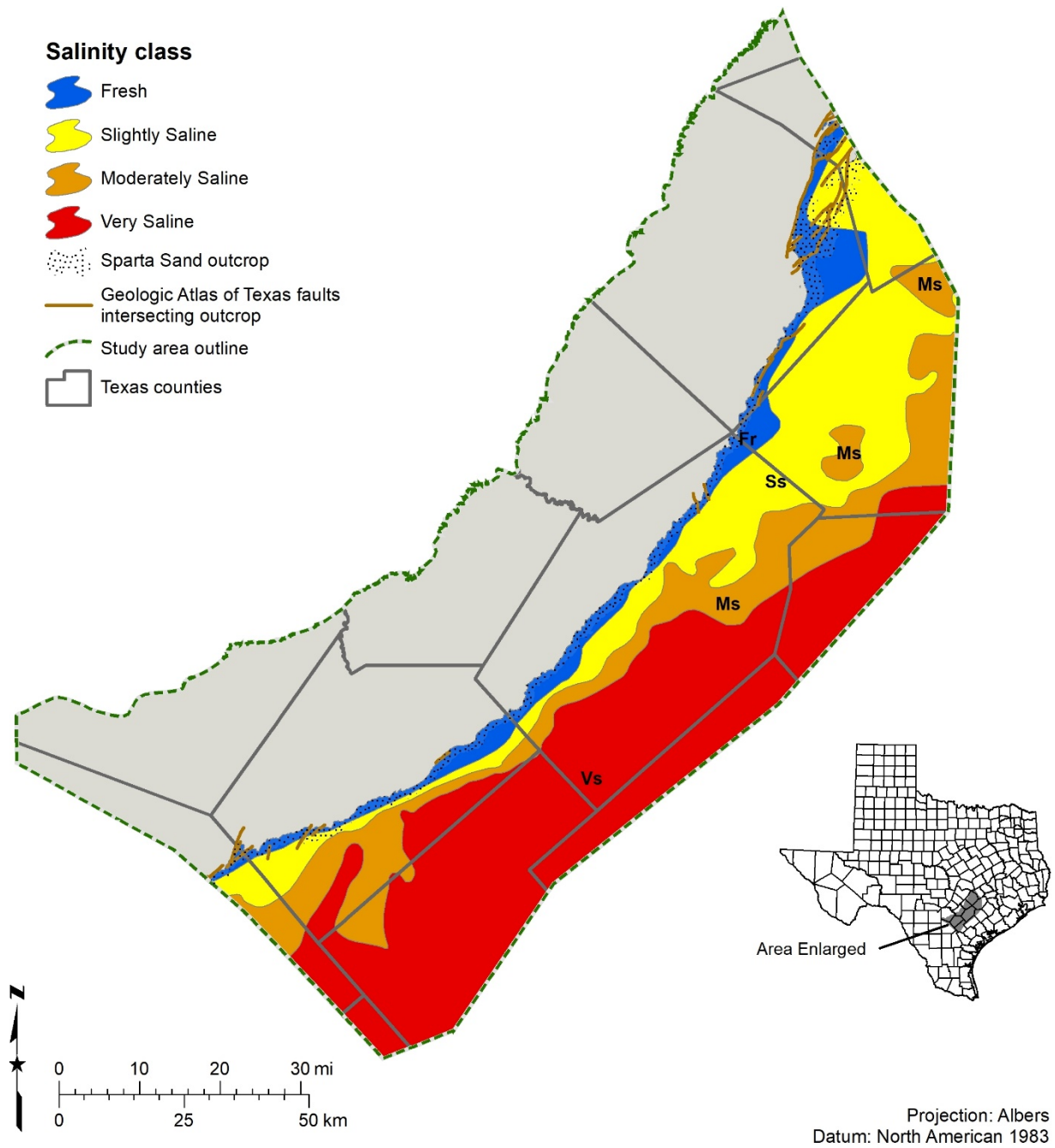


Figure 7.6.5-1. Sparta Sand salinity classes and identification names. Refer to Table 2-1 for salinity class definition.

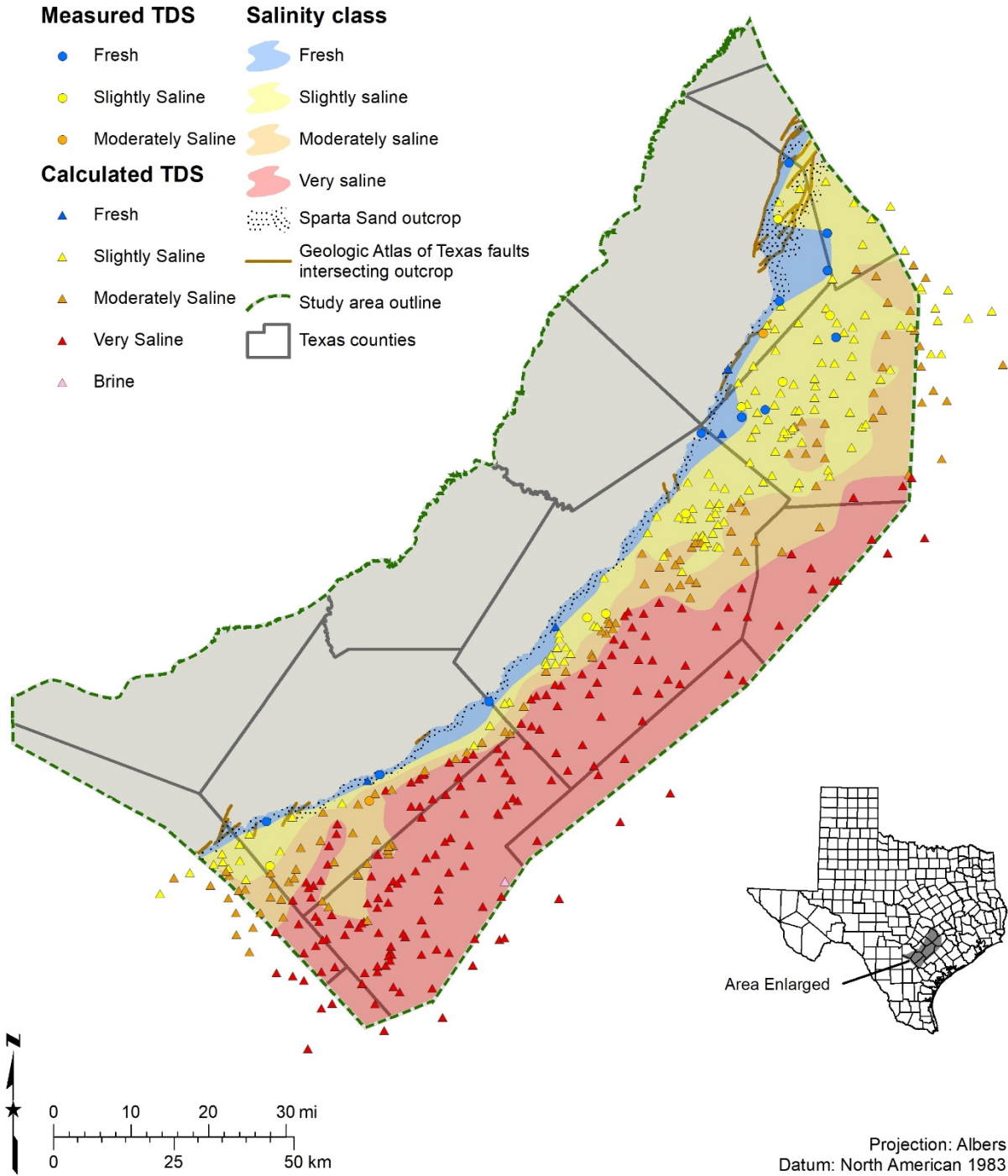


Figure 7.6.5-2. Sparta Sand salinity classes and well control consisting of water well quality data (circles) and interpreted geophysical well logs (triangles). Refer to Table 2-1 for salinity class definition. TDS = total dissolved solids.

7.6.6 Volume of brackish groundwater

We calculated the volume of in-place groundwater for the Sparta Sand based on salinity classes (Table 7.6.6-1). The Sparta Sand contains more than 6 million acre-feet of in-place brackish groundwater within the study area. The Sparta Sand contains a total of more than 11 million acre-feet of in-place groundwater of all salinity ranges within the study area.

Table 7.6.6-1. Total volume (acre-feet) of in-place groundwater in the Sparta Sand based on salinity class. Values summarized from Table 13.1.4-1. Volume values rounded to the nearest 10,000 acre-feet.

Salinity class	Volume groundwater (acre-feet)
Fresh	480,000
Slightly saline	3,550,000
Moderately saline	2,860,000
Very saline	4,860,000

Additionally, we subdivided the volumes based on administrative boundaries (Appendix 13.1, Tables 13.1.4-1, 13.1.4-2, 13.1.4-3, and 13.1.4-4). Appendix 13, Section 13.2 contains a complete discussion of volume methodology. Once salinity class mapping for the Sparta Sand was completed, we noticed that the study area did not include the entire available resource affecting some groundwater volume calculations. Specifically, the study area does not include the entire extent of Sparta Sand moderately saline water in the eastern part of the study area. Calculation of groundwater volumes used aquifer-based study area boundaries and some administrative boundaries are not coincident with the study area boundary. This resulted in partial volumes for some counties, groundwater conservation districts, and regional water planning areas. Future evaluation of the Sparta Sand to the northeast of the study area will address this issue.

7.6.7 Aquifer hydraulic properties

We compiled 50 sets of aquifer hydraulic property data from 50 wells completed in the Sparta Sand. The data is organized by hydraulic property (Table 7.6.7-1) and recorded in the BRACS Database table (tblUCPC_AquiferTestInformation). Sparta Sand records are identified using the field aquifer_new = SP. A full discussion of this dataset is provided in Section 6.7. We prepared a map showing the spatial distribution of wells with well yield, specific capacity, transmissivity, and hydraulic conductivity (Figure 7.6.7-1).

Table 7.6.7-1. Hydraulic properties of the Sparta Sand within the study area. Refer to the BRACS Database table (tblUCPC_AquiferTestInformation) for detailed information about each well and data. Refer to Figure 7.6.7-1 for a map of these parameters.

	Transmissivity (gallons per day per foot)	Hydraulic conductivity (feet per day)	Storage coefficient (dimensionless)	Specific capacity (gallons per minute per foot)	Well yield (gallons per minute)
Number of values	0	0	0	30	50
Low	-	-	-	0.18	8
High	-	-	-	12	250
Average	-	-	-	3.14	74

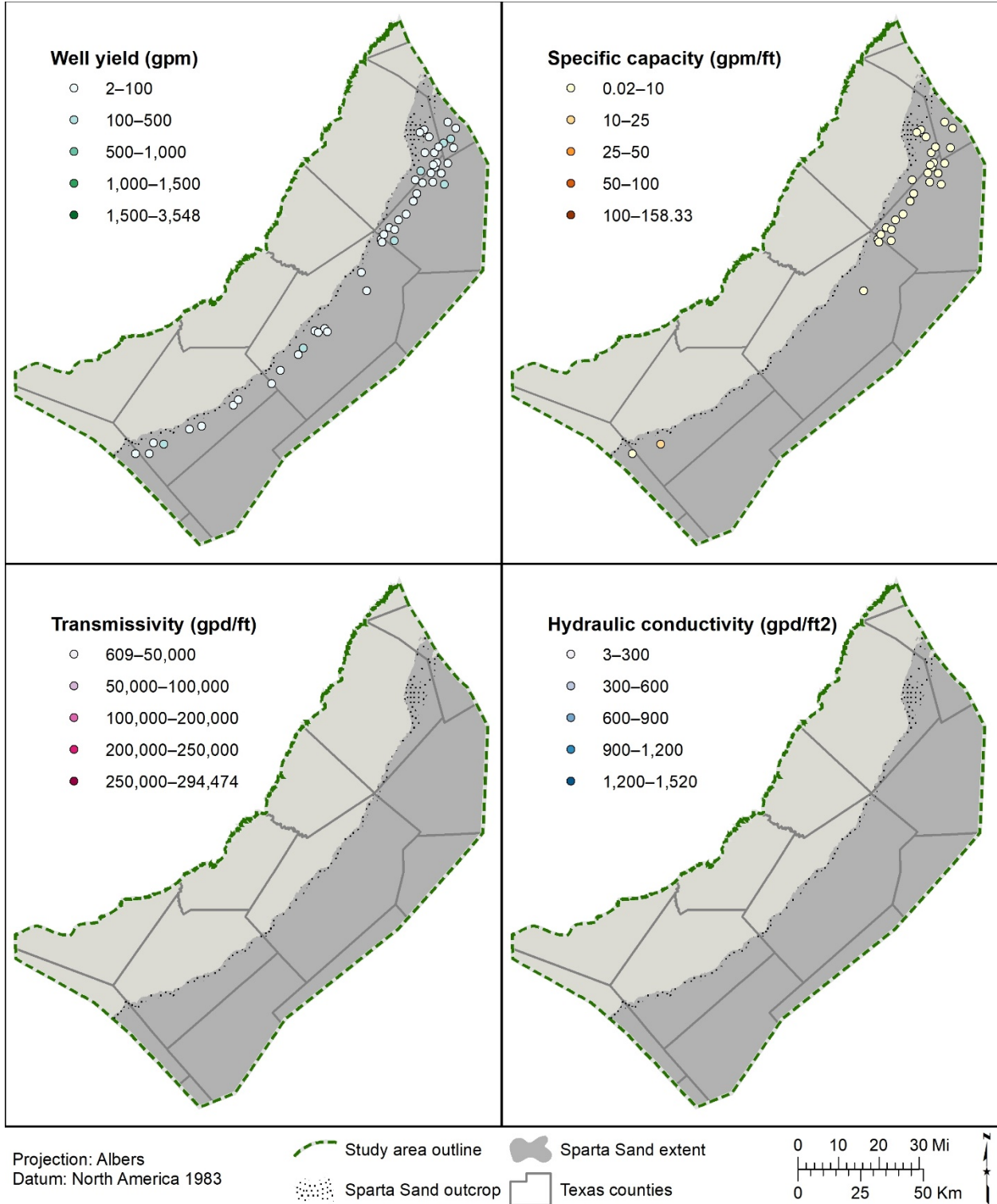


Figure 7.6.7-1. Sparta Sand hydraulic properties showing well yield (gallons per minute), specific capacity (gallons per minute per foot of drawdown), transmissivity (gallons per day per foot), and hydraulic conductivity (gallons per day per foot squared). Refer to Table 7.6.7-1 for a summary of these parameters.

7.7 Cook Mountain Formation

The Cook Mountain Formation of the Claiborne Group conformably underlies the Yegua Formation and unconformably overlies the Sparta Sand. The Cook Mountain Formation is a regional aquitard with low permeability compared to the sands of the Sparta and Yegua formations and can hinder vertical water movement between the two aquifers. For these reasons we did not evaluate the Cook Mountain Formation for groundwater potential.

The Cook Mountain Formation is referred to as the Crockett Formation (Sellards and others, 1932).

7.7.1 Well control

More than 550 wells were used in defining aspects of the Cook Mountain Formation stratigraphy, lithology, and water quality (Table 7.7.1-1).

Table 7.7.1-1. Cook Mountain Formation well control data points.

Well control with this information	Number of data points
Lithology	336
Top surface stratigraphic picks used for raster surface	410
Bottom surface stratigraphic picks used for raster surface	382
Top surface stratigraphic picks (database total*)	531
Bottom surface stratigraphic picks (database total*)	588
Net sand interpreted from wells	299**
Aquifer hydraulic properties	19 wells with 20 measurements
Water quality: wells	18 well with 21 measurements
TDS interpreted from geophysical well logs	0
Porosity	0

* Total number of stratigraphic picks in study counties

** Total number of wells with net sand values; however, these have not been verified for use

7.7.2 Stratigraphic analysis

Stratigraphic pick assignment of the upper contact of the Cook Mountain Formation was selected at the top of the shale subjacent to the base of the first significant progradational (coarsening upwards sequence) of the Yegua Formation. The bottom contact of the Cook Mountain Formation is at the base of the shale marker above the uppermost fining upwards sequence signature of the Sparta Sand. These contacts are based on lithostratigraphic correlations using geophysical log signatures without paleontology control for dating.

Geophysical well log signatures for the Cook Mountain Formation top depth in Fayette County are displayed in Figure 7.7.2-1. The Cook Mountain Formation top depth is 2,290 feet below ground surface (yellow line). The geophysical well log includes: the spontaneous potential recorded in the left track, depth below ground surface (feet) in the center track (each depth increment represents 10 feet), and induction (dotted line) and short guard resistivity (solid line) tools in the right. This log is from BRACS well id 39846 in southwestern Fayette County, Texas. The log was performed by Welex in 1979 with a kelly bushing height of 14 feet.

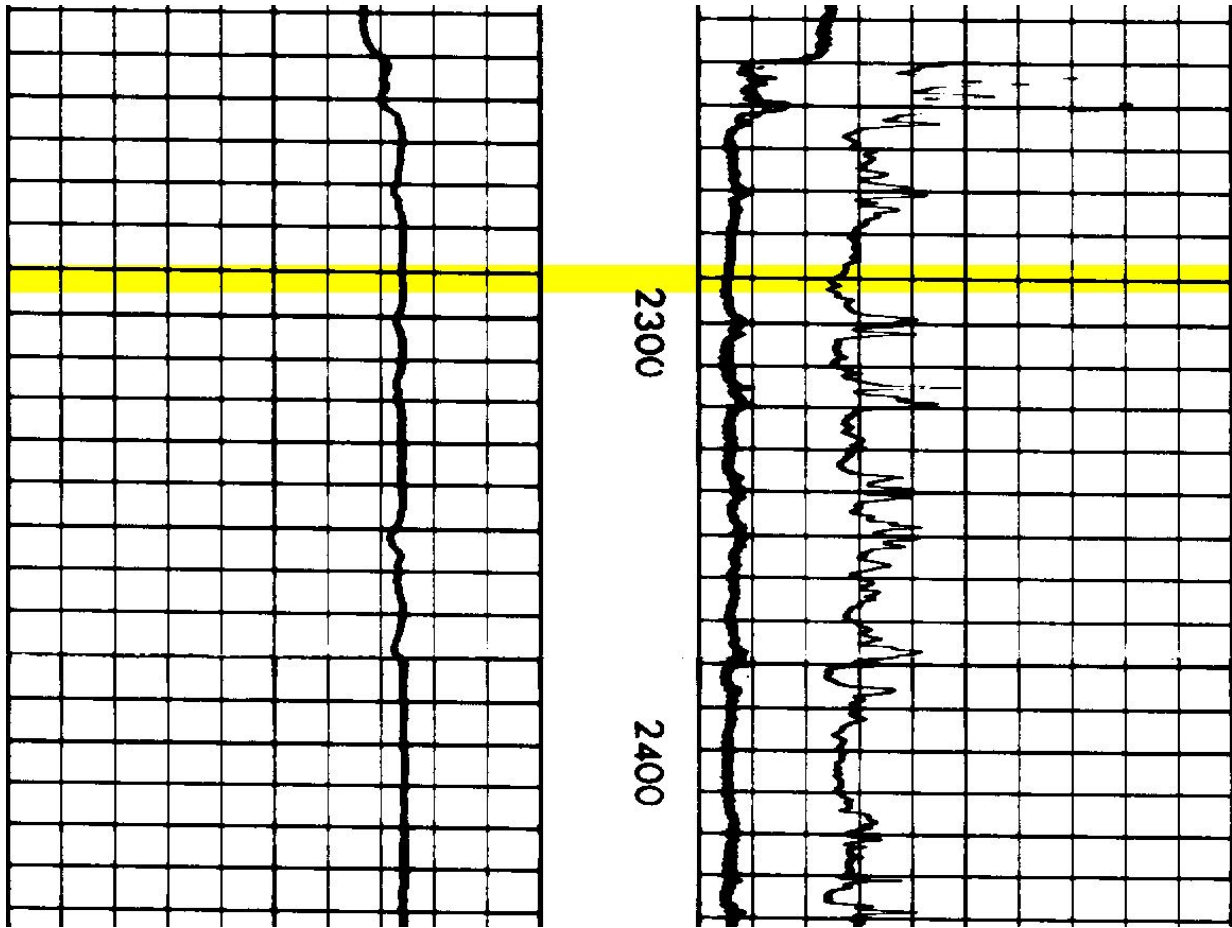


Figure 7.7.2-1. Cook Mountain Formation top depth interpreted on a geophysical well log in Fayette County, Texas.

Geophysical well log signatures for the Cook Mountain Formation bottom depth in Fayette County are displayed in Figure 7.7.2-2. The Cook Mountain Formation bottom depth is 2,690 feet below ground surface (yellow line). The geophysical well log includes: the spontaneous potential recorded in the left track, depth below ground surface (feet) in the center track (each depth increment represents 10 feet), and induction (dotted line) and short guard resistivity (solid line) tools in the right. This log is from BRACS well id 39846 in southwestern Fayette County, Texas. The log was performed by Welex in 1979 with a kelly bushing height of 14 feet.

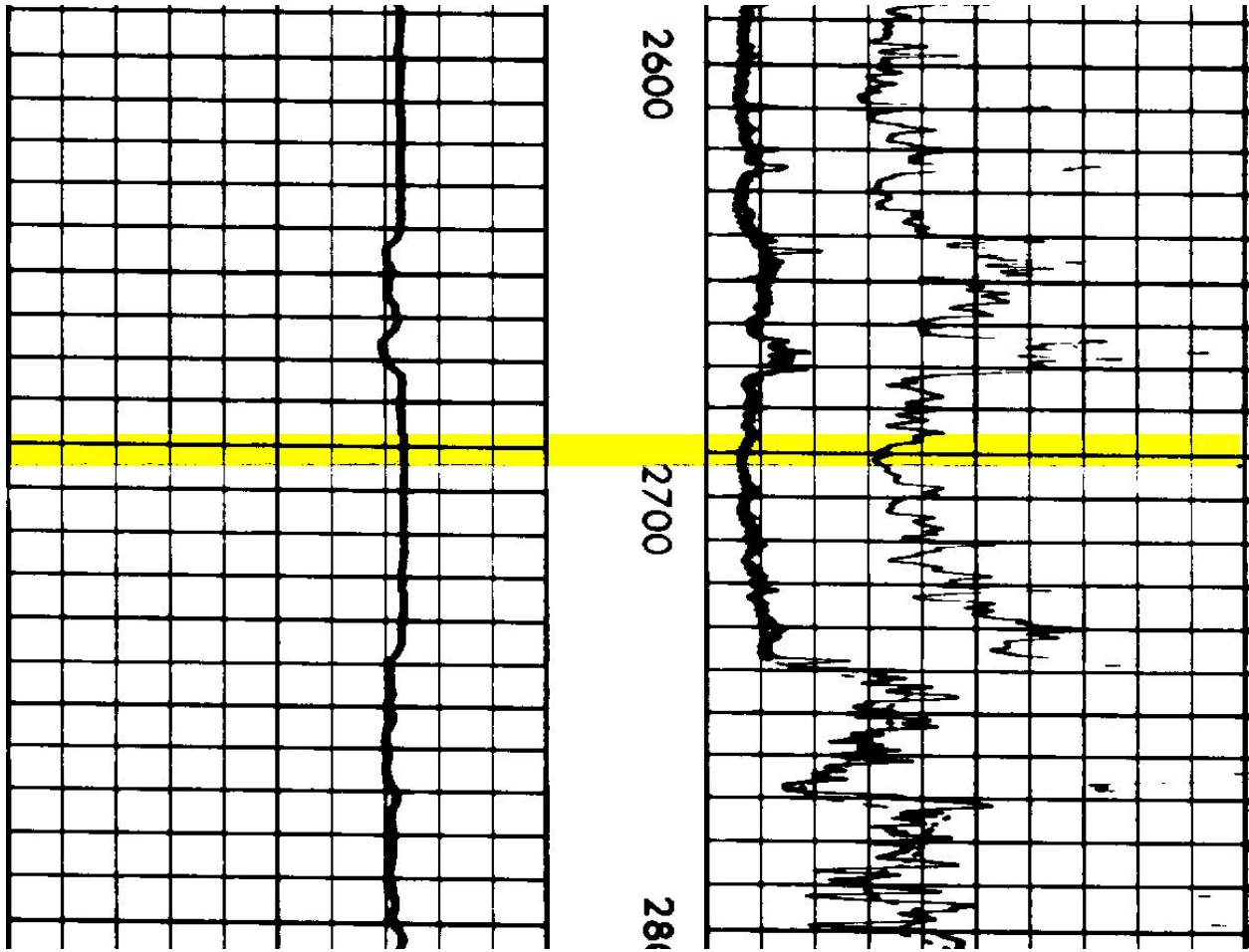


Figure 7.7.2-2. Cook Mountain Formation bottom depth interpreted on a geophysical well log in Fayette County, Texas.

Geophysical well log signatures for the Cook Mountain Formation top depth in Gonzales County are displayed in Figure 7.7.2-3. The Cook Mountain Formation top depth is 2,628 feet below ground surface (yellow line). The geophysical well log includes: the spontaneous potential recorded in the left track, depth below ground surface (feet) in the center track (each depth increment represents 10 feet), and induction (dotted line) and short normal resistivity (solid line) tools in the right track (these two curves are superimposed within the Cook Mountain). This log is from BRACS well id 15335 in southwestern Gonzales County, Texas. The log was performed by Schlumberger in 1960 with a kelly bushing height of 17 feet.

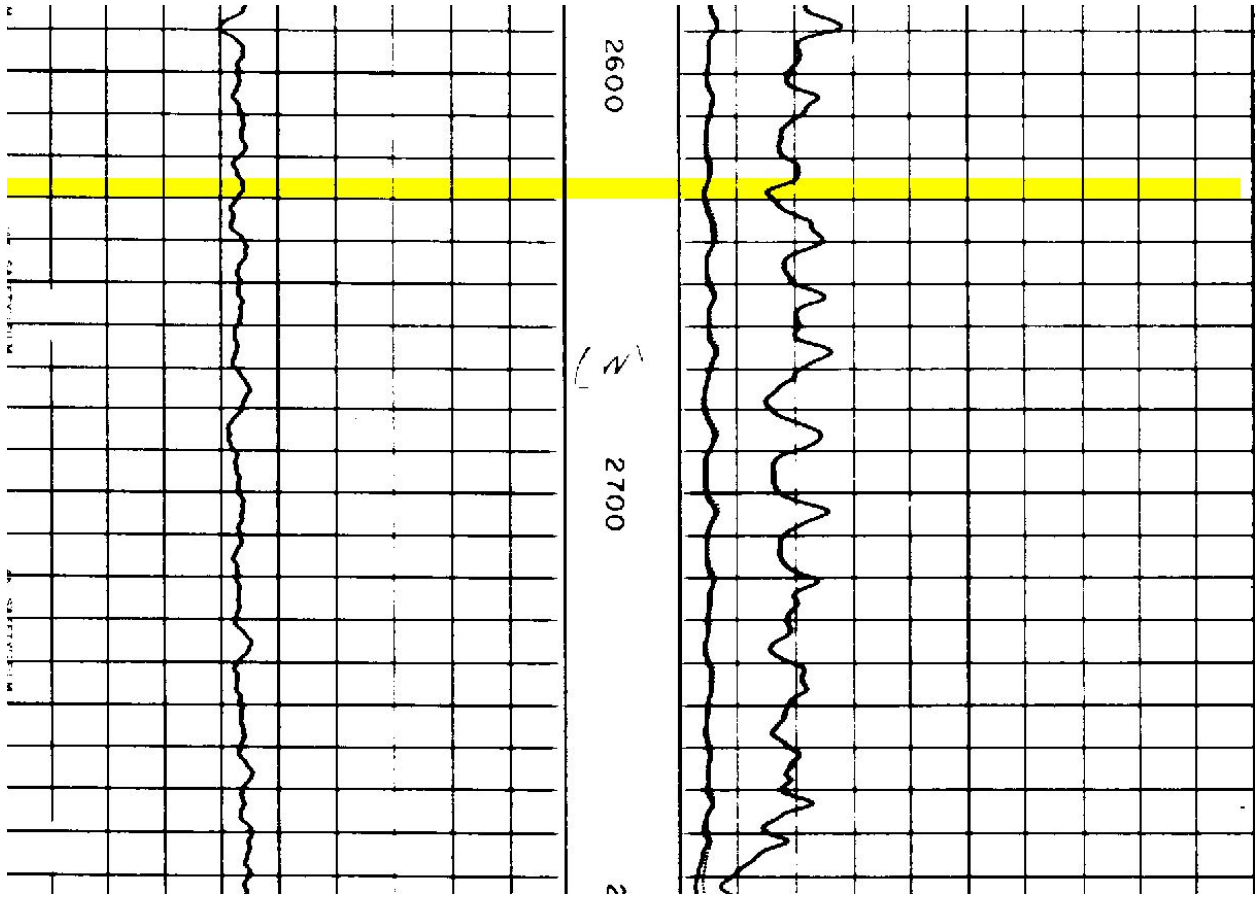


Figure 7.7.2-3. Cook Mountain Formation top depth interpreted on a geophysical well log in Gonzales County, Texas.

Geophysical well log signatures for the Cook Mountain Formation bottom depth in Gonzales County are displayed in Figure 7.7.2-4. The Cook Mountain Formation bottom depth is 3,110 feet below ground surface (yellow line). The geophysical well log includes: the spontaneous potential recorded in the left track, depth below ground surface (feet) in the center track (each depth increment represents 10 feet), and induction (dotted line) and short normal resistivity (solid line) tools in the right track (these two curves are superimposed within the Cook Mountain). This log is from BRACS well id 15335 in southwestern Gonzales County, Texas. The log was performed by Schlumberger in 1960 with a kelly bushing height of 17 feet.

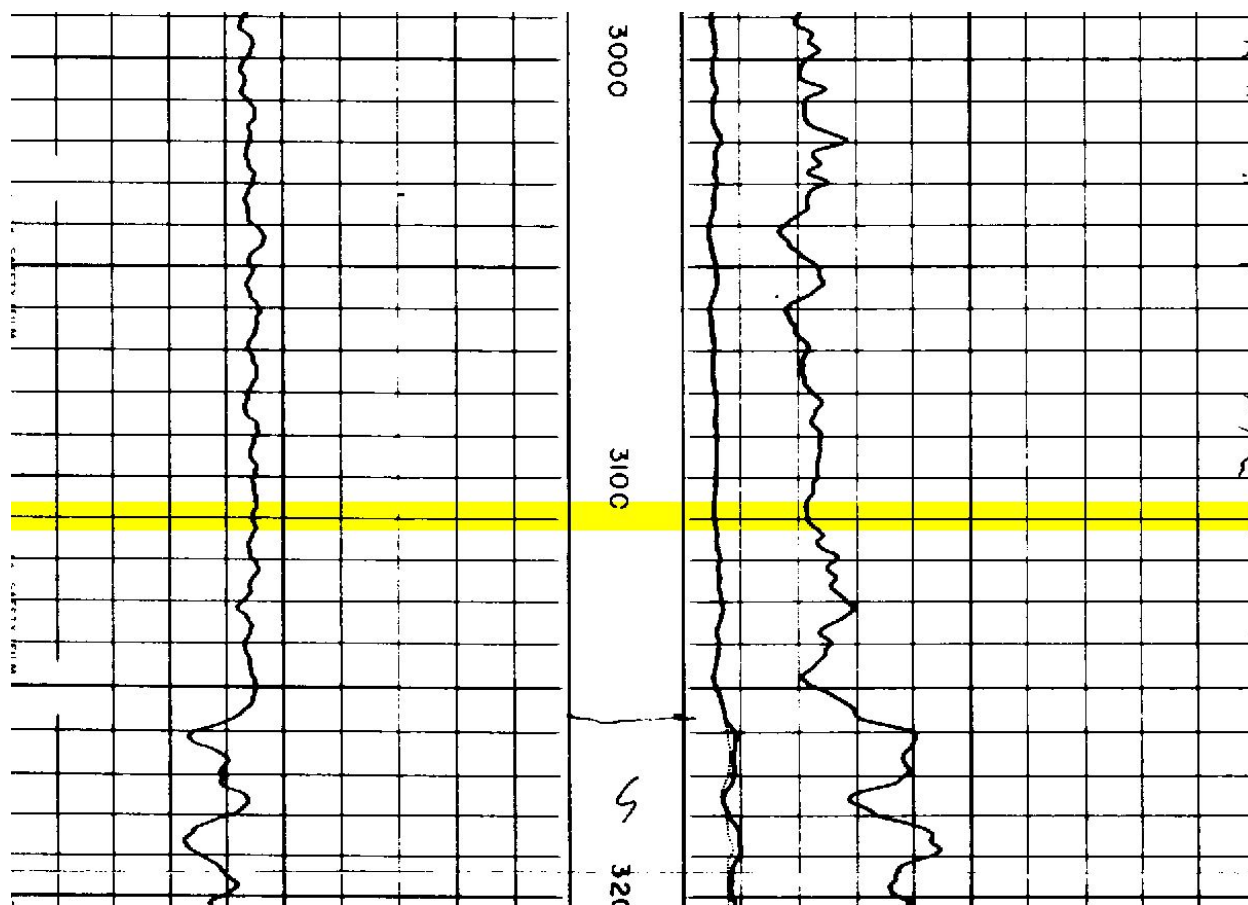


Figure 7.7.2-4. Cook Mountain Formation bottom depth interpreted on a geophysical well log in Gonzales County, Texas.

7.7.3 Formation top, bottom, thickness

Cook Mountain Formation top and bottom elevation maps (Figures 7.7.3-1 and 7.7.3-2) were prepared using 410 and 382 stratigraphic picks respectively from wells within the study area in addition to some wells immediately outside of the study area to control GIS raster edge effects. Cook Mountain Formation top and bottom depth maps (Figures 7.7.3-3 and 7.7.3-4) were prepared using elevation GIS rasters subtracted from the study area digital elevation model (refer to Appendix, Section 13.6 raster interpolation documentation).

The Cook Mountain Formation thickness was prepared by subtracting the bottom elevation GIS raster from the top elevation GIS raster. The Cook Mountain Formation thickness is 0 at the updip outcrop edge and over 590 feet in southwestern Karnes County (Figure 7.7.3-5).

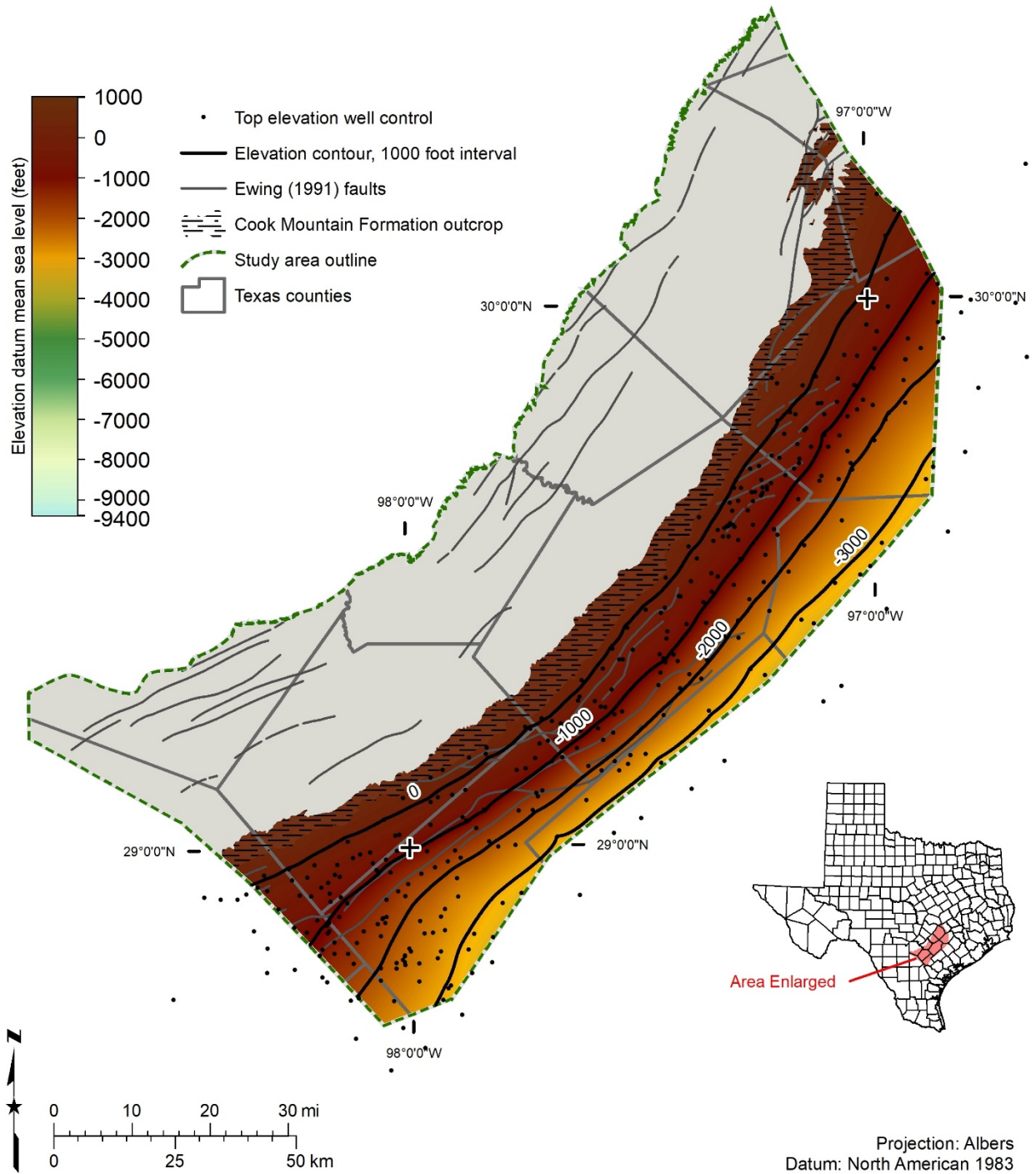


Figure 7.7.3-1. Cook Mountain Formation top elevation (feet above mean sea level), which was prepared using 410 wells for stratigraphic control (black dots).

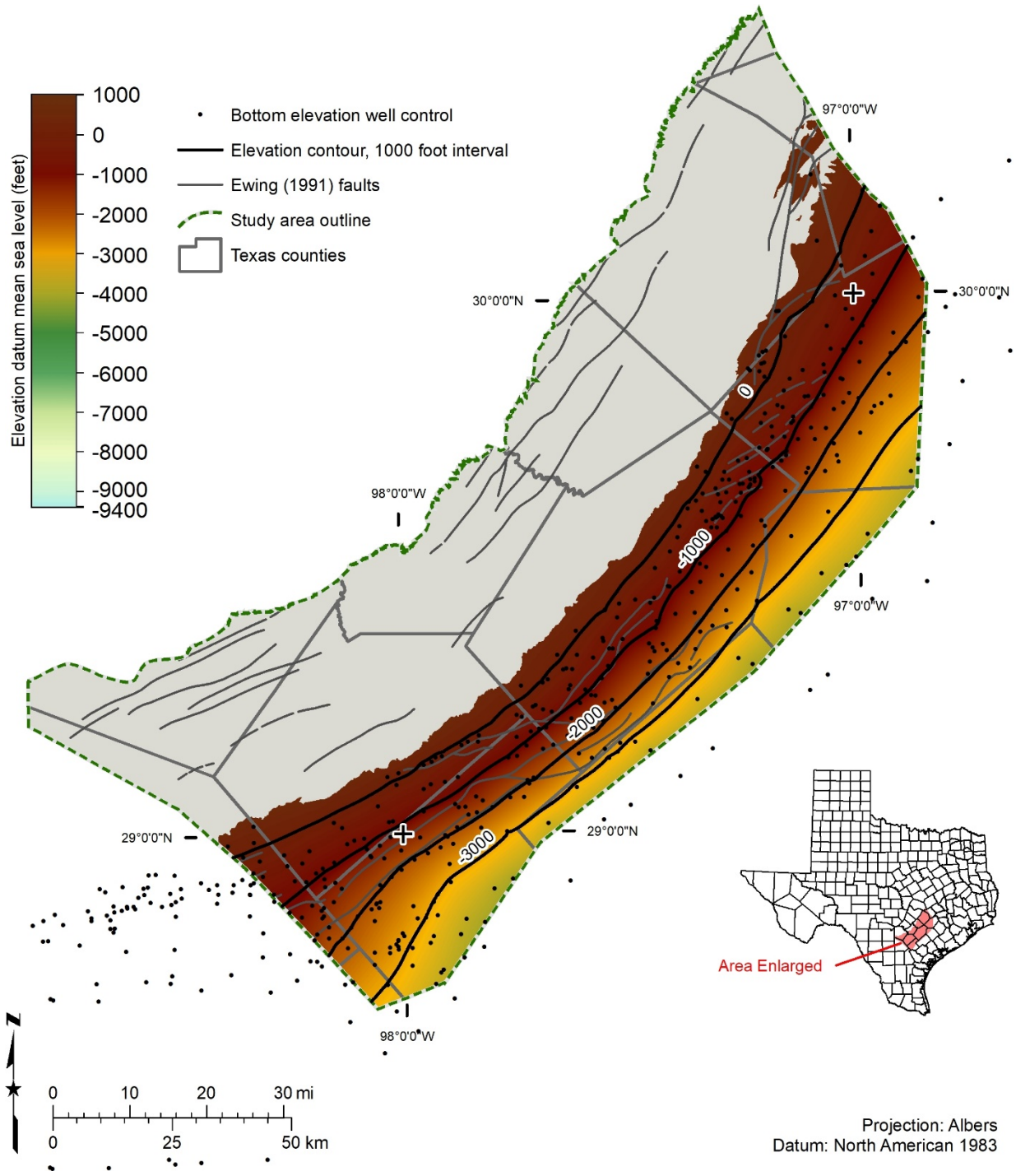


Figure 7.7.3-2. Cook Mountain Formation bottom elevation (feet above mean sea level), which was prepared using 382 wells for stratigraphic control (black dots).

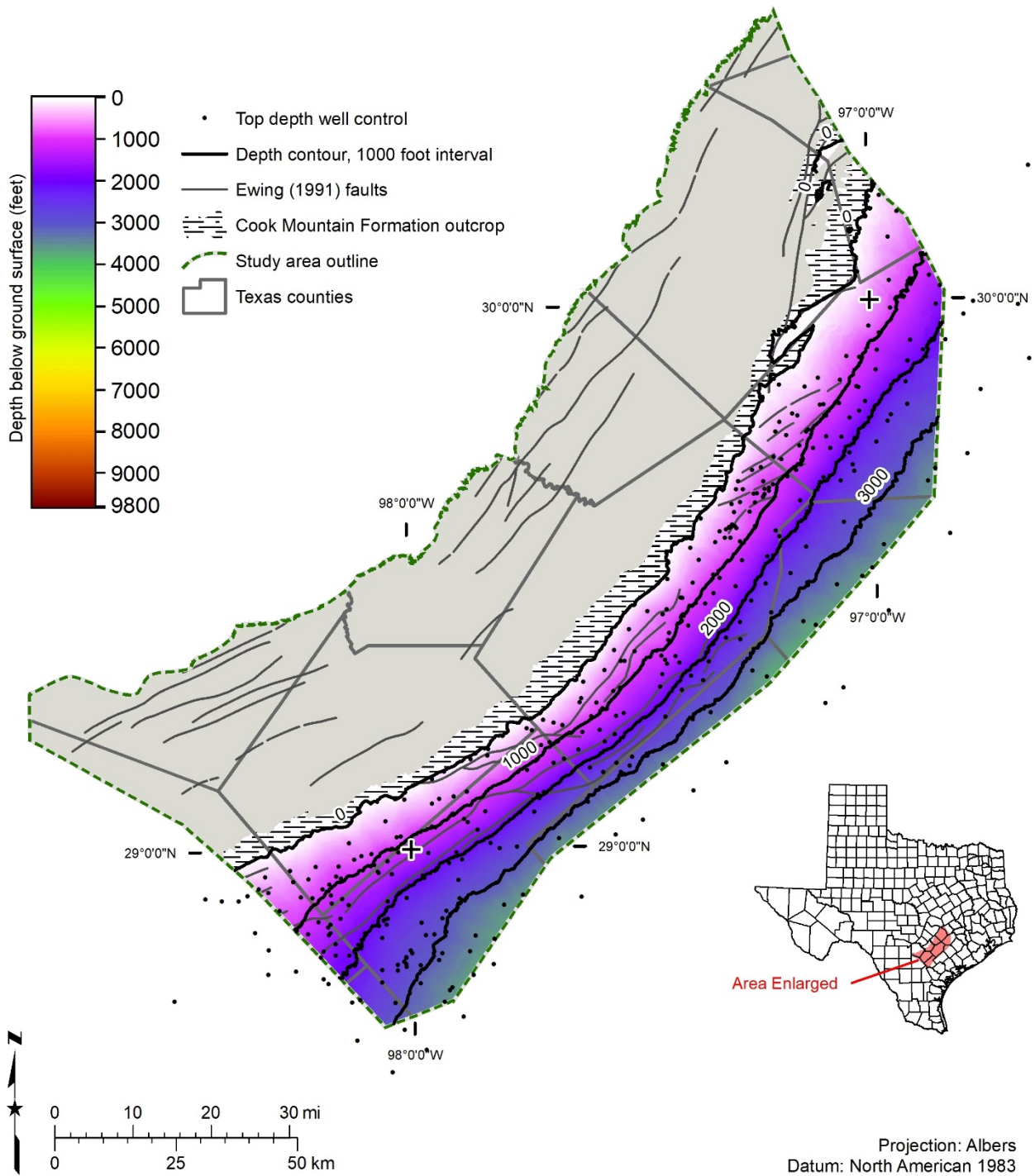


Figure 7.7.3-3. Cook Mountain Formation top depth (feet below ground surface), which was prepared using 410 wells for stratigraphic control (black dots).

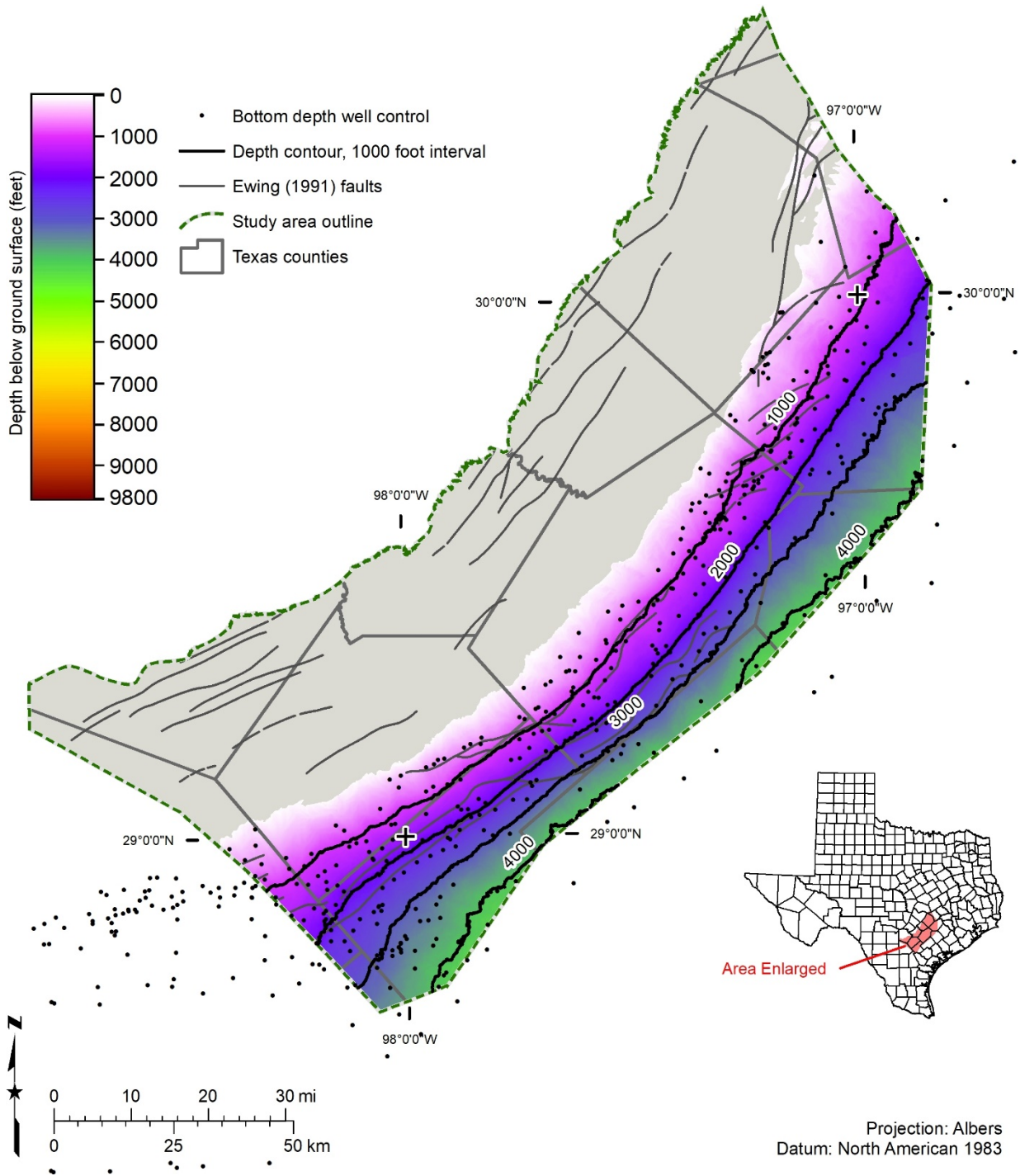


Figure 7.7.3-4. Cook Mountain Formation bottom depth (feet below ground surface), which was prepared using 382 wells for stratigraphic control (black dots).

7.7.4 Net sand

Due to the limited production potential of the Cook Mountain Formation, we did not conduct a thorough analysis of the net sands in the formation. Draft Cook Mountain Formation net sands were performed and recorded in the BRACS Database. Maps were not prepared for this geological formation.

7.7.5 Salinity classes

Sands containing groundwater are limited and isolated in the Cook Mountain Formation. As such, salinity classes were not calculated using geophysical well logs or mapped.

7.7.6 Volume of brackish groundwater

Brackish groundwater volume was not calculated for the Cook Mountain Formation since this formation is considered an aquitard and not a major or minor aquifer in Texas.

7.8 Yegua Formation

The Yegua Formation of the Claiborne Group unconformably underlies the Jackson Group and conformably overlies the Cook Mountain Formation. Lower Jackson Group strata consist of a regional transgressive shale known as the Caddell shale (Moody's Branch Formation). Yegua Formation strata represent the largest volume of sediment deposited in the Gulf of Mexico since the Wilcox Group and Carrizo Sand (Ewing, 2016).

The Yegua-Jackson Aquifer, wholly comprised of the Yegua Formation and Jackson Group, is a TWDB designated minor aquifer in Texas (George and others, 2011) that produces minor amounts of water over large geographic areas or large amounts of water over small geographic areas.

7.8.1 Well control

More than 400 wells were used in defining aspects of the Yegua Formation stratigraphy, lithology, and water quality (Table 7.8.1-1). We only used wells for water quality and aquifer hydraulic properties based on the aquifer determination analysis. Undoubtedly there are many other wells completed in the Yegua Formation, but without detailed well screen information it is not possible to accurately assign the Yegua Formation as the source of water produced from the wells.

Table 7.8.1-1. Yegua Formation well control data points.

Well control with this information:	Number of data points
Lithology	436
Top surface stratigraphic picks used for raster surface	302
Bottom surface stratigraphic picks used for raster surface	318
Top surface stratigraphic picks (database total*)	369
Bottom surface stratigraphic picks (database total*)	382
Net sand interpreted from wells	195
Aquifer hydraulic properties	146 wells with 148 measurements
Water quality: wells	63 wells with 79 measurements
TDS interpreted from geophysical well logs	282 wells with 638 depth intervals
Porosity	9

* Total number of stratigraphic picks in study counties

7.8.2 Stratigraphic analysis

Stratigraphic pick assignment of the upper contact of the Yegua Formation was selected at the top of the sand subjacent to the base of the first significant transgressive shale of the Jackson Group (Caddell shale). The bottom contact of the Yegua Formation is at the base of the lowest progradational (coarsening upwards sequence) signature above the upper shale of the Cook Mountain Formation. These contacts are based on lithostratigraphic correlations using geophysical log signatures without paleontology control for dating.

Geophysical well log signatures for the Yegua Formation top depth in Fayette County are displayed in Figure 7.8.2-1. The Yegua Formation top depth is 1,323 feet below ground surface (yellow line). The geophysical well log includes: the spontaneous potential recorded in the left track, depth below ground surface (feet) in the center track (each depth increment represents 10 feet), and induction (dotted line) and short guard resistivity (solid line) tools in the right. This log is from BRACS well id 39846 in southwestern Fayette County, Texas. The log was performed by Welex in 1979 with a kelly bushing height of 14 feet.

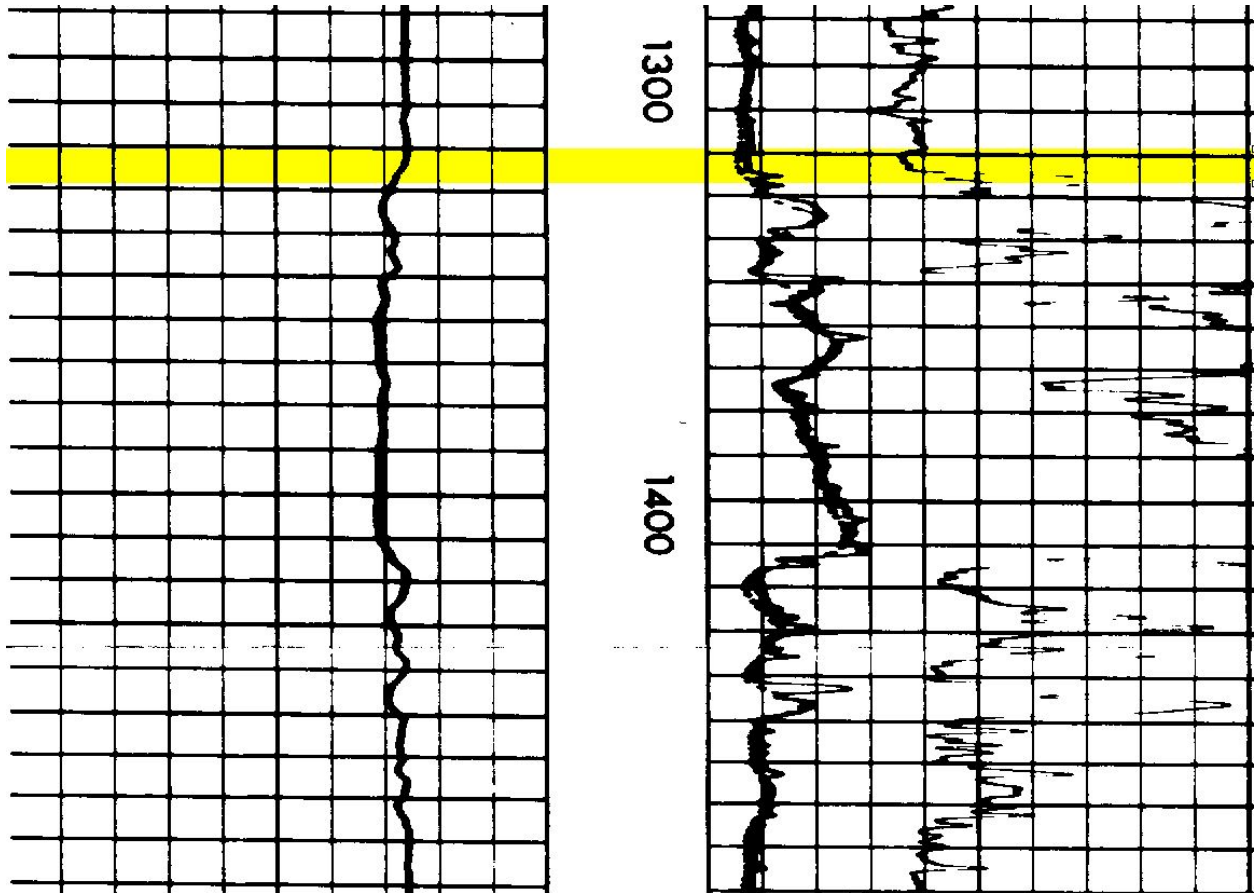


Figure 7.8.2-1. Yegua Formation top depth interpreted on a geophysical well log in Fayette County, Texas.

Geophysical well log signatures for the Yegua Formation bottom depth in Fayette County are displayed in Figure 7.8.2-2. The Yegua Formation bottom depth is 2,290 feet below ground surface (yellow line). The geophysical well log includes: the spontaneous potential recorded in the left track, depth below ground surface (feet) in the center track (each depth increment represents 10 feet), and induction (dotted line) and short guard resistivity (solid line) tools in the right. This log is from BRACS well id 39846 in southwestern Fayette County, Texas. The log was performed by Welex in 1979 with a kelly bushing height of 14 feet.

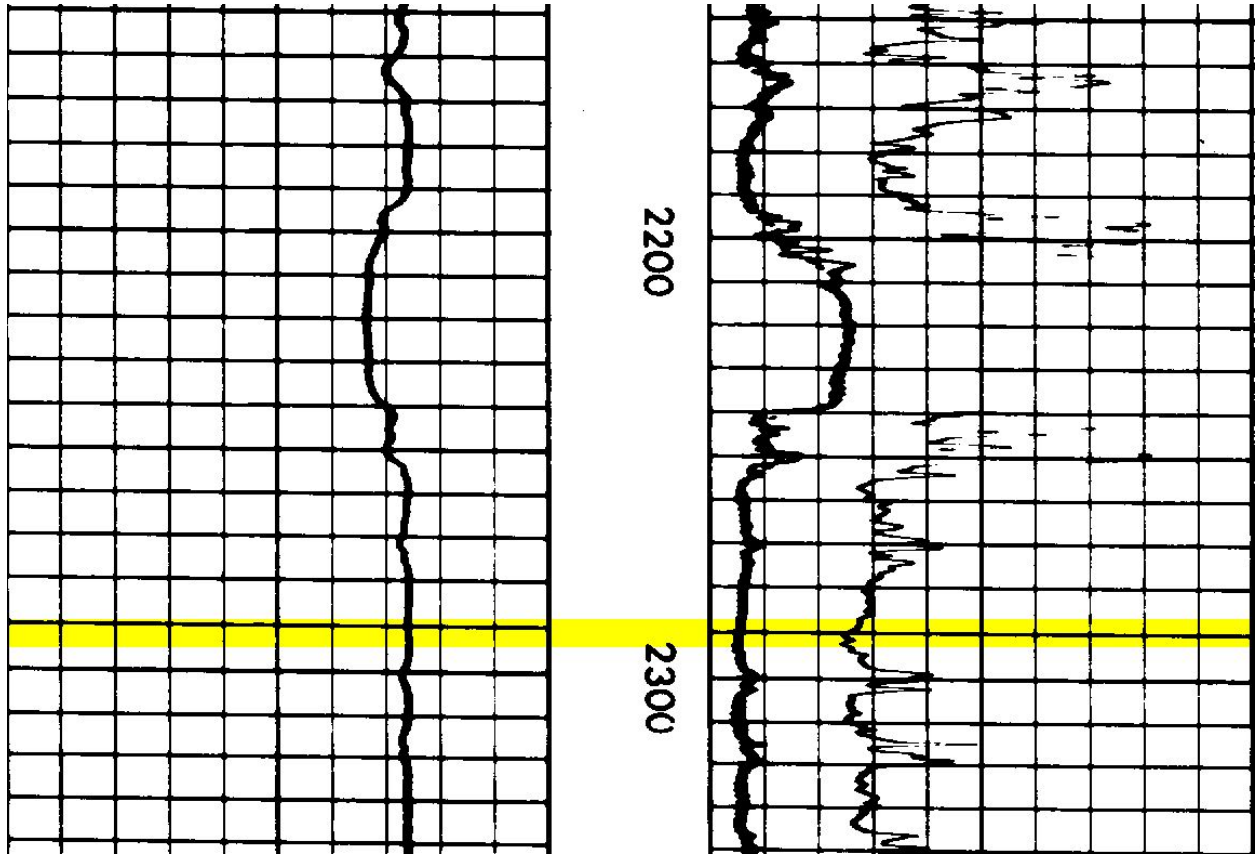


Figure 7.8.2-2. Yegua Formation bottom depth interpreted on a geophysical well log in Fayette County, Texas.

Geophysical well log signatures for the Yegua Formation top depth in Gonzales County are displayed in Figure 7.8.2-3. The Yegua Formation top depth is 1,562 feet below ground surface (yellow line). The geophysical well log includes: the spontaneous potential recorded in the left track, depth below ground surface (feet) in the center track (each depth increment represents 10 feet), and induction (dotted line) and short normal resistivity (solid line) tools in the right. This log is from BRACS well id 15335 in southwestern Gonzales County, Texas. The log was performed by Schlumberger in 1960 with a kelly bushing height of 17 feet.

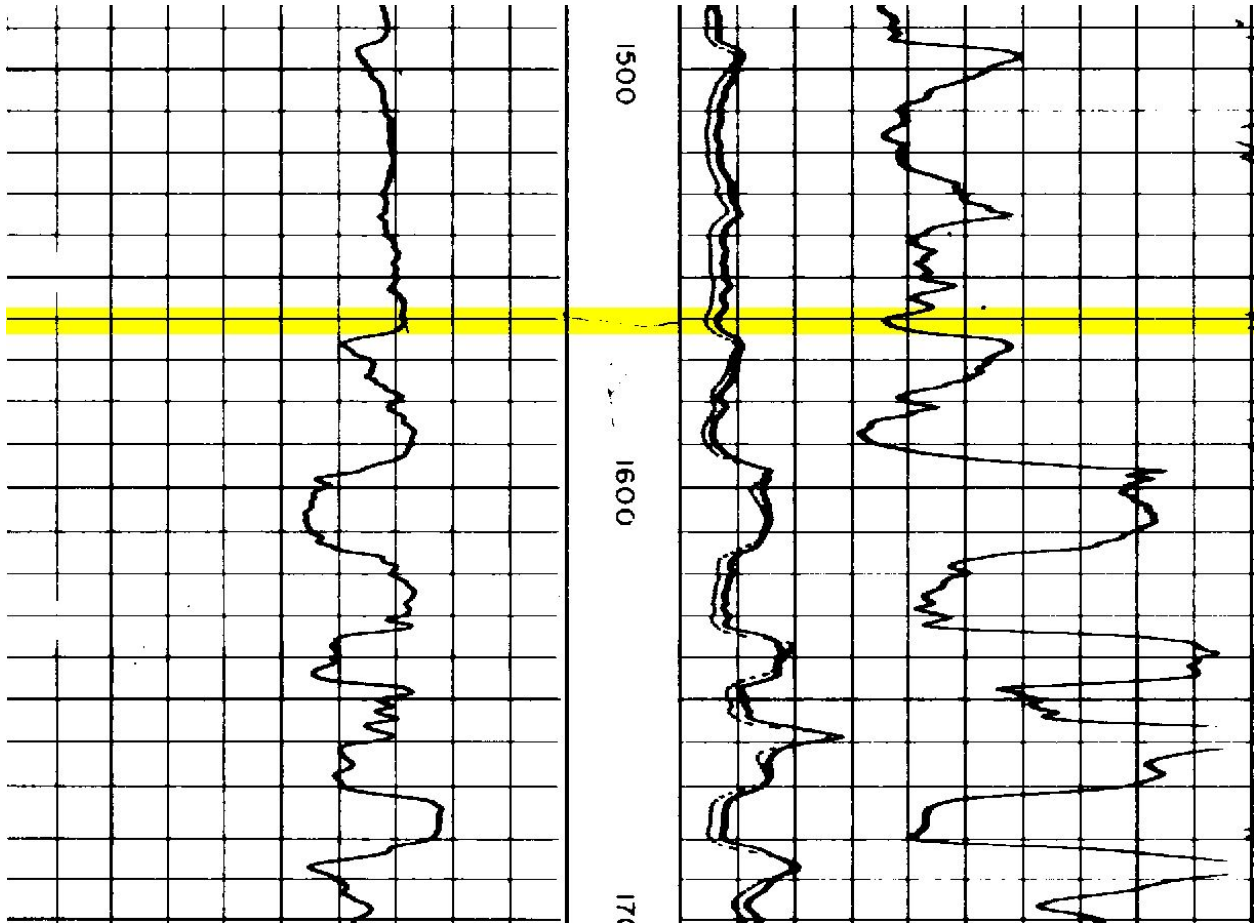


Figure 7.8.2-3. Yegua Formation top depth interpreted on a geophysical well log in Gonzales County, Texas.

Geophysical well log signatures for the Yegua Formation bottom depth in Gonzales County are displayed in Figure 7.8.2-4. The Yegua Formation bottom depth is 2,628 feet below ground surface (yellow line). The geophysical well log includes: the spontaneous potential recorded in the left track, depth below ground surface (feet) in the center track (each depth increment represents 10 feet), and induction (dotted line) and short normal resistivity (solid line) tools in the right track (these two curves are superimposed within the lower Yegua). This log is from BRACS well id 15335 in southwestern Gonzales County, Texas. The log was performed by Schlumberger in 1960 with a kelly bushing height of 17 feet.

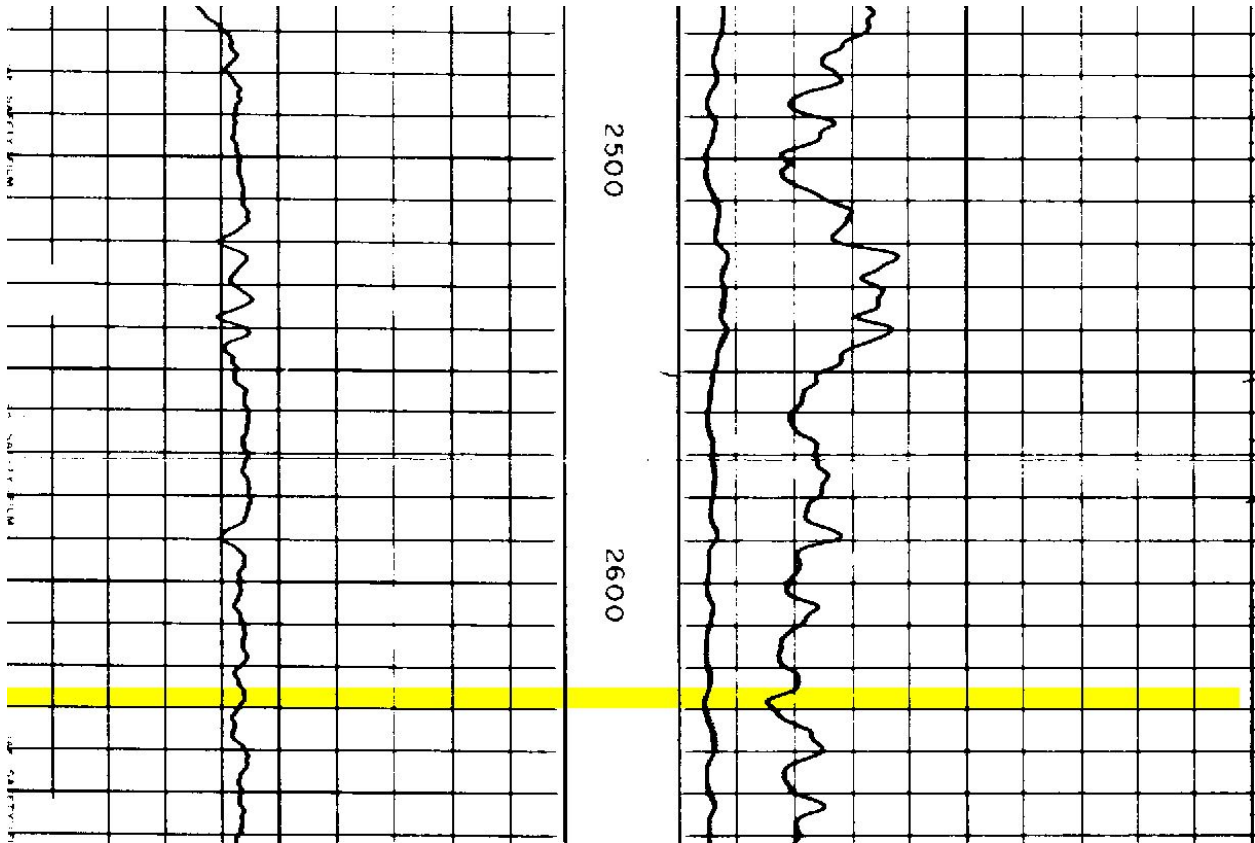


Figure 7.8.2-4. Yegua Formation bottom depth interpreted on a geophysical well log in Gonzales County, Texas.

7.8.3 Formation top, bottom, thickness

Yegua Formation top and bottom elevation maps (Figures 7.8.3-1 and 7.8.3-2) were prepared using 302 and 318 stratigraphic picks, respectively, from wells within the study area in addition to some wells immediately outside of the study area to control GIS raster edge effects. Yegua Formation top and bottom depth maps (Figures 7.8.3-3 and 7.8.3-4) were prepared using elevation GIS rasters subtracted from the study area digital elevation model (refer to Appendix, Section 13.6 raster interpolation documentation).

The Yegua Formation thickness was prepared by subtracting the bottom elevation GIS raster from the top elevation GIS raster. The Yegua Formation thickness is 0 at the updip outcrop edge and over 1,100 feet in northeastern Live Oak County (Figure 7.8.3-5).

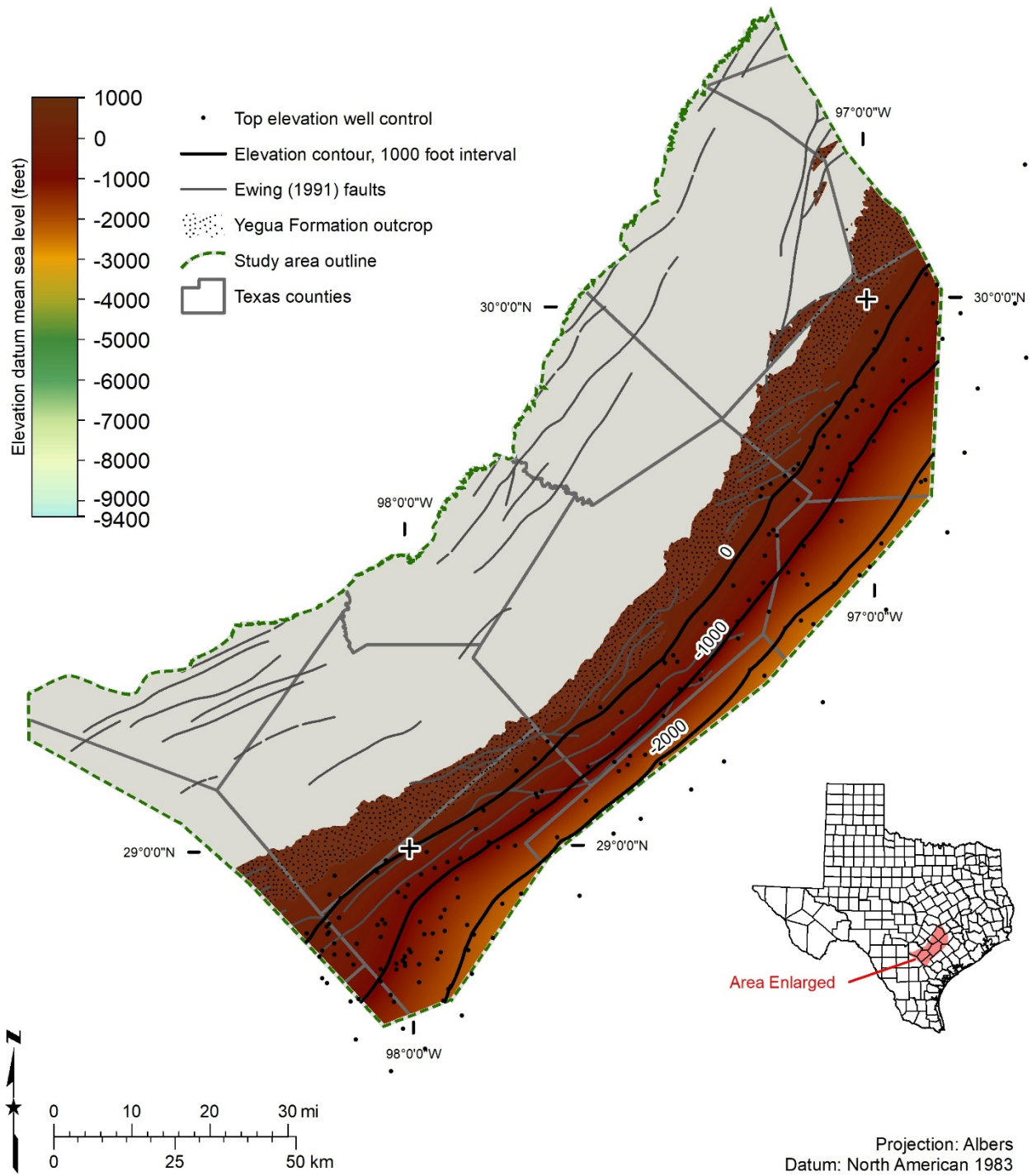


Figure 7.8.3-1. Yegua Formation top elevation (feet above mean sea level), which was prepared using 302 wells were stratigraphic control (black dots).

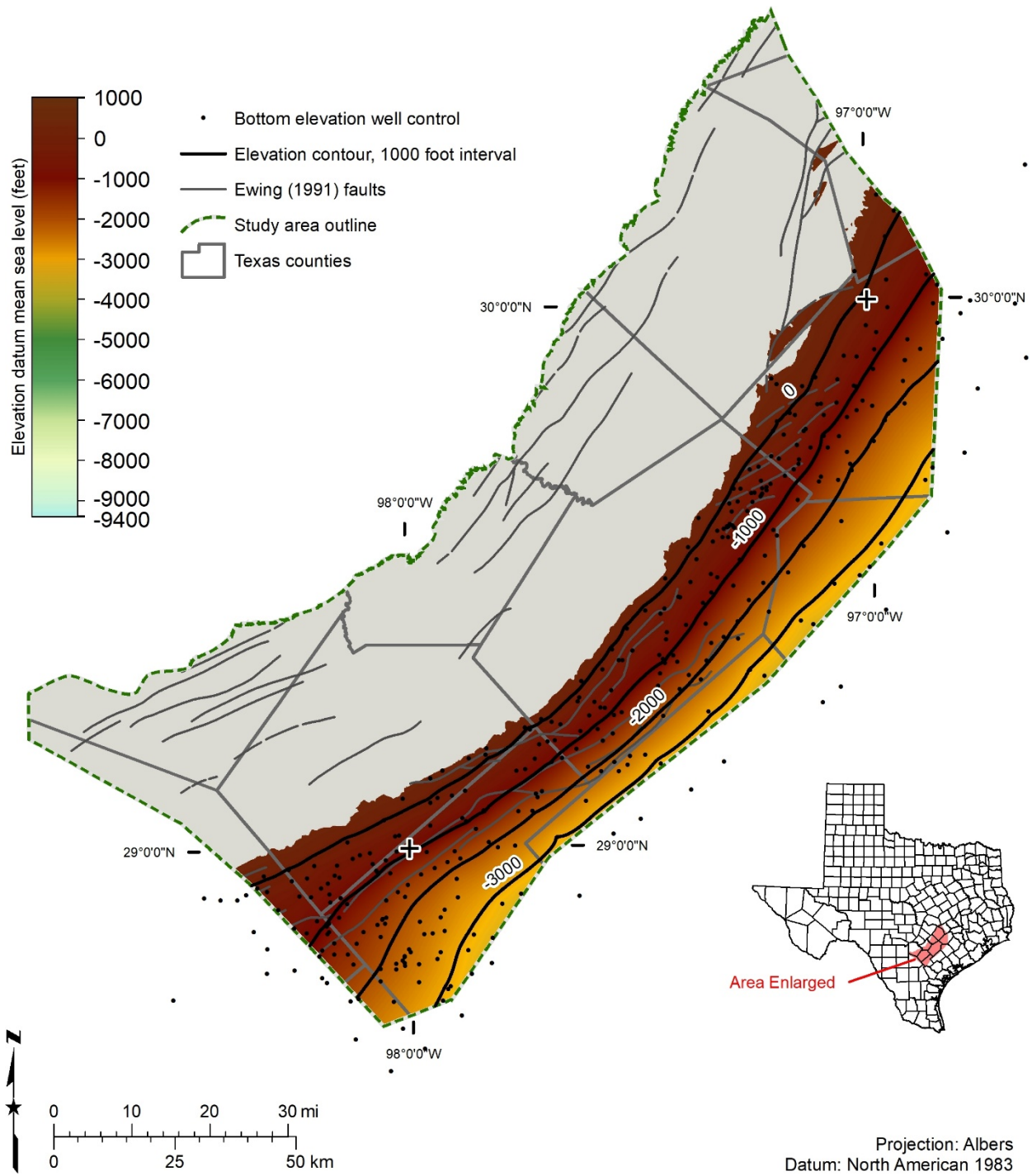


Figure 7.8.3-2. Yegua Formation bottom elevation (feet above mean sea level), which was prepared using 318 wells for stratigraphic control (black dots).

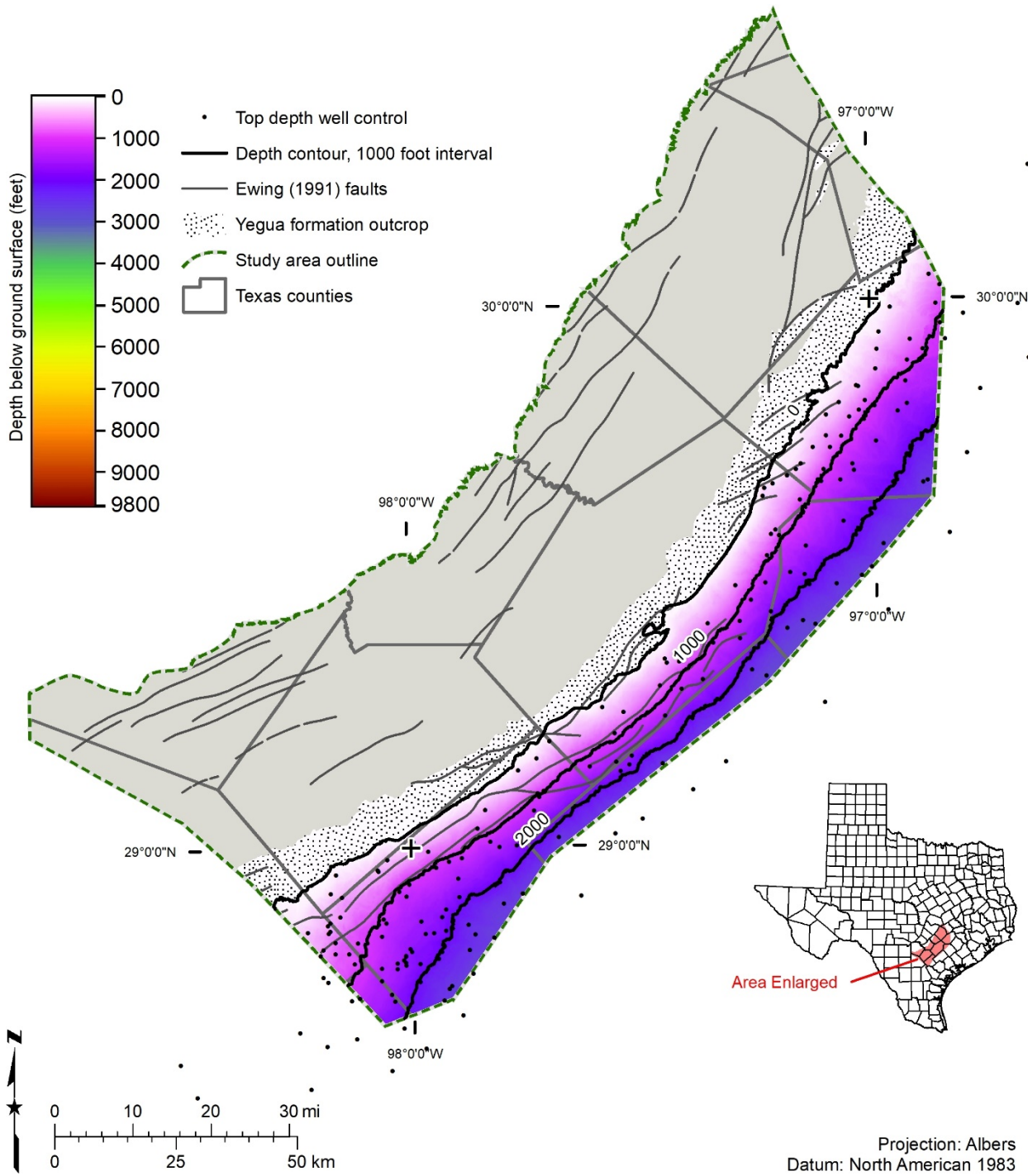


Figure 7.8.3-3. Yegua Formation top depth (feet below ground surface), which was prepared using 302 wells for stratigraphic control (black dots).

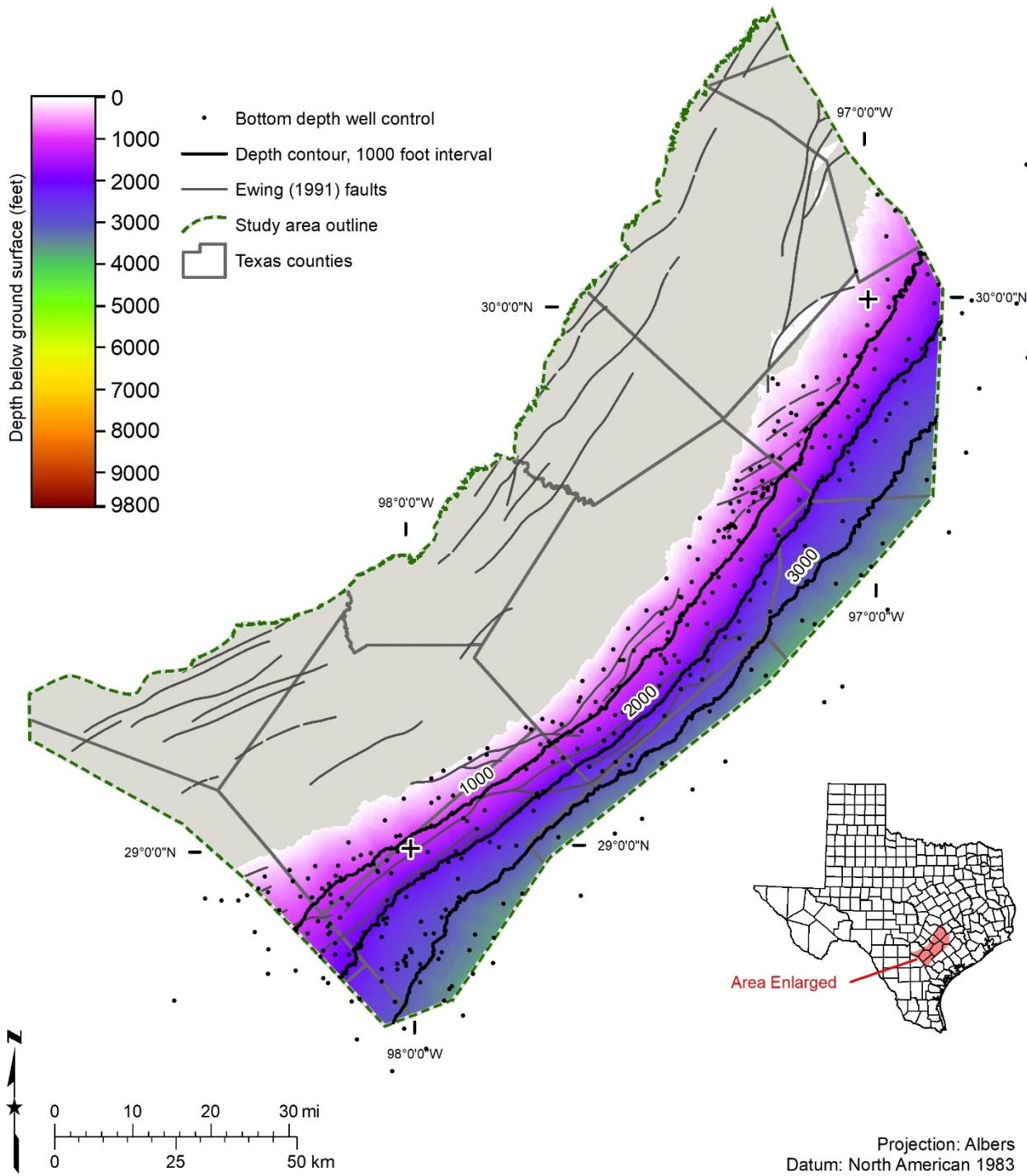


Figure 7.8.3-4. Yegua Formation bottom depth (feet below ground surface), which was prepared using 318 wells for stratigraphic control (black dots).

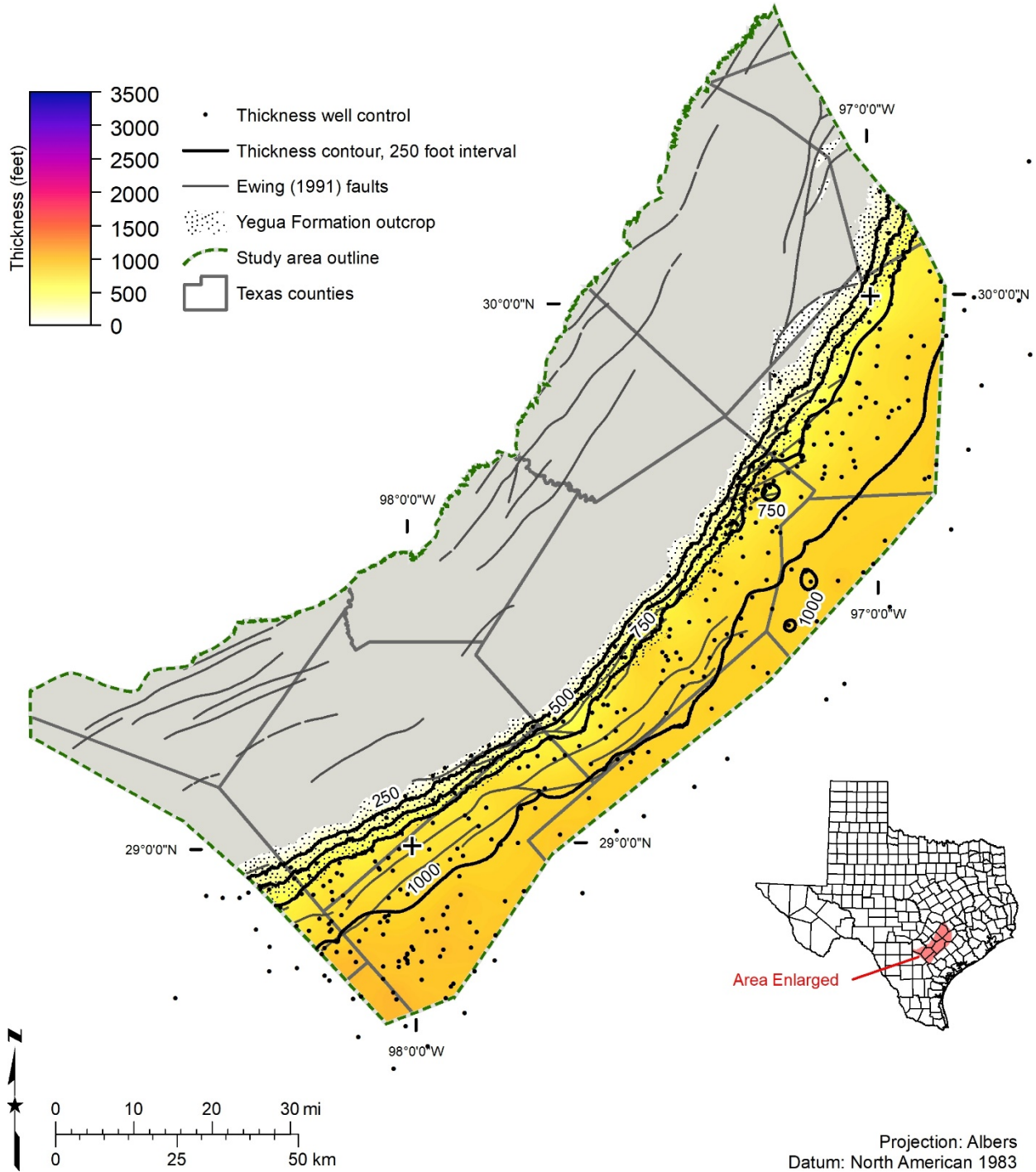


Figure 7.8.3-5. Yegua Formation thickness in units of feet, which was prepared using 302 wells for stratigraphic control (black dots).

7.8.4 Net sand

We evaluated 195 wells (Figure 7.8.4-1), of which 82 are water wells, 112 are oil and gas wells, and 1 well is classified as other (test hole). We used geophysical well logs for 121 wells and drillers' descriptions of lithology for the remaining 74 wells. Net sand values range from 0 at the

updip outcrop edge to over 500 feet in southwestern Karnes County. The individual depositional sequences (fluvial – deltaic) are masked by the net sand distribution of the entire formation. The study area does not extend to the delta margin facies on the shelf edge where the amount of sand decreases dramatically (Knox and others, 2007).

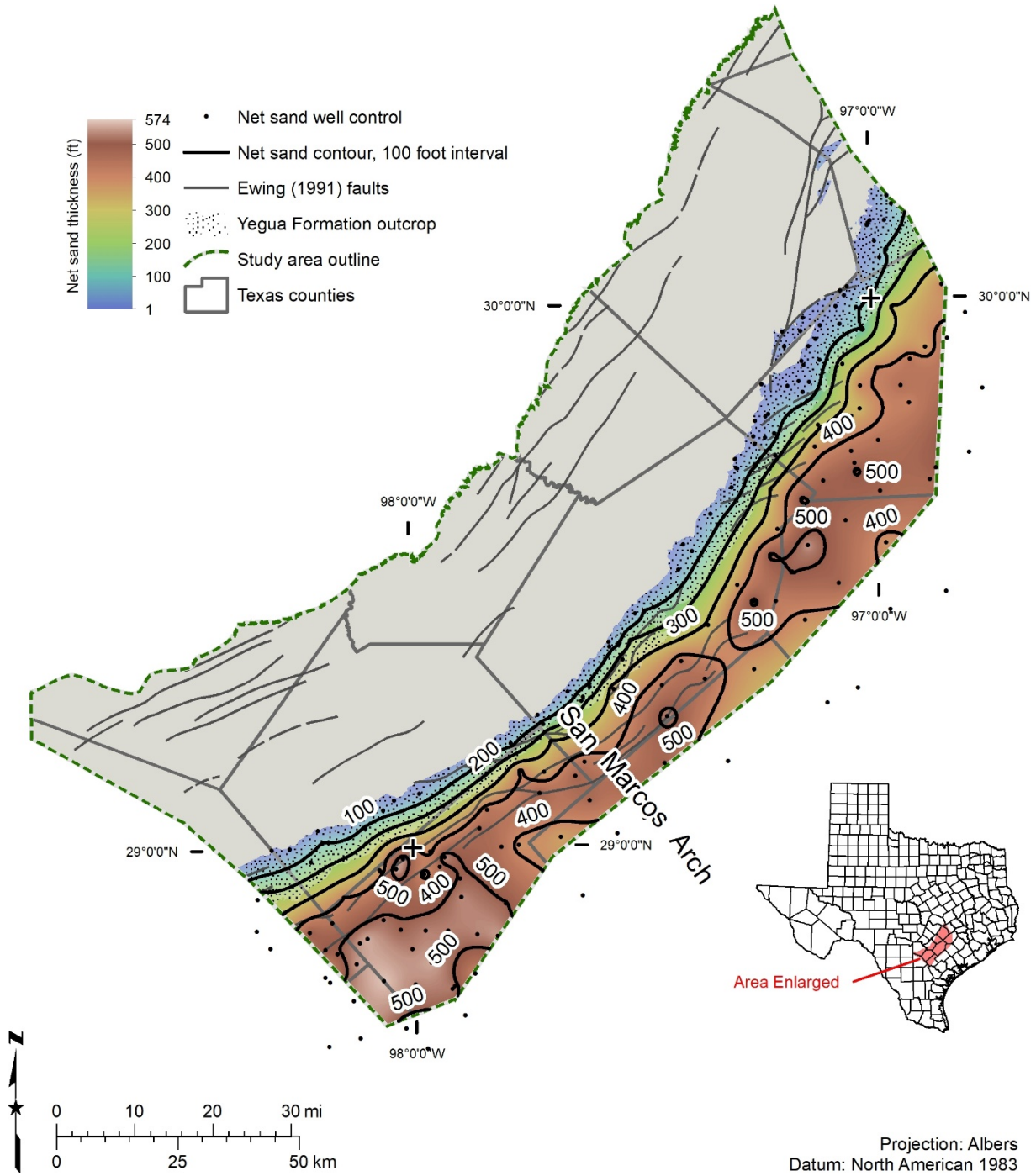


Figure 7.8.4-1. Yegua Formation net sand thickness in units of feet, which was prepared using 195 wells for net sand control (black dots).

7.8.5 Salinity classes

The Yegua Formation was mapped into defined salinity classes: (1) mixed fresh, slightly saline, and moderately saline, (2) moderately saline, (3) mixed moderately saline and very saline, and (4) very saline (Figures 7.8.5-1 and 7.8.5-2). Mapping was based on water quality samples (73 wells classified as: 36 fresh, 34 slightly saline, and 3 moderately saline) and estimated total dissolved solids calculations using geophysical well logs (287 wells with 643 depth intervals analyzed yielding 281 wells with 356 salinity class zones: 0 fresh, 38 slightly saline, 247 moderately saline, 71 very saline, and 0 brine). Fifty-five wells contain multiple salinity classes within the Yegua Formation ranging from two to seven vertical zones per well. The majority of the water well samples are in the eastern half of the study area.

Distribution of salinity within the Yegua Formation is quite complex with large areas mapped as mixed salinity classes, as these areas could not be subdivided into unmixed salinity classes. The largest mixed class includes the Yegua Formation outcrop and immediate downdip area represented by water wells containing fresh, slightly saline, and moderately saline groundwater and geophysical well logs interpreted as slightly saline to moderately saline (Plate 5). Some geophysical well logs show differences in salinity with depth, leading to two to seven vertical salinity classes per well. The outcrop area is particularly challenging since most water wells do not fully penetrate the aquifer. If a water well produces from multiple sands with different salinity classes, it is not apparent in the water quality sample that it represents a mixture. In addition, many geophysical well logs do not record strata within the cased portion of the well. Mapping mixed salinity classes was not a surprise since mixed water quality from fresh to poor quality was documented in Anders (1957) for Wilson County.

The other two mixed classes are represented by geophysical well logs showing moderately saline above very saline groundwater. The transition from moderately saline to very saline groundwater occurs in a wide zone, up to 15 miles wide, in the northeastern and southwestern parts of the study area. In contrast, the transition to very saline groundwater in southeast Gonzales County is immediately downdip of the outcrop, less than 1 mile wide. This is in the area of the San Marcos Arch.

We did not see evidence of brine (greater than 35,000 milligrams per liter total dissolved solids) in any of the geophysical well logs analyzed. This transition from very saline to brine occurs southeast of the study area. This transition will be documented in a future BRACS study addressing the Jackson and Yegua aquifers.

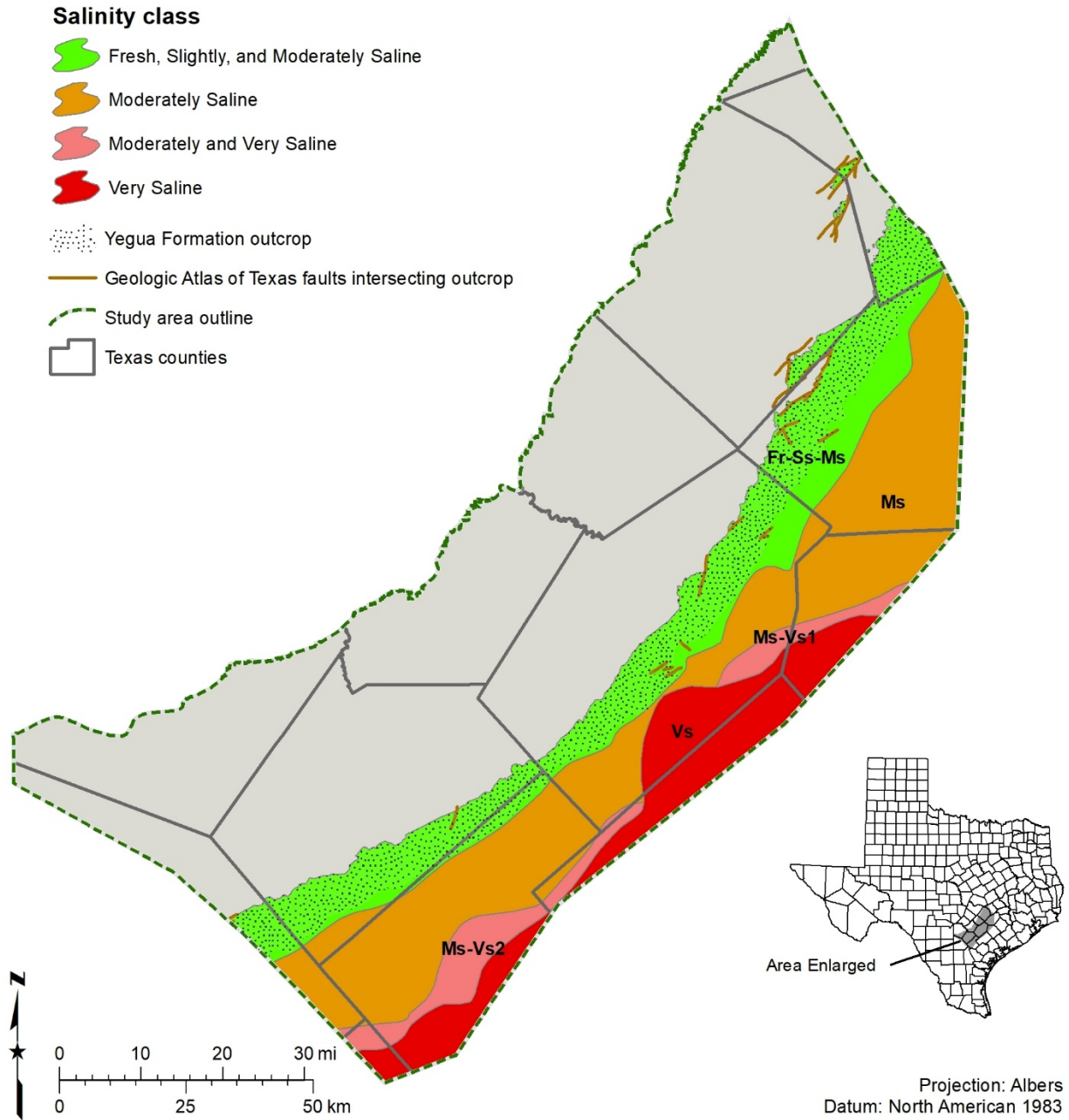


Figure 7.8.5-1. Yegua Formation salinity classes and identification names. Refer to Table 2-1 for salinity class definition.

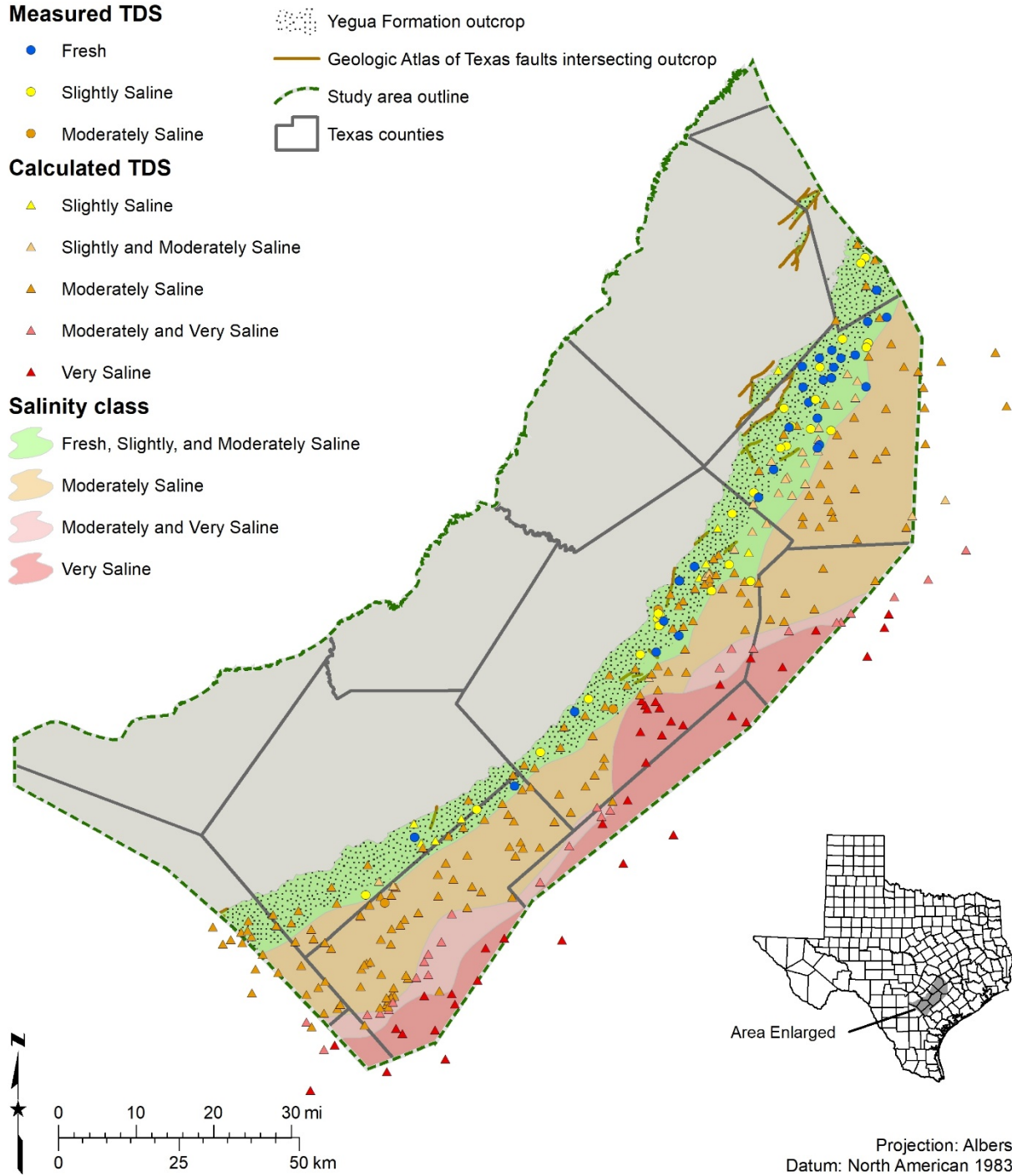


Figure 7.8.5-2. Yegua Formation salinity classes and well control consisting of water well quality data (circles) and interpreted geophysical well logs (triangles). Refer to Table 2-1 for salinity class definition. TDS = total dissolved solids.

7.8.6 Volume of brackish groundwater

We calculated the volume of in-place groundwater for the Yegua Formation based on salinity classes (Table 7.8.6-1). The Yegua Formation contains more than 42 million acre-feet of in-place brackish groundwater and additional significant brackish groundwater in mixed classes within the study area. The Yegua Formation contains a total of more than 78 million acre-feet of in-place groundwater of all salinity ranges within the study area.

Table 7.8.6-1. Total volume (acre-feet) of in-place groundwater in the Yegua Formation based on salinity class. Values summarized from Table 13.1.5-1. Volume values rounded to the nearest 10,000 acre-feet. Refer to Figure 7.8.5-1 for location of each salinity subclass.

Salinity class	Identification name	Volume groundwater (per salinity subclass) (acre-feet)	Volume groundwater (per salinity class) (acre-feet)
Fr - Ss - Ms	Fr-Ss-Ms1	10,160,000	10,160,000
Moderately saline	Ms	42,960,000	42,960,000
Ms - Vs	Ms-Vs1	2,140,000	8,110,000
	Ms-Vs2	5,970,000	
Very saline	Vs	16,900,000	16,900,000

Notes:

Fr - Ss - Ms is a mixed class of fresh, slightly, and moderately saline.

Ms - Vs is a mixed class of moderately and very saline.

Additionally, we subdivided the volumes based on administrative boundaries (Appendix 13, Tables 13.1.5-1, 13.1.5-2, 13.1.5-3, and 13.1.5-4). Appendix 13, Section 13.2 contains a complete discussion of volume methodology. Once salinity class mapping for the Yegua Formation was completed, we noticed that the study area did not include the entire available resource affecting some groundwater volume calculations. Specifically, the study area does not include the entire extent of Yegua Formation moderately saline water in the eastern part of the study area. Calculation of groundwater volumes used aquifer-based study area boundaries and some administrative boundaries are not coincident with the study area boundary. This resulted in partial volumes for some counties, groundwater conservation districts, and regional water planning areas. Future evaluation of the Yegua Formation to the northeast and southwest of this study area will address these issues.

7.8.7 Aquifer hydraulic properties

We compiled 148 sets of aquifer hydraulic property data from 146 wells completed in the Yegua Formation. The data is organized by hydraulic property (Table 7.8.7-1) and recorded in the BRACS Database table (tblUCPC_AquiferTestInformation). Yegua Formation records are recorded with the field aquifer_new = Y. A full discussion of this dataset is provided in Section 6.7. We prepared a map showing the spatial distribution of wells with well yield, specific capacity, transmissivity, and hydraulic conductivity (Figure 7.8.7-1).

Table 7.8.7-1. Hydraulic properties of the Yegua Formation within the study area. Refer to the BRACS Database table (tblUCPC_AquiferTestInformation) for detailed information about each well and data. Refer to Figure 7.8.7-1 for a map of these parameters.

	Transmissivity (gallons per day per foot)	Hydraulic conductivity (feet per day)	Storage coefficient (dimensionless)	Specific capacity (gallons per minute per foot)	Well yield (gallons per minute)
Number of values	1	0	0	87	146
Low	1,690	-	-	0.12	4
High	1,690	-	-	12.5	900
Average	1,690	-	-	4	105

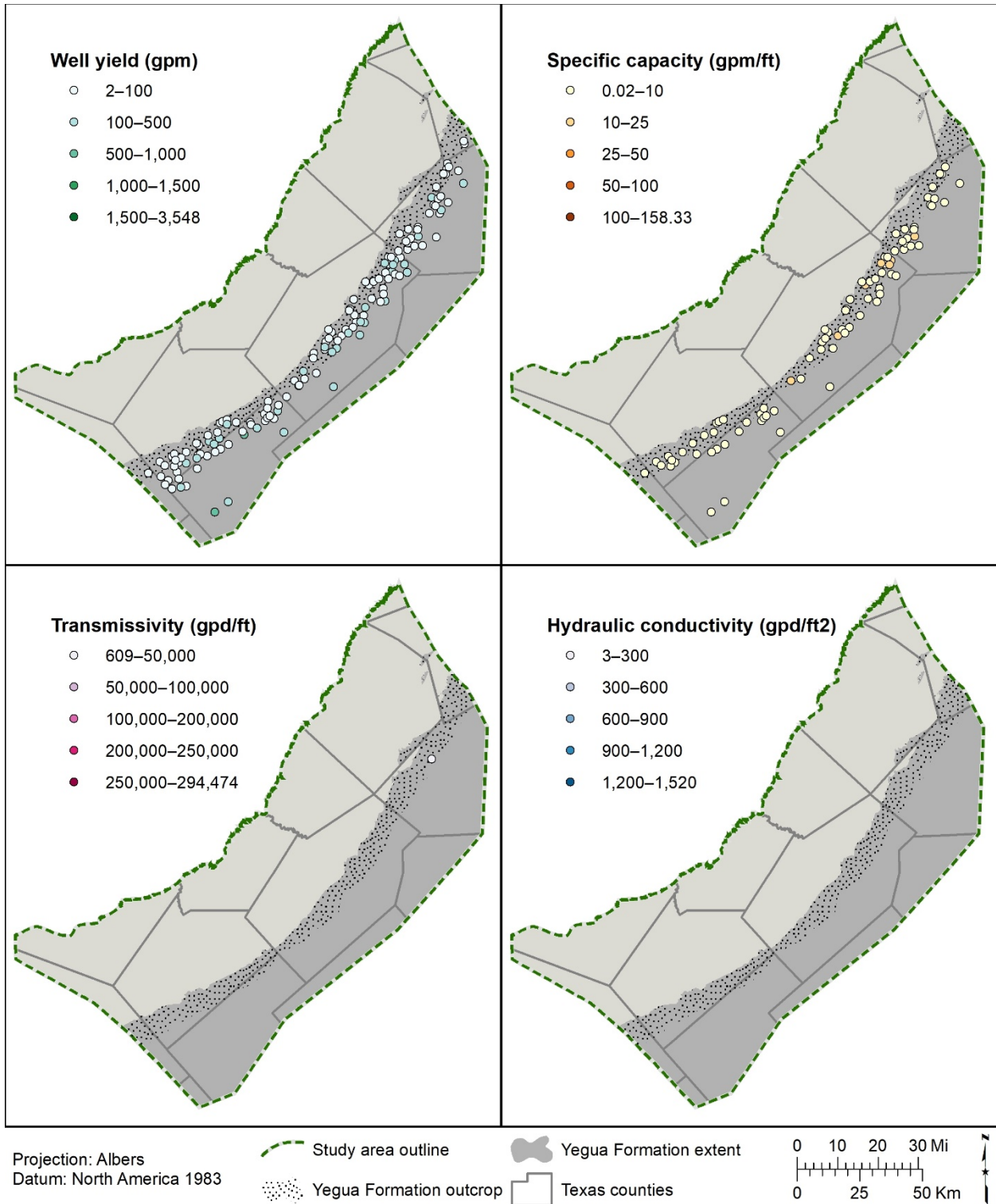


Figure 7.8.7-1. Yegua Formation hydraulic properties showing well yield (gallons per minute), specific capacity (gallons per minute per foot of drawdown), transmissivity (gallons per day per foot), and hydraulic conductivity (gallons per day per foot squared). Refer to Table 7.8.7-1 for a summary of these parameters.

8. Desalination concentrate disposal

Future development of brackish groundwater may require desalination depending on use. An important consideration of desalination is the disposal of concentrate as disposal can be costly and impede a project from moving forward. There is currently one existing brackish groundwater desalination plant in the study area (San Antonio Water System, H₂Oaks Center) that uses Class I injection wells to dispose the concentrate from the reverse osmosis process. San Antonio Water System is the first municipal water utility to permit a Class I injection well under the Texas Commission on Environmental Quality's Class I General Permit. The General Permit only applies to wells disposing of nonhazardous desalination concentrate or nonhazardous drinking water treatment residuals. The injection zone is within the Edwards Aquifer with native groundwater quality greater than 90,000 milligrams per liter total dissolved solids concentration.

Class II injection wells inject produced water, obtained from oil and gas wells, into subsurface zones where groundwater is greater than 10,000 milligrams per liter total dissolved solids (except in very specific circumstances). Class II injection wells can be used for disposal of nonhazardous desalination concentrate or nonhazardous drinking water treatment residuals if the following well types and conditions apply (CDM Smith, 2014):

Class II Type 1: Disposal injection well into a nonproductive oil and gas zone or interval. The well can be dually permitted as a Class I injection well under the Texas Commission of Environmental Quality General Permit. The well must meet all applicable construction standards of a Class I well, 30 Texas Administrative Code Section 331.62.

The Railroad Commission of Texas also refers to this as a (Railroad Commission of Texas Form) W-14 well. These wells are permitted under the Railroad Commission of Texas Statewide Rule 9.

Class II Type 2: Disposal injection well into a productive oil and gas zone or interval. The well can be dually permitted as a Class I injection well under the Texas Commission of Environmental Quality General Permit. The well must meet all applicable construction standards of a Class I well, 30 Texas Administrative Code Section 331.62.

The Railroad Commission of Texas also refers to this as an (Railroad Commission of Texas Form) H-1 well. These wells are permitted under the Railroad Commission of Texas Statewide Rule 46.

Class II Type 3: Enhanced recovery injection well into a productive oil and gas zone or interval. This type of well can receive a permit amendment from the Railroad Commission of Texas.

The Railroad Commission of Texas also refers to this as an (Railroad Commission of Texas Form) H-1 well. These wells are permitted under the Railroad Commission of Texas Statewide Rule 46.

If a Class II injection well is considered as a potential option for concentrate disposal, a considerable amount of research must be undertaken to ensure that the well meets construction requirements, appropriate permits are obtained, and a contract with the owner of the injection well can be obtained for the lifetime of the project (Mace and others, 2006; CDM Smith, 2014).

There are other concentrate disposal options that are currently being used by desalination plants in Texas: (1) disposal to surface water bodies, (2) disposal to wastewater treatment plants, (3) evaporation ponds, and (4) zero liquid discharge (partial stream of concentrate being evaluated at the Kay Bailey Desalination Plant in El Paso). These methods are specific to a site and require permits from the Texas Commission on Environmental Quality.

9. Future improvements

An important mission of the TWDB is to collect and disseminate groundwater data across the state. For this reason, we continue to be interested in obtaining additional study area data and information for inclusion into the BRACS Database. The BRACS Database is a living repository of data useful for mapping brackish groundwater, and it is a core purpose of the program to continue to gather data, even in areas where we have completed an aquifer study. Additional data that can be collected include water quality samples, aquifer tests, and geophysical well logs with complete headers and deep resistivity curves with readings in the formations of interest.

Collection of pumping tests in brackish portions of the study area aquifers is also very important because we presently have very few such tests and the tests will provide valuable information regarding the productivity and sustainability of these deeper and saltier portions of the aquifers.

The BRACS program continues to use geophysical well logs to interrupt the distribution of salinity classes in deeper portions of aquifers where water quality samples do not exist. However, there are significant challenges with these calculations, and additional investigations into some of the parameters used in log analysis would help improve the reliability of the results. These additional investigations include: (1) obtaining higher salinity water quality samples to support calibrating log analysis, (2) evaluating correction factors for mixed ion groundwater, (3) determining proper cementation factors, (4) mapping water quality data per geochemical facies and then developing water quality correction factors, (5) evaluating the effect and presence of grain-coating (pore-filling) clay, and (6) determining techniques of carbonate rock analysis for other aquifers in Texas.

Monitoring the brackish aquifers and adjacent aquifers with new monitor wells will provide answers to a number of frequently posed questions: (1) how development of brackish groundwater will impact fresh water resources in terms of quality and quantity, (2) how development of slightly saline water may be impacted by more saline sources during long-term development, (3) what is the sustainability of the brackish resource, and (4) what is the potential for subsidence. In addition, groundwater modeling, perhaps using variable-density tools, at pre- and post-development (using well-field production data) can provide site-specific data used to predict long-term aquifer response.

10. Conclusions

We selected the Central Texas area as a brackish groundwater study area because of the anticipated need for additional water in the region. For the study, we compiled over 8,000 water well and geophysical well logs for geologic, water chemistry, water level, and aquifer test data from a wide variety of sources to characterize groundwater in the study area. From this information, we (1) mapped the stratigraphy and lithology of the eight geological formations and prepared GIS raster maps, (2) mapped the salinity classes within the five aquifers and prepared GIS maps, (3) estimated groundwater volumes for the five aquifers, and (4) compiled supporting information for the five aquifers including water quality and aquifer hydraulic properties.

We estimate that the Upper Coastal Plain aquifers contain a significant volume of brackish groundwater. The Wilcox Group contains 112 million acre-feet of in-place brackish groundwater with additional brackish groundwater in mixed salinity classes. The Carrizo Sand contains more than 57 million acre-feet of in-place brackish groundwater with additional brackish groundwater in mixed salinity classes. The Queen City Sand contains more than 20 million acre-feet of in-place brackish groundwater with additional brackish groundwater in mixed salinity classes. The Sparta Sand contains more than 6 million acre-feet of in-place brackish groundwater and no mapped mixed salinity classes. The Yegua Formation contains more than 42 million acre-feet of in-place brackish groundwater with additional brackish groundwater in mixed salinity classes. We realize that not all brackish groundwater can be produced or economically developed; however, these estimates and detailed mapping provide users a beneficial tool to evaluate potential sites for brackish groundwater well fields. These volumes do not consider the effects of land surface subsidence, degradation of water quality, or any changes to surface water-groundwater interaction that may result from extracting groundwater from the aquifer. These volumes should not be used for joint groundwater planning or evaluation of achieving adopted desired future conditions because there is an established process in Texas Water Code §36.108.

One lower Wilcox Aquifer brackish groundwater production zone was designated in 2016 (TWDB, 2016) in parts of Atascosa, Frio, Dimmit, and Zavala counties. Recommendations for additional zones for the Carrizo-Wilcox, Queen City, and Sparta aquifers will be provided in a future report.

Finally, information contained in the report is not intended to serve as a substitute for site-specific studies that are required to evaluate local aquifer characteristics and groundwater conditions for a desalination plant. Well-field scale data collection using test and monitor wells is strongly recommended to evaluate the brackish groundwater resource. Collection and evaluation of additional well control in a prospective site area is essential in understanding potential target zones for groundwater development.

11. Acknowledgments

We would like to thank Greg Sengelmann, Manager of Gonzales County Underground Water Conservation District, for geophysical well logs and datasets in Gonzales County. We would like to thank Richard Donat, Kevin Morrison, and Saqib Shirazi of the San Antonio Water System for desalination plant data, water well data, and geophysical well logs from their aquifer storage and recovery (ASR) system and their Wilcox brackish groundwater well field. We would like to thank Jean Broce Perez (former BRACS team member) for net sand analysis. A special thank-you is extended to many staff members at the Railroad Commission of Texas for access to their Q-log collection of geophysical well logs, linen maps, log analysis methodology, and technical coordination meetings: Leslie Savage, James Harcourt, Sean Avitt, and last but not least John Estep (retired). We would like to thank Lauren Munguia, TWDB Communications, for editing and JoAnn Estrada, TWDB Communications, for cover graphic design and publication support. Finally, this work could not have been undertaken or completed without the support and encouragement of Texas Water Development Board management including Erika Mancha (Manager, Innovative Water Technologies), Kevin Kluge (Director, Conservation and Innovative Water Technologies), and John Dupnik (Deputy Executive Administrator, Office of Water Science and Conservation) and retired TWDB managers: Dr. Sanjeev Kalaswad (Director of Conservation and Innovative Water Technologies), Jorge Arroyo (Director of the Innovative Water Technologies Team), and Dr. Robert E. Mace (Former Deputy Executive Administrator of the Office of Water Science and Conservation).

12. References

- Alexander, W.H., and White, D.E., 1966, Ground-water resources of Atascosa and Frio counties, Texas: Texas Water Development Board Report 32, 200 p.
- Alger, R.P., 1966, Interpretation of electric logs in fresh water wells in unconsolidated sediments, *in* Society of Professional Well Log Analysts, Tulsa, Oklahoma, 7th Annual Logging Symposium Transaction, 25 p.
- Anders, R.B., 1957, Ground-water geology of Wilson County, Texas: Texas Board of Water Engineers Bulletin 5710, 62 p.
- Anders, R.B., 1960, Ground-water geology of Karnes County, Texas: Texas Board of Water Engineers Bulletin 6007, 107 p.
- Archie, G.E., 1942, The electrical resistivity log as an aid in determining some reservoir characteristics: *Petroleum Technology*, v. 5, p. 54-62.
- Arnow, T., 1959, Ground-water geology of Bexar County, Texas: Texas Board of Water Engineers Bulletin 5911, 52 p.
- Aronow, S., Brown, T.E., Brewton, J.L., Eargle, D.H., and Barnes, V.E., 1975 (revised 1987), Geologic Atlas of Texas Beeville—Bay City Sheet: The University of Texas at Austin, Bureau of Economic Geology, scale 1:250,000, 1 sheet.
- Asquith, G.B., 1982, Basic well log analysis for geologists: American Association of Petroleum Geologists Methods in Exploration Series, 216 p.
- Austin, G., 1954, Records of wells in Bastrop County, Texas: Texas Board of Water Engineers Bulletin 5413, 43 p. and one plate.
- Ayers, W.B., Jr., and Lewis, A.H., 1985, The Wilcox Group and Carrizo Sand (Paleogene) in east-central Texas: Depositional systems and deep-basin lignite: The University of Texas at Austin, Bureau of Economic Geology, 19 p. and 30 plates.
- Baker, E.T., Jr., 1979, Stratigraphic and hydrogeologic framework of part of the coastal plain of Texas: Texas Department of Water Resources Report 236, 43 p.
- Banerji, D.A., Hamlin, H.S., Scanlon, B.R., Reedy, R.C., Young, S.C., Jigmond, M., and Harding, J., 2019, Fresh, brackish, and saline groundwater resources in the Carrizo-Wilcox, Queen City, and Sparta aquifers in Groundwater Management Area 13—location, quantification, producibility, and impacts: The University of Texas at Austin, Bureau of Economic Geology, contract report to the Texas Water Development Board, 309 p. plus appendices.
- Bebout, D.G., Weise, B.R., Gregory, A.R., and Edwards, M.B., 1982, Wilcox sandstone reservoirs in the deep subsurface along the Texas Gulf Coast: The University of Texas at Austin, Bureau of Economic Geology Report of Investigations 117, 125 p.
- Blackwell, D., Richards, M., and Stepp, P., 2010, Texas geothermal assessment for the I 35 corridor east: Southern Methodist University, contract report to the Texas State Energy Conservation Office, variously paginated.

- Blondes, M.S., Gans, K.D., Rowan, E.L., Thordsen, J.J., Reidy, M.E., Engle, M.A., Kharaka, Y.K., and Thomas, B., 2016, U.S. Geological Survey national produced waters geochemical database v2.2 (Provisional): U.S. Geological Survey, 28 p. and database files.
- Breton, C., 2013, Digital GIS version of the tectonic map of Texas by Ewing (1991): The University of Texas at Austin, Bureau of Economic Geology, compact disk.
- Brown, L.F., Jr., and Loucks, R.G., 2009, Chronostratigraphy of Cenozoic depositional sequences and systems tracts: A Wheeler chart of the northwest margin of the Gulf of Mexico Basin: The University of Texas at Austin, Bureau of Economic Geology Report of Investigations 273, 28 p. and one plate.
- Brown, T.E., Waechter, N.B., Owens, F., Howeth, I., and Barnes, V.E., 1976, Geologic Atlas of Texas Crystal City—Eagle Pass Sheet: The University of Texas at Austin, Bureau of Economic Geology, scale 1:250,000, 1 sheet.
- Brown, T.E., Waechter, N.B., and Barnes, V.E., 1974 (revised 1983), Geologic Atlas of Texas San Antonio Sheet: The University of Texas at Austin, Bureau of Economic Geology, scale 1:250,000, 1 sheet.
- Bulling, T.P., and Breyer, J.A., 1989, Exploring for subtle traps with high-resolution paleogeographic maps: Reklaw 1 interval (Eocene), South Texas: American Association of Petroleum Geologists Bulletin, v. 73, p. 24-39.
- Carothers, J.E., 1968, A statistical study of the formation factor relation to porosity: The Log Analyst, v. 9, p. 38-52.
- Carothers, J.E., and Porter, C.R., 1970, Formation factor-porosity relation from well log data: Society Professional Well Log Analysts, 11th Annual Logging Symposium Transactions Paper D.
- Christian, B., and Wuerch, D., 2012, Compilation of results of aquifer tests in Texas: Texas Water Development Board Report 381, 106 p.
- Core Laboratories, 1972, A survey of the subsurface saline water of Texas: Texas Water Development Board Report 157, 8 volumes, variously paginated.
- CDM Smith, 2014, Guidance manual for permitting Class I and Class II wells for the injection and disposal of desalination concentrate: CDM Smith, contract report to the Texas Water Development Board, variously paginated.
- Davidson, S.C., Brown, B.J., and Mace, R.E., 2009, Aquifers of the Upper Coastal Plains, *in* Hutchison, W.R., Davidson, S.C., Brown, B.J., and Mace, R.E., editors, Aquifers of the Upper Coastal Plains of Texas: Texas Water Development Board Report 374, p. 1-16.
- Deeds, N.E., Kelley, V.A., Fryar, D., Jones, T.L., Whallon, A.J., and Dean, K.E., 2003, Groundwater availability model for the southern Carrizo-Wilcox Aquifer: INTERA, Inc., contract report to the Texas Water Development Board, variously paginated.
- Deeds, N.E., Yan, T., Singh, A., Jones, T.L., Kelley, V.A., Knox, P.R., Young, S.C., 2010, Groundwater availability model for the Yegua-Jackson Aquifer: INTERA, Inc., contract report to the Texas Water Development Board, 582 p.

- Dingus, W.F., and Galloway, W.E., 1990, Morphology, paleogeographic setting, and origin of the Middle Wilcox Yoakum Canyon, Texas coastal plain: *American Association of Petroleum Geologists Bulletin*, v. 74, p. 1055-1076.
- Dodge, M.M., and Posey, J.S., 1981, Structural cross sections, Tertiary formations, Texas Gulf Coast: The University of Texas at Austin, Bureau of Economic Geology, 6 p. and 26 plates.
- Doveton, J.H., 1999, Oil and gas log analysis: *Kansas Geological Survey*, 34 p.
- Duffin, G.L., 1974, Subsurface saline water resources in the San Antonio area, Texas: *Texas Water Development Board Open-file Report*, 39 p.
- Duffin, G.L., and Elder, G.R., 1979, Variations in specific yield in the outcrop of the Carrizo Sand in South Texas as estimated by seismic refraction: *Texas Department of Water Resources Report 229*, 56 p.
- Dutton, A.R., 1999, Groundwater availability in the Carrizo-Wilcox Aquifer in Central Texas—Numerical simulations of 2000 through 2050 withdrawal projections: *The University of Texas at Austin, Bureau of Economic Geology Report of Investigations 256*, 76 p.
- Dutton, A.R., 2016, Beyond the bad-water line: a model for the occurrence of brackish water in upper coastal plain aquifers in Texas: *South Texas Geological Society Bulletin*, p. 25-35.
- Dutton, A.R., Harden, B., Nicot, J.P., and O'Rourke, D., 2003, Groundwater availability model for the central part of the Carrizo-Wilcox Aquifer in Texas: *The University of Texas at Austin, Bureau of Economic Geology, contract report to the Texas Water Development Board*, 389 p.
- Dutton, A.R., and Nicot, J.P., 2006, Hydrodynamic convergence of hydropressured and geopressed zones, Central Texas, Gulf of Mexico basin, USA: *Hydrogeology Journal*, v. 14, p. 859-867.
- Dutton, S.P., Ambrose, W.A., and Loucks, R.G., 2016, Diagenetic controls on reservoir quality in deep Upper Wilcox sandstones of the Rio Grande delta system, South Texas: *Gulf Coast Association of Geological Societies*, v. 5, p. 95-110.
- Dutton, S.P., and Loucks, R.G., 2014, Reservoir quality and porosity-permeability trends in onshore Wilcox sandstone, Texas and Louisiana Gulf Coast: Application to deep Wilcox plays, offshore Gulf of Mexico: *Gulf Coast Association of Geological Societies*, v. 3, p. 33-40.
- Eargle, D.H., 1968, Nomenclature of formations of Claiborne Group, Middle Eocene Coastal Plain of Texas: *U.S. Geological Survey Bulletin 1251-D*, 25 p.
- Estep, J.D., 1998, Evaluation of ground-water quality using geophysical logs: *Texas Natural Resource Conservation Commission, unpublished report*, 516 p.
- Estep, J.D., 2010, Determining groundwater quality using geophysical logs: *Texas Commission on Environmental Quality, unpublished report*, 85 p.
- Ewing, T.E., 1991, The tectonic framework of Texas: *The University of Texas at Austin, Bureau of Economic Geology report to accompany the Tectonic Map of Texas*, 36 p. and one plate.
- Ewing, T.E., 2016, Texas through time: Lone star geology, landscapes, and resources: *The University of Texas at Austin, Bureau of Economic Geology Udden Series 6*, 431 p.

- Fisher, R.S., 1982, Diagenetic history of Eocene Wilcox sandstones and associated formation waters, south-central Texas: The University of Texas at Austin, Ph.D. dissertation, 185 p.
- Fisher, W.L., 1961, Stratigraphic names in the Midway and Wilcox groups of the Gulf Coastal Plain: Gulf Coast Association of Geological Societies Transactions, v. 11, p. 263-295.
- Fisher, W.L., and McGowan, J.H., 1967, Depositional systems in the Wilcox Group of Texas and their relationship to occurrence of oil and gas: Gulf Coast Association of Geological Societies Transactions, v. 17, p. 105-125.
- Fogg, G.E., 1980, Salinity of formation waters, *in* Kreitler, C.W., and others, Geology and geohydrology of the east Texas basin, a report on the progress of nuclear waste isolation feasibility studies (1979): The University of Texas at Austin, Bureau of Economic Geology Geological Circular 80-12, p. 68-72.
- Fogg, G.E., and Blanchard, P.E., 1986, Empirical relations between Wilcox ground-water quality and electric log resistivity, Sabine uplift area, *in* Kaiser, W.R., Geology and ground-water hydrology of deep-basin lignite in the Wilcox Group of east Texas: The University of Texas at Austin, Bureau of Economic Geology, p. 115-118.
- Fogg, G.E., Seni, S.J., and Kreitler, C.W., 1983, Three-dimensional ground-water modeling in depositional systems, Wilcox Group, Oakwood salt dome area, East Texas: The University of Texas at Austin, Bureau of Economic Geology Report of Investigations 133, 55 p.
- Follett, C.R., 1966, Ground-water resources of Caldwell County, Texas: Texas Water Development Board Report 12, 138 p.
- Follett, C.R., 1970, Ground-water resources of Bastrop County, Texas: Texas Water Development Board Report 109, 138 p.
- Forrest, J., Marcucci, E., and Scott, P., 2005, Geothermal gradients and subsurface temperatures in the northern Gulf of Mexico: Gulf Coast Association of Geological Societies Transactions Volume 55, p. 233-248.
- Fryar, D.G., Senger, R., Deeds, N.E., Pickens, J., Jones, T.L., Whallon, A.J., and Dean, K., 2003, Groundwater availability model for the northern Carrizo-Wilcox Aquifer: INTERA, Inc. and Parsons Corporation, contract report to the Texas Water Development Board, 529 p.
- Galloway, W.E., 1989a, Genetic stratigraphic sequences in basin analysis I: architecture and genesis of flooding-surface bounded depositional units: American Association of Petroleum Geologists Bulletin, v. 73, p. 125-142.
- Galloway, W.E., 1989b, Genetic stratigraphic sequences in basin analysis II: application to northwest Gulf of Mexico Cenozoic basin: American Association of Petroleum Geologists Bulletin, v. 73, p. 143-154.
- Galloway, W.E., Dingus, W.F., and Paige, R.E., 1988, Depositional framework and genesis of Wilcox submarine canyon systems, northwest Gulf Coast (abstract): American Association of Petroleum Geologists Bulletin Volume 72, p. 187-188.
- Galloway, W.E., Liu, X., Travis-Neuberger, D., and Xue, L., 1994, Reference high-resolution correlation cross sections, Paleogene section, Texas coastal plain: The University of Texas at Austin, Bureau of Economic Geology, 19 p. and 5 plates.

- Galloway, W.E., Ganey-Curry, P.E., Li, X., and Buffler, R.T., 2000, Cenozoic depositional history of the Gulf of Mexico basin: American Association of Petroleum Geologists Bulletin, v. 84, p. 1743-1774.
- Galloway, W.E., Whiteaker, T.L., and Ganey-Curry, P., 2011, History of Cenozoic North American drainage basin evolution, sediment yield, and accumulation in the Gulf of Mexico basin: *Geosphere*, v. 7, no. 4, p. 938-973.
- George, P.G., 2009, Geology of the Carrizo-Wilcox Aquifer, *in* Hutchison, W.R., Davidson, S.C., Brown, B.J., and Mace, R.E., editors, Aquifers of the Upper Coastal Plains of Texas: Texas Water Development Board Report 374, p. 17-34.
- George, P.G., Mace, R.E., and Petrossian, R., 2011, Aquifers of Texas: Texas Water Development Board Report 380, 172 p.
- Guevara, E.H., and Garcia, R., 1972, Depositional systems and oil-gas reservoirs in the Queen City Formation (Eocene) Texas: The University of Texas at Austin, Bureau of Economic Geology Geological Circular 72-4, 22 p.
- Hamlin, H.S., 1988, Depositional and ground-water flow systems of the Carrizo-Upper Wilcox, South Texas: The University of Texas at Austin, Bureau of Economic Geology Report of Investigations 175, 61 p.
- Hamlin, H.S., and de la Rocha, L., 2015, Using electric logs to estimate groundwater salinity and map brackish groundwater resources in the Carrizo-Wilcox Aquifer in South Texas: *Gulf Coast Association of Geological Societies Journal*, v. 4, p. 109-131.
- Hargis, R.N., 2009, Report on study of Wilcox Group northern Atascosa County and adjacent areas of Bexar and Wilson counties: Hargis, R.N., contract report to the Evergreen Underground Water Conservation District, variously paginated.
- Hargis, R.N., 2010, Report on study of Wilcox Group Wilson County study area and adjacent areas of Bexar and Guadalupe counties, Texas: Hargis, R.N., contract report to the Evergreen Underground Water Conservation District, 32 p. and various maps and cross-sections.
- Harris, H.B., 1965, Ground-water resources of La Salle and McMullen counties, Texas: Texas Water Commission Bulletin 6520, 59 p.
- Harris, J.R., 1962, Petrology of the Eocene Sabinetown-Carrizo contact, Bastrop County, Texas: *Journal of Sedimentary Petrology*, v. 32, p. 263-283.
- HDR Engineering, 2004, Data collection and analysis of aquifers in southern Gonzales County, Texas: HDR Engineering, LBG-Guyton Associates, contract report to the San Antonio Water System, 164 p. and well data.
- HDR Engineering, 2008, Preliminary assessment of potential water supplies from Wilcox Aquifer in parts of Bexar, Guadalupe, and Wilson counties: HDR Engineering, contract report to the San Antonio River Authority, variously paginated.
- HDR Engineering, 2011, Texas water system map: The compilation of a statewide geodataset and digital maps of water service area boundaries: HDR Engineering, contract report to the Texas Water Development Board, variously paginated with geodatabase.

- Hem, J.D., 1985, Study and interpretation of the chemical characteristics of natural water: U.S. Geological Survey Water-Supply Paper 2254, 263 p. and 4 plates.
- Henry, C.D., Basciano, J.M., and Duex, T.W., 1980, Hydrology and water quality of the Eocene Wilcox Group: significance for lignite development in East Texas: The University of Texas at Austin, Bureau of Economic Geology Geological Circular 80-3, 9 p.
- Hilchie, D.W., 1978, Applied openhole log interpretation for geologist and engineers: Hilchie, D.W., Inc., Golden, Colorado, variously paginated.
- Hoyt, W.V., 1959, Erosional channel in the Middle Wilcox near Yoakum, Lavaca County, Texas: Transactions Gulf Coast Association of Geological Societies, v. IX, p. 41-50.
- Hutchison, W.R., Davidson, S.C., Brown, B.J., and Mace, R.E., 2009, Aquifers of the Upper Coastal Plains of Texas: Texas Water Development Board Report 374, 204 p.
- Jackson, M.P.A., Rowan, M.G., and Trudgill, B.D., 2003, Salt-related fault families and fault welds in the northern Gulf of Mexico: The University of Texas at Austin, Bureau of Economic Geology Report of Investigations 268, 40 p.
- Jones, P.H., and Buford, T.B., 1951, Electric logging applied to ground-water exploration: Geophysics, v. 16, p. 115-139.
- Kalaswad, S., and Arroyo, J., 2006, Status report on brackish groundwater and desalination in the Gulf Coast Aquifer in Texas, *in* Mace, R.E., Davidson, S.C., Angle, E.S., and Mullican, III, W.F., editors, Aquifers of the Gulf Coast: Texas Water Development Board Report 365, p. 231-240.
- Keys, W.S., 1990, Borehole geophysics applied to ground-water investigations: U.S. Geological Survey Techniques of Water Resources Investigations Chapter E2, 150 p.
- Kelley, V.A., Deeds, N.E., Fryar, D.G., and Nicot, J.P., 2004, Groundwater availability models for the Queen City and Sparta aquifers: INTERA, Inc., contract report to the Texas Water Development Board, variously paginated.
- Kelley, V.A., Fryar, D.G., and Deeds, N.E., 2009, Hydrogeology of the Queen City and Sparta aquifers with an emphasis on regional mechanisms of discharge, *in* Hutchison, W.R., Davidson, S.C., Brown, B.J., and Mace, R.E., editors, Aquifers of the Upper Coastal Plains of Texas: Texas Water Development Board Report 374, p. 87-116.
- Klemt, W.B., Duffin, G.L., and Elder, G.R., 1976, Groundwater resources of the Carrizo Aquifer in the Winter Garden area of Texas: Texas Water Development Board Report 210, v. 1, 30 p.
- Knox, P.R., Deeds, N.E., Hamlin, H.S., and Kelley, V.A., 2009, Geology, structure, and depositional history of the Yegua-Jackson aquifers, *in* Hutchison, W.R., Davidson, S.C., Brown, B.J., and Mace, R.E., editors, Aquifers of the Upper Coastal Plains of Texas: Texas Water Development Board Report 374, p. 117-145.
- Knox, P.R., Kelley, V.A., Vreugdenhil, A., Deeds, N.E., and Seni, S.J., 2007, Structure of the Yegua-Jackson Aquifer of the Texas Gulf Coastal Plain: Baer Engineering and Environmental Consulting, Inc., INTERA, Inc., contract report to the Texas Water Development Board, 174 p.

- Kreitler, C.W., Bassett, R., Beach, J.A., Symank, L., O'Rourke, D., Papafotiou, A., Ewing, J., and Kelley, V.A., 2013, Evaluation of hydrochemical and isotopic data in Groundwater Management Areas 11, 12, and 13: LBG-Guyton Associates, Tetra Tech, and INTERA, Inc., contract report to the Texas Water Development Board, 454 p.
- Kwader, T., 1986, Use of geophysical logs for determining formation water quality: *Ground water*, v. 24, p. 11-15.
- Larkin, T.J., and Bomar, G.W., 1983, Climatic atlas of Texas: Texas Department of Water Resources Limited Printing Report 192, 151 p.
- Lawless, R.M., Jr., Fillon, R.H., and Lytton, III, R.G., 1997, Gulf of Mexico Cenozoic biostratigraphic, lithostratigraphic, and sequence event chronology: *Gulf Coast Association of Geological Societies Transactions*, v. 47, p. 297-282.
- LBG-Guyton Associates, 2003, Brackish groundwater manual for Texas regional planning groups: LBG-Guyton Associates, contract report to the Texas Water Development Board, 188 p.
- LBG-Guyton Associates, 2006, Site selection for San Antonio Water System's brackish groundwater resources in the Wilcox and Edwards aquifers in the vicinity of San Antonio, Texas: LBG-Guyton Associates, contract report to the San Antonio Water System, variously paginated.
- LBG-Guyton Associates, 2007, Preliminary evaluation of groundwater resources in the Wilcox Aquifer, Gonzales and eastern Wilson counties: LBG-Guyton Associates, contract report to the San Antonio Water System, 42 p.
- LBG-Guyton Associates, 2013, Well completion and data from SAWS brackish Wilcox wells BGD-1 through BGD-8, southern Bexar County, Texas: LBG-Guyton Associates, contract report to the San Antonio Water System, variously paginated.
- Lonsdale, J.T., 1935, Geology and ground-water resources of Atascosa and Frio counties, Texas: U.S. Geological Survey Water Supply Paper 676, 90 p.
- Mace, R.E., Nicot, J.P., Chowdhury, A.H., Dutton, A.R., and Kalaswad, S., 2006, Please pass the salt: Using oil fields for the disposal of concentrate from desalination plants: Texas Water Development Board Report 366, 198 p.
- Mace, R.E., and Smyth, R.C., 2003, Hydraulic properties of the Carrizo-Wilcox Aquifer in Texas: Information for groundwater modeling, planning, and management: The University of Texas at Austin, Bureau of Economic Geology Report of Investigations 269, 40 p. and compact disk.
- Mace, R.E., Smyth, R.C., Xu, L., and Liang, J., 2000, Transmissivity, hydraulic conductivity, and storativity of the Carrizo-Wilcox Aquifer in Texas—data and analysis: The University of Texas at Austin, Bureau of Economic Geology, contract report to the Texas Water Development Board, 76 p.
- Meyer, J.E., 2020, Brackish Resources Aquifer Characterization System Database data dictionary: Texas Water Development Board Open-File Report 12-02, Fifth Edition, 260 p.

- Meyer, J.E., Croskrey, A.D., Wise, M.R., and Kalaswad, S., 2014, Brackish groundwater in the Gulf Coast Aquifer, Lower Rio Grande Valley, Texas: Texas Water Development Board Report 383, 169 p.
- Miller, R.L., Bradford, W.L., and Peters, N.E., 1988, Specific conductance: Theoretical considerations and application to analytical quality control: U.S. Geological Survey Water Supply Paper 2311, 16 p.
- Miller, S.K., 1989, Genetic stratigraphic sequence analysis of the Upper Wilcox, Gulf Basin, Texas: The University of Texas at Austin, M.A. thesis, 127 p.
- Myers, B.N., 1969, Compilation of results of aquifer tests in Texas: Texas Water Development Board Report 98, 532 p.
- Novalis, S., 1999, Access 2000 Visual Basic for Applications handbook: Sybex, Inc., 845 p.
- Olariu, M.I., and Zeng, H., 2018, Prograding muddy shelves in the Paleogene Wilcox deltas, south Texas gulf coast: *Marine and Petroleum Geology* 91, p. 71-88.
- Payne, J.N., 1968, Hydrologic significance of the lithofacies of the Sparta Sand in Arkansas, Louisiana, Mississippi, and Texas: U.S. Geological Survey Professional Paper 569-A, 17 p.
- Pearson, F.J., Jr., and White, D.E., 1967, Carbon-14 ages and flow rates of water in Carrizo Sand, Atascosa County, Texas: *Water Resources Research*, v. 3, p. 251-261.
- Proctor, C.V., Jr., Brown, T.E., McGowan, J.H., Waechter, N.B., and Barnes, V.E., 1974a (revised 1981), *Geologic Atlas of Texas Austin Sheet*: The University of Texas at Austin, Bureau of Economic Geology, scale 1:250,000, 1 sheet.
- Proctor, C.V., Jr., Brown, T.E., Waechter, N.B., Aronow, S., and Barnes, V.E., 1974b, *Geologic Atlas of Texas Seguin Sheet*: The University of Texas at Austin, Bureau of Economic Geology, scale 1:250,000, 1 sheet.
- Railroad Commission of Texas, 2018a, Groundwater Advisory Unit Q-log geophysical well log collection.
- Railroad Commission of Texas, 2018b, Underground Injection Control Database: Railroad Commission of Texas.
- Railroad Commission of Texas, 2018c, Wellbore Database: Railroad Commission of Texas.
- Reedy, R.C., Nicot, J.P., Scanlon, B.R., Deeds, N.E., Kelley, V.A., and Mace, R.E., 2009, Recharge in the Carrizo-Wilcox Aquifer, *in* Hutchison, W.R., Davidson, S.C., Brown, B.J., and Mace, R.E., editors, *Aquifers of the Upper Coastal Plains of Texas*: Texas Water Development Board Report 374, p. 161-166.
- Ricoy, U.R., and Brown, L.F., Jr., 1977, Depositional systems in the Sparta Formation (Eocene) Gulf Coast Basin of Texas: The University of Texas at Austin, Bureau of Economic Geology Geological Circular 77-7, 16 p.
- Rogers, L.T., 1967, Availability and quality of ground water in Fayette County, Texas: Texas Water Development Board Report 56, 117 p.
- Ryder, P.D., 1996, Ground water atlas of the United States, segment 4 Oklahoma and Texas: U.S. Geological Survey Hydrologic Investigations Atlas 730-E, 30 p.

- Sams, R.H., 1990, The upper Wilcox-Reklaw marine transgression and its exploration consequences: *South Texas Geological Society Bulletin*, v. 30, p. 11-28.
- Sams, R.H., 1991, Stratigraphy of marine transgressive boundaries with the Gulf Coast Eocene Carrizo-Reklaw as an example: The University of Texas at Austin, Ph.D. dissertation, 180 p.
- Schlumberger, 1972, Log interpretation, Volume 1—Principles: Schlumberger Limited, 113 p.
- Schlumberger, 1979, Log interpretation charts: Schlumberger Limited, 93 p.
- Schlumberger, 1985, Log interpretation charts: Schlumberger Well Services, 112 p.
- Schlumberger, 1987, Log interpretation principles/applications: Schlumberger Educational Services, 198 p.
- Sellards, E.H., Adkins, W.S., and Plummer, F.B., 1932, The geology of Texas: Volume 1, Stratigraphy: *The University of Texas Bulletin* 3232, 1007 p.
- Shafer, G.H., 1965, Ground-water resources of Gonzales County, Texas: Texas Water Development Board Report 4, 89 p.
- Shafer, G.H., 1966, Ground-water resources of Guadalupe County, Texas: Texas Water Development Board Report 19, 93 p.
- Stumm, W., and Morgan, J.J., 1981, Aquatic chemistry (Second Edition): New York, John Wiley, 780 p.
- Sundstrom, R.W., and Follett, C.R., 1950, Ground-water resources of Atascosa County, Texas: U.S. Geological Survey Water Supply Paper 1079-C, p. 107-153.
- TCEQ (Texas Commission on Environmental Quality), 2010, Source Water Assessment Database: Texas Commission on Environmental Quality, Public Drinking Water Program.
- TCEQ (Texas Commission on Environmental Quality), 2015, Subchapter F: drinking water standards governing water quality and reporting requirements for public water systems: 30 Texas Administrative Code Chapter 290, §§ 290.101–290.122, 177 p.
- Thompson, G.L., 1966, Ground-water resources of Lee County, Texas: Texas Water Development Board Report 20, 131 p.
- Thorkildsen, D., Quincy, R., and Preston, R., 1989, A digital model of the Carrizo-Wilcox Aquifer within the Colorado River basin of Texas: Texas Water Development Board Limited Printing Report LP-208, 59 p.
- Thorkildsen, D., and Price, R.D., 1991, Groundwater resources of the Carrizo-Wilcox Aquifer in the Central Texas Region: Texas Water Development Board Report 332, 46 p.
- Torres-Verdín, C., 2017, Integrated geological-petrophysical interpretation of well logs: Department of Petroleum and Geosystems Engineering, The University of Texas at Austin, unpublished class notes, variously paginated.
- TWDB (Texas Water Development Board), 2007a, Water for Texas 2007, Volume II: Texas Water Development Board Report GP-8-1, 392 p.

- TWDB (Texas Water Development Board), 2007b, The Geologic Atlas of Texas: U.S. Geological Survey, contract geodatabase to the Texas Water Development Board, Version 3, one geodatabase.
- TWDB (Texas Water Development Board), 2012, 2012 Water for Texas: Texas Water Development Board State Water Plan, 299 p.
- TWDB (Texas Water Development Board), 2016, The future of desalination in Texas: 2016 biennial report on seawater and brackish groundwater desalination: Texas Water Development Board, variously paginated.
- TWDB (Texas Water Development Board), 2017, Water for Texas, 2017 State Water Plan: Texas Water Development Board, 133 p.
- TWDB (Texas Water Development Board), 2019a, BRACS Database: Texas Water Development Board.
- TWDB (Texas Water Development Board), 2019b, Groundwater Database: Texas Water Development Board.
- TWDB (Texas Water Development Board), 2019c, Submitted Driller's Report Database: Texas Water Development Board.
- Wade, S.C., and Bradley, R., 2013, GAM Task 13-036 (revised): Total estimated recoverable storage for aquifers in Groundwater Management Area 13: Texas Water Development Board Technical Note, 30 p.
- Wade, S.C., and Shi, J., 2014, GAM Task 13-035 version 2: Total estimated recoverable storage for aquifers in Groundwater Management Area 12: Texas Water Development Board Technical Note, 43 p.
- Winslow, A.G., and Kister, L.R., 1956, Saline-water resources of Texas: U.S. Geological Survey Water-Supply Paper 1365, 105 p.
- Wise, M.R., 2014, Queen City and Sparta aquifers, Atascosa and McMullen counties, Texas: Structure and brackish groundwater: Texas Water Development Board Technical Note 14-01, 67 p.
- Xue, L.Q., 1994, Genetic stratigraphic sequences and depositional systems of the lower and middle Wilcox strata, Texas Gulf Coast basin: The University of Texas at Austin, Ph.D. dissertation, 202 p.
- Xue, L.Q., and Galloway, W.E., 1993, Sequence stratigraphic and depositional framework of the Paleocene lower Wilcox strata, northwest Gulf of Mexico basin: Gulf Coast Association of Geological Societies Transactions Volume 43, p. 453-464.
- Xue, L.Q., and Galloway, W.E., 1995, High-resolution depositional framework of the Paleocene middle Wilcox strata, Texas coastal plain: American Association of Petroleum Geologists Bulletin, v. 79, p. 205-230.
- Young, S.C., Jigmond, M., Jones, T.L., and Ewing, T., 2018, Groundwater availability model for the central portion of the Sparta, Queen City, and Carrizo-Wilcox aquifers: INTERA, Inc. and Frontera, contract report to the Texas Water Development Board, variously paginated.

13. Appendices

13.1 Geological formation brackish groundwater volumes per administrative boundary

13.1.1 Wilcox Group

Table 13.1.1-1. In-place groundwater volume (acre-feet) of the Wilcox Group in each study area county per salinity class.

County	Fr - Ss	Fr - Ss - Ms	Ss	Ss - Ms	Ss - Ms - Vs	Ms
Atascosa	907,395	0	3,619,564	2,188,176	0	1,935,938
Bastrop	12,154,861	4,780,879	0	19,034,351	1,332,654	0
Bexar	2,564,910	0	368,086	0	0	0
Caldwell	3,032,517	2,093,163	0	1,708,758	0	531,977
DeWitt	0	0	0	0	0	0
Fayette	0	0	0	5,087,571	12,880,514	39,649
Gonzales	0	36,917	6,295,530	7,790,699	2,885,078	12,835,968
Guadalupe	2,875,578	56,828	2,465,216	62,254	0	0
Karnes	0	0	0	0	0	6,364,034
Lavaca	0	0	0	0	0	0
Lee	4,040,281	370,915	0	4,903,038	2,632,535	0
Live Oak	0	0	0	0	0	939,347
Williamson	195,087	0	0	0	0	0
Wilson	2,181,182	0	8,771,817	15,837,378	0	11,206,013
SUM	27,951,811	7,338,702	21,520,213	56,612,225	19,730,781	33,852,926

County	Ms - Vs	Ms - Vs - Br	Vs	Vs - Br	Br
Atascosa	93,916	0	0	0	0
Bastrop	0	0	0	0	0
Bexar	0	0	0	0	0
Caldwell	0	0	0	0	0
DeWitt	0	0	6,937,856	1,984,470	4,245,252
Fayette	14,278,776	3,969,383	4,319,076	11,836,911	12,955,455
Gonzales	19,718,621	0	19,797,443	3,663,731	0
Guadalupe	0	0	0	0	0
Karnes	7,348,351	0	15,074,684	3,370,494	1,249,383
Lavaca	567,581	0	6,606,566	9,091,558	5,020,155
Lee	1,925,798	94,199	0	0	0
Live Oak	101,137	0	0	0	0
Williamson	0	0	0	0	0
Wilson	0	0	0	0	0
SUM	44,034,180	4,063,582	52,735,625	29,947,164	23,470,245

Notes:

- Fr - Ss is a mixed class of fresh and slightly saline.
- Fr - Ss - Ms is a mixed class of fresh, slightly, and moderately saline.
- Ss is a slightly saline class.
- Ss - Ms is a mixed class of slightly and moderately saline.
- Ss - Ms - Vs is a mixed class of slightly, moderately, and very saline.
- Ms is a moderately saline class.
- Ms - Vs is a mixed class of moderately and very saline.
- Ms - Vs - Br is a mixed class of moderately, very saline and brine.
- Vs is a very saline class.

Vs - Br is a mixed class of very saline and brine.
 Br is a brine saline class.

Table 13.1.1-2. In-place groundwater volume (acre-feet) of the Wilcox Group in each Regional Water Planning Area (RWPA) per salinity class.

RWPA	Fr - Ss	Fr - Ss - Ms	Ss	Ss - Ms	Ss - Ms - Vs	Ms
G	4,235,368	370,915	0	4,903,038	2,632,535	0
K	12,154,861	4,780,879	0	24,121,922	14,213,167	39,649
L	11,561,582	2,186,909	21,520,212	27,587,266	2,885,078	32,873,930
N	0	0	0	0	0	939,347
P	0	0	0	0	0	0

RWPA	Ms - Vs	Ms - Vs - Br	Vs	Vs - Br	Br
G	1,925,798	94,199	0	0	0
K	14,278,776	3,969,383	4,319,076	11,836,911	12,955,455
L	27,160,888	0	41,809,983	9,018,694	5,494,635
N	101,137	0	0	0	0
P	567,581	0	6,606,566	9,091,558	5,020,155

Notes:

Fr - Ss is a mixed class of fresh and slightly saline.
 Fr - Ss - Ms is a mixed class of fresh, slightly, and moderately saline.
 Ss is a slightly saline salinity class.
 Ss - Ms is a mixed class of slightly and moderately saline.
 Ss - Ms - Vs is a mixed class of slightly, moderately, and very saline.
 Ms is a moderately saline salinity class.
 Ms - Vs is a mixed class of moderately and very saline.
 Ms - Vs - Br is a mixed class of moderately, very saline and brine.
 Vs is a very saline salinity class.
 Vs - Br is a mixed class of very saline and brine.
 Br is a brine salinity class.

Table 13.1.1-3. In-place groundwater volume (acre-feet) of the Wilcox Group in each Groundwater Management Area (GMA) per salinity class.

GMA	Fr - Ss	Fr - Ss - Ms	Ss	Ss - Ms	Ss - Ms - Vs	Ms
12	16,390,204	5,151,794	0	29,024,960	16,845,702	39,649
13	11,558,737	2,186,909	21,520,212	27,587,266	2,885,078	32,429,300
15	0	0	0	0	0	444,630
16	0	0	0	0	0	939,347

GMA	Ms - Vs	Ms - Vs - Br	Vs	Vs - Br	Br
12	15,334,844	3,448,870	1,955,494	2,351,808	0
13	24,083,842	0	23,461,721	3,947,653	0
15	4,514,357	614,711	27,318,410	23,647,705	23,470,245
16	101,137	0	0	0	0

Notes:

Fr - Ss is a mixed class of fresh and slightly saline.
 Fr - Ss - Ms is a mixed class of fresh, slightly, and moderately saline.
 Ss is a slightly saline class.
 Ss - Ms is a mixed class of slightly and moderately saline.
 Ss - Ms - Vs is a mixed class of slightly, moderately, and very saline.

Ms is a moderately saline class.
 Ms - Vs is a mixed class of moderately and very saline.
 Ms - Vs - Br is a mixed class of moderately, very saline and brine.
 Vs is a very saline class.
 Vs - Br is a mixed class of very saline and brine.
 Br is a brine salinity class.

Table 13.1.1-4. In-place groundwater volume (acre-feet) of the Wilcox Group in each groundwater conservation district per salinity class.

District	Fr - Ss	Fr - Ss - Ms	Ss	Ss - Ms	Ss - Ms - Vs	Ms
Evergreen UWCD	3,088,577	0	12,391,380	18,025,554	0	19,505,985
Fayette County GCD	0	0	0	5,087,571	12,880,514	39,649
Gonzales County UWCD	1,119,522	1,301,403	6,295,530	9,216,302	2,885,078	13,367,767
Guadalupe County GCD	2,875,578	56,828	2,465,216	62,254	0	0
Live Oak UWCD	0	0	0	0	0	939,347
Lost Pines GCD	16,195,143	5,151,794	0	23,937,389	3,965,189	0
Pecan Valley GCD	0	0	0	0	0	0
Plum Creek CD	1,621,646	703,149	0	269,425	0	0
No GCD present	3,051,345	125,529	368,086	13,730	0	178

District	Ms - Vs	Ms - Vs - Br	Vs	Vs - Br	Br
Evergreen UWCD	7,442,267	0	15,074,684	3,370,494	1,249,383
Fayette County GCD	14,278,776	3,969,383	4,319,076	11,836,911	12,955,455
Gonzales County UWCD	18,919,713	0	10,820,071	375,547	0
Guadalupe County GCD	0	0	0	0	0
Live Oak UWCD	101,137	0	0	0	0
Lost Pines GCD	1,925,798	94,199	0	0	0
Pecan Valley GCD	0	0	6,937,856	1,984,470	4,245,252
Plum Creek CD	0	0	0	0	0
No GCD present	1,366,490	0	15,583,938	12,379,741	5,020,155

Notes:

UWCD = Underground Water Conservation District.
 GCD = Groundwater Conservation District.
 CD = Conservation District.
 Fr - Ss is a mixed class of fresh and slightly saline.
 Fr - Ss - Ms is a mixed class of fresh, slightly, and moderately saline.
 Ss is a slightly saline class.
 Ss - Ms is a mixed class of slightly and moderately saline.
 Ss - Ms - Vs is a mixed class of slightly, moderately, and very saline.
 Ms is a moderately saline class.
 Ms - Vs is a mixed class of moderately and very saline.
 Ms - Vs - Br is a mixed class of moderately, very saline and brine.
 Vs is a very saline class.
 Vs - Br is a mixed class of very saline and brine.
 Br is a brine salinity class.

13.1.2 Carrizo Sand

Table 13.1.2-1. In-place groundwater volume (acre-feet) of the Carrizo Sand in each county per salinity class.

County	Fr	Fr - Ss	Ss	Ss - Ms	Ms	Ms - Vs
Atascosa	4,021,110	5,259,035	33,072	1,168,482	0	0
Bastrop	7,030,636	519,310	356,879	0	0	0
Bexar	1,185,008	0	0	0	0	0
Caldwell	1,378,684	390,465	0	0	0	0
DeWitt	0	0	0	0	0	0
Fayette	4,462,957	4,187,097	2,124,015	104,262	1,696,457	1,458,557
Gonzales	10,752,004	12,970,087	7,221,316	2,000,706	6,355,859	2,044,792
Guadalupe	1,635,244	0	0	0	0	0
Karnes	0	2,711,968	4,423,625	14,563,296	6,635,764	4,800,161
Lavaca	0	0	0	16,760	211	485,638
Lee	1,264,381	221,696	1,553,710	0	0	0
Live Oak	0	0	0	2,103,301	0	0
Williamson	0	0	0	0	0	0
Wilson	14,640,354	20,425,648	4,685,403	2,437,163	0	0
SUM	46,370,378	46,685,306	20,398,020	22,393,970	14,688,291	8,789,148

County	Vs	Vs - Br	Br
Atascosa	0	0	0
Bastrop	0	0	0
Bexar	0	0	0
Caldwell	0	0	0
DeWitt	6,212,798	371,655	3,297,943
Fayette	3,457,838	0	3,079,018
Gonzales	7,582,149	0	1,017,948
Guadalupe	0	0	0
Karnes	7,579,833	572,160	0
Lavaca	8,535,833	0	3,214,132
Lee	0	0	0
Live Oak	0	0	0
Williamson	0	0	0
Wilson	0	0	0
SUM	33,368,451	943,815	10,609,041

Notes:

- Fr is a fresh salinity class.
- Fr - Ss is a mixed class of fresh and slightly saline.
- Ss is a slightly saline class.
- Ss - Ms is a mixed class of slightly and moderately saline.
- Ms is a moderately saline class.
- Ms - Vs is a mixed class of moderately and very saline.
- Vs is a very saline class.
- Vs - Br is a mixed class of very saline and brine.
- Br is a brine salinity class.

Table 13.1.2-2. In-place groundwater volume (acre-feet) of the Carrizo Sand in each Regional Water Planning Area (RWPA) per salinity class.

RWPA	Fr	Fr - Ss	Ss	Ss - Ms	Ms	Ms - Vs
G	1,264,381	221,696	1,553,710	0	0	0
K	11,493,593	4,706,407	2,480,894	104,262	1,696,457	1,458,557
L	33,612,403	41,757,203	16,363,416	20,169,647	12,991,624	6,844,953
N	0	0	0	2,103,301	0	0
P	0	0	0	16,760	211	485,638

RWPA	Vs	Vs - Br	Br
G	0	0	0
K	3,457,838	0	3,079,018
L	21,374,780	943815	4,315,891
N	0	0	0
P	8,535,833	0	3,214,132

Notes:

- Fr is a fresh salinity class.
- Fr - Ss is a mixed class of fresh and slightly saline.
- Ss is a slightly saline class.
- Ss - Ms is a mixed class of slightly and moderately saline.
- Ms is a moderately saline class.
- Ms - Vs is a mixed class of moderately and very saline.
- Vs is a very saline class.
- Vs - Br is a mixed class of very saline and brine.
- Br is a brine salinity class.

Table 13.1.2-3. In-place groundwater volume (acre-feet) of the Carrizo Sand in each Groundwater Management Area (GMA) per salinity class.

GMA	Fr	Fr - Ss	Ss	Ss - Ms	Ms	Ms - Vs
12	12,757,975	4,913,313	3,632,521	0	1,025,156	316,073
13	33,612,403	41,757,203	14,858,811	11,857,533	8,094,328	2,044,792
15	0	14,790	1,906,689	8,433,136	5,568,808	6,428,283
16	0	0	0	2,103,301	0	0

GMA	Vs	Vs - Br	Br
12	7,007	0	0
13	7,582,149		1,017,948
15	25,779,294	943,815	9,591,093
16	0	0	0

Notes:

- Fr is a fresh salinity class.
- Fr - Ss is a mixed class of fresh and slightly saline.
- Ss is a slightly saline class.
- Ss - Ms is a mixed class of slightly and moderately saline.
- Ms is a moderately saline class.
- Ms - Vs is a mixed class of moderately and very saline.
- Vs is a very saline class.
- Vs - Br is a mixed class of very saline and brine.
- Br is a brine salinity class.

Table 13.1.2-4. In-place groundwater volume (acre-feet) of the Carrizo Sand in each groundwater conservation district per salinity class.

District	Fr	Fr - Ss	Ss	Ss - Ms	Ms	Ms - Vs
Evergreen UWCD	18,661,464	28,396,651	9,142,100	18,168,941	6,635,764	4,800,161
Fayette County GCD	4,462,957	4,187,097	2,124,015	104,262	1,696,457	1,458,557
Gonzales County UWCD	11,957,487	13,359,524	6,963,561	2,000,706	5,066,012	1,013,351
Guadalupe County GCD	1,635,244	0	0	0	0	0
Live Oak UWCD	0	0		2,103,301	0	0
Lost Pines GCD	8,295,017	741,006	1,910,589	0	0	0
Pecan Valley GCD	0	0	0	0	0	0
Plum Creek CD	173,201	725	0	0	0	0
No GCD present	1,185,008	303	257,755	16,760	1,290,059	1,517,079

District	Vs	Vs - Br	Br
Evergreen UWCD	7,579,833	572,160	0
Fayette County GCD	3,457,838	0	3,079,018
Gonzales County UWCD	1,062,480	0	0
Guadalupe County GCD	0	0	0
Live Oak UWCD	0	0	0
Lost Pines GCD		0	0
Pecan Valley GCD	6,212,798	371,655	3,297,943
Plum Creek CD	0	0	0
No GCD present	15,055,501	0	4,232,080

Notes:

UWCD = Underground Water Conservation District.

GCD = Groundwater Conservation District.

CD = Conservation District.

Fr is a fresh salinity class.

Fr - Ss is a mixed class of fresh and slightly saline.

Ss is a slightly saline class.

Ss - Ms is a mixed class of slightly and moderately saline.

Ms is a moderately saline class.

Ms - Vs is a mixed class of moderately and very saline.

Vs is a very saline class.

Vs - Br is a mixed class of very saline and brine.

Br is a brine salinity class.

13.1.3 Queen City Sand

Table 13.1.3-1. In-place groundwater volume (acre-feet) of the Queen City Sand in each county per salinity class.

County	Fr	Fr - Ss	Ss	Ss - Ms	Ss - Ms - Vs	Ms	Ms - Vs	Vs
Atascosa	48,255	801,108	1,022,761	757,023	0	576,757	208	488,113
Bastrop	819,671	1,299,152	349,717	0	0	0	0	0
Bexar	204	0	0	0	0	0	0	0
Caldwell	41,993	0	14,873	0	0	0	0	0
DeWitt	0	0	0	0	0	0	0	1,868,062
Fayette	280,839	30,214	3,514,303	1,043,763	0	1,407,886	230,613	1,410,934
Gonzales	1,239,918	490,127	1,621,078	348,713	0	1,661,577	29,210	5,098,744
Guadalupe	587	0	0	0	0	0	0	0
Karnes	0	0	0	0	0	94,136	121,654	10,692,108

County	Fr	Fr - Ss	Ss	Ss - Ms	Ss - Ms - Vs	Ms	Ms - Vs	Vs
Lavaca	0	0	0	0	0	116,580	0	1,857,273
Lee	158,106	392,280	1,113,990	0	0	0	0	0
Live Oak	0	0	0	0	0	0	0	537,843
Williamson	0	0	0	0	0	0	0	0
Wilson	895,381	1,206,887	3,182,467	723,029	415,796	2,742,728	234	1,158,951
SUM	3,484,954	4,219,768	10,819,189	723,029	415,796	6,599,664	381,919	23,112,028

Notes:

Fr is a fresh salinity class.
 Fr - Ss is a mixed class of fresh and slightly saline.
 Ss is a slightly saline class.
 Ss - Ms is a mixed class of slightly and moderately saline.
 Ss - Ms - Vs is a mixed class of slightly, moderately, and very saline.
 Ms is a moderately saline class.
 Ms - Vs is a mixed class of moderately and very saline.
 Vs is a very saline class.

Table 13.1.3-2. In-place groundwater volume (acre-feet) of the Queen City Sand in each Regional Water Planning Area (RWPA) per salinity class.

RWPA	Fr	Fr - Ss	Ss	Ss - Ms	Ss - Ms - Vs	Ms	Ms - Vs	Vs
G	158,106	392,280	1,113,990	0	0	0	0	0
K	1,100,511	1,329,367	3,864,020	1,043,763	0	1,407,886	230,613	1,410,934
L	2,226,337	2,498,122	5,841,179	1,828,765	415,796	5,075,197	151,305	19,305,979
N	0	0	0	0	0	0	0	537,843
P	0	0	0	0	0	116,580	0	1,857,273

Notes:

Fr is a fresh salinity class.
 Fr - Ss is a mixed class of fresh and slightly saline.
 Ss is a slightly saline class.
 Ss - Ms is a mixed class of slightly and moderately saline.
 Ss - Ms - Vs is a mixed class of slightly, moderately, and very saline.
 Ms is a moderately saline class.
 Ms - Vs is a mixed class of moderately and very saline.
 Vs is a very saline class.

Table 13.1.3-3. In-place groundwater volume (acre-feet) of the Queen City Sand in each Groundwater Management Area (GMA) per salinity class.

GMA	Fr	Fr - Ss	Ss	Ss - Ms	Ss - Ms - Vs	Ms	Ms - Vs	Vs
12	1,258,617	1,721,648	4,932,237	923,793	0	558,022	0	0
13	2,226,337	2,498,122	5,841,179	1,828,765	415,796	5,075,197	151,305	10,560,792
15	0	0	45,773	119,969	0	966,443	230,613	12,013,394
16	0	0	0	0	0	0	0	537,843

Notes:

Fr is a fresh salinity class.
 Fr - Ss is a mixed zone of fresh and slightly saline.
 Ss is a slightly saline class.
 Ss - Ms is a mixed class of slightly and moderately saline.
 Ss - Ms - Vs is a mixed class of slightly, moderately, and very saline.
 Ms is a moderately saline class.
 Ms - Vs is a mixed class of moderately and very saline.
 Vs is a very saline class.

Table 13.1.3-4. In-place groundwater volume (acre-feet) of the Queen City Sand in each groundwater conservation district per salinity class.

District	Fr	Fr - Ss	Ss	Ss - Ms	Ss - Ms - Vs	Ms	Ms - Vs	Vs
Evergreen UWCD	943,635	2,007,995	4,205,228	1,480,052	415,796	3,413,620	122,095	12,339,173
Fayette County GCD	280,839	30,214	3,514,303	1,043,763	0	1,407,886	230,613	1,410,934
Gonzales County UWCD	1,275,769	490,127	1,635,951	348,713	0	1,661,577	29,210	3,230,786
Guadalupe County GCD	587	0	0	0	0	0	0	0
Live Oak UWCD	0	0	0	0	0	0	0	537,843
Lost Pines GCD	977,777	1,691,433	1,463,707	0	0	0	0	0
Pecan Valley GCD	0	0	0	0	0	0	0	1,868,062
Plum Creek CD	6,142	0	0	0	0	0	0	0
No GCD present	204	0	0	0	0	116,580	0	3,725,231

Notes:

UWCD = Underground Water Conservation District.

GCD = Groundwater Conservation District.

CD = Conservation District.

Fr is a fresh salinity class.

Fr - Ss is a mixed class of fresh and slightly saline.

Ss is a slightly saline class.

Ss - Ms is a mixed class of slightly and moderately saline.

Ss - Ms - Vs is a mixed class of slightly, moderately, and very saline.

Ms is a moderately saline class.

Ms - Vs is a mixed class of moderately and very saline.

Vs is a very saline class.

13.1.4 Sparta Sand

Table 13.1.4-1. In-place groundwater volume (acre-feet) of the Sparta Sand in each county per salinity class.

County	Fresh	Slightly saline	Moderately saline	Very saline
Atascosa	3,090	113,814	198,278	195,609
Bastrop	177,459	235,594	0	0
Bexar	0	0	0	0
Caldwell	0	0	0	0
DeWitt	0	0	0	402,393
Fayette	91,955	1,811,243	922,414	119,988
Gonzales	105,782	715,843	755,669	1,264,627
Guadalupe	0	0	0	0
Karnes	0	0	151,251	1,940,663
Lavaca	0	0	212,102	411,797
Lee	5,025	445,320	11,689	0
Live Oak	0	0	0	94,633

Williamson	0	0	0	0
Wilson	91,969	229,739	604,920	430,463
SUM	475,280	3,551,553	2,856,323	4,860,173

Table 13.1.4-2. In-place groundwater volume (acre-feet) of the Sparta Sand in each Regional Water Planning Area (RWPA) per salinity class.

RWPA	Fresh	Slightly saline	Moderately saline	Very saline
G	5,025	445,320	11,689	0
K	269,414	2,046,837	922,414	119,988
L	200,841	1,059,396	1,710,118	4,233,755
N	0	0	0	94,633
P	0	0	212,102	411,797

Table 13.1.4-3. In-place groundwater volume (acre-feet) of the Sparta Sand in each Groundwater Management Area (GMA) per salinity class.

GMA	Fresh	Slightly saline	Moderately saline	Very saline
12	274,439	2,144,337	393,075	0
13	200,841	1,059,396	1,692,569	2,636,483
15	0	347,821	347,821	2,129,057
16	0	0	0	94,633

Table 13.1.4-4. In-place groundwater volume (acre-feet) of the Sparta Sand in each groundwater conservation district per salinity class.

District	Fresh	Slightly saline	Moderately saline	Very saline
Evergreen UWCD	95,059	343,553	954,449	2,566,735
Fayette County GCD	91,955	1,811,243	922,414	119,988
Gonzales County UWCD	105,782	715,843	645,132	895,945
Guadalupe County GCD	0	0	0	0
Live Oak UWCD	0	0	0	94,633
Lost Pines GCD	182,484	680,914	11,689	0
Pecan Valley GCD	0	0	0	402,393
Plum Creek CD	0	0	0	0
No GCD present	0	0	322,639	780,479

Notes:

UWCD = Underground Water Conservation District.

GCD = Groundwater Conservation District.

CD = Conservation District.

13.1.5 Yegua Formation

Table 13.1.5-1. In-place groundwater volume (acre-feet) of the Yegua Formation in each county per salinity class.

County	Fr - Ss - Ms	Moderately saline	Ms - Vs	Very saline
Atascosa	431,889	1,924,292	82,135	0
Bastrop	14,839	0	0	0
Bexar	0	0	0	0
Caldwell	0	0	0	0
DeWitt	0	435,618	926,330	5,369,081
Fayette	3,244,980	12,620,708	0	0
Gonzales	3,646,980	6,522,843	1,231,785	4,164,555
Guadalupe	0	0	0	0
Karnes	606,688	14,602,204	4,245,913	4,325,777
Lavaca	0	6,016,339	1,011,788	2,205,405
Lee	344,959	0	0	0
Live Oak	0	35,178	609,231	837,498
Williamson	0	0	0	0
Wilson	1,872,321	798,304	0	0
SUM	10,162,656	42,955,486	8,107,182	16,902,316

Notes:

Fr - Ss - Ms is a mixed class of fresh, slightly, and moderately saline.

Ms - Vs is a mixed class of moderately and very saline.

Table 13.1.5-2. In-place groundwater volume (acre-feet) of the Yegua Formation in each Regional Water Planning Area (RWPA) per salinity class.

RWPA	Fr - Ss - Ms	Moderately saline	Ms - Vs	Very saline
G	344,959	0	0	0
K	3,259,819	12,620,708	0	0
L	6,557,697	24,283,262	6,486,163	13,859,412
N	0	35,178	609,231	837,498
P	0	6,016,339	1,011,788	2,205,405

Notes:

Fr - Ss - Ms is a mixed class of fresh, slightly, and moderately saline.

Ms - Vs is a mixed class of moderately and very saline.

Table 13.1.5-3. In-place groundwater volume (acre-feet) of the Yegua Formation in each Groundwater Management Area (GMA) per salinity class.

GMA	Fr - Ss - Ms	Moderately saline	Ms - Vs	Very saline
12	3,604,778	3,515,242	0	0
13	6,557,697	15,382,764	1,313,920	4,164,555
15	0	24,022,303	6,184,031	11,900,262
16	0	35,178	609,231	837,498

Notes:

Fr - Ss - Ms is a mixed class of fresh, slightly, and moderately saline.

Ms - Vs is a mixed class of moderately and very saline.

Table 13.1.5-4. In-place groundwater volume (acre-feet) of the Yegua Formation in each groundwater conservation district per salinity class.

District	Fr - Ss - Ms	Moderately saline	Ms - Vs	Very saline
Evergreen UWCD	2,910,898	17,324,800	4,328,048	4,325,777
Fayette County GCD	3,244,980	12,620,708	0	0
Gonzales County UWCD	3,613,180	4,706,102	101,538	579,053
Guadalupe County GCD	0	0	0	0
Live Oak UWCD	0	35,178	609,231	837,498
Lost Pines GCD	359,798	0	0	0
Pecan Valley GCD	0	435,618	926,330	5,369,081
Plum Creek CD	0	0	0	0
No GCD present	0	0	0	0

Notes:

Fr - Ss - Ms is a mixed class of fresh, slightly, and moderately saline.

Ms - Vs is a mixed class of moderately and very saline.

UWCD = Underground Water Conservation District.

GCD = Groundwater Conservation District.

CD = Conservation District.

13.2 Calculation of groundwater volumes in GIS

A master grid polygon shapefile was created using the fishnet tool (Figure 13.2-1) to compile the multiple values and complex geological shapes and administrative boundaries into simple 3-dimensional cubes for the groundwater volume calculations. The shapefile polygons are coincident with the 250-foot by 250-foot extent of the snap grid cells. A total of 2,634,229 polygon cells were created to cover the entire snap grid of the study. Values from the stratigraphic and net sand rasters could be extracted without resampling by using polygons instead of rasters. These values are stored in the columns of the attribute table and used in calculations using Field Calculator.

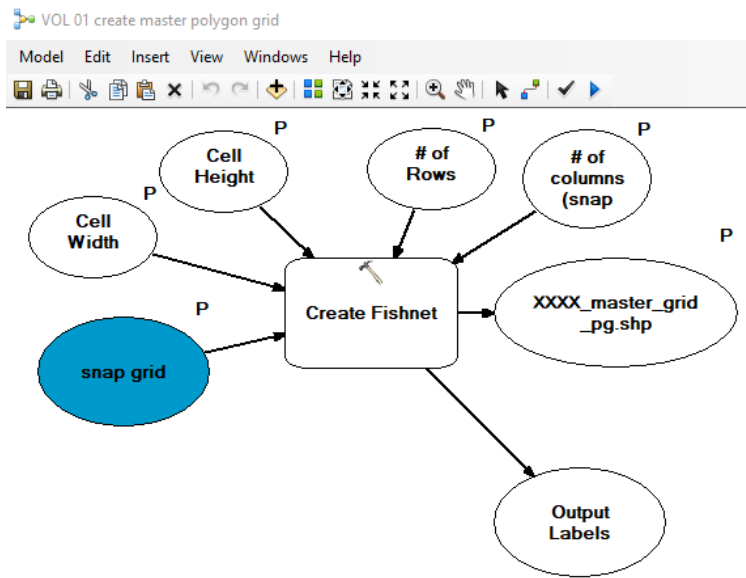


Figure 13.2-1. Model Builder diagram of inputs for the Fishnet tool used to create master grid polygons.

Since volumes of water will be listed for counties, groundwater conservation districts, groundwater management areas, and regional water planning areas, master grid cells were assigned to administrative boundaries using the centroid of the polygons. This ensures volumes calculated for a grid cell will not be double counted or overwritten for multiple, unique entities (Figure 13.2-2).

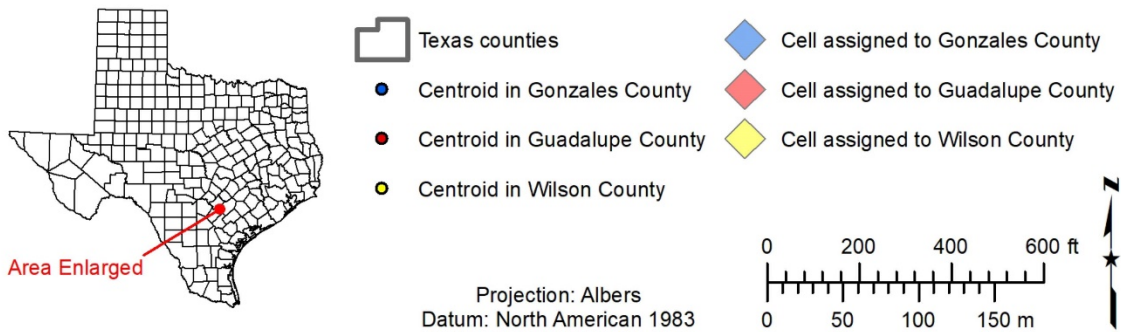
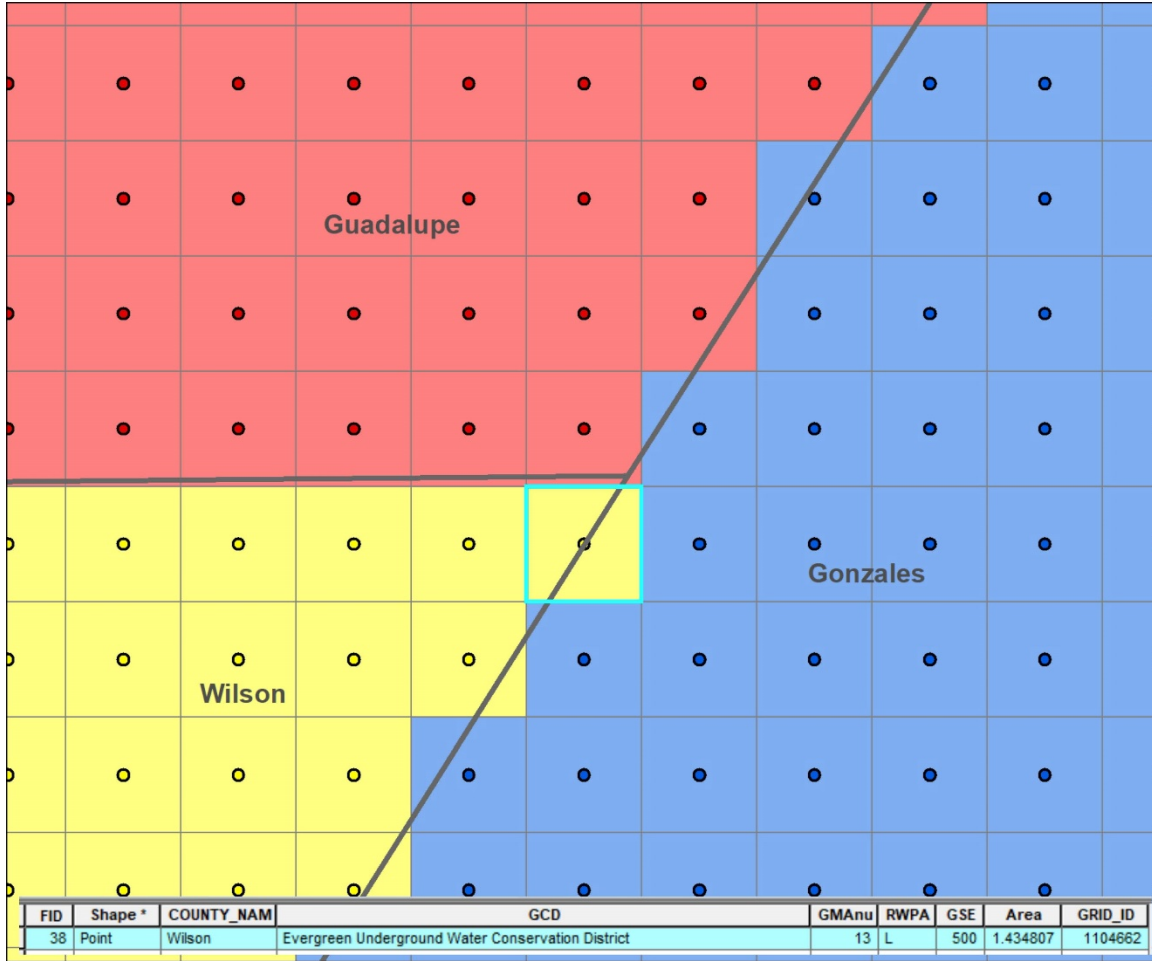


Figure 13.2-2. Grid cells were assigned to administrative areas based on their centroid.

13.2.1 Area

The area of each 250-foot grid cell is 1.4348 acres. This value for the [Area] field in the attribute table was calculated using the Calculate Geometry tool. To validate the tool result, the simple area equation and conversion factor below were used:

$$250 \text{ feet} \times 250 \text{ feet} \times \frac{1 \text{ acre}}{43,560 \text{ feet}^2} = 1.4348 \text{ acres}$$

The calculation for water volume per grid cell, regardless of salinity, is:

$$\text{Volume} = [\text{Area}] \times [\text{Saturated Thickness}] \times [\text{Specific Yield}]$$

13.2.2 Saturated thickness

Once the master grid polygon shapefile was attributed with administrative boundary designations, area values, and ground surface elevations, cells within each geological formation were selected by their centroid and exported to separate shapefiles. The bottom elevation, thickness, and net sand raster values were extracted for each geological formation-based polygon and added to the attribute table. If an end user requires the top elevation for each grid cell, a new column can be added and populated by summing the formation bottom elevation and thickness columns. If an end user prefers formation depths instead of elevations, the values in elevation fields can be subtracted from the values in the ground surface elevation field. The ground surface elevation for each grid cell in the master grid polygon shapefile was extracted from the study digital elevation model (DEM). Elevation values are in feet relative to mean sea level and are stored in the field [GSE]. ArcGIS® Model Builder (Figure 13.2.2-1) was used to:

1. clip out the centroids per geological formation,
2. extract geological formation bottom elevation [FMBE], formation thickness [FMTK], and net sand [FMNS] raster values,
3. assign a centroid to the outcrop or subcrop of the formation [FMOTC],
4. assign percent sand by dividing the net sand by the formation thickness [FMPS], and
5. create empty fields for the saturated thickness [FMSTK], specific yield [FMSY], cell groundwater volume [FM_h2o_vol], salinity class [FMSZ], and brackish groundwater production zone [BGPZ].



Figure 13.2.2-1. Model builder steps.

Saturated thickness was calculated in one of two ways depending on whether a cell was in the geological formation outcrop or subcrop. An attribute of “O” was applied to centroids in the formation outcrop. An “S” was applied to all cells with their centroid in the subcrop. For cells in the subcrop, it was assumed that the entire thickness of the geological formation was saturated. Therefore, the saturated thickness was set equal to the net sand in feet. The net sand values for each cell were extracted from the geological formation net sand raster using the Extract Multi Values to Points tool.

For cells in the outcrop of the formation, the saturated thickness [STK] was calculated using the static water level elevation [SWLE], formation bottom elevation [BE], and percent sand [PS] rasters. The percent sand was used as a substitute for net sand since it was not feasible to parse the amount of net sand below the static water level elevation.

$$STK_{\text{outcrop}} = (SWLE - BE) \times PS$$

$$STK_{\text{subcrop}} = FMNS$$

An example of the Field Calculator syntax for the Sparta Sand reads:

(!SPSWLE!-!SPBE!)*!SPPS!/100 if !SPOTC!=="O" else !SPNS!

13.2.3 Specific yield

Each geological formation of the study was assigned a specific yield value (Table 13.2.3-1). This value was then assigned to all the grid cells in that formation.

Table 13.2.3-1. Aquifer specific yield values.

Aquifer name	Reference	Specific yield
Wilcox Aquifer	Young and others (2018)	0.1
Carrizo Aquifer	Young and others (2018)	0.15
Queen City Aquifer	Young and others (2018)	0.1
Sparta Aquifer	Young and others (2018)	0.1
Yegua Aquifer	Deeds and others (2010)	0.15

With fields for area, saturated thickness, and specific yield attributed, we were able to multiply them together to calculate groundwater volumes in acre-feet for each aquifer grid cell. An example of the Field Calculator syntax for the Sparta Sand reads:

!Area! * !SPSTK! * !SPSY!

Random cells were then selected to have their attribute calculations checked by hand for quality assurance. An example cells for the Sparta Sand outcrop and subcrop are shown below (Figure 13.2.3-1). The cells were attributed with the salinity class using geological formation salinity class polygons. Brackish groundwater production zone designations can be applied when this work is completed in the future. With the entire attribute table populated, we then used the Summary Statistics tool to export tables containing the sum of all the groundwater values from individual cells into the entire groundwater volume per aquifer, salinity class, and administrative boundaries.

GSE	Area	spps	SPOTC	SPSTK	SPSY	SP_h2o_vol	SPSZ	BGPZ	spbe	sptk	spns	spswle	TKxSYxA	GRID_ID
383	1.434807	31	O	23	0.1	3.300056	fr		299	84	26	374	12.052379	1254690
388	1.434807	31	S	27	0.1	3.873979	fr		295	87	27	382	12.482821	1254691
393	1.434807	31	S	28	0.1	4.01746	fr		291	90	28	381	12.913263	1254692
389	1.434807	29	O	23	0.1	3.300056	fr		302	87	25	380	12.482821	1256087
390	1.434807	29	O	24	0.1	3.443537	fr		299	91	26	381	13.056744	1256088
394	1.434807	31	S	27	0.1	3.873979	fr		295	87	27	382	12.482821	1256089

Figure 13.2.3-1. Sparta Sand GRID_ID cells 1254692 and 1256087 (both highlighted in yellow) show attributes used for volume calculations. GRID_ID 1254692 is in the subcrop so the saturated thickness [SPSTK] is equal to the feet of net sands [spns], 28 feet. GRID_ID 1256087 is in the outcrop ([SPOTC] = "O"). Therefore [SPSTK] = ([spswle]-[spbe]) * [spps] or 23 = (380-302) * 29/100. For both cells [SP_h2o_vol] = [Area]*[SPSTK]*[SPSY].

13.3 List of reports performed in the study area.

County-wide hydrological studies by the TWDB (and predecessor agencies), the U.S. Geological Survey, and other agencies began in 1932 for the study area:

- Alexander and White (1966): Atascosa County
- Anders (1957): Wilson County
- Anders (1960): Karnes County
- Arnow (1959): Bexar County
- Austin (1954): Bastrop County
- Follett (1966): Caldwell County
- Follett (1970): Bastrop County
- Klemm and others (1976): Atascosa, Bexar, Caldwell, Dimmit, Frio, Gonzales, Guadalupe, Karnes, La Salle, Live Oak, McMullen, Maverick, Medina, Uvalde, Webb, Wilson and Zavala counties
- Lonsdale (1935): Atascosa and Frio counties
- Rogers (1967): Fayette County
- Sellards and others (1932): Texas
- Shafer (1965): Gonzales County
- Shafer (1966): Guadalupe County
- Sundstrom and Follet (1950): Atascosa
- Thompson (1966): Lee County
- Thorkildsen and Price (1991): Bastrop, Brazos, Burleson, Caldwell, Falls, Fayette, Freestone, Gonzales, Grimes, Lee, Leon, Limestone, Madison, Milam, Navarro, Robertson, and Williamson counties

Kreitler and others (2013) evaluated aquifer geochemistry in Groundwater Management Areas 11, 12, and 13. Hutchison and others (2009) compiled articles on the aquifers of the upper coastal plains.

The development of computer-based groundwater models of the study area aquifers began in 1983:

- Deeds and others (2003): Southern Carrizo-Wilcox Aquifer, Groundwater Availability Model
- Deeds and others (2010): Yegua-Jackson Aquifer, Groundwater Availability Model
- Dutton (1999): Carrizo-Wilcox Aquifer, Central Texas
- Dutton and others (2003): Central Carrizo-Wilcox Aquifer, Groundwater Availability Model
- Fogg and others (1983): Wilcox Group, Oakwood Dome, East Texas
- Fryar and others (2003): Northern Carrizo-Wilcox Aquifer, Groundwater Availability Model

- Kelley and others (2004): Queen City and Sparta Aquifers, added to the three Carrizo-Wilcox models, Texas
- Thorkildsen and others (1989): Carrizo-Wilcox Aquifer, Colorado Basin

Groundwater resource studies (including saline resources) in the study area began in 1956 in the study area:

- Winslow and Kister (1956): Texas
- Core Laboratories (1972): Texas
- Duffin (1974): Wilcox, Austin, Edwards, Glen Rose, and Travis Peak, San Antonio area
- Banerji and others (2019): Wilcox, Carrizo, Queen City, and Sparta aquifers, south Texas
- Hamlin and de la Rocha (2015): Carrizo-Wilcox Aquifer, South Texas
- HDR Engineering (2004): Carrizo Aquifer, southern Gonzales County
- HDR Engineering (2008): Wilcox Aquifer, Bexar, Guadalupe, and Wilson counties
- LBG-Guyton Associates (2006): Wilcox Aquifer, southern Bexar County
- LBG-Guyton Associates (2007): Wilcox Aquifer, Gonzales and Wilson counties
- Payne (1968): Sparta Aquifer, Texas and adjacent states
- Wise (2014): Queen City and Sparta aquifers, Atascosa and McMullen counties

Studies of the geological formations in the study area are too numerous to list, however the following are of particular significance:

- Ayers and Lewis, 1985
- Brown and Loucks, 2009
- Bulling and Breyer, 1989
- Davidson and others, 2009
- Dingus and Galloway, 1990
- Duffin and Elder, 1979
- Dutton, 2016
- Dutton and Nicot, 2006
- Dutton and Loucks, 2014
- Eargle, 1968
- Fisher, W., 1961
- Fisher, R., 1982
- Fogg, 1980
- Fogg and Blanchard, 1986
- Galloway, 1989a and 1989b
- Galloway and others, 1988, 1994, 2000

- George, 2009
- George and others, 2011
- Guevara and Garcia, 1972
- Harris, 1965
- Henry and others, 1980
- Kelley and others, 2009
- Klemt and others, 1976
- Knox and others, 2009
- Mace and Smyth, 2003
- Mace and others, 2000
- Miller, 1989
- Pearson and White, 1967
- Reedy and others, 2009
- Ricoy and Brown, 1977
- Sams, 1990 and 1991
- Sellards and others, 1932
- Xue, 1994
- Xue and Galloway, 1993 and 1995

Geologic cross-sections within the study area were prepared by many agencies starting in the 1950s:

- Alexander and White (1966): Atascosa County
- Anders (1957): Wilson County
- Anders (1960): Karnes County
- Arnow (1959): Bexar County
- Ayers and Lewis (1985): Wilcox Group and Carrizo Sand, east-central Texas
- Baker (1979): Gulf Coast Aquifer, Texas
- Dodge and Posey (1981): Tertiary Formations, Gulf Coast, Texas
- Follett (1966): Caldwell County
- Follett (1970): Bastrop County
- Hargis (2010): Wilcox Group, Wilson and adjacent areas of Bexar and Guadalupe counties
- Harris (1965): La Salle and McMullen counties
- Klemt and others (1976): Atascosa, Bexar, Caldwell, Dimmit, Frio, Gonzales, Guadalupe, Karnes, La Salle, Live Oak, McMullen, Maverick, Medina, Uvalde, Webb, Wilson and Zavala counties
- Knox and others (2007): Yegua-Jackson Aquifer, Texas

- LBG-Guyton Associates (2006): Wilcox Aquifer, southern Bexar County
- Rogers (1967): Fayette County
- Shafer (1965): Gonzales County
- Shafer (1966): Guadalupe County
- Thorkildsen and Price (1991): Carrizo-Wilcox Aquifer, central Texas
- Young and others (2018): Groundwater Management Area 12

13.4 BRACS Database

All point-based well and geophysical well log information for this study is managed in the BRACS Database using Microsoft® Access® 2016. When spatial analysis is required, copies of information are exported into ArcGIS® version 10.2.2. Information developed in GIS is then imported back to the BRACS Database and the tables are updated accordingly. Although this approach may be cumbersome, it takes advantage of the strengths of each software. The study also relied on other software for specific tasks, including Microsoft® Excel®, IHS Kingdom®, and Schlumberger Blueview® (for geophysical well log analysis).

For the study, we assembled information from external agencies and updated these databases frequently. Each of these supporting databases is maintained in Microsoft® Access® and GIS files were developed for spatial analysis and well selection. Many of the database objects were built from scratch or were redesigned to meet project objectives. Data from external agencies or projects were available in many different data designs, so establishing a common design structure proved beneficial in leveraging information compiled by other groups.

The BRACS and supporting databases are fully relational. Data fields common to multiple datasets have been standardized in data type and name with lookup tables shared between all databases. Database object names use a self-documenting style that follows the Hungarian naming convention (Novalis, 1999). The volume of project information required us to develop comprehensive data entry and analysis procedures (coded as tools) that were embedded on forms used to display information. Visual Basic for Applications® is the programming language used in Microsoft® Access®, and most code was written at the Microsoft® ActiveX® Data Objects level with full code annotation. The code for geophysical well log resistivity analysis was specifically designed with a custom BRACS class object to support a rapid analysis of information with the benefit of only appending data when the user approves the results.

The BRACS Database is documented in a data dictionary (Meyer, 2020) which is available with the public version of the BRACS Database from the TWDB website. We develop several custom tables and forms for each study and incorporate these into the BRACS Database and add these tables to the data dictionary in an appendix after study completion.

13.4.1 Table relationships

The BRACS Database contains 20 primary tables of information (Figure 13.4.1-1), 33 lookup tables, tables designed for GIS export, custom study tables, and many supporting tables for analysis purposes. A brief description of each of the primary tables is provided in this section. Lookup tables provide control on data entry codes or values for specific data fields (for example, a county lookup table with all 254 county names in Texas). The tables for GIS export are copies of information obtained from one or more tables and in some cases are reformatted to meet GIS analysis requirements. These tables are custom tailored to meet study needs and will not be discussed further.

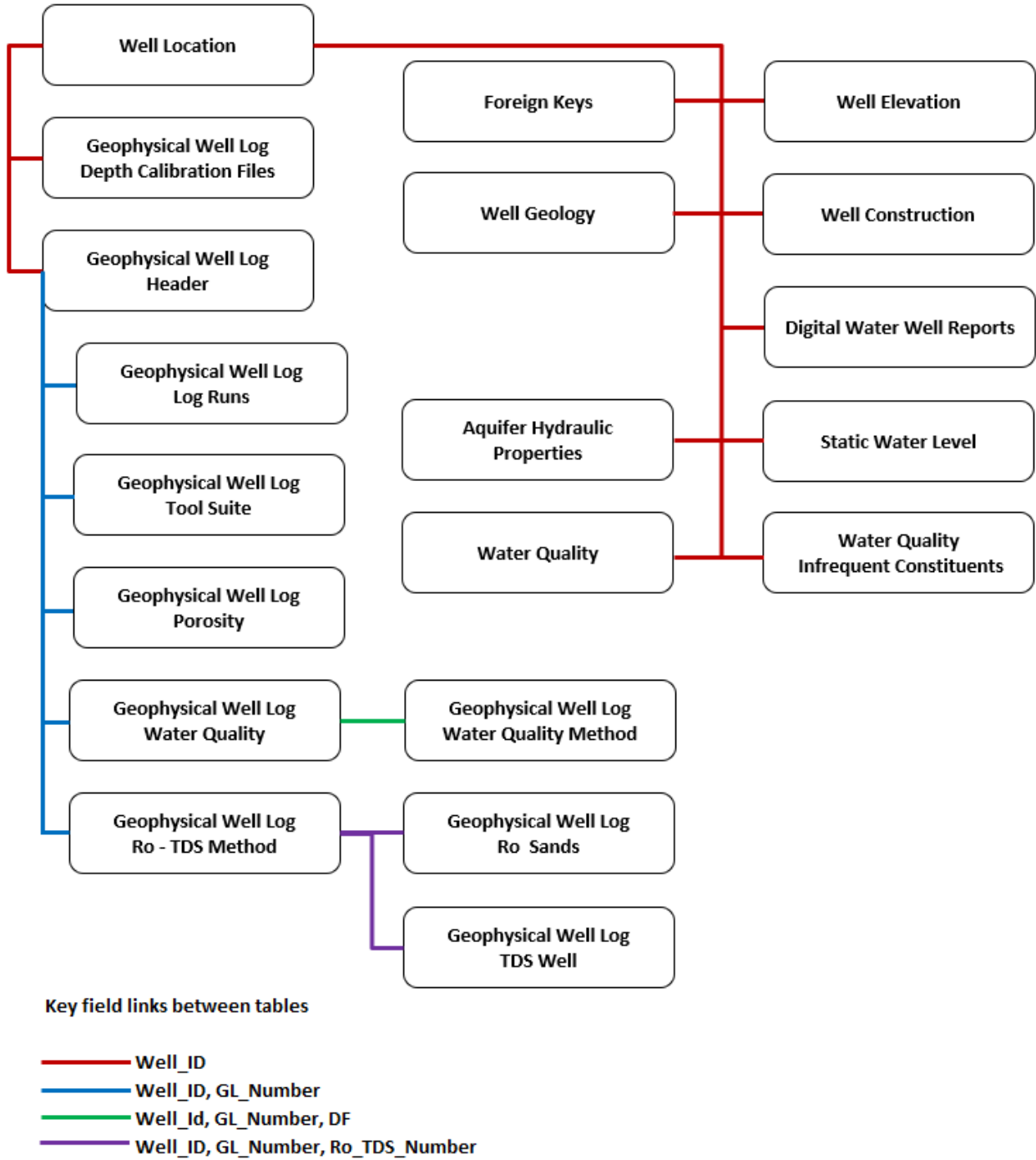


Figure 13.4.1-1. BRACS Database table relationships. Each rectangle represents a primary data table. The lines connecting the tables represent key fields: red represents the primary key well_id, blue represents the second key, green represents the third key, and purple represents the fourth key. New well records must be appended to the well location table to set the unique well_id. The tables, fields, and key fields are described in more detail in Meyer (2020).

A fully relational database design has information organized into tables based on a common theme. Information must be segregated into separate tables for each one-to-many data relationship. For example, one well may have many well screens with unique top and bottom depth values; each well screen constitutes one record. Tables are linked by key fields. The field well id is the primary key field for every table in the BRACS Database. For each one-to-many relationship at least one additional key field is required. Key fields are shown with colored lines in Figure 13.4.1-1.

Well locations

The table tblWell_Location contains one record for each well record in the BRACS Database and is assigned a unique integer in the well_id key field. The well_id field links all tables together. This table contains information such as well owner, well depth(s), location attributes (such as latitude and longitude), source of well information, county name, and date drilled.

Well elevation

The table tblBracs_Elevation has zero to many records for well site elevation. This table principally contains an elevation derived from a digital elevation model (DEM) with a 30-meter grid cell and eventually a 10-meter grid cell. All elevations used in this study used the 30-meter digital elevation model value.

Foreign keys

The table tblBracs_ForeignKey has zero to many unique well identification names or numbers assigned to it (for example, state well number and American Petroleum Institute number). These identifiers, known as foreign keys, permit database linkage to the supporting databases developed from external agencies and other TWDB studies. The table contains hyperlinks for additional documents from the Groundwater Database, Submitted Driller's Report Database, and USGS well data.

Digital well reports

The table tblBracsWaterWellReports contains zero to many records for digital copies of water well reports and miscellaneous records including oil and gas well scout tickets. The purpose of this table is to track the digital file names, file types, and hyperlinks to the documents.

Geophysical well logs

Information on the digital geophysical well logs is recorded in the table tblGeophysicalLog_Header. This includes the type of digital file, digital file name, data hyperlink to the log image, and well log parameters such as mean annual surface temperature at the well site. The well log parameters are only recorded if the well log is to be used for resistivity analysis for interpreted total dissolved solids.

Digital geophysical well logs can be downloaded directly from the web application Water Data Interactive (www3.twdb.texas.gov/apps/waterdatainteractive/groundwaterdataviewer). The table also has a hyperlink to download the log directly from the Cloud when using the public version of the BRACS Database. Stakeholders needing access to the entire log collection can contact TWDB for instructions.

Many geophysical logs have an associated depth calibration file used for geological analysis in software such as IHS Kingdom[®]. This information is recorded in the table `tblGeophysicalLog_DepthCalibrated`. The log and calibration file are stored in a separate folder schema. Stakeholders can contact TWDB for instructions on accessing this data.

Each geophysical well log may have one or more tools used to record subsurface parameters. This information is recorded in the table `tblGeophysicalLog_Suite`. Each tool name and its start and bottom depth values in units of feet below ground surface are recorded in this table.

A geophysical well log may be collected during different drilling stages (runs) within specific depth intervals. Each log run will usually have different drilling mud and temperature parameters. These parameters are recorded in the table `tblGeophysicalLog_Header_LogRuns`.

The results from resistivity analysis for interpreted total dissolved solids are recorded in several tables. Evaluating more than one depth interval per well necessitated designing the table `tblGeophysicalLog_WQ` to hold the depth of formation, temperature, and geological formation name for that interval. Evaluating more than one resistivity technique per depth interval dictated designing the table `tblGeophysicalLog_WQ_Method` to hold the analysis results including interpreted total dissolved solids, log correction values, method used, geophysical well log used, and a multitude of intermediate values.

One log analysis technique involves the comparison of log resistivity versus total dissolved solids concentration named the Ro-TDS Method. This information is placed in the following tables: `tblBRACS_GL_Analysis_Ro_TDS_Main`, `tblBRACS_GL_Analysis_Ro_Sands`, and `tblBRACS_GL_Analysis_TDS_Well`. These tables record the resistivity – water sample data pairs, the sands and their respective resistivity values, and the total dissolved solids concentration sample results for all wells used in the analysis.

Geophysical well log analysis is used to determine the porosity of specific geologic intervals. This information is recorded in the table `tblGeophysicalLog_Porosity`.

Well geology

The descriptions of rock types reported on drillers' well logs, simplified lithologic descriptions, stratigraphic picks, hydrochemical (salinity) classes, and faults are all contained in the table `tblWell_Geology`. Each record contains a top and bottom depth, thickness of the unit, top and bottom elevations, source of data, and a value for type of geologic pick (for example, lithologic, stratigraphic, or hydrogeologic). The latter field permits the storage of all this information in one table and the ability to view the information in one data entry form.

Well construction

Well casing and screen information is contained in the table `tblBracs_Casing`. This table design is similar to the original well-casing table in the Groundwater Database and contains top and bottom depths for casing and screen.

Water quality

Two tables contain the results of water quality analyses recorded for wells that are not in the Groundwater Database: `tblBracsWaterQuality` and `tblBracsInfrequentConstituents`. The table designs are similar to the original tables in the Groundwater Database.

All water quality records in the study area were appended to the tables tblBRACS_PE_sTx_MasterWaterQuality and tblBracs_PE_sTx_WQ_Radionuclide. These tables include records obtained from the Groundwater Database and records obtained from research for wells in the BRACS Database.

Static water level

Static water level information is contained in the table tblBRACS_SWL. The table design is similar to its equivalent in the original Groundwater Database. Information on dates, water levels, and source of measurement are recorded in the table.

Aquifer hydraulic properties

Information from existing aquifer tests conducted for all BRACS studies is contained in the table tblBRACS_AquiferTestInformation. The table contains fields for hydraulic conductivity, transmissivity, specific yield, storage coefficient, drawdown, pumping rate, specific capacity, the types of units for each measurement, date of analysis, source of information, and remarks. If an analysis included the top and bottom depths of the screen, well depth, and static water level, it was captured in this table in case the values differed from what is presented in the casing table (test may have been performed before total depth of the well was reached). The length of aquifer tests, values for drawdown versus recovery, pumping and static water levels, and two analysis remarks fields complete the table design. If additional data is listed in published reports, such as Report 98 (Myers, 1969), the page number of that report is listed.

Study area records were placed in the table tblUCPC_AquiferTestInformation.

Custom study tables

The aquifer determination table contains records of every well used in the study, with some wells located outside of the study area limits used to help constrain GIS raster surfaces. The purpose of this table is to assign well attributes to the correct geological formation(s) by comparing screen top and bottom depths to geological formation top and bottom depths.

The results of the aquifer determination process are presented in table tblAquiferDetermination_PaleoceneEocene_sTx. This table includes fields for the new aquifer decision, Groundwater Database aquifer code assigned to the well (if any), well and screen depths, whether the well has multiple screens, well owner, and latitude/longitude coordinates. Fields for geological formation top and bottom depths derived from GIS raster surfaces and the aquifer region code are listed.

The stratigraphic table contains records of every well with a stratigraphic pick used in the study, with some wells located outside of the study area limits used to help constrain GIS raster surfaces. The purpose of this table is to extract and process stratigraphic picks into a table that is exported to GIS for geological surface preparation. Stratigraphic depths and elevations are corrected for Kelly bushing height when this table is created.

The results of the stratigraphic table processing are presented in table gBRACS_ST_PE_sTx. The table includes well identification numbers, latitude and longitude, elevation, and fields for every study area geological formation with stratigraphic data in depth and elevation format.

Three tables were prepared to hold data for study area formation net sand analysis, with some wells outside of the study area limits used to help constrain GIS raster surfaces. One table contains records of every lithologic unit containing sand or a mixture of sand and clay (tblWell_Geology_NetSand_PaleoceneEocene_sTx_Temp). Another table summarizes the net sand and sand percent values per well per geological formation (tblWell_Geology_NetSand_PaleoceneEocene_sTx). The third table documents if a well is used for the GIS preparation of net sand raster files per geological formation (tblWell_Geology_NetSand_PaleoceneEocene_sTx_Well_Decisions).

13.5 Geographic Information System analysis and datasets

Many GIS datasets were created for this study and each of the GIS files prepared for this BRACS study is available for download from the Texas Water Development Board website. Many of the GIS techniques used to build the files are explained in this appendix and noted in the GIS file metadata. ArcGIS® 10.2 and the Spatial Analyst® extension software by Environmental Systems Research Institute, Inc. (ESRI) were used to create the GIS files.

Each point file is in the ArcGIS® shapefile format. Point files of well control used for general purposes are originally projected as a geographic projection North America with the North American Datum 1983 as the horizontal datum. Point files are re-projected to a TWDB Groundwater Availability Model projection and the North American Datum 1983 as the horizontal datum.

All surface files (for example elevation, depth, net sand) are in the ArcGIS® raster integer grid file format with a Groundwater Availability Model projection and the North American Datum 1983 as the horizontal datum. All raster files are snapped (coincident cell boundaries) to the study snap grid raster with a cell size of 250 by 250 feet.

Polygon and polyline files are in the ArcGIS® shapefile format with a Groundwater Availability Model projection and the North American Datum 1983 as the horizontal datum.

All well records are managed in the Microsoft® Access® BRACS Database. Well records are queried from the database and imported into ArcGIS® for spatial analysis. When new attributes are obtained for a well using ArcGIS® the information is imported into Microsoft® Access® and the well record is updated.

Every well record in each supporting database used for this study contains latitude and longitude coordinates in the format of decimal degrees with a North American Datum of 1983. These well records are imported into ArcGIS® and georeferenced in a geographic coordinate system North America with the North American Datum 1983 as the horizontal datum. A point shapefile was then saved in a working directory. Every well record then had an elevation assigned from the U.S. Geological Survey seamless 30-meter digital elevation model using the ArcGIS® ArcToolbox (Spatial Analyst® Tools, Extraction, and Extract Values to Points). The dbase file from each shapefile was then imported into Microsoft® Access® and the elevation data updated to each well record, along with date, method, vertical datum, and agency attributes. Each well record also recorded the kelly bushing height when available. GIS point files subsequently created for each geological formation and salinity class were corrected for kelly bushing height and elevation.

In many cases, new wells were plotted in ArcGIS® and the latitude, longitude, and elevation were determined and appended to the database tables manually. The Original Texas Land Survey obtained from the Railroad Commission of Texas was the principal base map used to plot well locations; county highway maps and topographic maps were used on occasion for original well locations in some of the supporting databases.

13.5.1 GIS filename codes

ArcGIS® raster files are limited to 12 characters, necessitating the development of a file naming scheme for all GIS files created for BRACS studies. The full list of codes can be found in BRACS Database table tblGisFile_NamingConventions and a study-specific list of codes is presented in Table 13.5.1-1.

Table 13.5.1-1. GIS filename codes applied to the Upper Coastal Plains Central BRACS study.

Code	Code type	Code description
BRACS	General	Brackish Resources Aquifer Characterization System
GCD	General	Groundwater Conservation District
GMA	General	Groundwater Management Area
GWDB	General	Groundwater Database
PWS	General	Public Water System
RWPA	General	Regional Water Planning Area
SWP	General	State Water Plan
TWDB	General	Texas Water Development Board
UCPC	BRACS Study	Upper Coastal Plains – Central (project acronym)
wx	Stratigraphic	Wilcox Group
cz	Stratigraphic	Carrizo Sand
r	Stratigraphic	Reklaw Formation
qc	Stratigraphic	Queen City Sand
w	Stratigraphic	Weches Formation
sp	Stratigraphic	Sparta Sand
cm	Stratigraphic	Cook Mountain Formation
y	Stratigraphic	Yegua Formation
j	Stratigraphic	Jackson Group
ns	Sand analysis	Net sand in cumulative feet
td	Value	Top depth in feet below ground surface
te	Value	Top elevation in feet relative to mean sea level
bd	Value	Bottom depth in feet below ground surface
be	Value	Bottom elevation in feet relative to mean sea level
dem	Value	Digital Elevation Model, ground surface elevation in feet relative to mean sea level
tk	Value	Isochore thickness in feet
swl	Value	Static water level
swle	Value	Static water level elevation, in feet relative to mean sea level
tds	Value	Total dissolved solids in milligrams per liter
i	Raster data value	Integer

Code	Code type	Code description
n or nd	Raster data value	Null data values are set
snap	Snap raster	Snap raster file used to snap all project cells into conformable alignment
250K	Data type	Shapefile was digitized from a 1:250,000 original
AD	Data type	Aquifer determination
AT	Data type	Aquifer test
calc	Data type	Calculated
con	Data type	Contour
depo	Data type	Depositional
ext	Data type	Extent
ft	Data type	Foot or feet
meas	Data type	Measured
MWQ	Data type	Master water quality
otc	Data type	Outcrop
pt	Data type	Point
pl	Data type	Polyline
pg	Data type	Polygon
sbc	Data type	Subcrop
wxsb	Data type	Wilcox Group – Simsboro Formation

These codes are used consistently in all digital files used in the project: BRACS Database field names, query variables, export files to GIS, GIS point, polyline, polygon, and raster files. Each code is separated from the next code with an underscore character. For example, the code wx_bd_trim refers to the Wilcox Group bottom depth created by the topo to raster surface interpolation as an integer value and masked.

13.5.2 Study GIS files organized by folder structure.

Table 13.5.2-1. GIS files for regional geology and the extent of mapped stratigraphic units in the study.
Folder structure: BRACS_UCPC_GIS_DATA\ucpc_Geology.

Formation name	File type	Point file name	Polyline file name	Polygon file name	Raster file name
Wilcox Group	Extent			UCPC_wx_extent_pg.shp	wx_ext_ndi
	Outcrop			UCPC_wx_otc_pg.shp	wx_otc_ndi
	Simsboro Formation outcrop			UCPC_wxsb_otc_pg.shp	
	Subcrop				wx_sbc_ndi
	Yoakum Canyon extent		UCPC_YoakumCanyon_pl.shp		
	Depositional axis		Fisher_McGowan_1967_DepoSystemWilcox_axis_pl.shp		
	Mapped faults in outcrop		UCPC_Fault250K_WXotc.shp		
Carrizo Sand	Extent			UCPC_cz_extent_pg.shp	cz_ext_ndi
	Outcrop			UCPC_cz_otc_pg.shp	cz_otc_ndi
	Subcrop				cz_sbc_ndi
	Depositional axis		Hamlin_1988_DepoSystemsCarrizo_axis_pl.shp		
	Mapped faults in outcrop		UCPC_Fault250K_CZotc_pl.shp		
Reklaw Formation	Extent				r_ext_ndi
	Outcrop			UCPC_r_otc_pg.shp	r_otc_ndi
Queen City Sand	Extent			UCPC_qc_extent_pg.shp	qc_ext_ndi
	Outcrop			UCPC_qc_otc_pg.shp	qc_otc_ndi
	Subcrop				qc_sbc_ndi
	Depositional axis		Guevarra_Garcia_1972_DepoSystemsQueenCity_axis_pl.shp		
	Mapped faults in outcrop		UCPC_Fault250K_QCotc_pl.shp		
Weches Formation	Extent				w_ext_ndi
	Outcrop			UCPC_w_otc_pg.shp	w_otc_ndi

Formation name	File type	Point file name	Polyline file name	Polygon file name	Raster file name
Sparta Sand	Extent			UCPC_sp_extent_pg.shp	sp_ext_ndi
	Outcrop			UCPC_sp_otc_pg.shp	sp_otc_ndi
	Subcrop				sp_sbc_ndi
	Depositional axis		Ricoy_Brown_1977_DepoSystemsSparta_axis_pl.shp		
	Mapped Faults in outcrop		UCPC_Fault250K_SPotc_pl.shp		
Cook Mountain Formation	Extent				cm_ext_ndi
	Outcrop			UCPC_cm_otc_pg.shp	cm_otc_ndi
Yegua Formation	Extent			UCPC_y_extent_pg.shp	y_ext_ndi
	Outcrop			UCPC_y_otc_pg.shp	y_otc_ndi
	Subcrop				y_sbc_ndi
	Mapped Faults in outcrop		UCPC_Fault250K_Yotc_pl.shp		
Jackson Group	Extent			UCPC_j_extent_pg.shp	j_ext_ndi
Regional Geology	Aquifer determination regions			UCPC_aquifer_determination_regions_pg.shp	
	Ewing (1991)		UCPC_Ewing_1990_faults_pl.shp		
			UCPC_Normal_Fault_DownToRight_pl.shp		
			UCPC_Normal_Fault_WithoutDirections_pl.shp		
			UCPC_Pinchout_pl.shp		
		UCPC_VolcanicCenter_pt.shp			
Geologic Atlas of Texas		UCPC_Fault250K_pl.shp	UCPC_GAT_RockUnitPoly250K_pg.shp		

Table 13.5.2-2. GIS files for the lithologic analysis in the study area. Folder structure: BRACS_UCPC_GIS_DATA\ucpc_Lithology.

Formation name	File type	Point file name	Polyline file name	Raster file name
Wilcox Group	Net sand	UCPC wxns pt.shp	UCPC wxns con 400ft pl.shp	ucpc wxns
	Outcrop control	UCPC_wxns_otc_zero_pt.shp		
	Guide control	UCPC wxns guide pt.shp	UCPC wxns guide con 500ft pl.shp	
			UCPC_wxns_guide_con_1000ft_pl.shp	
Interpolated net sands without contour guides			wxns_noguide.tif	
Carrizo Sand	Net sand	UCPC czns pt.shp	UCPC czns con 200ft pl.shp	ucpc czns
	Outcrop control	UCPC_czns_otc_zero_pt.shp		
	Guide control	UCPC_czns_guide_pt.shp		
Queen City Sand	Net sand	UCPC qcns pt.shp	UCPC qcns con 50ft pl.shp	ucpc qcns
	Outcrop control	UCPC_qcns_otc_zero_pt.shp		
Sparta Sand	Net sand	UCPC spns pt.shp	UCPC spns con 20ft pl.shp	ucpc spns
	Outcrop control	UCPC_spns_otc_zero_pt.shp		
Yegua Formation	Net sand	UCPC y ns pt.shp	UCPC y ns con 100ft pl.shp	ucpc y ns
	Outcrop control	UCPC_y_ns_otc_zero_pt.shp		

Table 13.5.2-3. GIS files for geological formation salinity class maps in the study. Folder structure: BRACS_UCPC_GIS_DATA\ucpc_SalinityClass.

Formation name	File type	Point file name	Polygon file name
Wilcox Group	Salinity class	UCPC_salinity_class_wx_pt.shp	UCPC_salinity_class_wx_pg.shp
	Measured water quality	UCPC_TDSmeas_wx_pt.shp	
	Calculated water quality	UCPC_TDScalc_wx_pt.shp	
Carrizo Sand	Salinity class	UCPC_salinity_class_cz_pt.shp	UCPC_salinity_class_cz_pg.shp
	Measured water quality	UCPC_TDSmeas_cz_pt.shp	
	Calculated water quality	UCPC_TDScalc_cz_pt.shp	
Queen City Sand	Salinity class	UCPC_salinity_class_qc_pt.shp	UCPC_salinity_class_qc_pg.shp
	Measured water quality	UCPC_TDSmeas_qc_pt.shp	
	Calculated water quality	UCPC_TDScalc_qc_pt.shp	
Sparta Sand	Salinity class	UCPC_salinity_class_sp_pt.shp	UCPC_salinity_class_sp_pg.shp
	Measured water quality	UCPC_TDSmeas_sp_pt.shp	
	Calculated water quality	UCPC_TDScalc_sp_pt.shp	
Yegua Formation	Salinity class	UCPC_salinity_class_y_pt.shp	UCPC_salinity_class_y_pg.shp
	Measured water quality	UCPC_TDSmeas_y_pt.shp	
	Calculated water quality	UCPC_TDScalc_y_pt.shp	
General	Salinity class template		UCPC_salinity_class_template_pg.shp
	Master water quality	UCPC_MWQ_pt.shp	

Table 13.5.2-4. GIS files for geologic formation surfaces. Folder structure: BRACS_UCPC_GIS_DATA\ucpc_Stratigraphy.

Formation name	File type	Point file name	Polyline file name	Raster file name
Wilcox Group	Top elevation		UCPC_wxte_con_1500ft_pl.shp	ucpc_wxte
	Bottom elevation	UCPC_wxbe_pt.shp	UCPC_wxbe_con_1500ft_pl.shp	ucpc_wxbe
	Top depth		UCPC_wxtd_con_1500ft_pl.shp	ucpc_wxtd
	Bottom depth		UCPC_wxbd_con_1500ft_pl.shp	ucpc_wxbd
	Thickness		UCPC_wxtdk_con_500ft_pl.shp	ucpc_wxtdk
	Outcrop control	UCPC_wxbe_DEM_pt.shp		
Carrizo Sand	Top elevation		UCPC_czte_con_1500ft_pl.shp	ucpc_czte
	Bottom elevation	UCPC_czbe_pt.shp	UCPC_czbe_con_1500ft_pl.shp	ucpc_czbe
	Top depth		UCPC_cztd_con_1500ft_pl.shp	ucpc_cztd
	Bottom depth		UCPC_czbd_con_1500ft_pl.shp	ucpc_czbd
	Thickness		UCPC_cztdk_con_250ft_pl.shp	ucpc_cztdk
	Outcrop control	UCPC_czbe_DEM_pt.shp		
Reklaw Formation	Top elevation		UCPC_r_te_con_1500ft_pl.shp	ucpc_r_te
	Bottom Elevation	UCPC_r_be_pt.shp	UCPC_r_be_con_1500ft_pl.shp	ucpc_r_be
	Top Depth		UCPC_r_td_con_1500ft_pl.shp	ucpc_r_td
	Bottom Depth		UCPC_r_bd_con_1500ft_pl.shp	ucpc_r_bd
	Thickness		UCPC_r_tdk_con_100ft_pl.shp	ucpc_r_tdk
	Outcrop control	UCPC_r_be_DEM_pt.shp		
	Guide control	UCPC_r_be_guide_pt.shp		
Queen City Sand	Top elevation		UCPC_qcte_con_1500ft_pl.shp	ucpc_qcte
	Bottom elevation	UCPC_qcbe_pt.shp	UCPC_qcbe_con_1500ft_pl.shp	ucpc_qcbe
	Top depth		UCPC_qctd_con_1000ft_pl.shp	ucpc_qctd
	Bottom depth		UCPC_qcbd_con_1500ft_pl.shp	ucpc_qcbd
	Thickness		UCPC_qctdk_con_250ft_pl.shp	ucpc_qctdk
	Outcrop control	UCPC_qcbe_DEM_pt.shp		

Formation name	File type	Point file name	Polyline file name	Raster file name
	Guide control	UCPC_qcbe_guide_pt.shp		
Weches Formation	Top elevation		UCPC_w_te_con_1000ft_pl.shp	ucpc_w_te
	Bottom Elevation	UCPC_w_be_pt.shp	UCPC_w_be_con_1000ft_pl.shp	ucpc_w_be
	Top Depth		UCPC_w_td_con_1000ft_pl.shp	ucpc_w_td
	Bottom Depth		UCPC_w_bd_con_1000ft_pl.shp	ucpc_w_bd
	Thickness		UCPC_w tk_con_50ft_pl.shp	ucpc_w tk
	Outcrop control	UCPC_w_be_DEM_pt.shp		
	Guide control	UCPC_w_be_guide_pt.shp		
Sparta Sand	Top elevation		UCPC_spte_con_1000ft_pl.shp	ucpc_spte
	Bottom elevation	UCPC_spbe_pt.shp	UCPC_spbe_con_1000ft_pl.shp	ucpc_spbe
	Top depth		UCPC_sptd_con_1000ft_pl.shp	ucpc_sptd
	Bottom depth		UCPC_spbd_con_1000ft_pl.shp	ucpc_spbd
	Thickness		UCPC_sptk_con_100ft_pl.shp	ucpc_sptk
	Outcrop control	UCPC_spbe_DEM_pt.shp		
	Guide control	UCPC_spbe_guide_pt.shp		
Cook Mountain Formation	Top elevation		UCPC_cmte_con_1000ft_pl.shp	ucpc_cmte
	Bottom Elevation	UCPC_cmbe_pt.shp	UCPC_cmbe_con_1000ft_pl.shp	ucpc_cmbe
	Top Depth		UCPC_cmtd_con_1000ft_pl.shp	ucpc_cmtd
	Bottom Depth		UCPC_cmbd_con_1000ft_pl.shp	ucpc_cmbd
	Thickness		UCPC cmtk con 200ft pl.shp	ucpc cmtk
	Outcrop control	UCPC_cmbe_DEM_pt.shp		
	Guide control	UCPC_cmbe_guide_pt.shp		
Yegua Formation	Top elevation		UCPC_y_te_con_1000ft_pl.shp	ucpc_y_te
	Bottom elevation	UCPC_y_be_pt.shp	UCPC_y_be_con_1000ft_pl.shp	ucpc_y_be
	Top depth		UCPC_y_td_con_1000ft_pl.shp	ucpc_y_td

Formation name	File type	Point file name	Polyline file name	Raster file name
	Bottom depth		UCPC_y_bd_con_1000ft_pl.shp	ucpc_y_bd
	Thickness		UCPC y tk con 250 pl.shp	ucpc y tk
	Outcrop control	UCPC_y_be_DEM_pt.shp		
	Guide control	UCPC_y_be_guide_pt.shp		
Jackson Group	Bottom elevation	UCPC_j_be_pt.shp		
	Outcrop control	UCPC_j_be_DEM_pt.shp		

**Table 13.5.2-5. Study support GIS files. Folder structure:
BRACS_UCPC_GIS_DATA\ucpc_StudyAreaData.**

File type	Point file name	Polyline file name	Polygon file name	Raster file name
Project snap grid				ucpc_snap
Project elevation				ucpc_dem_ni
Project boundary		UCPC_study_area_pl.shp	UCPC_study_area_pg.shp	ucpc_extent
Aquifer determination	UCPC_AD_pt.shp			
BRACS well control	TWDB_BRACS_pt.shp			
GWDB well control	TWDB_GWDB_Wells_pt.shp			
Cross-sections	Cross_Section_pt.shp	Cross_Section_pl.shp		
Estimated cross-sections	Estimated_Cross_section_pt.shp	Estimated_Cross_section_pl.shp		
Cross-sections made from this study	UCPC_CrossSection_plates_pl.shp			
Existing desalination plants	UCPC_desal_existing_pt.shp			
Recommended desalination plants	UCPC_desal_recommended_plant_2017_SWP_pt.shp			
Public water supply boundary within the study area			UCPC_pws_inside_pg.shp	
Public water supply boundary outside the study area			UCPC_pws_outside_pg.shp	
Major Texas rivers		major_Texas_rivers_pl.shp		
Texas counties			TWDB_counties_GAM_pg.shp	
Texas groundwater conservation district within the study area			UCPC_GCD_pg.shp	
Texas groundwater conservation district outside the study area			UCPC_GCD_outside_pg.shp	
Texas groundwater management areas			GMA_pg.shp	
Texas regional water planning area			RWPA_pg.shp	
Texas cities			UCPC_cities_2014_txdot_pg.shp	

File type	Point file name	Polyline file name	Polygon file name	Raster file name
Texas cities within the study area			UCPC_cities_2014_txdot_inside_pg.shp	
Texas cities outside the study area			UCPC_cities_2014_txdot_outside_pg.shp	
U.S. highways		UCPC_us_highways_pl.shp		
Interstate highways		UCPC_interstate_highways_pl.shp		
State highways		UCPC_state_highways_pl.shp		
Figure feathering			UCPC_study_area_feathering_mask_pg.shp	
Study area universe			UCPC_universe_pg.shp	
Study area universe mask			UCPC_universemask_pg.shp	
Aquifer test data	UCPC_AT_pt.shp			

Table 13.5.2-6. Geological formation groundwater volume files. Folder structure: BRACS_UCPC_GIS_DATA\ucpc_Volume.

Formation name	File type	Point file name	Polyline file name	Polygon file name	Raster file name
Wilcox Group	Static water level	UCPC_wx_swl_pt.shp			wx_swle_otc
	Static water level outcrop control		UCPC_wx_swl_otc_zero_pl.shp		
	Volume grid	UCPC_master_grid_wx_pt.shp			
	Volumes by county	UCPC_WX_volumes_by_county.dbf			
	Volumes by GCD	UCPC_WX_volumes_by_GCD.dbf			
	Volumes by GMA	UCPC_WX_volumes_by_GMA.dbf			
	Volumes by RWPA	UCPC_WX_volumes_by_RWPA.dbf			
	Volumes by salinity class	UCPC_WX_volumes_by_salinity_class.dbf			
Carrizo Sand	Static water level	UCPC_cz_swl_pt.shp			cz_swle_otc
	Static water level outcrop control		UCPC_cz_swl_otc_zero_pl.shp		
	Volume grid	UCPC_master_grid_cz_pt.shp			
	Volumes by county	UCPC_CZ_volumes_by_county.dbf			
	Volumes by GCD	UCPC_CZ_volumes_by_GCD.dbf			
	Volumes by GMA	UCPC_CZ_volumes_by_GMA.dbf			
	Volumes by RWPA	UCPC_CZ_volumes_by_RWPA.dbf			
	Volumes by salinity class	UCPC_CZ_volumes_by_salinity_class.dbf			
Queen City Sand	Static water level	UCPC_qc_swl_pt.shp			qc_swle_otc
	Static water level outcrop control		UCPC_qc_swl_otc_zero_pl.shp		
	Volume grid	UCPC_master_grid_qc_pt.shp			
	Volumes by county	UCPC_QC_volumes_by_county.dbf			
	Volumes by GCD	UCPC_QC_volumes_by_GCD.dbf			
	Volumes by GMA	UCPC_QC_volumes_by_GMA.dbf			

Formation name	File type	Point file name	Polyline file name	Polygon file name	Raster file name
	Volumes by RWPA	UCPC_QC_volumes_by_RWPA.dbf			
	Volumes by salinity class	UCPC_QC_volumes_by_salinity_class.dbf			
Sparta Sand	Static water level	UCPC_sp_swl_pt.shp			sp_swle_otc
	Static water level outcrop control	UCPC_sp_swl_otc_zero_pt.shp			
	Volume grid	UCPC_master_grid_sp_pt.shp			
	Volumes by county	UCPC_SP_volumes_by_county.dbf			
	Volumes by GCD	UCPC_SP_volumes_by_GCD.dbf			
	Volumes by GMA	UCPC_SP_volumes_by_GMA.dbf			
	Volumes by RWPA	UCPC_SP_volumes_by_RWPA.dbf			
	Volumes by salinity class	UCPC_SP_volumes_by_salinity_class.dbf			
Yegua Formation	Static water level	UCPC_y_swl_pt.shp			y_swle_otc
	Static water level outcrop control		UCPC_y_swl_otc_zero_pl.shp		
	Volume grid	UCPC_master_grid_y_pt.shp			
	Volumes by county	UCPC_Y_volumes_by_county.dbf			
	Volumes by GCD	UCPC_Y_volumes_by_GCD.dbf			
	Volumes by GMA	UCPC_Y_volumes_by_GMA.dbf			
	Volumes by RWPA	UCPC_Y_volumes_by_RWPA.dbf			
	Volumes by salinity class	UCPC_Y_volumes_by_salinity_class.dbf			
General	Volume grid	UCPC_master_grid_pt.shp		UCPC_master_grid_pg.shp	

13.6 Raster interpolation documentation

Interpolation of values between known data points is a method to estimate and predict values where they don't currently exist on surfaces presumed to be continuous. This is an especially useful methodology when new data is expensive to obtain, such as in subsurface geologic mapping which would require drilling or seismic surveys. As useful as this tool is, there are many considerations and assumptions made. The reliability of the values estimated between known values is reliant on the homogeneity of the property or feature, predictive capabilities of the modeling, the density and distribution of the known values, and the scale and magnitude of variations in values. It is easier to predict the values of a smooth surface with few points than an erratic surface.

13.6.1 Stratigraphic surface interpolation

Create the input data

Combinations of source data were tested in creating modeled elevation surfaces for the nine geological formations in this study. The best results came from using (1) geological formation boundary polygons created from the Geologic Atlas of Texas (TWDB, 2007b) that we edited to remove surficial Quaternary alluvial deposits and conform to the study digital elevation model, (2) outcrop digital elevation model points derived by sampling the earth surface elevation at points generated at even intervals along the outcrop lines, and (3) stratigraphic elevations points exported and projected from the BRACS Database.

Geological formation boundaries

We edited the geological formation polygons in the study area to remove all surficial units (Quaternary, Tertiary, and water) to create continuous outcrop polygons for the formations in the study area. These edited polygons were as used to create geological formation extent shapefiles for selecting and clipping data. Section 6.5 discusses these aquifer determination polygons with their region codes.

Outcrop elevation points

Digital elevation model outcrop points were created along the updip outcrop line. We then used the Extract Values to Points tool to attribute the points with the elevation value from the study digital elevation model.

Stratigraphic elevation points

Stratigraphic picks are saved as depths in the BRACS Database. We used the kelly bushing height and surface elevation from the well location table to correct the stratigraphic depths and elevations for interpolation (refer to Section 6.3 for additional discussion). Interpolating elevations is more predictable since it only requires one variable (changes in subsurface topography) instead of the two variables represented by depth (changes in surface topography and changes in subsurface topography).

Creation and export of stratigraphic picks from the BRACS Database used these steps:

1. Database queries appended stratigraphic picks from study area counties (Atascosa, Bastrop, Bexar, Caldwell, Dewitt, Fayette, Gonzales, Guadalupe, Karnes, Lavaca, Lee, Live Oak, Williamson, and Wilson) with geological formation names (Jackson Group,

Yegua Formation, Cook Mountain Formation, Sparta Formation, Weches Formation, Queen City Formation, Reklaw Formation, Carrizo Formation, and Wilcox Group) into a study stratigraphic table (gBRACS_ST_PE_sTx) for export into GIS. Very specific formation name nomenclature is used for different studies to avoid unintentional comingling of stratigraphic picks from various studies. For example, this report uses “Sparta Sand” but the exact nomenclature used in the database is “Sparta Formation.”

2. Stratigraphic depth and elevations values were corrected with the Kelly bushing height and well site elevation to represent true depth below ground surface and elevation above mean sea level, respectively.
3. Exported the table from the BRACS Database as a dBase® IV file version.
4. Imported table into ArcGIS®. Used the tool “Make XY Event Layer” to create an event file.
5. Exported the event into to a shapefile in a Geographic Coordinate System North America with a North American Datum 83 horizontal datum.
6. Projected the shapefile into the custom TWDB Groundwater Availability Model projection.
7. Used GIS definition queries to extract geological formation picks into individual point shapefiles.

Refer to Figure 13.6.1-1 for an example of interpolation inputs from the Sparta Sand.

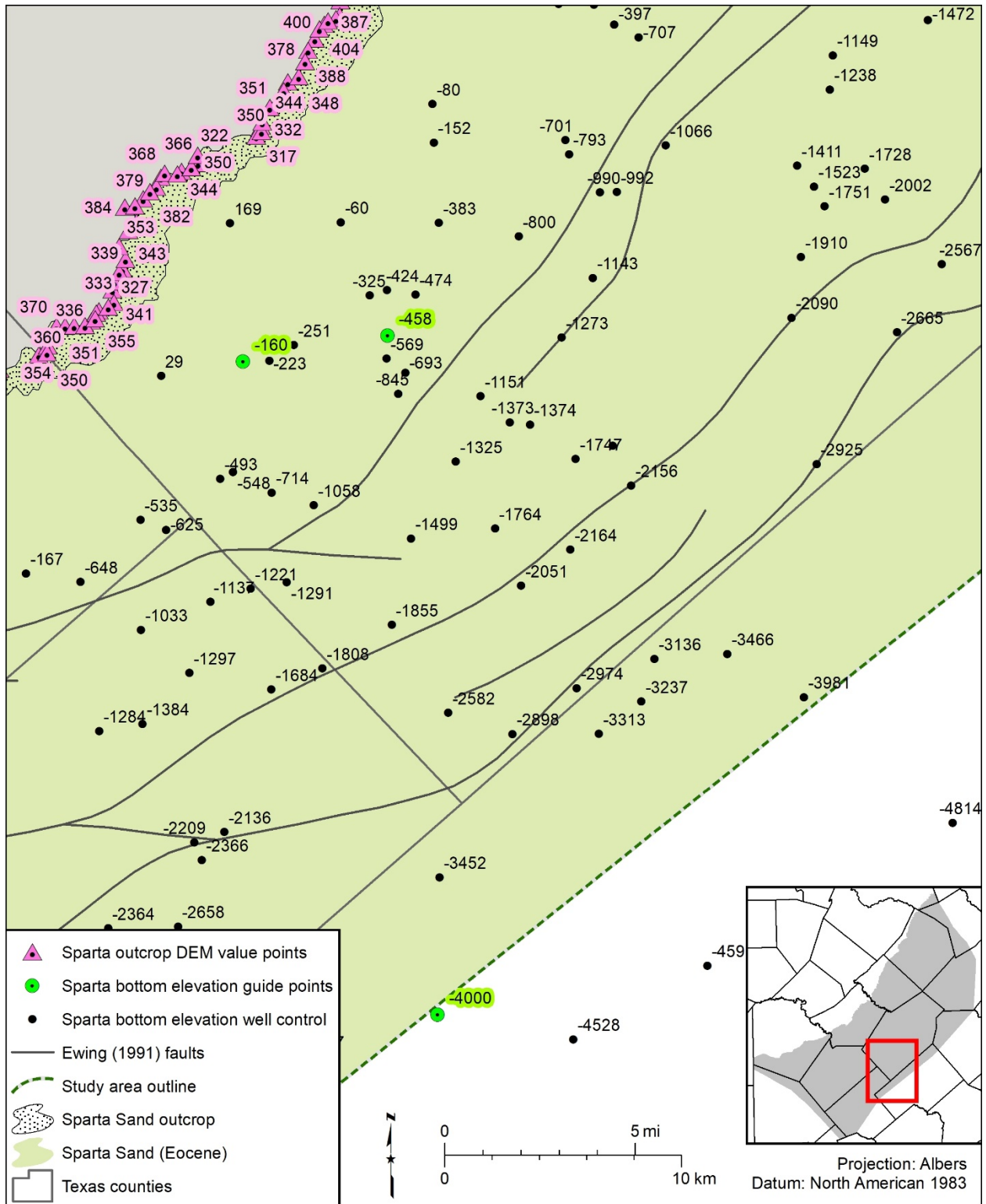


Figure 13.6.1-1. Sample of the point inputs to interpolate the bottom elevation surface for the Sparta Sand.

Predictive surface modeling using the Topo to Raster tool

Several surface modeling methods are available in ESRI's Advanced ArcGIS® 10.2.2 for Desktop (ArcGIS®, 2017). After creating and comparing raster surfaces created from stratigraphic depth values using ESRI's interpolation tools (Inverse Distance Weighted, Kriging, Natural Neighbor, Spline, and Topo to Raster) we selected the Topo to Raster tool. The Topo to Raster tool was designed for representation of surfaces modified by hydrologic processes. This tool allows the inclusion of points, polygons, and polylines as source data. There are also multiple parameters that can be set. To ensure the coincidence of the grid between the various rasters created in the study, four environmental parameters were always set with reference to the snap grid file (ucpc_snap): (1) output coordinate system, (2) extent, (3) snap grid, and (4) cell size. We did not use contour lines to preserve regional trends in the formation bottom rasters because these created striping interpolation artifacts in the formation thickness rasters. We did not use fault lines from the Geologic Atlas of Texas or the tectonic framework of Texas (Ewing, 1991) as "cliff" inputs for the interpolation because they resulted in errors, presumable because the available well control wasn't dense enough to represent and define the fault offsets.

Topo to Raster tool inputs for interpolating the bottom elevation rasters (where xx = geological formation abbreviation [for example, cz = Carrizo]):

1. Input feature data
 - a. UCPC_xx_be_pt.shp
 - i. Field: XX_B_E
 - ii. Type: PointElevation
 - b. UCPC_xx_be_DEM_pt.shp
 - i. Field: XX_B_E
 - ii. Type: PointElevation
 - c. UCPC_xx_be_guide_pt.shp*
 - i. *not needed for the bottom of the Jackson and Wilcox groups and the Carrizo Sand.
 - ii. Field: XX_B_E
 - iii. Type: PointElevation
 - d. UCPC_xx_extent_pg.shp
 - i. Field: none
 - ii. Type: Boundary
2. Output surface raster: xx_be_raw.
3. Output cell size: snap_ucpc (study snap grid raster).
4. Output Extent: snap_ucpc.
5. Margin in cells: 20.
6. Smallest z value to be used in interpolation (optional).
7. Largest z values to be used in interpolation (optional).
8. Drainage enforcement (optional): NO_ENFORCE.
9. Primary type of input data (optional): SPOT.

10. Maximum number of iterations (optional): 20.
11. Roughness penalty (optional).
12. Profile curvature roughness penalty (optional).
13. Discretization error factor (optional): 1.
14. Vertical standard error (optional): 0.
15. Tolerance 1 (optional): 0.
16. Tolerance 2 (optional): 200.

Steps to build a top elevation raster:

1. Export the individual outcrop polygons from the aquifer determination polygon shapefile described above.
2. Create an outcrop extent raster using the Feature to Raster tool and formation outcrop polygon.
3. Modify the outcrop extent raster so all the grid cells in the outcrop are equal to 0 and all of the null cells in the snap grid area are equal to -9 using the Raster Calculator tool
 - a. Example syntax: *Con(IsNull("WXotcExtUCPC"),-9,"WXotcExtUCPC")*
 - b. Example output: *"wx_otc_ndi"*
4. Interpolate the subcrop portion of the overlying formation using the Topo to Raster tool. For example, we used the interpolated bottom elevation raster of the Carrizo Sand (czbe) as the subcrop portion to build the top elevation raster for the Wilcox Group. See the inputs for interpolation mentioned earlier in this section.
5. Use the outcrop extent raster, DEM raster, interpolated subcrop raster, and conditional statements in Raster Calculator to combine the values from the DEM in the outcrop with interpolated values for the subcrop into one raster.
 - a. Example syntax: *Con("wx_otc_ndi" == 0,"ucpc_dem_ni","czbe")*
 - b. Example output: *"wxte"*
 - c. The raster calculator condition is set so if the outcrop raster cell = yes, the value assigned to the new raster will be from the study digital elevation model; if outcrop raster cell = "no", the new raster value will be from the overlying geological formation bottom elevation raster. The geological formation raster top elevation represents digital elevation model values in the outcrop and the overlying geological formation bottom elevation raster elsewhere.

Quality control, errors, and anomalies

The interpolated stratigraphic picks were reviewed within the context of regional geological structure and depositional environments for irregularities. Geological formations generally strike subparallel to the current coast and dip in wedges that thicken toward the Gulf of Mexico. Stratigraphic picks were expected to have similar elevations along strike.

Visual inspection

Stratigraphic picks that deviated from these expectations were given extra scrutiny, including verification of well location, geologic interpretation, and collection and interpretation of additional well control where possible to verify interpretations. Anomalies that resulted from

erroneous well locations or stratigraphic picks in the database were updated, exported, and interpolation was run again. Other anomalies were explained by knowledge of geologic features, for example geological faults, the Wilcox Group Yoakum Canyon, or the San Marcos Arch. Stratigraphic elevation variance near the Karnes, Luling, and Milano fault zones mapped in the Geologic Atlas of Texas (TWDB, 2007b) and in tectonic framework of Texas (Ewing, 1991), was attributed to fault offsets. We also recognized that changes in sediment depositional axes exist on either side of the San Marcos Arch. We expected that the Wilcox Group is thicker northeast of the arch and that the Carrizo Sand is thicker southwest of the arch. We discovered that the Carrizo Sand thickens within the Yoakum Canyon. The dip slope angle of the geological formation bottom along the arch axis tended to be steeper than the limbs. The Queen City, Weches, and Sparta formations are thicker to the southwest than the northeast. Some incongruities are inexplicable and remain in the dataset. Once bottom elevations were geologically acceptable, we calculated the thickness of the geological formation, evaluated it for irregularities, and made additional database edits as necessary.

Slope analysis

In addition to a visual inspection of the interpolated surfaces, we performed slope analysis to look for abrupt changes or high angles in slope. We created the slope raster using the formation top elevation raster and the Spatial Analyst[®] Surface Slope tool with output measurements set to degrees. Areas of the resulting raster with slope grades greater than 4° were reviewed for errors.

We identified areas where the Geologic Atlas of Texas outcrop lines were offset from the digital elevation model or didn't agree with well control. We made edits to the outcrop polylines and aquifer determination polygon shapefiles to accommodate these observations.

To ensure no gaps were created between the polygons, the following steps were used:

1. Edit the the polyline.
2. Use the Split Polygons tool using the new outcrop line.
3. Find and merge slivers with new attribution.

Layer inversions

Negative thickness raster values occur when the geological formation bottom elevation has values that are higher in elevation than the formation top elevation. Most of these errors occurred (1) near the outcrop, (2) where the geological formations become higher in elevation, (3) as the thickness decreased towards the outcrop, (4) where the spatial density of well control is low, (5) where the digital elevation model topography was irregular, (6) near interpolation tool anomalies, and (7) where the rasters are influenced by edge effects. The influence of Geologic Atlas of Texas outcrop mapping is critical. Areas with negative thickness values were identified and cells values in the stratigraphically lower geological formation were altered to be equal to the overlying geological formation surface elevation minus 1 foot.

Steps to correct inverted layers:

Create the quality control thickness raster by subtracting the formation bottom elevation raster from the top elevation raster using the Raster Calculator tool.

Example syntax: "w_xte" – "w_xbe"

Example output: "qcw_xTE-BE_01"

For every cell with a negative thickness value, change the geological formation bottom value to the top elevation value minus 1.

Example syntax: `Con("qcwxTE-BE_01"<0, "wxte"-1, "wxbe_i _____###")`

Guide points

Formation interpolations sometimes resulted in anomalies that create formations that were too thin, too thick, or even inverted. We would examine the location and elevation of picks in these areas. If the location of the well and interpretation of the stratigraphic pick seemed reliable, we tried to find more well control within the area. Sometimes more well control could not be discovered. When this was the case, we guided the interpolations in these areas to more geologically defensible results by inserting a guide point with an estimated formation elevation. Adding guide points as an input feature steered the interpolation results towards a raster that better reflected our predictions of where the bottom of a formation would be. Bottom elevation raster guide points applied to avoid geologically unlikely features included the Yegua (2), Cook Mountain (33), Sparta (19), Weches (50), Queen City (11), and Reklaw (12). The location and elevation of guide points used to interpolate rasters are provided in the GIS deliverables as point shapefiles. Although every effort was made to use guide points to correct overthickening artifacts in the thickness surfaces, some of these interpolation artifacts remain. Most are near the outcrop due to the same reasons stated above for layer inversions. Some of these may be interpolation artifacts from trying to match the geological formation raster with the Geologic Atlas of Texas outcrops, especially in areas where the geological formation is overlain by Quaternary sediments or where the Geologic Atlas of Texas Army map service topographic base map does not match this study's digital elevation model.

When both bottom elevation and test thickness rasters were satisfactory, bottom elevation rasters could be finalized, and final top elevation, bottom depth, top depth, and thickness rasters were generated (Figure 13.6.1-2).

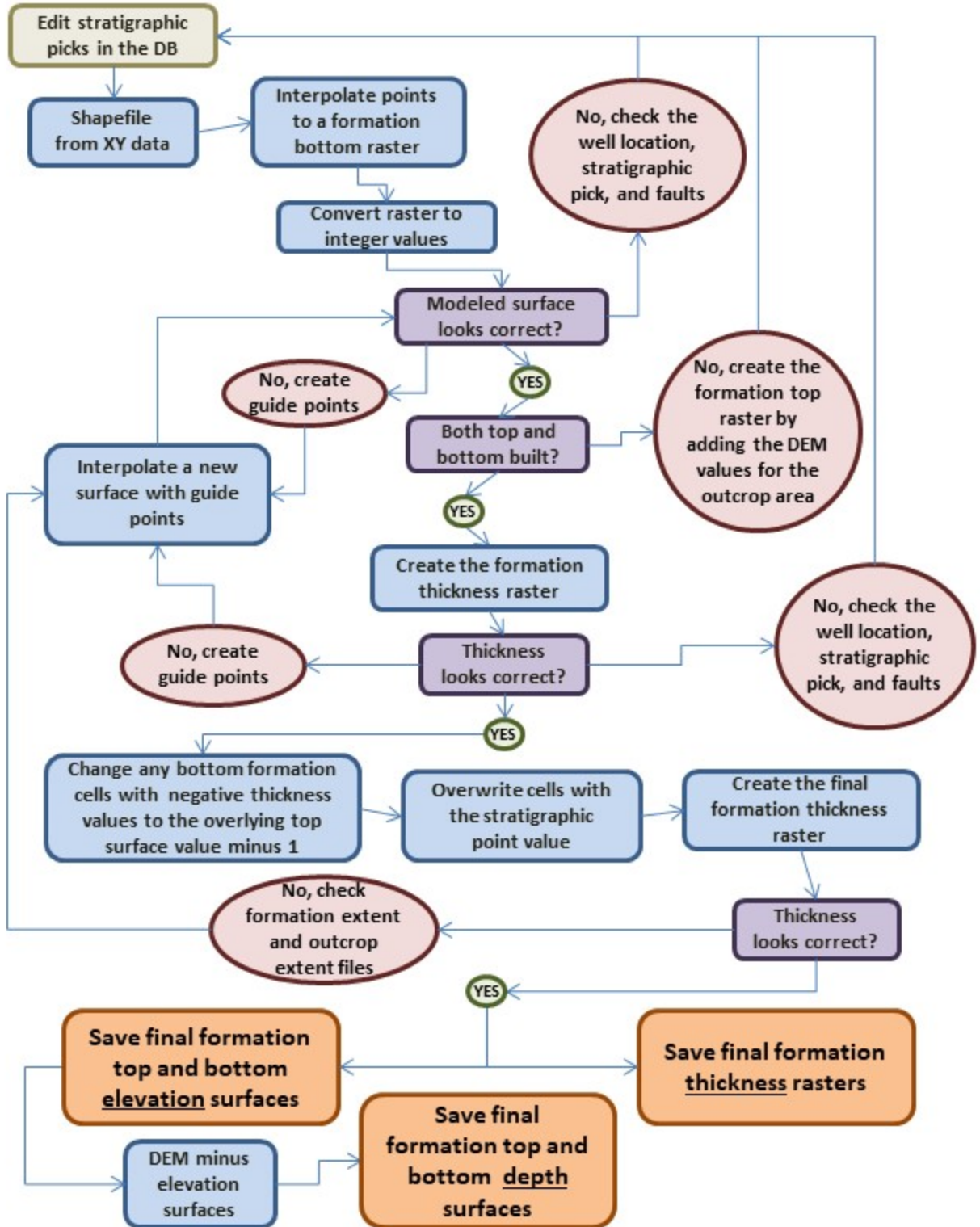


Figure 13.6.1-2. Diagram shows the iterative work flow of data export, interpolation, and editing necessary to create the geological formation surface raster files for top elevation and depth, bottom elevation and depth, and the thickness. DEM = digital elevation model; DB = BRACS Database.

Raster completion

We compared the stratigraphic picks in the database to the interpolated formation top and bottom surfaces generated with well control exported from the database in February 8, 2017. A summary of the differences (Table 13.6.1-1) is discussed in Section 6.3.

Table 13.6.1-1. Table of minimum, maximum, and mean offsets between a well log geological formation elevation pick and the interpolated geological formation elevation. Negative average differences indicate the interpolated surface is below the log derived stratigraphic elevation on average.

Stratigraphic unit	Number	Minimum (ft)	Maximum (ft)	Average (ft)	Area (sq mi)
Jackson Group	166	-13	11	0	1829
Yegua Formation	318	-11	50	0	2470
Cook Mountain Fm.	381	-68	49	0	2869
Sparta Sand	405	-61	31	-1	3045
Weches Formation	414	-73	21	-1	3163
Queen City Sand	578	-35	73	0	3687
Reklaw Formation	634	-46	14	-1	4005
Carrizo Sand	683	-68	27	0	4441
Wilcox Group	901	-43	28	-1	5842

Burn points

Cells that had an interpolated stratigraphic elevation different than a co-located stratigraphic pick point were corrected with a process we call “burning points”. For this process we use the Raster Calculator tool to overwrite the interpolated cell value with the precise stratigraphic elevation from the database-derived point shapefile.

Steps to burn point values to the raster:

1. Create a raster of the point values using the stratigraphy point shapefile using the Feature to Raster tool to create cell values that contain stratigraphic elevation values from the database.
 - a. Example output: *wxbe_fr*
2. Within the snap grid extent, convert the point raster no data cells to -99999 using the Raster Calculator tool.
 - a. Example syntax: *Con(IsNull("wxbe_fr"), -99999, "wxbe_fr")*
 - b. Example output: *wxbe_fr_nd*
3. Using the Raster Calculator tool, overwrite interpolated bottom elevation raster cell values with the precise stratigraphic pick raster cell values. This ensures the raster value matches the database and geophysical well log picks (with the kelly bushing correction applied).
 - a. Example syntax: *Con("wxbe_fr_nd"== -99999, "wxbe", "wxbe_fr_nd")*

Discussion of integer grid, snap grid, and projection

We checked every raster to ensure it had integer values, was coincident with the snap grid, and was in the GAM projection. We used the TWDB custom Groundwater Availability Model Albers Equal Area map projection because it preserves area and X, Y, and Z all use the same units. This is essential when calculating volume.

The custom Groundwater Availability Model projection is a Texas State Mapping System, Albers Equal Area ESRI projection. Projection parameters are:

Projection: Albers
False_Easting: 4921250.0
False_Northing: 19685000.0
Central_Meridian: -100.0
Standard_Parallel_1: 27.5
Standard_Parallel_2: 35.0
Latitude_Of_Origin: 31.25
Linear Unit: Foot_US (0.3048006096012192)
Geographic Coordinate System: GCS_North_American_1983
Angular Unit: Degree (0.0174532925199433)
Prime Meridian: Greenwich (0.0)
Datum: D_North_American_1983
Spheroid: GRS_1980
Semimajor Axis: 6378137.0
Semiminor Axis: 6356752.314140356
Inverse Flattening: 298.257222101

Thickness

Thickness (isochore) rasters were created using the Raster Calculator tool by subtracting the bottom elevation raster from the top elevation raster for every geological formation. The thickness raster values precisely match the mathematical subtraction of the input rasters. If we had interpolated the thickness point values to create the thickness rasters, the math between our formation top and bottom rasters would be out of sync with the thickness raster. Comparing the mathematically derived thickness with the interpolated thickness raster is a good quality control check.

Depth rasters

Depth rasters were needed to perform aquifer determination and are of value when determining how deep to drill to a geological formation top. They were easily created by subtracting the formation elevation rasters from the study digital elevation model. The digital elevation model for this study was created by resampling the United States Geological Survey 30-meter digital elevation model to the 250-foot grid cells defined by the study snap grid file (Figure 13.6.1-2).

Color ramps

We symbolized the interpolated geological formation raster surfaces with great care and thoughtfulness. Using “Bilinear Interpolation” can hide errors by making the grids appear smoother than the scale allows. This gives a false sense of data resolution where data appears more precise than reality. Additionally, during the stratigraphic pick reviews we used full color scales for each geological formation raster to highlight as many changes in elevation or thickness value as possible. However, for the report maps we utilized standardized color maps to ensure elevation, depth, or thickness values were assigned the same color between figures. This

provides fewer colors for defining thinner or shallower formations but allows the reader to use the same color value association between figures. Users can download the study GIS files and modify symbolization to meet their needs if necessary.

Stratigraphy rasters locked down

The stratigraphic information was finalized on February 8, 2017 so we could create geological formation surfaces. Since we are constantly acquiring and processing new data, there are stratigraphic picks in the current BRACS Database that weren't used in the interpolation of formation surface rasters. Also, geological formation top and bottom surface depths in the BRACS_ST_PE_sTX.shp will not equal those read directly from the BRACS Database since the depths in the shapefile have been corrected to reference the ground surface reference datum instead of the Kelly Bushing reference datum.

13.6.2 Net sand thickness raster interpolation

Predictive surface modeling using the Topo to Raster tool

We selected the Topo to Raster tool for interpolating net sands. This tool reasonably honored input point values while creating rasters that resembled our best professional judgement. We made this decision after evaluating net sand raster surfaces created using ArcGIS® 10.2.2 Kriging (from the Spatial Analyst and Geostatistical Analyst toolboxes), ArcGIS® 10.2.2 Topo to Raster, and Surfer® Kriging. To ensure the coincidence of the cells between the various rasters created in the study, four environmental parameters were always set with reference to the snap grid file (ucpc_snap) (1) output coordinate system, (2) extent, (3) snap grid, and (4) cell size. Net sand rasters were interpolated for five geological formations in the study (Yegua, Sparta, Queen City, Carrizo, and Wilcox). Preparation of net sand rasters for the Cook Mountain, Weches, and Reklaw formations was not a requirement of this study since these are not aquifers.

Methodology

The net sand interpolation input features included the net sand point and zero value outcrop point (net sand value set to zero) shapefiles. Section 6.4 describes processing driller's report formation descriptions and geophysical well log interpretations for net sand analysis. After these lithology picks were entered into the BRACS Database, they were exported to GIS using the following steps.

1. BRACS Database tables tblWell_Geology_NetSand_PaleoceneEocene_sTx and tblWell_Geology_NetSand_PaleoceneEocene_sTx_Well_Decisions were exported as dBase® IV files. This creates the tables gUCPC_NetSand and gUCPC_NS_WDec.
2. The dBase® files were imported into ArcGIS®.
3. The gUCPC_NetSand table was plotted in ArcMap using the tool "Make XY Event Layer" to create an event file.
4. The event file was exported to a shapefile in the Geographic Coordinate System, North American Datum 83 horizontal datum.
5. The shapefile was then projected into the custom TWDB Groundwater Availability Model projection

6. The shapefile was then joined to the gUCPC_NS_WDec table to utilize the field [USEWELL].
7. Definition queries were designed to reduce the features to formation specific net sand data:
 - a. Yegua: "Y_USEWELL" <> 0
 - b. Sparta: "SP_USEWELL" <> 0
 - c. Queen City: "QC_USEWELL" <> 0
 - d. Carrizo: "CZ_USEWELL" <> 0
 - e. Wilcox: "WX_USEWELL" <> 0
8. The formation specific data was then exported to individual shapefiles.
9. Excess fields were deleted from the formation specific net sands attribute tables for conciseness.

Zero value net sand outcrop points were created along the updip outcrop line. These zero value points forced the interpolated raster to smaller values towards the outcrop. These points were created in GIS using the following steps.

1. In ArcCatalog, right click on the "net_sand_pt" folder -> New...-> shapefile
 - a. Name the file "fmns_xxxx_otc_zero_pt.shp"
 - b. Feature Type: Point
 - c. Click the "Edit..." button
 - d. Choose the GAM projection
 - e. Click "OK", Click "OK"
2. In ArcMap, add the fmbe_otc_pl.shp from the "extent" folder and fmns_xxxx_otc_zero_pt.shp from the "net_sand_pt" folder
3. Start an editing session
4. Click the Edit Tool on the Editor toolbar.
5. Click a single line feature along which you want to generate points.
6. Click the Editor menu and click Construct Points.
7. Choose the fmns_xxxx_otc_zero_pt.shp in which the new feature will be created.
8. Choose Distance and enter "13200 ft"
 - a. 13,200 feet = 2.5 miles
 - b. This is the shortest distance across a 2.5-minute grid cell (our ideal data density) and would theoretically create one point per 2.5-minute grid cell.
9. Click "OK".
10. Save edits.
11. Add "FM_NET_SAN" field (Data Type = Double, Precision=18, Scale=5) and attribute it as "0"

Guide points were only used to improve the interpolation of the net sands for the Carrizo and Wilcox. The placement of these points was determined based on trouble areas where the interpolation was creating artifacts that did not reflect the existing data and geologic

understanding of the formation. The Wilcox Group interpolation used two guide points with values of 47 and 77 feet. The Carrizo Sand interpolation used three guide points with values of 214, 375, and 650 feet of net sand.

The preparation of the Wilcox Group required additional work to incorporate the extent of the shale-filled Yoakum Canyon. Maps by Hoyt (1959) and Dingus and Galloway (1990) were georeferenced and digitized to help understand the extent, morphology, and lithology of the Yoakum Canyon. Net sand contours were hand drawn for 700- and 1000-foot values based on these references, net sand points from the BRACS Database, and computer-generated contours from the interpolation of those points and outcrop zero value points. These contour intervals were included in the second round of Topo to Raster interpolation (Figure 13.6.2-1).

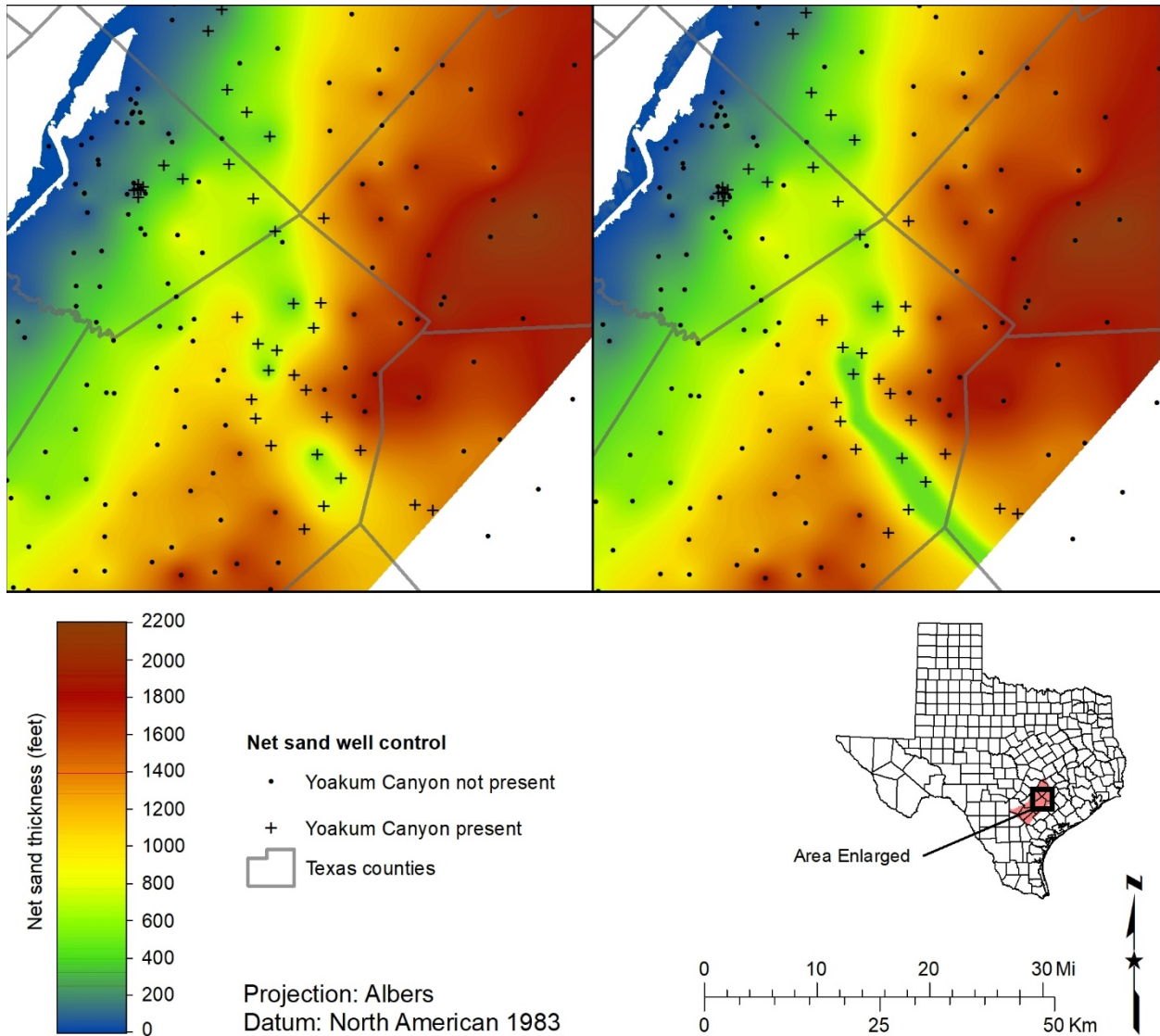


Figure 13.6.2-1. Wilcox net sand rasters in the Yoakum Canyon area. The image on the left was interpolated without the hand drawn contours. The image on the right incorporated the contours.

Topo to Raster tool inputs for the Wilcox Group net sands:

1. Input feature data:

Feature layer	Field	Type
wxns_guide_pt	wxns_guide	PointElevation
wxns_otc_zero_pt.shp	WX_NET_SAN	PointElevation
wxns_pt.shp	WX_NET_SAN	PointElevation
wxns_contour_guides_500ft	guide_con	Contour
wxns_contour_guides_1000ft	guide_con	Contour

2. Output surface raster: wxnstrog__11.
3. Output cell size: snap_ucpc (study snap grid raster).
4. Output Extent: snap_ucpc.
 - a. Top: 19465088.468617
 - b. Left: 5272452.803318
 - c. Right: 5943452.803318
 - d. Bottom: 18728588.468617
5. Margin in cells: 20.
6. Smallest z value to be used in interpolation (optional): 0.
7. Largest z values to be used in interpolation (optional).
8. Drainage enforcement (optional): NO_ENFORCE.
9. Primary type of input data (optional): SPOT.
10. Maximum number of iterations (optional): 20.
11. Roughness penalty (optional).
12. Profile curvature roughness penalty (optional).
13. Discretization error factor (optional): 1.
14. Vertical standard error (optional): 0.
15. Tolerance 1 (optional): 0.
16. Tolerance 2 (optional): 200.
17. Environments...
 - a. Output Coordinates
 - i. Same as snap_gird
 - b. Processing Extent
 - i. Extent – same as snap_grid
 - ii. Snap Raster – snap_grid
 - c. Raster Analysis
 - i. Cell Size – snap_grid
 - ii. Mask - none

Quality control, errors, and anomalies

Net sand well points represent cumulative feet of sand per geological formation based on driller's logs and geophysical well log interpretations. Quality assurance was applied to the net sand points, as outlined below, but the quality of the picks varied by source. Quality assurance and quality control (QA/QC) checks performed on net sand points and rasters for each of the five aquifers in the study included database queries, histograms, hot spot and slope analysis, and GIS queries.

The three coded database queries we ran were 1) negative lithologies, 2) gaps, and 3) outliers. The negative lithology queries checked for inversions in the lithology records for the project by subtracting the top depth from the bottom depth of the same record. We examined wells with negative thickness intervals. In some cases, these wells were corrected because the lithology came from well log interpretation. In other cases, the error could not be corrected because the data came from a submitted driller's report. Wells with this error were not used in the interpolation of net sands.

The gap query checks adjacent lithology records to see if the overlying bottom depth is a different value than the underlying top depth. We run this query since users can introduce an error in the top and bottom depths. Sometimes there may be unanalyzed log sections without a corresponding unanalyzed record value. Gaps result from overlapping or underlapping lithology records. If these gaps were based on a geophysical well log interpretation, we fixed the interval values. Gaps in submitted driller's reports that could not be fixed were culled from use in the study using the net sand decision table.

The outlier query utilizes statistics compiled for the thickness of each simplified lithologic description from tblWell_Geology from the BRACS Database. For example, code would compare the thickness of a sand record from the study dataset to statistics compiled from all of the sand records in the BRACS Database. If the thickness of the sand record from the study dataset exceeded the thickness of 98% of the sand records in the database, these records were flagged, reviewed, and edited as necessary. In some cases, "lumped" lithology was described more finely, and in other cases, for example the Yoakum Canyon, the very thick interval of clay seemed reasonable and was left alone. If lithology records from a submitted driller's report are flagged in this check, that well was set to "NO" in the decision table for net sands data. Often these wells had one lithology record that was thicker than the geological formation and was presumably inaccurate.

Histograms of point data detected wells where the net sand seemed too thin or too thick within the study dataset. The lithology for these wells was checked in IHS Kingdom[®], corrected as needed, and then updated in the BRACS Database.

The hot spot and slope tests relied on ArcToolbox tools to highlight geometric anomalies in the predictive raster surface. The Hot Spot Analysis (Getis-Ord G_i^*) tool is in the Mapping Cluster toolset in the Spatial Statistics Tools toolbox. The Hot Spot Analysis tool is used to identify well points where the net sand value was unusually high or low compared to its neighbors before an interpolation is performed. When the tool identified a hot spot (a point with a high value compared to its neighbors) or a cold spot (a point with low values compared to its neighbors), we investigated the well lithology. If the lithology was interpreted from a geophysical well log, we described thicker lithology units in more detail. If the lithology came from a submitted driller's report and seemed unreasonable, we set the well to "NO" in the net sand decision table.

The Slope tool is in the Surface toolset in the Spatial Analyst Tools toolbox. To leverage the slope tool for QA/QC, a specific slope angle in degrees was identified as a cutoff and the slope raster was symbolized so that cells with a slope value below the cutoff were considered fine and cells above the slope cutoff needed to be cross-examined. We reassessed well points that fell within the cells above the slope cutoff using IHS Kingdom[®] and adjusted values as needed. The BRACS Database was updated with corrected data.

A GIS query was performed selecting wells with net sand values equal to or greater than the formation thickness. Well lithology for these wells was examined in IHS Kingdom[®]. If changes were made to the lithology it was updated in the BRACS Database and exported to the net sand shapefile for a new round of interpolation. If some wells with unusual lithology persisted, we audited the location of wells. In some cases, the flagged lithology looked fine, but the location was inaccurate.

Net sand raster cell values were extracted at each net sand well point for each geological formation using the Extract Values to Points tool. The difference between the interpolated net sand value and the well net sand value was calculated and saved to a new field in the net sand point attribute table. We then ran summary statistics on that field to get the minimum, maximum, and average difference between the point value we assigned after interpreting logs or importing driller’s lithology and the raster value the software predicted for that location after weighing the surrounding values. These offsets can serve as a metric to evaluate interpolation accuracy. The value ranges and averages per formation can be reviewed in Table 13.6.2-1. Each formation interpolation average underestimated the net sand thickness by about 1 foot. The Sparta Sand net sand raster was the most predictable with the lowest spread of offsets. The Queen City net sand was the least predictable with the largest minimum and maximum offset values. Net sand well density per square mile per formation can also be calculated from this table. The Yegua Formation had the lowest amount at 0.079 wells per square mile and the Carrizo Sand had the most at 0.118 wells per square mile. There was an average of 0.099 wells per square mile of formation.

Table 13.6.2-1. Table of minimum, maximum, and mean differences between measured net sand thickness from wells and the interpolated net sand thickness. Negative averages indicate the interpolation underestimated the net sand thickness on average.

Formation	Number of wells with net sand picks	Minimum (ft)	Maximum (ft)	Average (ft)	Area (sq mi)
Yegua Formation	194	-33	31	-1	2,470
Sparta Sand	334	-15	15	-1	3,045
Queen City Sand	383	-90	89	-1	3,687
Carrizo Sand	525	-41	40	0	4,441
Wilcox Group	499	-66	35	-1	5,842

Raster finalization

Several data processing steps were required (Figure 13.6.2-2) to prepare final net sand rasters once we were satisfied with interpolation results.

1. Check that cells are coincident with the snap grid
2. Check that the raster is in the GAM projection
3. Ensure rasters have integers values
4. Overwrite precise net sand point values into raster cells
5. Correct interpolated net sand values that are greater than formation thickness values

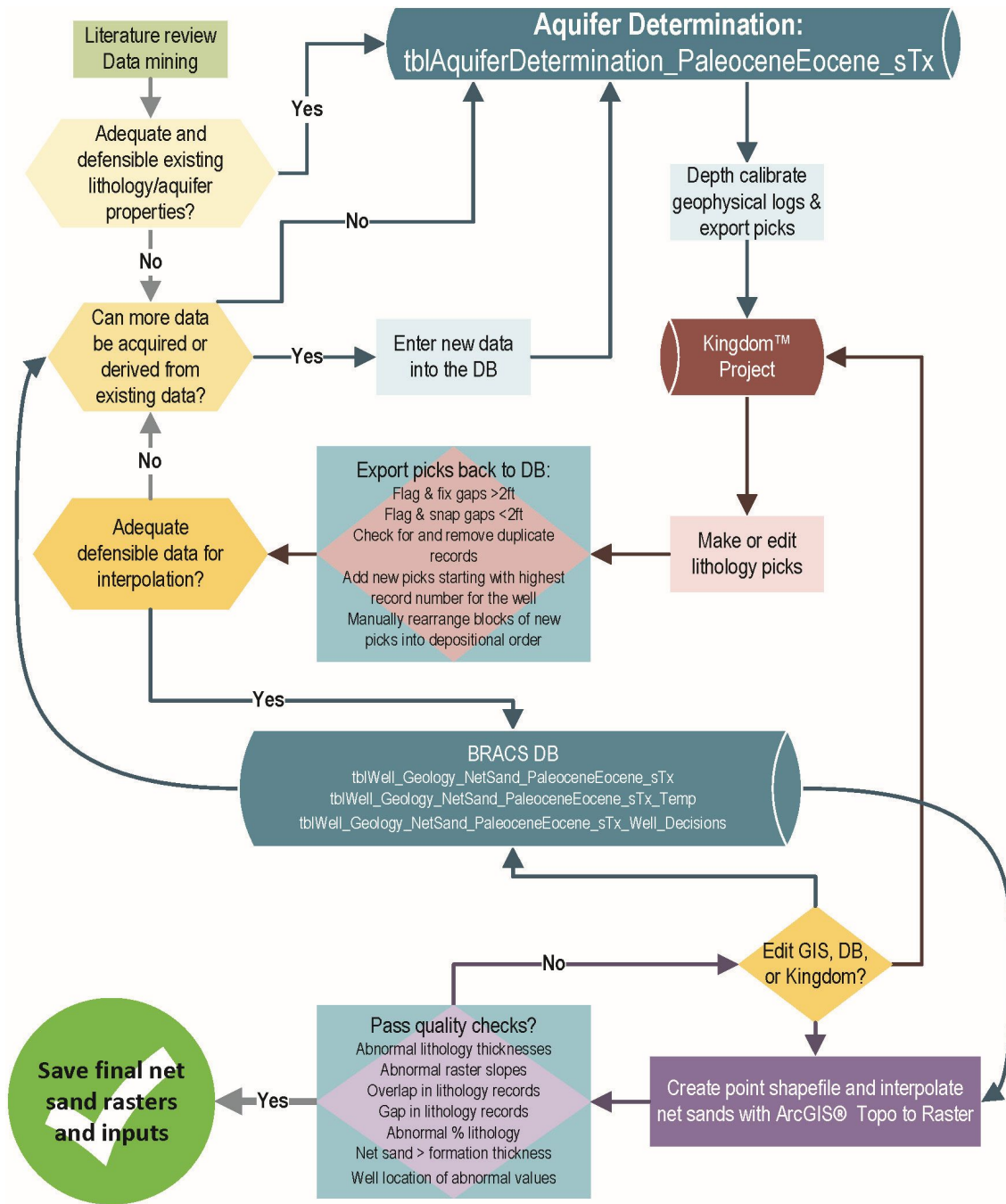


Figure 13.6.2-2. Diagram showing the iterative work flow of data export, interpolation, and editing necessary to create the net sand rasters. DB = BRACS Database, GIS = Geographic Information System.

We utilized ArcMap® Pixel Inspector to visually confirm that cells in the net sand rasters were coincident with the snap grid cells. Cells need to be coincident with other rasters in the study to run volume calculations. We checked the raster properties to certify that the Spatial Reference was the GAM projection and the Pixel Type was signed integer.

We overwrote (burning points) cell values at each well point with the net sand value. The first step we took to enforce this rule was to create a raster where well values were set to the individual cells intersected and all other cells set to -9. We achieved this by converting points to a raster using the Feature to Raster tool. Then we used Raster Calculator to combine IsNull and conditional statements to assign -9 to all the remaining cells. We used a conditional statement in Raster Calculator to overwrite the net sand well point values to the matching net sand grid cell while retaining the interpolated values in all grid cells that did not contain a well.

Given the nature of predictive interpolated values, areas without enough well control could have a net sand cell value greater than formation thickness. We subtracted the net sand raster from the formation thickness raster. Negative cell values were corrected with a conditional statement in Raster Calculator to equal the formation thickness. Additionally, any net sand cells with a value equal to zero were overwritten with a value of 1 foot.

We did not use Bilinear Interpolation to symbolize the interpolated geological formation net sand raster surfaces. This option can hide errors by making the grids appear smoother than the scale of the grid size allows. This gives a false sense of data resolution that is more precise than reality. We used the same color ramp for each geological formation net sand map, however the data range for each ramp is specific to the formation. For example, the Wilcox Group net sand color ramp has a range of 1 to 2,168 feet and the Sparta Sand net sand color ramp has a range of 1 to 159 feet. Users can download the study GIS files and modify symbolization to meet their needs if necessary.

13.6.3 Static water level raster interpolation

Static water levels were interpolated for each of the five aquifers. These rasters were used to determine the saturated thickness for the outcrop regions used to estimate groundwater volume. We considered using the potentiometric surfaces from the southern and central Carrizo-Wilcox and Queen City-Sparta GAM models for our study (Young and others, 2018; Kelly and others, 2004). Upon examination of the surfaces, we did not find them suitable for our study for two reasons. First is that the GAM combines the Carrizo and Wilcox into one layer and the Queen City and Sparta into another layer. Second is that the GAM used pre-development data for the Queen City-Sparta layer and pre-2000 data for the Carrizo-Wilcox layer. Using these surfaces would underestimate the unsaturated thicknesses of the aquifers near outcrop and result in an overestimation of groundwater volume.

Methodology

Creation and export of static water level measurements from the BRACS and Groundwater (GWDB) databases used these steps:

1. The GWDB was imported into a MS Access® format and tables were linked to the BRACS Database
2. Database queries appended static water level measurements from the two source databases into a study static water level table. These queries used the study aquifer determination table to select measurements from wells completed in the Yegua Formation (field [AQ_New] = Y), Sparta Sand (field [AQ_New] = SP), Queen City Sand (field [AQ_New] = QC), Carrizo Sand (field [AQ_New] = CZ), and the Wilcox Group (field [AQ_New] = WX)

3. Wells without a measurement date or related information were removed from the table
4. Wells with a static water level at or above the ground surface were checked to ensure they were artesian wells
5. Wells with a reported static water level below the total depth of the well or the drilled hole were assumed to be data entry errors and removed from the table
6. Exported table from BRACS Database
7. Imported table into GIS and used “Display XY data” tool, selected Geographic Coordinate System North America with a North American Datum 83 as the horizontal datum
8. Exported the event and projected the resulting shapefile into the custom TWDB GAM projection
9. The static water level elevation was calculated using the project Digital Elevation Model value from the study resampled elevation raster
10. Definition queries to select only wells completed in a single study aquifer and with a static water level measurement from year 2000 to present were used to generate each static water level interpolation raster
11. Interpolate the depth to static water level points with updip outcrop points set to zero in Topo to Raster
12. Convert the raster from depth to elevation value using the study DEM
13. Clip the raster to just the geological formation outcrop extent
14. Check the raster for any water levels that are above the top of the formation/earth’s surface. This would represent artesian conditions, which we assume to be improbable in outcrop. No corrections were needed.
15. Check the raster for any water levels that are deeper than the bottom of the geological formation
16. Correct the raster for any water levels that are deeper than the bottom of the formation to be equal to the bottom of the formation

The static water level information was finalized on October 12, 2018 so we could create aquifer static water level interpolated surfaces. Since we are continually acquiring data for both the GWDB and BRACS databases, there may be static water level measurements that were not used in this study. We selected measurements from the year 2000 to present to more accurately reflect current aquifer saturation conditions near outcrop, while still maintaining a set of data with enough measurements and spatial distribution for interpolation. We used the TWDB GAM projection because this projection preserves area, which is essential when calculating volumes.

Spatial distribution of well control data

Water wells are typically drilled to the first water-bearing formation with suitable water quality and quantity. Therefore, we had more static water level measurements near the outcrop of a geological formation and measurements become sparser downdip. This resulted in a roughly strike-oriented belt of data with an interpolated static water level surface dipping less steeply than the geological formation surface downdip, reflecting the change from water table to artesian

conditions. The Topo to Raster interpolation method incorporates data trends when creating the surfaces so the best value predictions are within the areas with well control points. The predicted surface was poorly-constrained where we lacked data, especially in the downdip portion of the aquifer. This is not a problem since we clipped the raster to the geological formation outcrop extent.